Department of Bioengineering & Strathclyde
Institute of Pharmacy and Biomedical Sciences

Deep brain stimulation of the mediodorsal thalamic nucleus and its implications for the treatment of schizophrenia

Samuel G. Ewing

A thesis presented in fulfillment of the requirements for
the degree of Doctor of Engineering

March 7, 2011

Copyright Statement

Signed: Date:

Acknowledgements

To my parents. You gave me the most valuable gift on earth - a proper education. I doubt that I will ever fully appreciate the sacrifices you made to provide me the best schooling in England. Without your continued support I would not have made it to where I am now and I certainly would never have made it to where I am going. I hope you agree that it has all been worth it!

To my brothers. I could not wish for three better friends. You made me competitive and the worst case scenario never seems so bad knowing I can never fall farther than one of your floors!

To my friends and supporters. Many of you need do nothing more than buy me a pint at the end of the week which is more than enough. To those who have contributed in the discussion and creation of this text, you know who you are and you know you have my thanks.

Contents

Abbreviations

Anatomical

AC	anterior limb of the internal capsule
Acb	nucleus accumbens
AcbC	accumbens core
AcbSh	accumbens shell
AGI	agranular insular cortex
ATN	anterior thalamic nucleus
BLA	basolateral amygdaloid nucleus
CeM	centeromedial amygdaloid nucleus
Cg	cingulate cortex
Cg1	cingulate cortex, area 1
Cg2	cingulate cortex, area 2
CL	centerolateral thalamic nucleus
CM	centromedian thalamic nucleus
CPu	caudate-putamen
dm	dorsomedial
dl	dorsolateral
DLO	dorsolateral orbital cortex
DRN	dorsal raphe nucleus
EP	entopeduncular nucleus
GP	globus pallidum
IAM	interanteromedial thalamic nucleus
IL	infralimbic cortex
IMD	intermediodorsal thalamic nucleus
LaDL	lateral amygdaloid nucleus
LH	lateral hypothalamus
LO	lateral orbital cortex
LSI	lateral septal nucleus, intermediate part
LSV	lateral septal nucleus, ventral part
M1	primary motor cortex
M2	secondary motor cortex
MD	mediodorsal thalamic nucleus
MDL	mediodorsal thalamic nucleus, lateral part
MDM	mediodorsal thalamic nucleus, medial part
MO	medial orbital cortex
MTL	medial temporal lobe
OFC	orbitofrontal cortex
PF	parafasicular thalamic nucleus

PFC	prefrontal cortex
PrL	prelimbic cortex
PT	paratenial thalamic nucleus
PV	paraventricular thalamic nucleus
PPN	pedunculopontine nucleus
Re	reuniens thalamic nucleus
Rh	rhomboid thalamic nucleus
Rt	reticular thalamic nucleus
Sone	primary somatosensory cortex
Stwo	secondary somatosensory cortex
SNc	substantia nigra, compacta part
SNr	substantia nigra, reticular part
STN	subthalamic nucleus
vm	ventromedial
VM	ventromedial thalamic nucleus
VO	ventral orbital cortex
VP	ventral pallidum
VS	ventral striatum
vSub	ventral subiculum of the hippocampus
VTA	ventral tegmental area
ZI	zona incerta

Miscellaneous

A	amplitude
CT	computer assisted tomography
DBS	deep brain stimulation
DTI	diffusion tensor imaging
ECG	electro-cardiogram
ECoG	electro-corticography
EEG	electro-encephalography
EPSP	excitatory post synaptic potential
F	frequency
FFT	fast Fourier transform
GABA	γ-aminobutryic acid
HF	high frequency
IEG	immediate early gene
ISH	*in situ* hybridisation
IPSP	inhibitory post synaptic potential
LFP	local field potential
MRI	magnetic resonance imaging
NMDA	*N*-methyl-D-aspartate
OCD	obsessive compulsive disorder
PCP	phencyclidine
PET	positron emission tomography
PW	pulse width
rCBF	regional cerebral blood flow
ROD	relative optical density

Abstract

Schizophrenia is a devastating mental illness affecting 1% of the population. Existing antipsychotic drugs treat the positive symptoms associated with the disease but they have limited effects against the negative symptoms and cognitive deficits. Here a deep brain stimulation (DBS) strategy analogous to that used in Parkinson's disease is proposed. Methods for the validation of this strategy in a phencyclidine (PCP) rat model of schizophrenia are described. Given the weight of evidence implicating disruption of the thalamo-cortical system, particularly the mediodorsal thalamic nucleus and prefrontal cortex, studies have focused on investigation of the consequences of high frequency stimulation of the mediodorsal thalamic nucleus and results from biomolecular, electrophysiological and behavioural investigations reported.

Bipolar stimulating electrodes were fabricated and implanted, bilaterally, into the mediodorsal thalamic nucleus of rats. In all experiments high frequency DBS was delivered unilaterally via a custom designed and built stimulation device.

Brains were removed, sectioned and radio labeled for the immediate early gene (IEG) *zif-268*. In anaesthetised rats DBS of mediodorsal thalamic nucleus produced robust increases in the expression of *zif-268* localised to the efferent targets of the mediodorsal thalamic nucleus, indicating an increase in neural activity in the prefrontal cortex.

Spectral analysis of the electro-cortigram (ECoG) was explored in both saline and PCP treated rats. Increases in low frequency (delta and theta) power were demonstrated in PCP treated animals. DBS of the mediodorsal thalamic nucleus appears to transiently exacerbate the already augmented increase in delta/theta power.

Open-field locomotor activity, pre-pulse inhibition (PPI) and PCP induced hyperlocomotion were explored in conscious animals. DBS of the mediodorsal thalamic nucleus was found to have no effect on locomotor activity whilst yielding an improvement in prepulse inhibition of the startle response. In addition DBS of the mediodorsal thalamic nucleus was shown to augment the hyperlocomotion induced by the acute administration of PCP.

Impairment in the ability to recruit the prefrontal cortex is frequently reported in schizophrenia. The results of the IEG experiments demonstrate activation of frontal cortical regions as a consequence of deep brain stimulation of the mediodorsal thalamic nucleus. In addition quantitative analysis of the ECoG demonstrates a spectral profile, in rats treated sub-chronically with PCP, similar to that seen in schizophrenic patients. Furthermore DBS of the mediodorsal thalamic nucleus may improve PPI performance - a deficit commonly reported in schizophrenia - although this same stimulation protocol exacerbates the PCP hyperlocomotion purported to reflect some of the positive symptoms of schizophrenia.

Part I

General Introduction & Methods

Chapter 1

Introduction

> *"Multi-disciplinary research in this area is at the cutting-edge of understanding the basis of symptomatology and fundamentally impacting the treatment and prevention of schizophrenia."*
>
> Goghari *et al.* (2009)

Whilst DBS for movement disorders is well established, DBS for psychiatric disorders is in its infancy. Clinical trials for Tourette's syndrome (Kuhn *et al.*, 2007; Ackermans *et al.*, 2008; Visser-Vandewalle *et al.*, 2003; Diederich *et al.*, 2005; Welter *et al.*, 2008), obsessive-compulsive disorder (OCD) (Abelson *et al.*, 2005; Greenberg *et al.*, 2006) and treatment resistant depression (Mayberg *et al.*, 2005; Schlaepfer *et al.*, 2008) are underway. These conditions have a history of being successfully treated with lesioning procedures (Larson, 2008) so, by analogy with the successful replacement of thalamotomy and pallidotomy in Parkinson's disease and dystonia, seem likely candidates for the extension of DBS to psychiatric illness. Psychotic disorders have no such history of successful treatment by lesioning techniques. There are currently no studies into the application of DBS in schizophrenia (Larson, 2008). However, it is the aim of this thesis to do just that and provide the first evidence that DBS may be a strategy worth consideration in the treatment schizophrenia.

1.1 Schizophrenia

Schizophrenia, at the level of the individual sufferer and at the level of the global economy, is a devastating illness. Occasionally grabbing headlines with tales of maniacal homicide it is the quietly tragic stories of broken minds, broken families and suicide that go unreported. Omitting diseases of old age it ranks as the third greatest cause of disability worldwide (Murthy *et al.*, 2001) affecting approximately 1% of the global population (Satorius N & Korten, 1986). Schizophrenia is most commonly diagnosed in late adolescence afflicting people just as they are to begin their productive lives, making it nearly impossible for them to complete their education, maintain gainful employment, marry or have a family (see Andreasen 1995). As such it has recently been estimated that the total service costs for England in 2007 was £2.2 billion and is predicted to rise to £3.7 billion by 2026. Less than a fifth of these service costs are incurred through the prescription of medication. Including the costs incurred through lost employment the total has been estimated to be £4 billion at present rising to £6.5 billion by 2026 (McCrone *et al.*, 2008). The global cost is clearly an astronomical multiple of these figures.

The personal cost is even greater. Schizophrenics often feel that they have lost their identity, autonomy and mental capacity whilst relatives witness the disease as the loss of a previously normal relation, who continues to live but seems a different person (see Andreasen 1995). The disease is often so unbearable that many *choose* to take their own lives: approximately 30% of schizophrenics attempt suicide with a third of these succeeding (Black & Fisher, 1992).

Schizophrenia produces a severe fragmentation of thinking and personality. The etymology, schizo = split, phrenia = mind, tends to generate the popular misunderstanding that schizophrenics have a "split personality". However, this condition, technically known as dissociative disorder, is far less common than schizophrenia itself (see Andreasen 1995).

Schizophrenia comprises a diverse array of symptoms with an equally diverse array of brain systems affected. The criteria for the diagnosis of schizophrenia are detailed in the ICD-10 (The Tenth International Classification of Disease) and the DSM-IV (The American Psychiatric Association's Diagnostic and Statistical Manual) and are not discussed in detail here.

Suffice it to say that the diagnosis of this disease is complex. However it is helpful to classify the symptoms as:

positive: those which occur in addition to normal experience.

negative: those that occur which depreciate one's normal experience.

cognitive deficits: deficits in cognitive function.

Positive symptoms include: hallucinations, delusions, thought broadcasting (the belief that one's thoughts can be heard by others), thought insertion (the belief that the thoughts of other's are being inserted into one's mind) and inappropriate affect (emotional behaviour which is unsuited to the social context). Negative symptoms include: depression, anhedonia (the inability to feel pleasure), self-neglect, social withdrawal, avolition (lack of motivation) and alogia (poverty of speech). The symptoms of cognitive dysfunction include: deficits in working memory, selective attention and mental flexibility (the ability to plan and anticipate outcomes).

1.1.1 Biology of schizophrenia

Amphetamine acts to increase dopamine transmission in the brain and its abuse in otherwise healthy humans can lead to a psychotic episode with positive symptoms that are almost indistinguishable from those seen in schizophrenia. In addition many of the typical antipsychotics (see section 1.1.4, page 10) achieve their therapeutic benefit through blocking dopamine receptors. These evidences support the **dopamine hypothesis of schizophrenia** which suggests that psychotic episodes in schizophrenia are caused by the activation of dopamine receptors. Alternatively phencyclidine (PCP) abuse is also known to exhibit a profile of positive and negative symptoms, in otherwise healthy humans, that closely resembles that seen in schizophrenia. However PCP is known to act at NMDA receptors affecting glutamatergic transmission in the brain. This evidence underpins **glutamate hypothesis of schizophrenia** and suggests that schizophrenia is due, at least in part, to diminished activation of NMDA receptors (see Bear *et al.* 2001).

Schizophrenia is highly heritable with estimates of a heritability risk of the order of 80% (see Ross *et al.* 2006) suggesting a predominant genetic component in the neurobiology of this disease. Family studies demonstrate that simple major gene effects are unlikely indicating cumulative effects from multiple candidate genes (see Harrison & Weinberger 2005). The schizophrenia genome project, launched in November 2008, aims to identify "all inherited elements important in schizophrenia within 3 years." As of the date of the publication of this thesis the

schizophrenia genome project has identified 188 candidate genes for schizophrenia (http://schizophrenia.ncgr.org). To discuss one would invite discussion of them all and is beyond the scope of this introduction.

Whilst the positive and negative symptoms associated with this disease may vary in their severity, the cognitive dysfunction, acknowledged as a central feature (see Antonova *et al.* 2004; Gold 2004), remains stable. Furthermore cognitive deficits are also observed in relatives of schizophrenic patients (Snitz *et al.*, 2006) suggesting that at least some of features of the cognitive dysfunction associated with schizophrenia may be under specific genetic control.

However the probability of an identical twin developing schizophrenia given that their sibling also has schizophrenia is of the order of 50% (see Bear *et al.* 2001), indicating that genetics alone are insufficient to cause schizophrenia. This suggests that additional environmental factors must contribute to the underlying genetic anomalies in the development of this disease. Such environmental factors include; stress, substance abuse, in utero infections (such as rubella, influenza, and poliovirus (Brown & Susser, 2002)), season of birth and parental age (see Messias *et al.* 2007) and obstetric complications (such as premature birth (Cannon *et al.*, 2002)). This complex interplay between genes and the environment is thought to lead to a subtle yet complicated disturbance of neurodevelopment early in life, the consequence of which may be reached by multiple pathogenetic pathways, yielding the syndrome recognised as schizophrenia (see Lewis & Levitt 2002). This aberrant development leads to an equally subtle pathology in the developing nervous system with alterations commonly reported in the thalamo-cortical system. This pathology is explored in some detail below.

1.1.2 Pathology of schizophrenia

Both Kraepelin and Bleuler who first described "dementia praecox" (1907) and the "schizophrenias" (1911) (see Bear *et al.* 2001) believed that the etiology of the disease would be linked to structural abnormalities in the brain. However the tools necessary to accurately interrogate this assertion are only more recently available. Initial computer assisted tomography (CT) has been superceded by ever evolving imaging modalities (magnetic resonance imaging (MRI), positron emission tomography (PET) and diffusion tensor imaging (DTI)). A large number of imaging studies have explored structural abnormalities in schizophrenia, the results of which are well corroborated in post-mortem investigations. As such it has become clear that schizophrenia is associated with a highly characteristic pattern

of anatomical changes in the central nervous system, centred on interconnected circuitry involving cortical, limbic and thalamic brain structures. Furthermore some studies indicate that these structural changes may be progressive (Rapoport *et al.*, 2005).

Whilst the following explores anatomically specific abnormalities commonly associated with schizophrenia it is worth noting that, at a gross anatomical level, schizophrenics exhibit a reduction in total cerebral volume and an increase in total ventricular volume (Wright *et al.*, 2000; Chua *et al.*, 2007). Unless otherwise stated all differences are relative to healthy control subjects.

1.1.2.1 Frontal Cortices

Prefrontal cortex: The dorsolateral prefrontal cortex, once considered unique to primates (Uylings *et al.*, 2003), is a region critical in working and episodic memory (Andrews *et al.*, 2006). Whilst differences in total volume of the prefrontal cortex have not been reported, Gilbert *et al.* (2001) have demonstrated a reduction in the volume of the grey matter in the dorsolateral prefrontal cortex, localised to the left hemisphere, in new-onset schizophrenics, indicating that grey matter volume reduction may be part of the primary pathology of this disease. This finding has been "duplicated", although in the right hemisphere of new-onset schizophrenics (Chua *et al.*, 2007). Dysfunction in the prefrontal cortex has been correlated with the severity of the negative symptoms and cognitive deficits (Schroder *et al.*, 1996; Hazlett *et al.*, 2000; Perlstein *et al.*, 2001; Potkin *et al.*, 2002; Callicott *et al.*, 2003). Deficits in working memory that correlate with reduced activation of the dorsolateral prefrontal cortex have been reported in schizophrenic patients (Barch *et al.*, 2002, 2003)

1.1.2.2 Thalamus

The thalamus acts as a critical relay between the cortex and structures of the basal ganglia and cerebellum. The thalamus is a heterogeneous structure with different thalamic nuclei reciprocally connected with anatomically (and, therefore, functionally) distinct regions of the cortex. Whilst it is the pathology of specific thalamic nuclei that are of greatest importance it is interesting to note that reductions in whole thalamic volume are a consistent finding in both new-onset and chronic schizophrenia (Gilbert *et al.*, 2001; Konick & Friedman, 2001; Andreasen *et al.*, 1994; Coscia *et al.*, 2009). Shimizu *et al.* (2008) indicate that reduction in whole thalamic volume is specific to the right hemisphere. However

no differences in glucose metabolism have been reported at the level of the whole thalamus with abnormalities only being reported in the mediodorsal thalamic nucleus and centromedian thalamic nucleus (see below). Correlations between total thalamic volume and executive functioning have been noted (Coscia *et al.*, 2009) although they reported no correlation between thalamic volume and the severity of either positive or negative symptoms.

Mediodorsal thalamic nucleus: The mediodorsal thalamic nucleus is reciprocally connected with the prefrontal cortex and, whilst not unique in this role, is the predominant input to the prefrontal cortex.

Post-mortem studies have shown reductions in the volume (Danos *et al.*, 2003; Byne *et al.*, 2002), neuronal size and number in the mediodorsal thalamic nucleus (Byne *et al.*, 2002; Popken *et al.*, 2000; Young *et al.*, 2000) and imaging studies confirm this finding *in vivo* (Kemether *et al.*, 2003; Shimizu *et al.*, 2008). In addition Hazlett *et al.* (2004) has reported abnormal glucose metabolism in this nucleus. Healthy subjects had higher relative glucose metabolism in the left mediodorsal nucleus when compared with the right, whilst schizophrenic patients exhibited an opposing pattern with no differences in the right hemisphere but a reduction in the left. This finding mirrors the finding of reduced grey matter volume in the left dorsolateral prefrontal cortex (Gilbert *et al.*, 2001) although this correlation, to the author's knowledge, has not been demonstrated in a unified study.

The mediodorsal thalamic nucleus is activated in tasks involving memory and attention (see Hazlett *et al.* 2004) and is reciprocally connected with the prefrontal cortex. These cortical regions play a vital role in working and episodic memory (Andrews *et al.*, 2006) and reductions in the magnitude of the correlations between the [^{18}F]fluorodeoxyglucose PET signal in the mediodorsal thalamic nucleus and the prefrontal cortex have been reported (Mitelman *et al.*, 2005). Human schizophrenics, when compared with controls, exhibit a reduction in the task related activation of the mediodorsal thalamic nucleus (Andrews *et al.*, 2006).

Anterior thalamic nucleus: Human schizophrenics, when compared with controls, exhibit a reduction in the task related activation in the anterior thalamic nucleus (Andrews *et al.*, 2006) although no reduction in the volume of this nucleus has been reported in post-mortem studies (Byne *et al.*, 2002; Young *et al.*, 2000).

Pulvinar nuclei: The pulvinar is the largest thalamic nucleus in humans (Byne *et al.*, 2007) accounting for almost 25% of the total thalamic volume (Romanski *et al.*, 1997). It provides a considerably smaller source of thalamic input to the prefrontal cortex and is also reciprocally connected with the parieto-occiptal cortex (Romanski *et al.*, 1997) and the entorhinal cortex (see Coscia *et al.* 2009). The central/lateral divisions project to the dorsolateral and orbital frontal cortices whilst the dorsomedial and medial prefrontal cortex receive input from the more caudal/medial aspects of the pulvinar nuclei (Romanski *et al.*, 1997).

Post-mortem studies have shown reductions in the volume of the pulvinar (Byne *et al.*, 2002; Danos *et al.*, 2003; Kemether *et al.*, 2003) through significant reduction in the number of cells within it localised specifically to the medial division (Byne *et al.*, 2007). However no reduction in the task related activation during a working memory task (Andrews *et al.*, 2006) nor any reduction in glucose metabolism have been reported (Hazlett *et al.*, 2004).

Centromedian thalamic nucleus: The centromedian thalamic nucleus projects to areas of the motor cortex and the striatum. When compared with healthy controls it has been shown that schizophrenics have reduced glucose metabolism in this nucleus (Hazlett *et al.*, 2004).

Ventral lateral posterior nucleus: The ventral lateral posterior nucleus is the major thalamic recipient of cerebellar afferents and projects to various areas of the motor cortex (see Danos *et al.* 2002). Schizophrenics show a reduction in volume and a reduction in total cell number in the ventral lateral posterior nucleus (Danos *et al.*, 2002).

1.1.2.3 Hippocampus

The hippocampus is a structure of the medial temporal lobe and is involved in short term and working memory (Razi *et al.*, 1999) and it is thought that abnormalities in this structure may specifically underpin the thought disorder associated with schizophrenia (see Andreasen *et al.* (1994). The hippocampus, amongst others, projects to the prefrontal cortex and the thalamus via the fornix.

The hippocampus in schizophrenics shows a reduced volume in comparison with healthy controls (Gur *et al.*, 2000; Nelson *et al.*, 1998; Wright *et al.*, 2000) although Csernansky *et al.* (2002) suggests that this is more likely attributable to

a reduction in total cerebral volume. Schizophrenics do show a marked exaggeration of the asymmetry between the left and right hippocampus seen in controls (Csernansky *et al.*, 2002). The structural abnormality in this nucleus is not a crude volume reduction but more a deformity in the head of the hippocampus (Csernansky *et al.*, 2002). This is the area in which the CA1 neurons are found (see Csernansky *et al.* 2002) and, since these neurons project to the mediodorsal thalamic nucleus, suggests a disruption in the indirect projection between the hippocampus and the prefrontal cortex (see Csernansky *et al.* 2002)

Reductions in the volume of the left hand side of the parahippocampal gyrus and the hippocampus of female schizophrenics have been reported in chronic schizophrenics (Razi *et al.*, 1999). New-onset schizophrenics show no reduction in hippocampal volumes indicating a degenerative process secondary to the primary pathology (Razi *et al.*, 1999).

1.1.2.4 Striatum

Reductions in the volume of the caudate (Chua *et al.*, 2007) but not in the putamen of new-onset schizophrenics have been found (Keshavan *et al.*, 1998). The ventral striatum appears unaffected. However similar reductions in the volume of this structure are observed in patients with depression (see Keshavan *et al.* 1998) so may not be contributary in the primary pathology of schizophrenia.

1.1.2.5 White matter tracts

Andreasen *et al.* (1994) tentatively reported reduction in the volume of the white matter that "may implicate tracts connecting the thalamus and the prefrontal cortex". Imaging techniques have improved greatly over the last 15 years and continue to do so. Kito *et al.* (2009) has since convincingly demonstrated a reduction in the volume of the anterior thalamic peduncle - the connection between the mediodorsal thalamic nucleus and the prefrontal cortex (via the anterior limb of the internal capsule) - using DTI imaging techniques. White matter volume reductions are also reported in the internal capsule and in the corpus callosum (Chua *et al.*, 2007). Bilateral reductions in the fractional anisotropy (an indicator of white matter integrity) in the fornix - the major white matter tract connecting the hippocampus with other regions of the brain - have also been reported (Fitzsimmons *et al.*, 2009).

1.1.3 Summary

Time and time again imaging studies implicate abnormalities of structure in the thalamus, particularly the mediodorsal thalamic nucleus and the pulvinar; the frontal cortices, particularly the prefrontal cortex; the hippocampus, particularly the CA1 region which projects to the mediodorsal thalamic nucleus and the white matter tracts which link these regions. Whilst hippocampal deformations may be a consequence, rather than a cause, deformation of the thalamocortical system seems a robust finding in the primary pathology of schizophrenia. The anomalies in these systems are further evidenced through dysfunctional behaviours and electrophysiological disturbances. To describe the full spectrum of observables associated with schizophrenia is beyond the scope of this introduction. Discussion of further schizophrenia specific dysfunction, including behavioural and electrophysiological anomalies, is limited to the chapters pertaining specifically to these phenomena.

1.1.4 Treatment strategy

1.1.4.1 First generation antipsychotics

The first antipsychotic, chlorpromazine, developed as an antihistamine, was found to have effects against the positive symptoms of schizophrenia in the 1950s (Bear *et al.*, 2001). Chlorpromazine and haloperidol, along with a plethora of related antipsychotics act through the antagonism of the dopamine system, commonly at D_2 receptors, although they also have affinity for other receptors including $5HT_2$ receptors. In addition to the clinical benefit achieved through the mesocortical dopamine system these drugs act in the nigral-striatal dopamine pathways yielding numerous side effects including drug-induced Parkinsonism (see Bear *et al.* 2001).

1.1.4.2 Second generation antipsychotics

Modern antipsychotics - atypical neuroleptics - offer similar clinical outcomes as the typical neuroleptics but with fewer adverse side effects through diminished action in the striatum (see Bear *et al.* 2001). These include clozapine, risperidone and olanzapine.

1.1.4.3 Negative symptoms and cognitive dysfunction

As eluded to above it is the positive - psychotic - symptoms of schizophrenia that respond best to treatment. Negative symptoms and cognitive deficits responded poorly (or not at all) to conventional antipsychotic treatment (see Carpenter Jr & Gold 2002) and, although some studies suggest that atypical antipsychotics confer a cognitive benefit (see Carpenter Jr & Gold 2002; Green 2006), serious concerns have been voiced regarding bias in these studies (Carpenter Jr & Gold, 2002) and recent evidence from the CATIE (Clinical Antipsychotic Trials of Intervention Effectiveness) studies confirms that there are no clear differences in clinically efficacy between typical and atypical drugs (Lieberman *et al.*, 2005). There is no compelling evidence to support clinical benefit on cognitive dysfunction and it is these symptoms that contribute most to the long term morbidity, poor functional outcomes and reduced quality of life in patients (see Carpenter Jr & Gold 2002). Alternative approaches are urgently required for schizophrenia, particularly therapies that specifically target the negative symptoms and deficits in cognitive function. As such the National Institute of Mental Health (NIMH) have established initiatives including the Measurement and Treatment Research to Improve Cognition in Schizophrenia (MATRICS) and Treatment Units for Research on Neurocognition and Schizophrenia.

1.2 Deep brain stimulation (DBS)

Deep brain stimulation (DBS) is the electrical stimulation, via chronically implanted electrodes connected to a device similar to a cardiac pacemaker, of specific brain regions. Whilst the technology continues to improve, the fundamental components of a DBS system have remained relatively unchanged. Such a system typically consists of implantable 4-contact electrodes, extension leads which are tunnelled under the skin to a intraclavicularly implanted pulse generator. Stimulation parameters are programmed via an external radio frequency transmitter (Coffey, 2008).

Current advances in research into DBS for neuropsychiatric disorders stems largely from the pioneering work investigating the efficacy of DBS of the subthalamic nucleus and globus pallidum in the treatment of Parkinson's disease (Limousin *et al.*, 1998; Krack *et al.*, 1998). DBS is accepted as a standard alternative treatment, for patients refractory to conventional treatments, in a variety of movement disorders including; Parkinson's disease, Essential Tremor, dystonia and cerebellar outflow tremor and in 2007 it was estimated that over 35 000 patients had undergone surgery for the implantation of DBS electrodes (Hardesty & Sackheim, 2007).

Trials are underway in an increasing number of psychiatric and other neurological disorders including; depression (Mayberg *et al.*, 2005; Schlaepfer *et al.*, 2008), obsessive-compulsive disorder (OCD) (Abelson *et al.*, 2005; Greenberg *et al.*, 2006), Tourette's syndrome (Kuhn *et al.*, 2007; Ackermans *et al.*, 2008; Visser-Vandewalle *et al.*, 2003; Diederich *et al.*, 2005; Welter *et al.*, 2008), epilepsy (Boon *et al.*, 2007; Chkhenkeli *et al.*, 2004; Dinner *et al.*, 2002) and minimally conscious states (Schiff *et al.*, 2007). The increasing application of DBS stands as a testament to the effectiveness of this treatment strategy yet despite this the mechanism by which DBS effects its therapeutic benefit remains unclear.

The experience from the clinic, particularly from the early work of Benabid (see McIntyre *et al.* 2004), demonstrated effects through DBS analogous to those achieved via surgical lesioning. This observation lead quickly to the reasonable hypothesis that high frequency stimulation yielded a "functional lesion" by inhibiting the activity of the stimulated nucleus. As such DBS techniques have largely replaced ablative procedures for Parkinson's disease. By analogy the application of DBS has been extended to other neurological disorders with histories of successful treatment via surgical lesioning. However the clinical experience

from these investigators indicates that the traditional lesioning hypothesis is inadequate to explain the full spectrum of effects nor does it account for many observations made in animal studies, a topic to which this introduction returns shortly (see section 1.3, page 17).

1.2.1 Treatment-resistant depression

Major depression is the most common of all psychiatric illnesses and, omitting diseases of old age is the leading cause of disability in both the UK (Murthy *et al.*, 2001; McCrone *et al.*, 2008) and the USA (Mayberg *et al.*, 2005). Nearly a fifth of those diagnosed with major depression fail to respond to conventional therapies (see Mayberg *et al.* 2005). The treatment of depression via DBS demonstrates some of the most innovative approaches to neurosurgery through the stimulation of cortical targets (Mayberg *et al.*, 2005) and the stimulation of targets to deliberately affect a network rather than "functional lesioning" of the stimulated target (Schlaepfer *et al.*, 2008).

Mayberg *et al.* (2005) identified, through functional imaging (PET), a cortical nucleus - the subgenual cingulate (Cg25) - that was hyperactive in major depression. By analogy with the Parkinson's experience the group sought to impose a functional lesion on this hyperactive region via DBS of the adjacent white matter tracts. Using typical Parkinson's parameters (F, 130Hz; PW, 60μs; A, 4V) they achieved a reduction in depression symptoms in 4/6 patients with 3 achieving remission or near remission of the disease.

Schlaepfer *et al.* (2008) stimulated the nucleus accumbens in three patients (F, 145Hz; PW, 90μs; A, 4V) obtaining a reduction in the severity of their depression symptoms. PET imaging demonstrated significant activation of the ventral striatum, dorsolateral and dorsomedial prefrontal cortex, the cingulate cortex and bilateral amygdala. Concurrent deactivation was seen in the ventrolateral and venteromedial prefrontal cortex, the dorsal caudate and thalamus.

1.2.2 Obsessive-compulsive disorder

Obsessive-compulsive disorder (OCD) is a common disorder afflicting 2-3% of the general population (Aouizerate *et al.*, 2004; Gabriëls *et al.*, 2003; Anderson & Ahmed, 2003; Rauch *et al.*, 2006). Characterised by repetitive intrusive thoughts and compulsive time consuming behaviours, OCD is also frequently comorbid with major depression and anxiety disorders (Gabriëls *et al.*, 2003). Almost a

third of patients fail to respond to standard pharmacological and cognitive behavioural therapies (Aouizerate *et al.*, 2004; Rauch *et al.*, 2006) so for these treatment refractory patients ablative neurosurgical techniques are often considered as a last resort (Abelson *et al.*, 2005). However advances in DBS look likely to supercede these irreversible lesioning methods with controllable, reversible and minimally invasive stimulation of brain regions including the anterior limb of the internal capsule and regions of the striatum (Nuttin *et al.*, 1999; Abelson *et al.*, 2005; Greenberg *et al.*, 2006; Aouizerate *et al.*, 2004; Gabriëls *et al.*, 2003; Anderson & Ahmed, 2003; Rauch *et al.*, 2006). Curiously Mallet *et al.* (2002) noted, whilst attempting to alleviate the symptoms of Parkinson's disease in a patient with coincidental OCD, that DBS of the subthalamic nucleus significantly reduced the severity of the OCD symptoms in this patient, a finding that has been corroborated by Fontaine *et al.* (2004).

1.2.3 Tourette's syndrome

Tourette's syndrome is a childhood onset, neurodevelopmental disorder characterised by vocal and/or motor tics (sudden, brief, intermittent involuntary sounds or movements) (Welter *et al.*, 2008; Temel & Visser-Vandewalle, 2004; Ackermans *et al.*, 2006). The literature is unclear as to the prevalence of Tourette's syndrome with reports indicating between 0.0004% and 0.15% (Temel & Visser-Vandewalle, 2004). Whilst symptoms may subside, a significant number of patients continue to suffer with the condition into adulthood (Larson, 2008) causing social disability (Welter *et al.*, 2008). Of these, many patients require chronic pharmacological treatment with some failing to respond or developing intolerable side effects (Temel & Visser-Vandewalle, 2004; Ackermans *et al.*, 2006; Visser-Vandewalle *et al.*, 2003). Those refractory to pharmacological intervention have received ablative surgical treatments; typically thalamic lesions, although interventions as severe as prefrontal lobotomy have been reported (Temel & Visser-Vandewalle, 2004). More recently DBS, first introduced for Tourette's syndrome in 1999 (Ackermans *et al.*, 2008) has emerged as a safer, reversible and controllable alternative for irreversible ablative neurosurgey with thalamic (centromedian thalamic nucleus) and pallidal (globus pallidum) targets proving effective (Welter *et al.*, 2008; Houeto *et al.*, 2005; Ackermans *et al.*, 2006; Bajwa *et al.*, 2007; Diederich *et al.*, 2005; Visser-Vandewalle *et al.*, 2003; Kuhn *et al.*, 2007).

1.2.4 Epilepsy

Epilepsy, characterised by recurrent seizures caused by outbursts of excessive brain activity, is the most common brain disorder (Murthy *et al.*, 2001). In excess of 30% of patients are refractory to conventional therapies suffering uncontrolled seizures or unacceptable side effects (Boon *et al.*, 2007). Of these 35% fail to respond to newly developed antiepileptic drugs or ablative surgery (Boon *et al.*, 2007). By analogy with DBS for movement disorders, epilepsy seems a likely candidate for successful intervention by DBS. However, in the majority of individuals with epilepsy it is difficult to identify an obvious brain abnormality, other than the electrical activity, (Murthy *et al.*, 2001) making it difficult to identify a target.

Boon *et al.* (2007) have demonstrated some success in treating medial temporal lobe (MTL) epilepsy with chronic HF DBS by identifying regions of the amygdala and hippocampus as the origin of the seizure activity. However only a proportion of patients suffer specifically with MTL epilepsy and the remainder would not benefit from this intervention.

Whilst Boon *et al.* (2007) have concentrated on suppressing the initiating structure others have focused on preventing seizure propagation reaching the cortex by stimulating the thalamus. However, as one might expect, with a poorly defined originating nucleus it is difficult to identify a specific thalamic relay for stimulation. The centromedian thalamic nucleus and anterior thalamic nucleus have both received some attention with promising results (Zumsteg *et al.* 2006 and for review see Chkhenkeli *et al.* 2004; Halpern *et al.* 2008; Theodore & Fisher 2004).

Successful interventions have also been reported through DBS of the subthalamic nucleus (Handforth *et al.*, 2006; Kerrigan *et al.*, 2004; Vesper *et al.*, 2007), the head of the caudate nucleus, the cerebellum, the hippocampus and stimulation of the vagus nerve (for review see Halpern *et al.* (2008); Chkhenkeli *et al.* (2004); Theodore & Fisher (2004)).

1.2.5 Minimally conscious states

Schiff *et al.* (2007), to the author's knowledge, are the only group other than Schlaepfer *et al.* (2008) that have applied DBS clinically to affect activation of efferent targets rather than suppression of the stimulated target. Bilateral stimulation of the anterior thalamic nuclei and the adjacent paralaminar regions of

the thalamic association nuclei (F, 100Hz; PW, - ;[†] A, 4V) yielded improvements in arousal level, motor control and behavioural persistence in a patient that had been in a minimally conscious state for 6 years. Of particular interest is their assertion that these improvements were likely due to activation of frontal regions via stimulation of central thalamic nuclei.

1.2.6 Summary

Whilst it is the aim of this author, and of the authors who's work is discussed above, to encourage the reader that DBS is a good treatment strategy one should not consider it a "silver bullet". Great care should be taken when considering the ramifications of these studies. Many are case reports with a small number of participants. In those studies with more than one subject it is important to note that no study shows beneficial effects in all subjects. And, in those subjects where effects are reported the effects are rarely complete. DBS is not a cure. If anything the DBS literature further consolidates the complexity of neurological disease. The very fact that some patients respond to conventional pharmacological and/or behavioural therapies and others do not is a testament to the heterogeneity of these disorders. Epilepsy is particularly challenging in that it lacks the identification of a clearly dysfunctional nucleus or system. Of those who are refractory to pharmacological intervention only a proportion of those respond to DBS. Whilst a single root cause may yet be identified the difference in response indicates great subtlety in the final pathology that underpins the final presentation of the psychiatric disease. To better predict who may benefit from DBS requires a considerable effort to elucidate the mechanisms by which DBS produces its therapeutic benefit. To this end an increasing number of investigators have turned to animal models to explore DBS and the following section explores this literature and its findings.

[†]- indicates that the pulse width is not given in the publication

1.3 DBS - Mechanism of action

Deep brain stimulation (DBS) has greatly improved the treatment of movement disorders such as Parkinson's disease, essential tremor and dystonia. As evidenced in the clinical literature there is a commonly held belief that DBS effects its therapeutic benefit by creating a "functional lesion" in the stimulated target. This hypothesis is drawn largely from the clinically analogous outcomes in ablative surgical procedures, such as a lesions of the thalamus (ventralis intermedius thalamic nucleus) for tremor (see Wichmann & DeLong 2006) or lesions of the subthalamic nucleus or globus pallidum for the cardinal motor symptoms of Parkinson's disease, and chronic high frequency electrical stimulation of the same territories.

This "lesioning hypothesis" has lead to the extension of DBS techniques to psychiatric conditions with histories of successful treatment by neurosurgical lesions, including obsessive-compulsive disorder and Tourette's syndrome. The success of these experimental procedures has further fueled the "lesion hypothesis" but its prevalence throughout the clinical literature is misleading and one should consider the context in which it arises. Since its initial inception DBS has predominantly been applied in patients in whom it would be expected that an ablative procedure would yield a positive outcome. Any positive outcome has then been attributed to a "functional lesion" without recourse to more thorough scientific examination.

However, as the academic literature expands it is becoming increasingly apparent that the conventional "lesioning hypothesis" is insufficient to explain the full spectrum of effects observed in pre-clinical studies, particularly the modulation of nuclei in the stimulated network. The challenge is to then explain the comparable lesioning effects of DBS seen in the clinic given the knowledge garnered in the laboratory. Furthermore this expanding body of pre-clinical literature indicates excitatory effects in the stimulated network. How then are these to be explained and may they be of clinical benefit in disorders that are typically unresponsive to ablative intervention?

There is increasingly compelling evidence to suggest that, rather than inhibition of the stimulated region, DBS actually leads to excitation as evidenced by increased output from the stimulated region. This dichotomy of neuronal excitation or inhibition is the subject of frequent and thorough debate as evidenced by the wealth of published reviews (Vitek, 2002; Garcia *et al.*, 2005; Birdno & Grill, 2008) and it is to this dichotomy that the remainder of this section is dedicated.

1.3.1 Effects in the stimulated nucleus

Computational simulations predict the suppression of intrinsic activity in thalamocortical relay neurons by extracellular high frequency electrical stimulation (McIntyre *et al.*, 2003). If one accepts the extrapolation of this result to neurons in other nuclei then this prediction has been realised in neurons of the subthalamic nucleus *in vitro* (Beurrier *et al.*, 2001; Meissner *et al.*, 2005), in man (Filali *et al.*, 2004) and neurons of the globus pallidum (Dostrovsky *et al.*, 2000; Wu *et al.*, 2001) in man. Although Beurrier *et al.* (2001) argued in favour of an inhibitory effect through direct electrical stimulation of the soma, the majority of the literature asserts that the inhibition is mediated by neurotransmitter release from afferent axons synapsing onto the stimulated target (McIntyre *et al.*, 2003; Meissner *et al.*, 2005). This synaptic driven inhibition is well documented in studies targeting the globus pallidum which receives a large number of GABAergic afferents from the striatum (Dostrovsky *et al.*, 2000). However, whilst inhibition is still observed, it is less robust in studies targeting the subthalamic nucleus, possibly since this nucleus receives a proportionally higher number of glutamatergic afferents than the globus pallidum (Filali *et al.*, 2004).

Electrophysiological studies are often confounded by the presence of stimulation artifacts. To negate them investigators often resort to exploring the epoch immediately after the cessation of stimulation and infer the activity of cells immediately prior (Benazzouz *et al.*, 1995; Wu *et al.*, 2001), leading some investigators to question the validity of these observations when considering the effects during stimulation (Bar-Gad *et al.*, 2004). However it has been shown that sustained HFS of subthalamic nucleus neurons *in vitro* surpresses subthalamic nucleus neurons during stimulation verifying the same conclusions made in the post-stimulation period (Magariños-Ascone *et al.*, 2002). Thus the majority of the literature agrees that, whether an inference from the post-stimulation period or an observation during stimulation, that DBS yields inhibition of the stimulated nucleus.

The results of these studies provide substantial support for the "lesion hypothesis" with significant agreement between *in vitro* and *in vivo* studies, and *in silico* predictions. Whilst there may still be some debate as to the nature of the inhibition, be it direct or mediated by the activation of inhibitory afferents, the evidence in favour of stimulation induced reduced neuronal output is compelling. However, there is equally compelling evidence inferring precisely the opposite. DBS, rather than inhibiting the stimulated structure, increases neuronal output suggesting activation of the stimulated structure.

1.3.2 Effects in the stimulated network

Studies in the subthalamic nucleus have shown major modifications in the firing rates of its major efferent targets (substantia nigra - reticular part, entopeduncular nucleus, globus pallidum) (Benazzouz *et al.*, 1995). The subthalamic nucleus projects to these nuclei via excitatory glutamatergic fibres (see Benazzouz *et al.* 1995). Superficially activation of the globus pallidum is easily understood given the direct projection from the subthalamic nucleus but one may also expect to see excitation of the entopeduncular nucleus and the substantia nigra - reticular part. Indeed the same study reports excitation of the substantia nigra - reticular part by single stimuli but inhibition through repeated stimuli. It is reasonable to posit that the single stimulus increases activity in the substantia nigra - reticular part and the globus pallidum through direct glutamatergic excitation. Repeated stimuli continue to release glutamate in both efferent targets but with the resulting excitation of the globus pallidum causing increased GABAergic transmission in the substantia nigra - reticular part. This inhibition then dominates in the substantia nigra - reticular part yielding inhibition in response to repeated stimulation. The lack of inhibition in response to a single stimulus may be explained through the delayed arrival of the GABA release given its generation through an indirect pathway.

The electrophysiological evidence indicating excitation/inhibition of the stimulated network are further supported by evidence garnered from micro-dialysis studies. HFS of the subthalamic nucleus yields sustained increases in glutamate levels *in vivo* in both the globus pallidum and the substantia nigra - reticular part with a concurrent increase in GABA in the substantia nigra - reticular part (Windels *et al.*, 2000, 2003). Increases were seen to be frequency dependent with an optimum release at 130Hz (Windels *et al.*, 2003). Interestingly glutamate increases were seen only in the hemisphere ipsilateral to stimulation in the globus pallidum. Glutamate increases were seen both ipsilateral and contralateral to stimulation in the substantia nigra - reticular part but with only ipsilateral increases in GABA. In a later study Windels *et al.* (2005) demonstrated the need for an intact globus pallidum to mediate the increase in substantia nigra - reticular part GABA indicating the importance of considering effects in the extended network rather than merely in the stimulated nucleus and its immediately efferent targets.

1.3.3 Somatic inhibition and axonal activation are concurrent

The evidence indicates that DBS is both inhibitory and excitatory. The question then becomes: "are these contradictory data mutually exclusive and, if not, how may they be reconciled?". The most parsimonious explanation comes from the observation that electrical stimulation of neuronal tissue preferentially activates axons rather than the soma (Nowak & Bullier, 1998a,b; Ranck, 1975). The observations of "functional lesions" can be explained by increased GABA release in the stimulated targets due to the large number of GABAergic afferents in structures such as the globus pallidum internus and subthalamic nucleus. This notion is largely supported in the DBS literature with Anderson *et al.* (2004) concluding that DBS effects are "primarily of synaptic origin" and similarly (Dostrovsky *et al.*, 2000) suggest that DBS "preferentially excites the axon terminals". Preferential axonal activation also explains the observations of increased neuronal output from stimulated nuclei. This output however, in no way reflects the activity in the soma and is driven purely by the extracellular stimulation. This inhibition of the soma with activation of the axon removes the processing power of the stimulated nucleus creating a "functional deafferentation" (Anderson *et al.*, 2004) whereby the afferent input to the stimulated nucleus no longer influences the nucleus' output.

1.3.3.1 Functional deafferentation: a working hypothesis

This working hypothesis is sufficient to reconcile the observations of "functional lesions" from the clinic and the evidence of increased efferent output from the laboratory and is popularly held in numerous reviews (Vitek, 2002; Garcia *et al.*, 2005; Birdno & Grill, 2008). It is this hypothesis of DBS action that shall form the basis for determining targets for stimulation in this thesis.

However it is important to note that this is merely one of several hypotheses by which DBS affects its therapeutic benefit. There is evidence to suggest that antidromic activation of regions projecting to the stimulated nucleus may also play an important role in mediating the effects of DBS (McCracken & Grace, 2007, 2009). Furthermore there is increasing evidence to suggest that the effects may depend not only on "conventional" parameters such as frequency, pulse width and voltage/current amplitude but also on the temporal patterning of the pulse delivery (Quinkert *et al.*, 2010; Cota *et al.*, 2009). As if the possible modes of action were not daunting enough there is still all too little evidence on the effects

of chronic (as opposed to acute) stimulation. Whilst evidence may be scant it is clear from clinical OCD and dystonia trials that the effects of DBS may take months to manifest indicating a role for long term plastic processes.

Clearly there is still much to be done in determining all of the effects that high frequency stimulation may have. At the time of writing it seems plausible that these effects may, in the very least, include; activation of synaptic terminals in the stimulated region, antidromic activation of neurons in the upstream regions, orthodromic activation of neurons in the downstream targets and activation of inhibitory interneurons in the all three of these regions (see figure 1.1). All these possible forms of activation are likely to depend on the frequency, pulse width and amplitude of the stimulation, the pattern by which the stimulation is delivered and the length of time for which the stimulation is delivered.

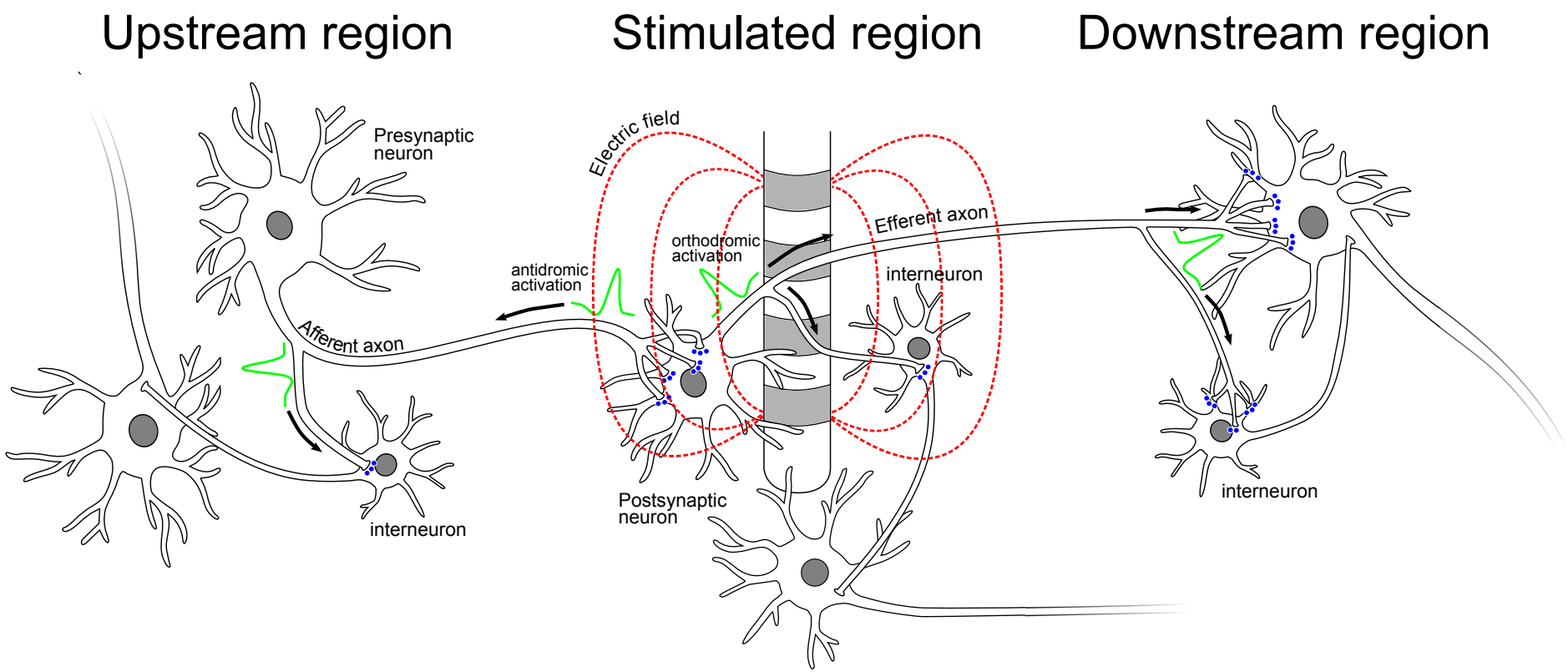

Figure 1.1: Functional deafferentation. DBS preferentially excites the axons leading to increased synaptic transmission in the synaptic terminals of the axons that afferent to the stimulated nucleus and excitation of the axon hillock and initial segment yielding increased synaptic transmission in the efferent synaptic terminals. Stimulation of the afferent axons also leads to antidromic activation of neurons in the upstream region, particularly interneurons via axon collaterals. It is likely that DBS also activates interneurons in the stimulated region, either through direct excitation or through activation of local recurrent collaterals. Activation of the efferent axons in the stimulated region may lead to excitation/inhibition of both the principal cells and interneurons in the downstream region. Not to scale.

1.4 Neuroanatomy

The pathology of schizophrenia indicates dysfunction, not of a single nucleus, but rather a widespread disruption of a large network. Whilst this pattern of anomalies and aberrant activity may have a single perpetrator it has thus far been impossible to identify such a singular locus. To best consider the effects of potential DBS in this schizophrenia it is vital to understand the underlying anatomy. A description follows herein.

1.4.1 Overview

What follows is a description of the cortico-basal-ganglia-thalamo-cortical anatomy specific to the rat since this animal, and the associated models, will be the platform from which the hypotheses of this thesis are tested. There is no inclusion of the pulvinar nuclei which are unique to primates (Romanski *et al.*, 1997). These nuclei, as discussed above, contribute to the pathology of schizophrenia and investigations concerning them are beyond the scope of rodent models. This said the notion of a rodent prefrontal cortex has previously been the subject of debate (see Uylings *et al.* 2003; Brown & Bowman 2002) and it may transpire that a functional analogue of the pulvinar will be demonstrated in the rat. It is now widely accepted that rodents *do* have a prefrontal cortex.

Widespread disruption is reported in schizophrenia with perhaps the most robust data implicating significant anomalies in the thalamo-cortical system. As a gross generalisation the cortex receives input from the thalamus which relays input from a myriad of regions in the basal ganglia and cerebellum. The cortex reciprocates its thalamic input whilst projecting back to the basal ganglia via the striatal-pallidal complex.

1.4.2 Thalamo-cortical architecture

The predominant hypothesis describing cortico-basal-ganglia-thalamo-cortical architecture is that different "affector" circuits are organised in parallel with little or no overlap between circuits processing distinct functions. Five cortico-basal-ganglia-thalamo-cortical circuits have been described in primates affecting motor, oculomotor, associative and limbic functions (Temel *et al.*, 2005). Uylings *et al.* (2003) describes four similar circuits in the rat, although Temel *et al.* (2005) and Nakano (2000) describe only three such loops.

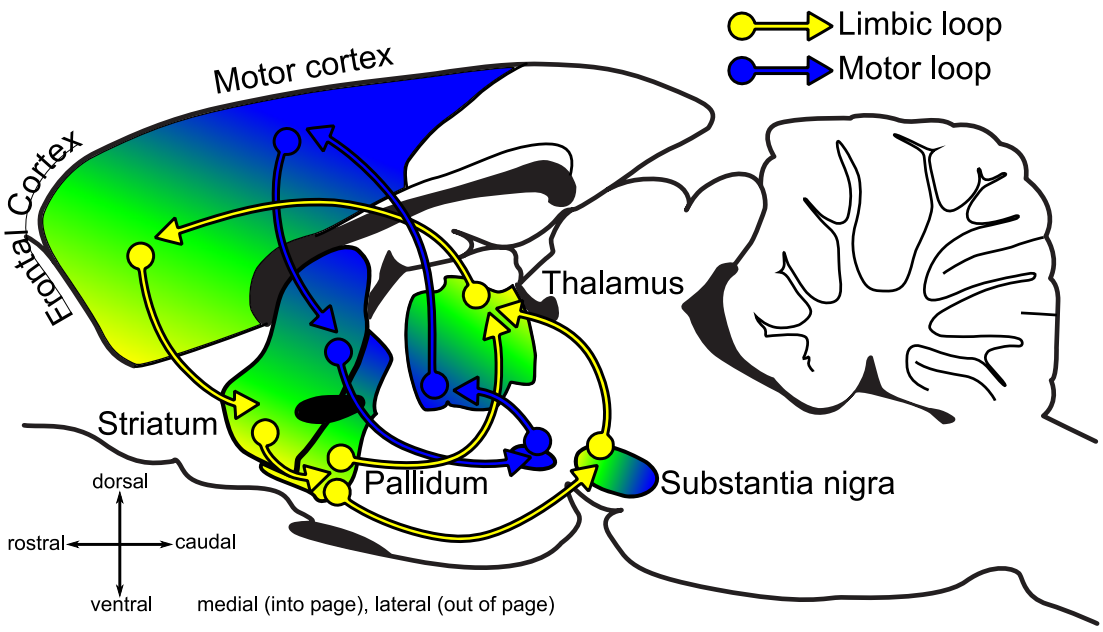

Figure 1.2: Generalised cortico-basal-ganglia-thalamo-cortical architecture. For clarity two of the four loops described by Uylings *et al.* (2003) are depicted. In general the more dorsal-caudal cortices project to more dorsal regions of the striatum before returning to their origin via the globus pallidum and the ventral anterior and ventrolateral regions of the thalamus. The more rostral-ventral regions of the cortex project to the ventral striatum, returning to their origin via the ventral pallidum and the mediodorsal nuclei of the thalamus. Adapted from Uylings *et al.* 2003

These circuits are topographically organised with anatomically and functionally distinct areas of the cortex projecting to specific striatal and thalamic nuclei and subsequently back to themselves. Uylings *et al.* (2003) describes a "motor loop", a "dorsal shoulder prefrontal loop", a "medial prefrontal/anterior cingulate loop" and a "lateral prefrontal/agranular insular loop". These re-entrant circuits originate and return to the dorsolateral, dorsomedial, medial and ventrolateral areas of the frontal cortex via topographically organised pathways through the striatum, pallidum and thalamus. Of specific interest in research involving rodent models of schizophrenia is the loop rising in the medial prefrontal cortex - the rodent analogue of the primate dorsolateral prefrontal cortex. The "medial prefrontal/anterior cingulate loop" has been called the "limbic loop" by others (Nakano, 2000) and the principle components are decribed below.

1.4.3 The limbic loop

The limbic loop originates in the medial prefrontal cortex which projects to the ventral striatum (see figure 1.2, page 24). The ventral striatum directs its output to both the ventral pallidum and dorsomedial substantia nigra - reticular

part. The loop returns to the medial prefrontal cortex predominantly via the mediodorsal thalamic nucleus but also via the medial portion of the ventromedial thalamic nucleus. The mediodorsal thalamic nucleus receives its input predominantly from the ventral pallidum although a small contribution comes from the substantia nigra - reticular part. The ventromedial thalamic nucleus draws its input solely from the substantia nigra - reticular part (Uylings *et al.*, 2003).

1.4.4 Medial prefrontal cortex

The medial prefrontal cortex is the major cortical node of the limbic loop. It comprises the regions of frontal cortex immediately adjacent to the midline; the secondary motor cortex, cingulate cortex - area 2, cingulate cortex - area 1, prelimbic cortex and the infralimbic cortex (Vertes, 2004; Hoover & Vertes, 2007) (see figure 1.3, page 27).

Afferents: In general the more dorsal regions, secondary motor cortex, cingulate cortex - area 2 and cingulate cortex - area 1, receives widespread input from the whole cortex and associated thalamic nuclei. The more ventral regions, the prelimbic cortex and infralimbic cortex, receive comparatively smaller input than do the dorsal regions. Cortical inputs include the medial orbitofrontal, agranular insular and entorhinal cortices. Non-cortical input arises in the hippocampus, the midline thalamic nuclei and the amygdala (Hoover & Vertes, 2007). Dopaminergic input comes from the ventral tegmental area.

Efferents: Of specific interest are the connections with the prefrontal cortex, temporal lobe, thalamus and basal ganglia. Within the frontal cortices the infralimbic cortex distributes to the cingulate cortex, medial orbital cortex, prelimbic cortex and back to itself. The infralimbic cortex projects to the medial, basomedial and central nuclei of the amygdala in the temporal lobe. Thalamo-cortical projections are primarily to medial thalamic nuclei including the paratenial thalamic nucleus, paraventricular thalamic nucleus, mediodorsal thalamic nucleus, intermediodorsal thalamic nucleus, interanteromedial thalamic nucleus, centromedian thalamic nucleus and reuniens thalamic nucleus. The infralimbic cortex projects to only the medial shell of the nucleus accumbens and specifically to the substantia nigra - compacta part (Vertes, 2004). The prelimbic cortex projects to cortical structures including, the secondary motor cortex, infralimbic cortex, cingulate cortex - area 2 and cingulate cortex - area 1, medial orbital cortex, agranular insular cortex and the entorhinal cortex. In the striatum projections

are directed to the medial caudate putamen and the shell and core of the nucleus accumbens. Thalamocortical projections are primarily to medial thalamic nuclei including the paratenial thalamic nucleus, paraventricular thalamic nucleus, mediodorsal thalamic nucleus, intermediodorsal thalamic nucleus, interanteromedial thalamic nucleus, centromedian thalamic nucleus and reuniens thalamic nucleus. The central and basolateral nuclei of the amygdala receive projections as do the ventral tegmental area and the substantia nigra - compacta part (Vertes, 2004).

1.4.5 Midline thalamic nuclei

The subdivisions of the midline thalamic nuclei project to the frontal cortices in topographic manner (see figure 1.3, page 27). Broadly speaking the more medial the thalamic nucleus then the the more medial the projection to the frontal cortices. Moreover axons originating in thalamic nuclei are seen to travel ipsilaterally, with the ascending projections being topographically distributed through the caudate-putamen - the more medial the thalamic nucleus the more medial the pathway through the caudate-putamen. Axons originating in the mediodorsal thalamic nucleus project heavily to the cingulate cortex - area 1, prelimbic cortex, lateral orbital cortex and ventral orbital cortex and to a lesser extent the infralimbic cortex, medial orbital cortex, cingulate cortex - area 2 and agranular insular cortex. Axons originating in the mediodorsal thalamic nucleus - lateral part project less heavily to the cingulate cortex - area 1 and to a greater extent to the primary motor cortex and secondary motor cortex. Axons originating in the centerolateral thalamic nucleus project heavily to the primary motor cortex and to a lesser extent to primary somatosensory cortex, secondary somatosensory cortex and secondary motor cortex (Wang & Shyu, 2004).

The mediodorsal thalamic nucleus projects to the dorsolateral prefrontal cortex and orbital cortical areas and, in conjunction with other midline thalamic nuclei to areas of the anterior cingulate cortex. These thalamo-cortical pathways are reciprocal in that the cortical area receiving a thalamic innervation projects back to the same thalamic nucleus. However the same is not true of cortico-thalamic pathways in that cortical areas may project to thalamic regions without there being a reciprocal connection. As such specific regions of the thalamus derive a greater and broader input from the cortex than that which is simply reciprocated from its cortical target (see Haber & McFarland 2001).

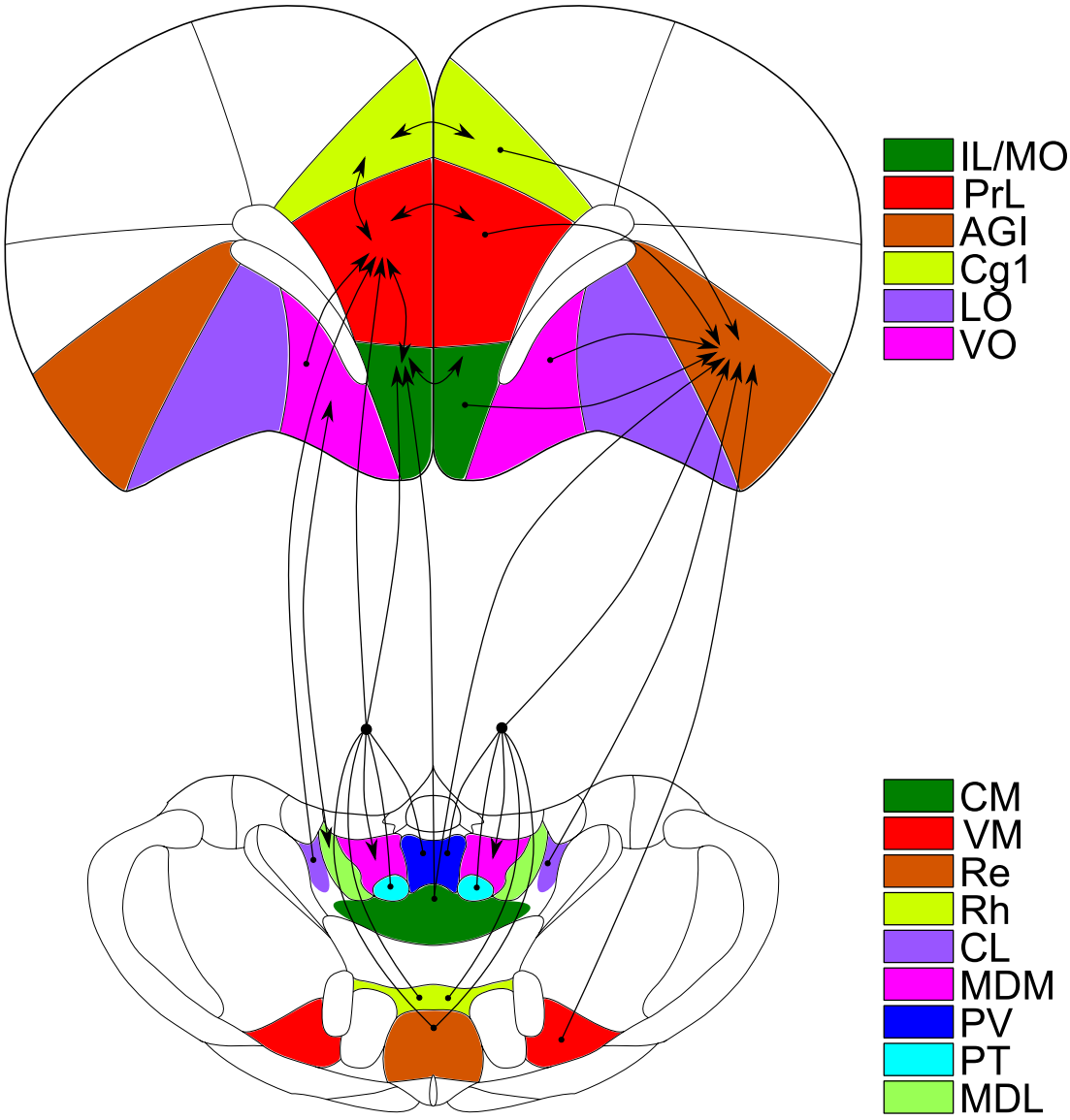

Figure 1.3: The thalamo-cortical, cortico-thalamic and cortico-cortical connections within the frontal cortices and the midline thalamic nuclei. Connections between identical regions across the midline indicate a projection back to the originating cortical region (ipsilateral) rather than a connection to the contralateral hemisphere. **Abbreviations:** IL, infralimbic cortex; MO, medial orbital cortex; PrL, prelimbic cortex; AGI, agranular insular cortex; Cg1, cingulate cortex - area 1; LO, lateral orbital cortex; VO, ventral orbital cortex; CM, centromedian thalamic nucleus; VM, ventromedial thalamic nucleus; Re, reuniens thalamic nucleus; Rh, rhomboid thalamic nucleus; CL, centerolateral thalamic nucleus; MDM, mediodorsal thalamic nucleus - medial part; PV, paraventricular thalamic nucleus; PT, paratenial thalamic nucleus; MDL, mediodorsal thalamic nucleus - lateral part.

Afferents: The primary inputs to the midline thalamic nuclei are the ventral pallidum and substantia nigra - reticular part. The projections from the ventral pallidum dominate in the mediodorsal thalamic nucleus whereas those from the substantia nigra - reticular part dominate in the ventromedial and intralaminar nuclei of the thalamus (Groenewegen *et al.*, 1999).

Efferents: The ventromedial thalamic nuclei and mediodorsal thalamic nucleus project to overlapping areas of prefrontal cortex (Groenewegen *et al.*, 1999). Topographically organised projections to the dorsal striatum have also been reported (Erro *et al.*, 2002).

1.4.6 The basal ganglia

The principle components of the basal ganglia are the striatum, the pallidum, the subthalamic nucleus and the substantia nigra; interconnected to form a complex network in the forebrain and midbrain tegmentum (Groenewegen *et al.*, 1999; Temel *et al.*, 2005).

Input: The input structure - the striatum - can be subdivided into two subterritories. The dorsal striatum, including the caudate and the putamen, is a component of the basal ganglia with connections to the motor cortex. The ventral striatum, comprising the shell and core areas of the nucleus accumbens (Heimer *et al.*, 1991; Kelley, 2004) is a component of the limbic system with connections to the limbic and frontal cortices (see figure 1.4, page 32).

Output: The output structures of the basal ganglia are considered to be the subdivisions of the pallidal complex and the substantia nigra - reticular part (Groenewegen *et al.*, 1999). The primary output of the basal ganglia, via specific thalamic relays, are to the prefrontal and premotor cortices (Groenewegen *et al.*, 1999). The dorsal pallidum, particularly the internal segment, is associated more with motor output and the ventral pallidum with limbic output.

1.4.7 Ventral striatum

The afferent and efferent connections of the accumbens shell and the accumbens core are anatomically and functionally distinct (Kelley, 2004) with the accumbens core seemingly more greatly involved in affecting motor control circuits and the accumbens shell involved in limbic functions.

1.4.7.1 Core of the nucleus accumbens

The accumbens core surrounds the anterior commisure (Kelley, 2004).

Afferents: The accumbens core recieves input from the dorsal subiculum of the hippocampus and the prelimbic cortex and dopaminergic input from the ventral tegmental area.

Efferents: The accumbens core projects to pallidal and ganglial structures including; the dorsolateral part of the ventral pallidum, the medial entopeduncular nucleus, the medial subthalamic nucleus, the globus pallidum, the pedunculopontine nucleus, the substantia nigra - reticular part and the substantia nigra - compacta part (Usud *et al.*, 1998; Nakano, 2000; Groenewegen *et al.*, 1999).

1.4.7.2 Shell of the nucleus accumbens

The shell of the nucleus accumbens forms the ventral and medial borders of the accumbens extending medially, ventrally and laterally around the core of the nucleus accumbens (Zaborszky *et al.*, 1985).

Afferents: The entirety of the accumbens shell recieves dense projections from the hippocampus (Zahm, 2000; Usud *et al.*, 1998) whilst projections from the amygdala are concentrated in the medial accumbens shell (Ghitza *et al.*, 2003). The accumbens shell receives further afferents from the ventral subiculum of the hippocampus, infralimbic cortex, medial prefrontal cortex, the anterior cingulate and piriform cortices (Haber *et al.*, 1995; Friedman *et al.*, 2002). The accumbens shell also receives input from areas of the hypothalamus and brainstem including; the lateral hypothalamus and the nucleus of the solitary tract (Kelley, 2004). The accumbens shell receives dopaminergic input from the ventral tegmental area.

Efferents: The accumbens shell projects to subcortical limbic structures including the ventromedial part of the ventral pallidum (Groenewegen *et al.*, 1999), hypothalamic regions including the lateral hypothalamus (Kelley, 2004) and paraventricular hypothalamic nucleus, the lateral preoptic area, the ventral tegmental area and back to itself (Chang & Kitai, 1985; Zahm, 2000; Meredith *et al.*, 1993). A small direct projection from the medial portion of the accumbens shell to the mediodorsal thalamic nucleus has also been reported (Otake & Nakamura, 2000).

1.4.8 Ventral tegemental area

The mesocortical limbic dopamine system rises in the ventral tegmental area (Bear *et al.*, 2001). The ventral tegmental area contains the A10 dopaminergic neurons (Del-Fava *et al.*, 2007).

Afferents: The ventral tegmental area receives GABAergic input from the accumbens shell and glutamatergic input for the prelimbic cortex (Vertes, 2004).

Efferents: The ventral tegmental area projects to the ventral pallidum in a topographic manner. The more medial ventral tegmental area, including the nucleus interfasicularis and the nucleus linearis caudalis project almost exclusively to the ventromedial ventral pallidum. The more lateral nuclei, including the nucleus parabrachialis pigmentosus and the nucleus paranigralis project to the ventromedial and the dorsolateral ventral pallidum. Of the order of 50% projections from the ventral tegmental area to the ventral pallidum are estimated to be dopaminergic (Klitenick *et al.*, 1992).

The ventral tegmental area projects back to the accumbens shell and accumbens core via dopaminergic projections. The ventral tegmental area also has a direct dopaminergic input to areas of the prefrontal cortex and reciprocal projections back to the ventral pallidum have been reported (Klitenick *et al.*, 1992). Projections from the rostral linear region of the ventral tegmental area to the mediodorsal thalamic nucleus and the lateral habenula have been described. This region is reported to contain a lower density of dopamine neurons and is putatively considered to be GABAergic (Del-Fava *et al.*, 2007).

1.4.9 Ventral pallidum

The ventral pallidum is a subcommissural region considered to be a rostroventral extension of the globus pallidum functioning as the major output nucleus of the cortico-striatal-pallidal circuits (Klitenick *et al.*, 1992; Maurice *et al.*, 1997). The ventral pallidum is not a homogeneous structure and can be further delineated into ventromedial and dorsolateral subterritories (Maurice *et al.*, 1997).

Afferents: The ventral pallidum receives topographically organised input from the ventral striatum such that the ventromedial portion receives its input from the accumbens shell and the dorsolateral portion recieves its input from the accumbens core (Klitenick *et al.*, 1992; Nakano, 2000; Maurice *et al.*, 1997). The

ventral pallidum also receives dopaminergic input from the ventral tegmental area (Klitenick *et al.*, 1992).

Efferents: The ventral pallidum projects to the mediodorsal thalamic nucleus, amygdala, hypothalamus, ventral tegmental area, subthalamic nucleus, substantia nigra - reticular part and reciprocally back to the nucleus accumbens via inhibitory GABAergic axons in a topographic manner (Klitenick *et al.*, 1992; Nakano, 2000; Maurice *et al.*, 1997; Wu *et al.*, 1996; Groenewegen *et al.*, 1999). Projections to the ventral tegmental area and mediodorsal thalamic nucleus arise predominantly in the ventromedial portion of the ventral pallidum - the accumbens shell innervated region - whereas projections to the subthalamic nucleus and substantia nigra - reticular part arise predominantly in the dorsolateral portion of the ventral pallidum - the accumbens core innervated region (Klitenick *et al.*, 1992; Maurice *et al.*, 1997). The ventral pallidum projects, rather prominently, to the habenular complex and rostral part of the reticular thalamic nucleus. A small projection from the ventral pallidum is directed to the medial part of the ventromedial thalamic nucleus and reuniens thalamic nucleus (Groenewegen *et al.*, 1999).

1.4.10 Hippocampus

The hippocampus is a component of the limbic system thought to be involved in memory formation and spatial navigation. It has been the subject of extensive research, so much so that it has been afforded its own journal (Hippocampus, ISSN 1050-9631) and discussion of its role here is limited.

Afferents: The reuniens thalamic nucleus is almost the only source of thalamic input to the hippocampus, providing excitatory input predominantly in the CA1 regions of Ammon's horn and the subiculum (Vertes *et al.*, 2007; Vertes, 2006).

Efferents: The hippocampus distributes heavily to the medial prefrontal cortex via glutamatergic projections. In rats projections arise predominantly in the temporal CA1 region and subiculum and terminate in the ventromedial prefrontal cortex (see Vertes *et al.* 2007; Vertes 2006).

1.4.11 Subthalamic nucleus

The rat subthalamic nucleus is a relatively small densely populated biconvex-shaped nucleus located between the dorsal region of the zona incerta and the

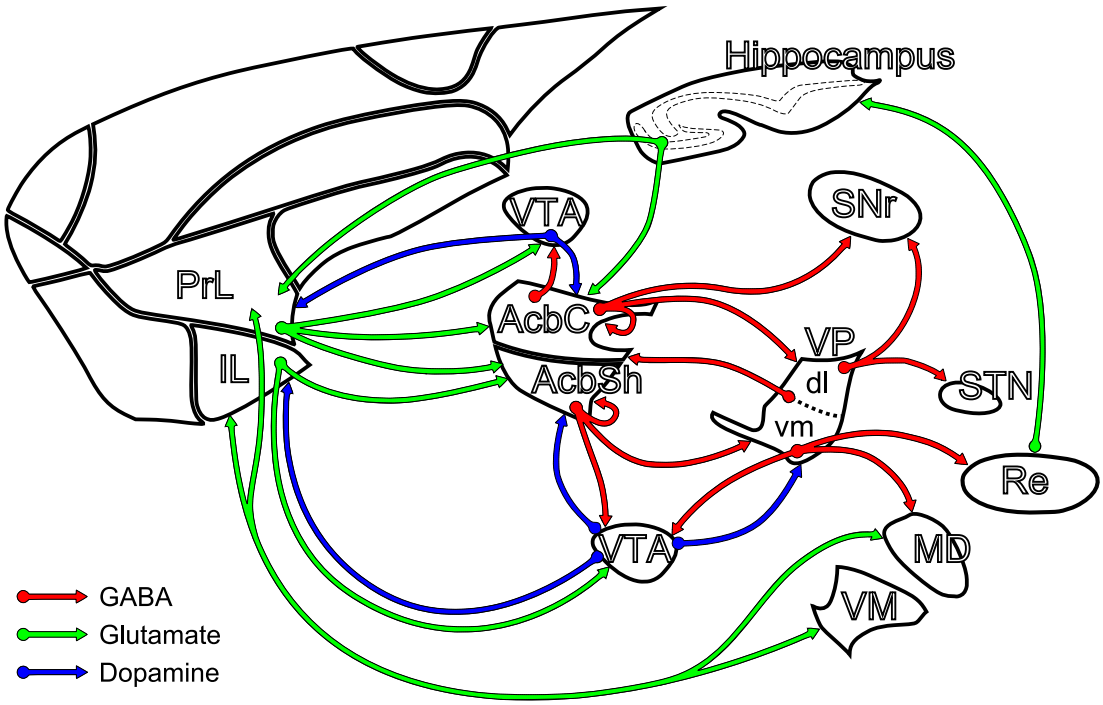

Figure 1.4: The cortico-basal-ganglia-thalamo-cortical system. The figure above is a simplification of the myriad of connections described in this section but shows the primary cortico-basal-ganglia-thalamo-cortical pathways through the medial prefrontal cortex . **Abbreviations:** PrL, prelimbic cortex; IL, infralimbic cortex; AcbC, accumbens core; AcbSh, accumbens shell; VP, ventral pallidum (dl, dorsolateral part, vm, ventromedial part); MD, mediodorsal thalamic nucleus; VM, ventromedial thalamic nucleus; VTA, ventral tegmental area; Re, reuniens thalamic nucleus; STN, subthalamic nucleus; SNr, substantia nigra - reticular part.

posterior nigral complex in the upper midbrain. It is surrounded by dense bundles of myelinated fibers such as the internal capsule and is the only glutamatergic nucleus in the basal ganglia. It can be further delineated into a medial part, associated more with limbic functions, and a dorsolateral part, associated more with sensorimotor functions (Temel *et al.*, 2005).

Afferents: The main inputs arise in regions of the cortex, entopeduncular nucleus, ventral pallidum (primarily connected with the medial subthalamic nucleus), parafasicular thalamic nucleus, centromedian thalamic nucleus, substantia nigra - compacta part, pedunculopontine nucleus and the dorsal raphe nucleus (see Temel *et al.* 2005).

Efferents: The subthalamic nucleus projections are predominantly directed to globus pallidum, substantia nigra - reticular part, substantia nigra - compacta part and the pedunculopontine nucleus (see Temel *et al.* 2005).

1.5 Summary, hypotheses & aims

The previous sections serve to introduce the major themes which motivated the work described in this thesis. Briefly,

1. Schizophrenia is a prevalent illness, the understanding and treatment of which remain incomplete.

2. Deep brain stimulation has been shown to be a potentially successful therapy in patients, with a range of neuropsychiatric conditions, who are otherwise refractory to more conventional treatments.

3. The pathology of schizophrenia implicates, amongst others, dysfunction of the thalamo-cortical system as a consistent anomaly in schizophrenia.

4. The current understanding of the mechanism by which DBS affects its therapeutic action is one of "functional deafferentation", whereby the processing power of a stimulated region is diminished and its output is driven by the stimulation.

Given the above it is suggested here that DBS may be a plausible intervention in the modulation of the aberrant thalamo-cortical circuitry in schizophrenia.

Whilst there is no target in schizophrenia implicated as a potential candidate for "functional lesioning", the literature lends support for the use of DBS as a tool to activate distal targets rather than inhibit dysfunctional regions. Cortical disruption, particularly diminished activity in the medial prefrontal cortex is consistently reported in schizophrenia. The OCD literature indicates improvements in tasks that recruit the prefrontal cortex due to DBS of striatal regions (Aouizerate *et al.*, 2004; Greenberg *et al.*, 2006). However the mechanism is still unclear. Antidromic activation of the orbital frontal cortices is a plausible explanation (McCracken & Grace, 2009) so too is an indirect mechanism through inhibition of the ventral pallidum yielding disinhibition of the mediodorsal thalamic nucleus. It is perhaps not unreasonable to hypothesise that a similar DBS paradigm may be of merit in tackling the cognitive dysfunction associated with schizophrenia. However the pathological evidence indicating a disruption in the thalamo-cortical network seems more compelling than the evidence implicating the striatum. Furthermore whilst DBS of the nucleus accumbens has been shown to activate the frontal cortices it also deactivated the thalamus (Schlaepfer *et al.*, 2008).

Evidence suggests that aberrant hippocampal activity may underlie some of the positive symptoms of schizophrenia (see Andreasen *et al.* (1994)). In keeping with this, aberrant hippocampal activity has been shown to underpin dopamine dysregulation *in vivo* (Lodge & Grace, 2007). These data strongly implicate the hippocampus in the pathology of the positive symptoms of schizophrenia. However alterations in hippocampal morphology may be a secondary effect rather than a primary cause (Razi *et al.*, 1999) in schizophrenia.

Thalamic disruption, particularly reduced glucose metabolism in the mediodorsal thalamic nucleus is a core pathophysiological deficit in schizophrenia (Hazlett *et al.*, 2004). DBS of the anterior thalamic nucleus leads to increased glucose metabolism in the stimulated region (Gao *et al.*, 2009) so it is logical to assert that DBS of the mediodorsal thalamic nucleus would similarly reverse this deficit associated with schizophrenia. Furthermore lesions of the prefrontal cortex have been shown to increase the rate of spontaneous firing in the mediodorsal thalamic nucleus whilst concurrently reducing the rate of spontaneous firing in the ventral pallidum (Lavin & Grace, 1997). The implication being that diminished activity in the prefrontal cortex yields compensatory changes in pallidal and thalamic regions which act to increase mediodorsal thalamic nucleus output.

Given the weight of evidence implicating the mediodorsal thalamic nucleus in the pathology of schizophrenia it is to this region that this thesis focuses its attention. The mediodorsal thalamic nucleus provides a significant glutamatergic input to prefrontal cortex, in addition to cortico-cortical connections. The working hypothesis by which DBS affects its action is by dual activation of synaptic afferents and axonal efferents (Anderson *et al.*, 2004; Vitek, 2002; Dostrovsky *et al.*, 2000). So, invoking this hypothesis one would expect that DBS of the mediodorsal thalamic nucleus would activate efferent axons generating action potentials which would be propagated to the distal target - the prefrontal cortex - leading to an increase in neurotransmitter release. The mediodorsal thalamic nucleus projects via glutamatergic axons so the influence in the prefrontal cortex may be excitatory although it is also reasonable to posit an inhibitory influence through feedforward inhibition. Activation of cortical structures via stimulation of thalamic nuclei has been evidenced in the treatment of minimally conscious states (Schiff *et al.*, 2007). It is interesting to consider the possible effects of DBS on the soma in the mediodorsal thalamic nucleus cells. The mediodorsal thalamic nucleus receives a significant GABAergic projection from the ventral pallidum. Activation of these synaptic inputs would yield inhibition in the mediodorsal

thalamic nucleus. The mediodorsal thalamic nucleus also receives reciprocal projections from the prefrontal cortex. These synaptic inputs are glutamatergic so activation of these would activate the soma, presumably contributing further to the axonal output. It is difficult to predict how DBS might affect the balance of excitation and inhibition in the mediodorsal thalamic nucleus itself. However it is suggested here that excitation of efferent axons alone will be sufficient to increase activity in the prefrontal cortex. Based on this the following is posited:

1.5.1 Parameter selection

The number of variables available when designing a stimulation protocol are significant. As discussed previously these most commonly include; **frequency**, **pulse width** and **amplitude**. It is well established that high frequency (>100Hz) stimulation provides the greatest clinical benefit whereas low frequencies (of the order of 10Hz) have at best no effect. This said there is modest interest in low frequency stimulation of the pedunculopontine tegmental nucleus (PPTg) for the gait anomalies associated with Parkinson's disease (Mazzone *et al.*, 2009). Common pulse widths lie in a range between 60 - 200μA with pulse widths at the lower end of this range becoming increasingly prevalent. Amplitude may refer to either current or voltage amplitude depending on the mode of stimulation. Constant voltage stimulation has long been the norm, limited as the clinicians have been by available technologies. Constant voltage stimulation suffers in that as the tissue impedance increases (as a consequence of stimulation) current delivery decreases. More recently constant current stimulators have become available in the clinic and look set to become the new standard. As such the work detailed herein will only be concerned with constant current stimulation. There is scant published clinical work describing constant current stimulation. As such it is difficult to define a standard range of clinical effective currents. Typical currents applied in preclinical research range over widely, from around 10μA up to the milliamp range. Whilst there is little agreement on a "standard" current it is most common to see currents of the order of 100-200μA.

There are myriad further variables - all of which are likely to be of interest in the application of DBS. These include electrode separation, charge balancing, temporal patterning (including cycling), duration and whether to use unilateral or bilateral stimulation. Electrode separation pertains to the distance between the active contact and ground and influences the volume of tissue activated. All clinical DBS is charge balanced such that the net delivery of current over a single

cycle is zero. This is achieved using a biphasic stimulation pattern. However the majority of preclinical literature deals with simpler monophasic stimulation. Whilst there is some indication that temporal patterning of stimulation may be an important factor (Cota *et al.*, 2009) it has yet to be applied clinically where constant duty cycle stimulation is still standard. Clinical opinion leans towards minimising the invasiveness of the procedure. As such it is common to apply DBS unilaterally in the first instance with recourse to bilateral stimulation required as necessary. As such the parameters explored in this thesis will be:

Mode: Constant current, constant duty cycle, monophasic, unilateral

Frequency: ≈130Hz

Pulse width: ≈100μs

Amplitude: ≈100μA

1.5.2 Hypotheses

Electrical stimulation of the mediodorsal thalamic nucleus using parameters demonstrated to be clinically effective in a variety of disorders will:

1. Increase activation of the efferent targets of the prefrontal cortex.
2. Reverse schizophrenia like EEG and behavioural deficits in a PCP model that mirrors the prefrontal cortex dysfunction seen in schizophrenia.

1.5.3 Aims

It is the aim of this thesis;

1. To develop the necessary methodology to investigate DBS in freely moving conscious rats, particularly to develop techniques for the construction of deep brain electrodes and stimulation devices appropriate for this species.
2. To test the hypotheses by investigation of the consequences of DBS of the mediodorsal thalamic nucleus in both normal animals and in a PCP rat model of schizophrenia. This will be achieved using biomolecular, electrocorticographic and behavioural methods.

The details of this methodological development and of results of these investigations are detailed herein.

Chapter 2

General methods

2.1 Equipment design & fabrication

2.1.1 Deep brain electrodes

2.1.1.1 Electrode fabrication

Bipolar deep brain electrodes are fabricated by sticking pairs of ultra-fine (25μm diameter) Teflon™ insulated nickel-chromium (nichrome (The Scientific Wire Company)) to the outside of a supporting structure, providing the necessary mechanical strength to drive the electrode wires deep into the brain.

The supporting structure is made by inserting a 100μm insect pin (Watkins & Doncaster) into a 30mm long, gauge 30 stainless steel syringe needle (Coopers Needle Works Ltd.). A small amount of fine (low viscosity) superglue (Javis MFG. Co, Ltd.) is then applied to the join. The superglue is drawn into the join by capillary forces firmly attaching the insect pin to the needle. The length of the insect pin protruding from its supporting needle can be adjusted before gluing to best suit the application - the deeper the stimulation target the longer the exposed length of the insect pin.

Two 40mm lengths of nichrome wire are then cut with a scalpel against a glass block. The microwires are then glued to the outside of the supporting structure by quickly dragging the microwires and the support backwards through a drop of fine superglue. The microwires should be allowed to extend beyond the tip of the insect pin and subsequently cut back to the end of the insect pin with a scalpel against a glass block under a top illuminated 3-5× magnification dissection microscope. Care should be taken to not allow the wires to become glued to the 30G needle; they should only be glued to the protruding insect pin.

Two solder pads are then prepared by cutting a 4×4mm (approximately) square from a piece of double sided copper clad board (Farnell) with a piercing saw. The resulting small piece of board can then be held between heatshrink sheathed forceps (to prevent damage to the copper surfaces of the board) and split with a Stanley™ knife. The pads are then glued, back to back, on to the 30G needle, over the microwires, just below the join between the insect pin and the needle. This join is made with rapid setting araldite™ which withstands the temperatures generated in the subsequent soldering; the electrode will fall apart during soldering if this join is made with superglue.

The free ends of each microwire are then wrapped around one of the solder pads and fixed on either side of the pad with a drop of fine superglue. Care must be taken to insure that no glue runs onto the surface of the solder pads. Any excess microwire can be trimmed away at this stage with very sharp scissors. The Teflon™ insulation can then be removed from the microwire immediately above the solder pad by gently scraping it away with a scalpel under under a top illuminated 3-5× magnification dissection microscope. An electrical connection can then be made between the microwire and the solder pad by flooding the pad with low melting point lead-free silver solder (RS Components).

Two 30mm lengths of 0.25mm diameter kynar insulted wire (The Scientific Wire Company) are then cut, the ends stripped of their insulation and soldered to the pads making an electrical connection between the kynar wire and the electrode wires. The pads and connections are then sealed in an appropriately sized piece of heatshrink and any voids filled with superglue. The free ends of the kynar wires are then soldered to connectors cut from turned pin DIL sockets (RS Components) and insulated with heatshrink. The connectors are made by cutting pairs of adjacent pins from 8 pin DIL sockets with a piercing saw.

It should be noted that this method for fabricating bipolar stimulating electrodes yields an unsatisfactory variability in interelectrode separation. This should be addressed in future work.

2.1.1.2 Electrode testing & sterilisation

Electrodes are tested by lowering them into physiological saline to at least the depth that they would be implanted into the brain. A cathodal current is then driven through the electrode by applying a DC voltage of 3V between each electrode connector and a wire immersed in the saline at a distance from the electrode. Electrons form the exposed tip of the electrode combine with the H^+

ions in the electrolyte (saline) to form bubbles of H_2 which stream to the surface, indicating that the electrical connections made in the production of the electrode are satisfactory. Any breaches in the Teflon™ insulation will also cause the production of H_2 identifying any breaks in the insulation (Westby & Wang, 1997). Electrodes with breaks in the insulation would provide additional current delivery to structures outwith the intended target and these electrodes should be discarded. Electrodes are sterilised by briefly (5-10 seconds) submerging them in 70% ethanol.

2.1.2 Deep brain stimulation device design & fabrication

2.1.2.1 Pulse generator

DBS pulses were generated using a dual retriggerable monostable multivibrator (74HC123D (RS Components)). These so called "one-shots" generate an output pulse width that is independent of the pulse width of the triggering pulse. This output pulse width can be programmed by an external resistor-capacitor network (see figure 2.1(b)).

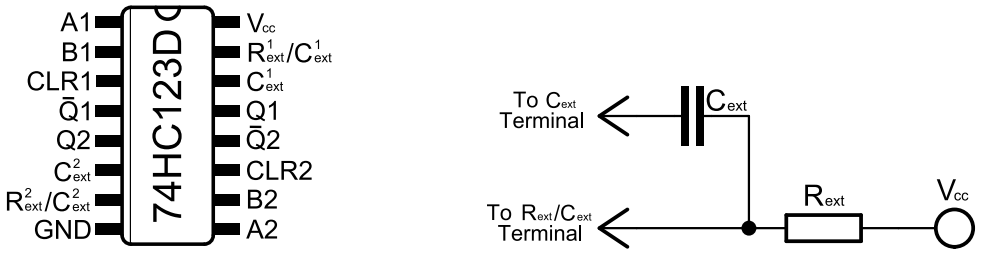

(a) SO16 Pin outs

(b) Timing components

Figure 2.1: (a) Pin outs of a dual retriggerable monostable multivibrator. (b) Frequency and pulse width are controlled via external timing components

The dual one-shot simply houses two one shots in a single package. These can be wired as a pulse generator with independent frequency and duty cycle control (see figure 2.2). The frequency (F) generated at the output of the first one-shot (Q1) is determined by the values of R^1_{ext} and C^1_{ext};

$$F = \frac{1}{0.7\ R^1_{ext} C^1_{ext}} \tag{2.1}$$

The pulse width (PW) is a function of the duty cycle;

$$\text{Duty Cycle} = \frac{R^2_{ext} C^2_{ext}}{R^1_{ext} C^1_{ext}} \quad \Rightarrow \quad PW = 0.7\ R^2_{ext}\ C^2_{ext} \tag{2.2}$$

As can be seen from the logic table (see figure 2.2) the dual one-shot can be wired in a variety of ways. The first one shot was wired according to row 1 of this table. With A1 held LOW (GND) and CLR1 held HIGH (+3V) the one shot develops, on its outputs a HIGH signal level on Q1 and a low signal level on $\bar{Q}1$. As the pulse on $\bar{Q}1$ transits from LOW→HIGH it retriggers the device via pin B1 generating a frequency given by equation 2.1. The second one shot was then also wired according to row 1. A2 is held LOW and CLR2 HIGH. The one-shot is triggered by the LOW→HIGH transition from Q1, generating an output waveform with a frequency defined by the resistor-capacitor network connected to the first one-shot and a pulsewidth defined by the resistor-capacitor network connected to the second one-shot (see equation 2.2).

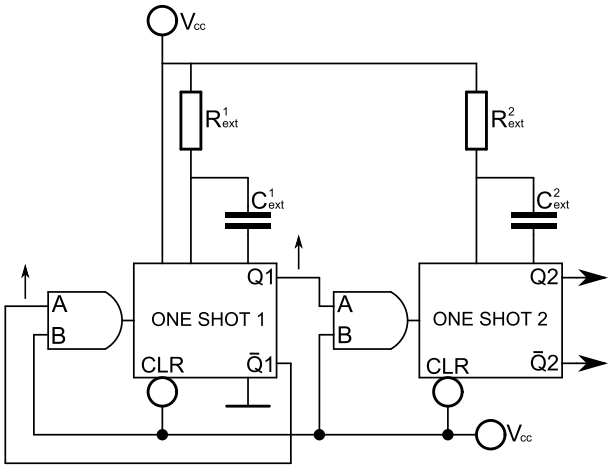

Inputs			Outputs	
CLR	**A**	**B**	**Q**	**$\bar{Q}$**
H	L	↑	⎍	⎏
H	↓	H	⎍	⎏
↑	L	H	⎍	⎏

H = logic level HIGH

L = logic level LOW

↑ = logic transition LOW→HIGH

↓ = logic transition HIGH→LOW

Figure 2.2: Wiring diagram and logic table for a pulse generator using two one-shot devices. **Abbreviations:** R/C^1_{ext}, external resistor/capacitor for one-shot number 1; R/C^2_{ext}, external resistor/capacitor for one-shot number 2; Q, output; $\bar{Q}$, inverted output; CLR, clear; V_{cc}, control voltage.

2.1.2.2 Charge pump

Tissue is capable of increasing its resistivity over 10 fold in response to electrical stimulation. To be certain of constant current delivery to the stimulated nucleus it is necessary to provide sufficient voltage at the input to the current sources that they will be capable of delivering current over a wide range of tissue impedences. To generate a large enough voltage from batteries small enough to be comfortably carried by a rat a charge pump (LM2704 (Farnell)) is used to supply 20V from a 3V supply (see figure 2.3). The charge pump, by storing and accumulating charge, is capable of generating significantly larger output voltages than it receives on its input.

2.1.2.3 Current sources

Constant current sources are used to drive the electrical stimulation into the brain. The current sources are switched via a high speed NPN transistor switch driven by the pulse generator (see figure 2.3). This generates, on the output of the device, a high frequency pulsed constant current source capable of driving currents with a maximum voltage of 20V.

2.1.2.4 PCB design considerations

The timing components of the pulse generator should be placed as close to the device output pins as is possible to reduce timing errors in the output frequency and pulse width (see figures 2.4 & 2.5). Circuit boards were printed by the department of Electronics and Electrical Engineering at The University of Glasgow.

2.1.2.5 Deep brain stimulation device - complete schematic

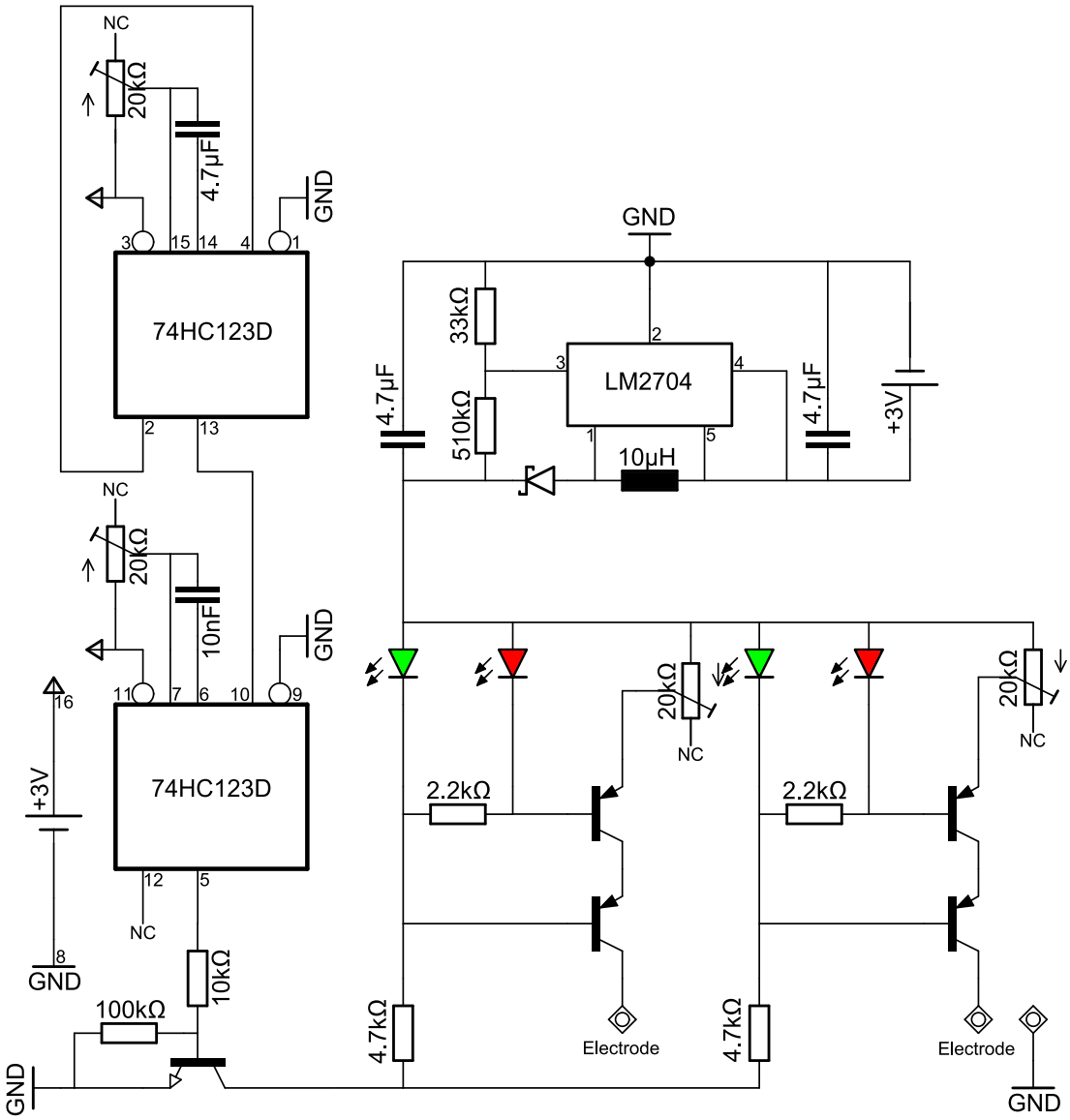

Figure 2.3: Circuit diagram of the DBS device. Small numbers indicate specific device pin outs. NC indicates no connection. LM2704, charge pump; 74HC123D, dual monostable multivibrator.

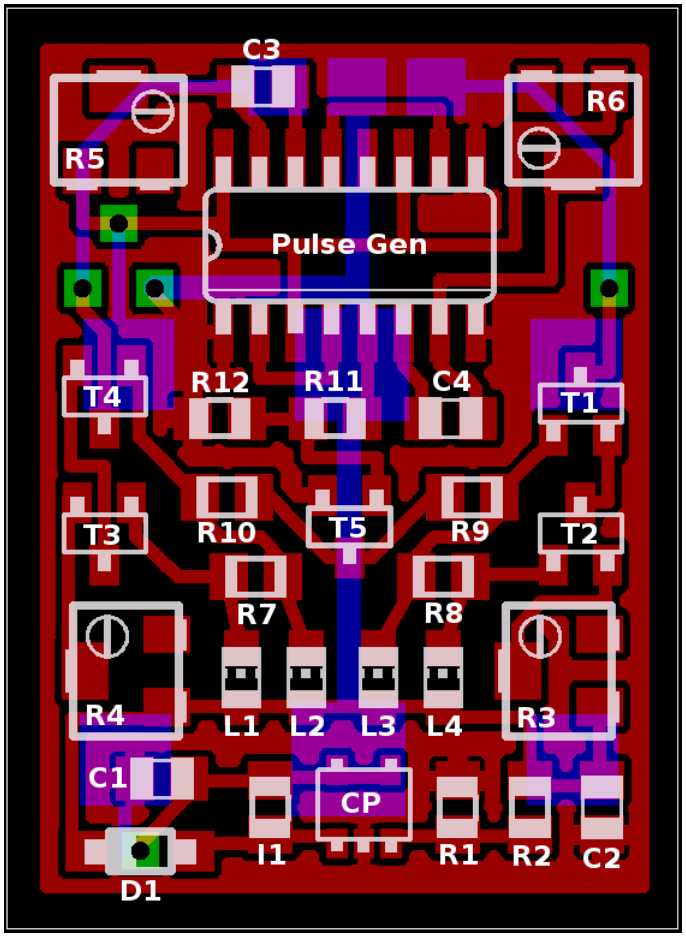

Apprev.	Component	Package	Value
R1	Fixed resistor	0805	33k
R2	Fixed resistor	0805	510k
R3,4,5,6	Variable resistor	-	20k
R7,8	Fixed resistor	0805	2.2k
R9,10	Fixed resistor	0805	4.7k
R11	Fixed resistor	0805	10k
R12	Fixed resistor	0805	100k
C1,2,3	Capacitor	0805	4.7μF
C4	Capacitor	0805	10nF
T1,2,3,4	Transistor	SOT23	PNP
T5	Transistor	SOT23	NPN
D1	Schottky diode	SOD123	-
L1,4	LED	0805	Red
L2,3	LED	0805	Green
Pulse Gen	74HC123D	SO16	-
CP	LM2704	SOT23	-
I1	Inductor	0805	10μH

Figure 2.4: PCB components

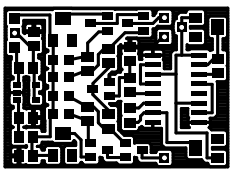

(a) PCB: top

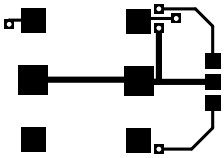

(b) PCB: bottom

Figure 2.5: (a) PCB layout for the top of the DBS device and (b) PCB layout for the bottom of the DBS device. Images are actual size. This print can be used to etch, via a photo-lithographic process, this design onto the surfaces of double sided copper clad board (EEE, The University of Glasgow). Components can then be soldered to the surface of the board to construct the device (see figure 2.4). **Abbreviations:** PCB, printed circuit board.

2.1.2.6 Deep brain stimulation device testing

The waveform generated by the deep brain stimulation device is easily scrutinised with a standard oscilloscope. Frequency, pulse width and the voltage amplitude of a pulse are readily measurable. By stimulating a dummy load of known resistance (*i.e:* a fixed value resistor) with the device the current output can be calculated from the measured voltage and known resistance using Ohm's law (V = IR). The device should deliver the same current regardless of the load resistance (up to a finite limit). The constancy of the current delivered by the device can be verified simply by measuring the voltage delivered by the device when driving a current through an assortment of fixed resistors.

2.1.2.7 Habituation Devices

Devices used in the habituation phase of behavioural testing are constructed by preparing a piece of stripboard (Maplin Electronics) of an equivalent size to the finished PCB described above (see figure 2.5). The board is weighted to a similar mass to that of the finished devices by sticking a penny to the top-most surface. Cables and connectors, identical to those used in the "live" devices, are super-glued to the front edge of the board in a position identical to that of the "live" devices and the board and penny wrapped in insulating tape. The habituation devices are then prepared for attaching to the small rodent jackets (Royem Scientific Limited/Harvard Apparatus Ltd.) (see figure 2.6) by sticking the hooked side of adhesive hook-and-loop tape to the top-most surface of the the device. The looped side of the hook-and-loop tape was stuck to the underside of the device to cushion the battery housings which would otherwise have been

adjacent to the animals back.

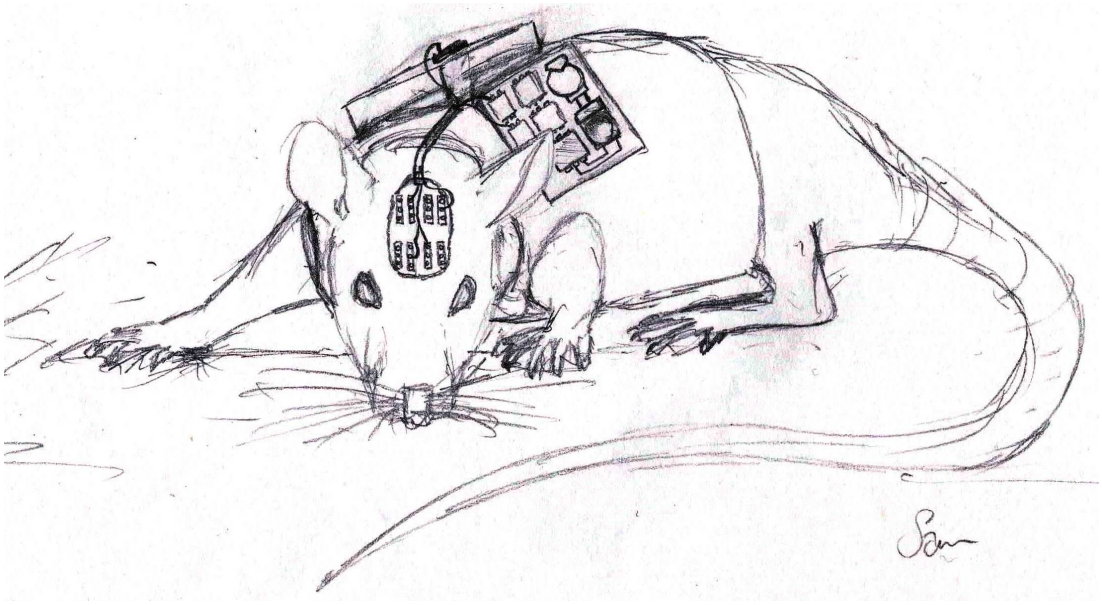

Figure 2.6: Devices were designed to be carried by the animals by attaching them to rodent jackets.

2.2 *in vivo* procedures

2.2.1 Surgical protocol

2.2.1.1 Preparation

Analgesics are prepared immediately prior to surgery. Rimadyl™ (Pfizer Animal Health) is used to provide general analgesia lasting well into the post-operative period (24 hours). Rimadyl™ contains the non-steroidal anti-inflammatory drug carprofen in a concentration of 50mg.ml^{-1}. A 1:10 dilution is made up in sterile water for administration at a dose of 5mg.kg^{-1}. The drug is not particularly stable in water and should be made fresh prior to every surgical procedure. Fast acting, short duration, local anaesthesia and analgesia is provided with a cocktail of lidocaine hydrochloride 1% (Hameln Pharmaceuticals Ltd) and bupivacaine hydrochloride 0.25% (Marcain Polyamp® (AstraZeneca UK Ltd)). The drugs are drawn into a 1ml syringe in a ratio of approximately 20:14 (bupivicaine:lidocaine) for administration at 1ml.kg^{-1}.

Drapes, gown and instruments are all autoclaved prior to surgery. The surgical table is covered with a sterile drape and all remaining exposed surfaces wiped

down with 70% ethanol.

2.2.1.2 Anaesthesia & analgesia

Animals are first weighed to determine appropriate levels for the injectible anaesthetics and analgesics before being anaesthetised via the inhalation of isoflurane (Isoflo® (Abbott Animal Health)). Anaesthesia is initially induced in a clear acrylic chamber flooded with isoflurane (level 4-5% (Flecknell, 1996)), oxygen (0.3l.min^{-1}) and nitrous oxide (0.7l.m^{-1}). Level of anaesthesia is assessed via the pedal withdrawal reflex and tail pinch. Induction is deemed complete following the abolition of responses to these painful stimuli. Following induction, the fur from the area above the cranial surface is shaved with a small set of clippers, the animal transferred to a stereotaxic frame (David Kopf Instruments) and the level of anaesthesia lowered to 2% (Flecknell, 1996). From this point the animal's body temperature is maintained with a small heat pad (Fine Science Tools Inc.). Any remaining hair clippings are cleaned away and the shaved scalp sterilised with 70% ethanol applied with a small sterile gauze swap (Sterets, (Seton Healthcare Group PLC.)). The eyes are protected via the application of an ocular lubricant (Lacrilube™ (Allergen Pharmaceuticals (Ireland) Ltd.)). At this point, should the animal be undergoing surgery with recovery, the animal receives a single subcutaneous injection of Rimadyl™ administered at 1ml.kg^{-1} and a bolus injection of approximately three quarters of the lidocaine/bupivacaine cocktail into the scalp. The bolus injection is allowed sufficient time to absorb into the tissues before continuing.

2.2.1.3 Surgery

The animal is mounted in the frame using atraumatic (blunt) ear bars (David Kopf Instruments) to prevent damage to the inner surfaces of the ear and potential rupturing of the ear drum. A single rostral-caudal incision is made from between the eyes to between the ears with a fresh scalpel. The skin from above the cranial surface is drawn back and the wound held open with two two-pronged 16cm retractors (Royem Scientific Limited). Any remaining connective tissue is removed via "blunt" dissection with a cotton bud. Should the animal be undergoing surgery with recovery the remaining lidocaine/bupivacaine cocktail is then applied to the open wound and allowed time (approximately 5 minutes) to be absorbed by the cranial surface and the wound margins. Any remaining drug and bleeding is cleaned away with cotton buds.

The position of the animal is then adjusted to ensure a flat-skull position. The relative height of bregma and lambda (Paxinos & Watson, 2007) are measured using a "dummy" electrode and the height of the incisor bar adjusted such that the height of bregma and lambda are equal. The position of bregma is then recorded and the coordinates for the electrode implants calculated. The positions for the burr holes are marked by scoring the skull surface lightly with the drill. The position is then checked before drilling carefully through the skull with a 1mm diameter dental burr (Royem Scientific Limited). The dura beneath the breach is then resected with a small needle. In general four further burr holes are drilled with a 0.8 diameter dental burr fore and aft of the larger electrode holes. These holes are drilled to take the supporting stainless steel screws (M1×2mm (Royem Scientific Limited)) and do not penetrate the skull. The supporting screws are then screwed into the skull by holding them in a pair of needle grips. After affixing the screws the electrodes are lowered, bilaterally, into the target though the 1mm burr holes. The electrodes are then secured to the anchor screws with dental cement (Kemdent). A low viscosity dental cement is made up by filling a standard eppendorf with Simplex Rapid™ powder (Kemdent) to just below the 1ml line and mixing it with 400µl of Simplex Rapid™ liquid (Kemdent) by repeatedly drawing it in and out of a 1ml pipette tip. The cement is then applied to the electrodes and anchor screws by flooding the skull surface with this mixture. The cement is allowed to cure and the electrode holders withdrawn. Before the cement has cured completely the skin from the scalp is gently pulled away from the cement to prevent it fixing to the implant. The supporting 30G stainless steel tubing supporting the implanted electrode is then clipped away with a small pair of pincers. The connectors and cabling for the deep brain electrodes are then arranged to minimise its size and the loose skin drawn tightly around the implant. The wound is sutured closed with vicryl sutures (Ethicon 4-0 coated vicryl (Dunlop's Vetinary Supplies)). Any remaining voids within the wound are then filled by forcing more dental cement into the space between the implant and the scalp through gaps in the sutures with a pipette. Again the cement is allowed to cure before further experimentation or recovery. The procedure for implanting EEG electrodes is slightly different and is dealt with specifically in the chapter pertaining to this technique.

2.2.1.4 Recovery

Animals are then moved to a warmed cage lined with tissue paper and allowed to recover until their righting reflex has returned. Following this, animals are

returned to their home cages and allowed to recover for at least 7 days before undergoing any behavioural tests.

2.2.1.5 Electrolytic lesions

Electrolytic lesions are made to mark the exact location of the electrode tip for verification of position in subsequent sectioning. Direct current (DC) was delivered between the two electrode contacts at 100μA for approximately 10 seconds. Animals used in recovery experiments were briefly re-anaesthetised as previously described (2.2.1.2, page 46) before electrolytic lesioning. It should be noted that, whilst it is standard practice to generate an electrolytic lesion to verify electrode placement, it also makes it difficult to determine whether the stimulation itself causes any local damage. To assess this accurately a separate cohort of animals should be run. At the end of the experiment these animals should not receive an electrolytic lesion and any damage caused by the stimulation itself should be determined histologically.

There are several populations of cells involved in the inflammatory response to electrodes inserted into the brain. Neurons themesleves make up less than 25% of these cells. The remaining 75% comprises glial cells and vascular tissue. 30-65% of the glial cells are astrocytes. Immunostaining for GFAP is the most common method of assessing the astrocytic response ("reactive gliosis") to injury (see Polikov *et al.* (2005)). 5-10% of the glial cells are microglia which also participate in the brain's response to injury. They are a potent source of pro-inflammatory cytokines, including; IL-1 and TNF-α. In addition they are a known to secrete neurotrophic growth factors including NGF, BDNF and NT-3 in reponse to injury (see Polikov *et al.* (2005)). The brain tissue response to chronically implanted electrodes is characterized by the presence of both reactive astrocytes and activated microglia. Staining for some of the inflammatory markers detailed above would be of interest to determine the extent of the damage caused by, and the response to electrode insertion.

2.3 *ex vivo* procedures

2.3.1 Euthanasia, dissection & fixation

All animals used in the course of this research were euthanased via cervical dislocation and then decapitated. Brains were removed by peeling away the overlying skull and scooping the brain out with a small spatula. Brains were then snap

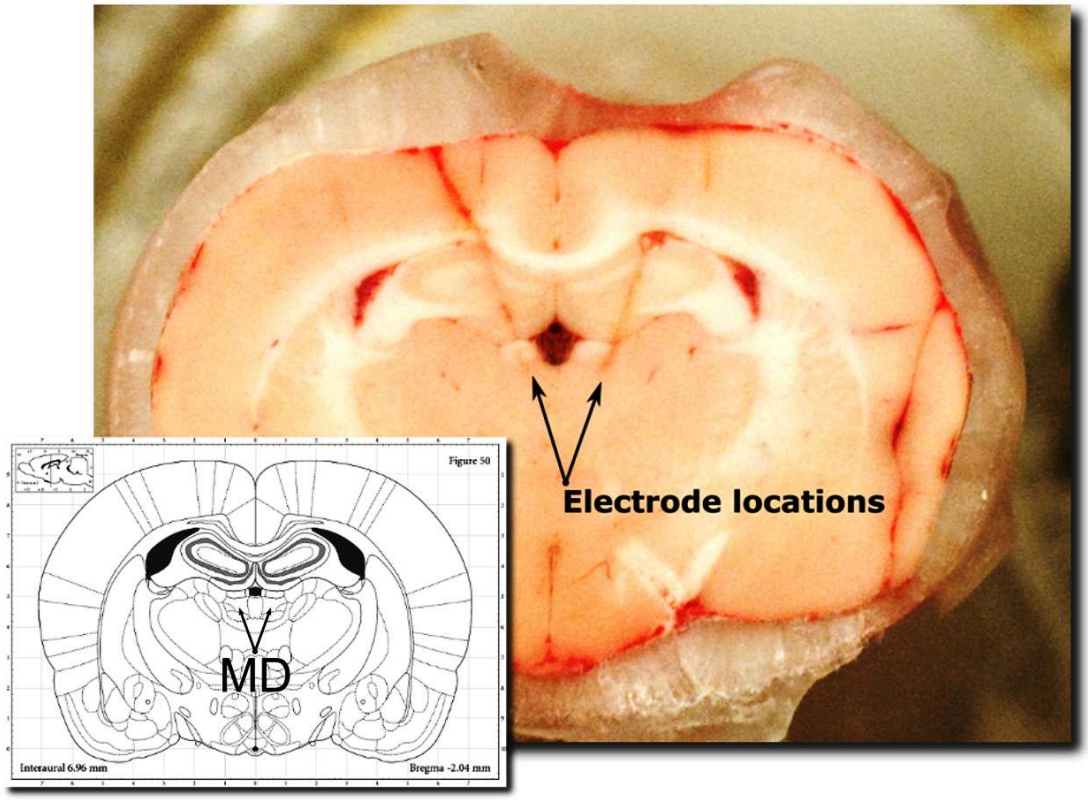

Figure 2.7: Determining electrode locations. In the region of the electrode implant 10µm sections were cut and the sectioned surface of the brain observed. The location of the tip of the electrode was identified as the most ventral point of the electrode track. Electrode locations were plotted onto atlas sections. The mediodorsal thalamic nucleus is the region immediately below the stria medullaris of the thalamus.

frozen by dropping them into iso-Pentane (VWR International Ltd) cooled to -42°C on dry ice. The frozen brain was then coated in an embedding matrix (Shandon M-1 embedding matrix (Thermo Electron Corporation)), wrapped in aluminium foil and stored at -80°C until required.

2.3.2 Electrode location verification

Brains were removed from -80°C frozen storage and warmed to -16°C and 60µm coronal sections cut on a rotary microtome in a cryostat (Leica Microsystems (UK) Ltd). In the region of the electrode implant 10µm sections were cut, the sectioned surface of the brain observed and electrode locations plotted onto atlas sections (see figure 2.7).

2.3.3 Expression of immediate early genes

2.3.3.1 Cryotomy & Fixation

Brains were removed from -80°C frozen storage and warmed to -16°C and 20µm coronal sections cut on a rotary microtome in a cryostat (Leica Microsystems (UK) Ltd). Two consecutive sections were taken at 6 levels, including the rostral prefrontal cortex, caudal prefrontal cortex, ventral striatum (including the rostral cingulate cortex), caudal cingulate cortex, rostral thalamus and dorsal hippocampus (Bregma ≈ 4.68mm, 3.00mm, 1.32mm, -1.20mm, -2.04mm and -3.24mm respectively according to the atlas of Paxinos & Watson (2007), see figures 2.8 and 2.9) and thaw mounted onto poly-L-lysine (Sigma-Aldrich) coated slides (Raymond A Lamb Ltd). Sections were allowed to air dry, at room temperature, before being fixed in an ice cold (≈ 0°C) 4% solution of depolymerised paraformaldehyde (Sigma-Aldrich) for 5 minutes. 1 extra section per level per IEG was taken for subsequent use as a "cold-probe" control section. Sections were then washed in phosphate buffered saline for 5 minutes (1× PBS (Sigma-Aldrich)) before being dehydrated through graded concentrations (70%, 95% and 100%, 5 minutes each) of AR grade ethanol (Sigma-Aldrich). Sections were then stored in glass racks in 100% ethanol at 4°C.

2.3.3.2 IEG labelling

The *in situ* hybridisation technique was based on the method described by (Wisden & Morris, 2002). A 45-mer oligonucelotide probe with sequences complementary to mRNA encoding the immediate early genes *zif-268* (`CCG TTG CTC AGC ATC ATC TCC TCC AGT TTG GGG TAG TTG TCC`) (PerkinElmer LAS (UK) Ltd) and *c-fos* (`CA GCG GGA GGA TGA CGC CTC GTA GTC CGC GTT GAA ACC CGA GAA`) (Cruachem Ltd.) was labelled with [^{33}P]-dATP (PerkinElmer LAS (UK) Ltd) via reaction with the TdT enzyme using a terminal deoxynucleotidyl transferase kit (Roche Applied Science). A reaction mixture containing 2.9µl DEPC (Sigma-Aldrich) treated water, 0.6µl $CoCl_2$, 2.0µl TdT reaction buffer (5×), 2.0µl [^{33}P]-dATP, 1.5µl oligonucleotide probe (5ng.µl^{-1}) and 1.0µl TdT enzyme was incubated at 37°C for 1 hour. The reaction was terminated via the addition of 40µl of DEPC treated water. Probes were purified and eluted using a QIAquick nucleotide removal kit (QIAGEN Ltd). Specific activity of each probe was quantified by liquid scintillation counting and those with an activity between 2.5 and 7.5kBq.µl^{-1} were stored at -20°C until required.

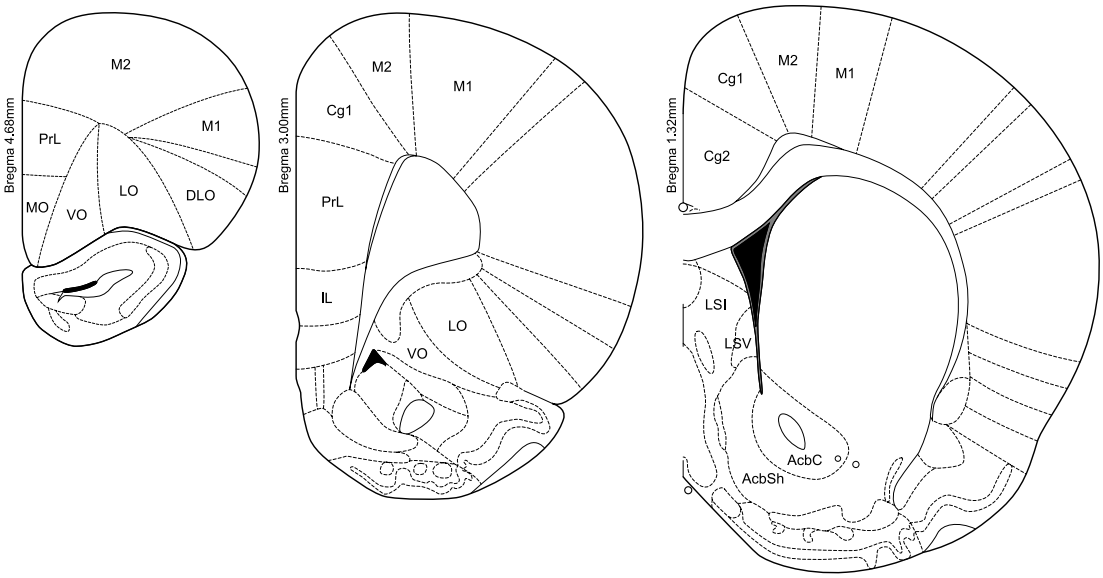

Figure 2.8: Atlas sections at the level of the prefrontal cortex and ventral striatum. **Abbreviations:** AcbC, core of the nucleus accumbens; AcbSh, shell of the nucleus accumbens; Cg1, cingulate cortex area 1; Cg2, cingulate cortex area 2; DLO, dorsolateral orbital cortex; IL, infralimbic cortex; LO, lateral orbital cortex; LSI, lateral septal nucleus, intermediate part; LSV, lateral septal nucleus, ventral part; MO, medial orbital cortex; M1, primary motor corex; M2, secondary motor cortex; PrL, prelimbic cortex; VO, ventral orbital cortex.

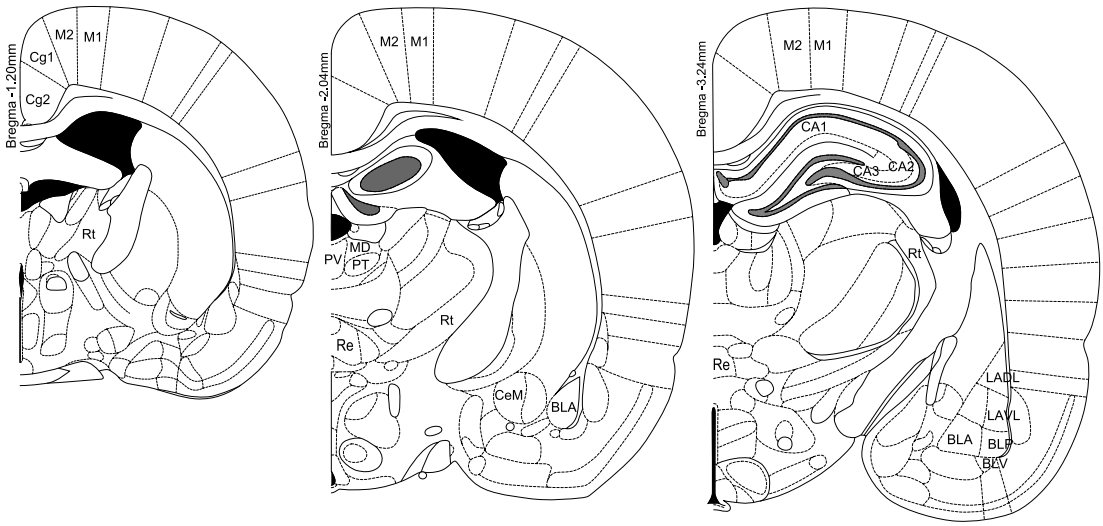

Figure 2.9: Atlas sections at the level of the thalamus and hippocampus. **Abbreviations:** BLA, basolateral amygdala; CA1/CA2/CA3, regions of the hippocampus; CeM, centromedian amygdala; Cg1, cingulate cortex area 1; Cg2, cingulate cortex area 2; MD, mediodorsal thalamic nucleus; M1, primary motor corex; M2, secondary motor cortex; PT, paratenial thalamic nucleus; PV, paraventricular thalamic nucleus; Re, reuniens thalamic nucleus; Rt, reticular thalamic nucleus

2.3.3.3 Hybridisation of brain sections

Slides were removed from storage and allowed to dry for approximately 30 minutes. Experimental slides (4 sections) were coated with a hybridisation mix containing 4µl of radio-labeled probe suspended in 200µl of hybridisation buffer. To determine the level of non-specific hybridisation test sections were coated with a hybridisation mix containing 16µl of unlabelled oligonucleotide in addition to the 4µl of labelled probe. Slides were incubated overnight at 42°C before being washed, to remove unhybridised probe, in 1×SSC (sodium citrate) in a gently shaking water bath maintained at 60°C for approximately 30 minutes. Slides were washed further through graded concentrations of SSC (1× and 0.1×) at room temperature before being dehydrated through graded concentrations of ethanol (70% and 95%). Slides were air dried for approximately 30 minutes before exposure to x-ray film (Kodak Biomax MR-1 (Sigma-Aldrich)) for several days (≈ 8). Films were developed using an X-MAT (Kodak) automated film developer.

2.3.3.4 Quantification of IEG expression

The subsequent autoradiograms were analysed using `MCID` (Imaging Research Inc.), an optical densitometer software package. Quantative optical density measurements are made from discrete brain regions as anatomically defined in the atlas of Paxinos & Watson (2007). For each brain, measurements are taken from two parallel sections, in both hemispheres, for each region, at each level (see figures 2.8 and 2.9 on pages 51 and 51). Measurements for a single region of interest (ROI) are determined by sampling the relative optical density (ROD) within the region. This is preformed by measuring the optical density of a small square area well within the anatomical boundaries of the ROI three times. The three samples from each ROI are then averaged for each animal. Non-specific hybridisation was quantified by sampling the ROD from sections hybridised with a "cold-probe" containing an excess of non-labelled oligonucleotide. The RODs for each region are then averaged over animals from the same group, the ROD due to non-specific binding subtracted and the computed mean RODs between the hemispheres ipsilateral and contralateral to stimulation statistically compared via a paired Student's t-test in `Prism5` (Graphpad Software Inc.).

Part II

Molecular markers of neural activity

Chapter 3

Deep brain stimulation of the mediodorsal thalamic nucleus yields differential effects in the expression of *zif-268* and *c-fos* in frontal regions of the anaesthetised rat.

3.1 Introduction

Immediate early genes (IEGs) are widely used as general markers of neural activity as they are induced by many stimuli. Neurotransmitters regulate gene expression, the initial phase of which is charactersied by the induction of IEGs. In the absence of cellular excitation IEGs are usually only expressed at low levels. However when synaptic inputs are activated they are rapidly, though transiently, induced; mRNA levels may be significantly increased within 15 minutes and may remain elevated for only 30-60 minutes (see Davis *et al.* 2003). Second phase, late onset genes depend on the actions of the protein products generated by the IEGs. Location and regulation of IEGs in the brain can be studied by *in situ* hybridisation for IEG mRNA. This chapter explores the location and regulation of the IEGs *zif-268* and *c-fos* as a result of DBS of the mediodorsal thalamic nucleus.

3.2 Immediate early genes as markers of neuronal activity

Immediate early genes (IEGs) are those genes which can be induced without the activation of any other responsive genes and, by definition, represent the earliest genomic response to a stimulus. The total number of such genes has been estimated to be of the order of 30-40 (Lanahan & Worley, 1998) and broadly speaking these can be placed into categories based on their protein products (see Clayton 2000; Loebrich & Nedivi 2009):

1. **Regulatory IEGs:** encode proteins that return to the nucleus after their synthesis to regulate the subsequent expression of specific genes (delayed early genes).

2. **Direct effector IEGs:** encode proteins that have structural or enzymatic roles that may immediately affect the cells physical organization.

Regulatory IEGs (transcription factors) account for one-third to one-half of the total number (Lanahan & Worley, 1998) and much of what is know about the neuronal IEG response is based on a fraction of these transcription factors. Particular attention has been paid to *c-fos* and *zif-268* (also known as: *Egr-1, NGFI-A, Krox-24, TZS8* and *Zenk*) (see Clayton 2000) and the expression of the mRNA and protein products of them are commonly used as markers of neural activity (Zangenehpour & Chaudhuri, 2002). So much so that this field is the subject of extensive reviews (see Hughes & Dragunow 1995; Clayton 2000; Loebrich & Nedivi 2009; Davis *et al.* 2003; Kovács 1998; Herdegen & Leah 1998) and is afforded its own volume in the *Handbook of Chemical Neuroanatomy* (Kaczmarek & Robertson, 2002). Suffice it to say that IEGs, particularly *c-fos* and *zif-268*, are used routinely to map the neural substrates of stimuli, be it pharmacological, behavioural or electrical in origin. *zif-268* has high basal expression whereas *c-fos* has low basal expression. It is these IEGs that will be used to elucidate the patterns of neural activation resulting from DBS of the mediodorsal thalamic nucleus since, whilst *c-fos* is the most commonly employed, it is not useful for determining reductions in activity. The high basal expression of *zif-268* makes it a more appropriate marker for determining reductions in expression.

3.2.1 *c-fos*

c-fos is a regulatory IEG with low basal expression (Sagar *et al.*, 1988) which can be induced by a wide range of stimuli (see Clayton 2000; Davis *et al.* 2003;

Kovács 1998). *c-fos* mRNA expression peaks between 30 and 60 minutes after the inducing stimuli with expression of its protein product peaking between 1 and 3 hours later (see Kovács 1998).

3.2.2 *zif-268*

zif-268 is a regulatory IEG (see Clayton 2000; Davis *et al.* 2003) with high basal expression in the neocortex (primarily in layers IV and VI), primary olfactory and entorhinal cortices, amygdaloid nuclei, nucleus accumbens, striatum, cerebellar cortex and the hippocampus (primarily in CA1) (see Davis *et al.* 2003; Hughes & Dragunow 1995). *zif-268* mRNA is induced via the activation of different receptors which include at least, all subtypes of glutamatergic receptors, dopaminergic, adrenergic and opiate receptors (see Hughes & Dragunow 1995).

3.3 *in situ* hybridisation

The expression of IEG mRNA can be detected with a high degree of anatomical resolution using *in situ* hybridisation (ISH) techniques described in depth by Wisden & Morris (2002) and in section 2.3.3.2, page 50. Simply, oligonucleotide probes with sequences complementary to mRNA expressed by a particular IEG can be tagged with (in this case) radiolabelled molecules. The tagged probe, under the appropriate conditions, will hybridise to only the mRNA expressed by the specific IEG. Subsequent exposure to x-ray film detects the location of the radioactive probe and, therefore, the location of the expressed IEG. The relative optical density of regions within the autoradiogram provides an indication of the number of cells expressing the IEG mRNA and therefore a means by which to identify and localise regions of increased cellular activity.

3.4 IEG expression in response to anaesthesia

The results described in this chapter are from aneasthetised animals. Obviously it is important to consider the effects of this potential confound on IEG expression. Anaesthetic via inhalation of isoflurane yields upregulation of *c-fos* in the brain after 30 minutes with a return to baseline expression after 60 minutes (Hamaya *et al.*, 2000). Given the time course of *c-fos* expression in response to isoflurane anaesthesia time courses for stimulation in these studies have been chosen such that there should be no potential overlap between the anaesthetic induced expression and any DBS induced expression. Furthermore the design of the following

experiments uses a within animal control (contralateral hemisphere) to further account for any anaesthetic confounds.

3.5 IEG expression in response to DBS

There have been few studies investigating the induction of IEGs as a consequence of DBS of subcortical nuclei. Previous studies have focused on "traditional" parkinson's targets (subthalamic nucleus, Schulte *et al.* 2006) or alternative thalamic targets (Sun *et al.*, 2006).

It has been previously shown that stimulation of the medial thalamus, including the mediodorsal thalamic nucleus - medial part, mediodorsal thalamic nucleus - central part, mediodorsal thalamic nucleus - lateral part, centerolateral thalamic nucleus and strai medullaris of the thalamus, yields increases in the expression of *c-fos* in the ipsilateral medial prefrontal cortex (including secondary motor cortex, cingulate cortex - area 1 and prelimbic cortex regions) in a frequency dependent manner (Sun *et al.*, 2006). Whilst *c-fos* immunolabelling was not localized to specific sub territories within the medial prefrontal cortex it was more prevalent in layers II/III than in other cortical layers. Stimulation at both 1Hz and 10Hz yielded significant increases in *c-fos* expression when compared to the sham-stimulated contralateral control hemisphere. However stimulation at 10Hz yielded significantly greater increases than did 1Hz stimulation of the same site. Interestingly, despite not being highlighted in the text of the paper, unilateral stimulation of the medial thalamus seems to effect a bilateral response in *c-fos* immunoreactivity: 10Hz stimulation yields an apparent increase in *c-fos* expression in the contralateral sham stimulated hemisphere when compared with completely stimulation naive controls. This bilateral effect is not apparent at 1Hz (Sun *et al.*, 2006). The stimulation target studied by Sun *et al.* (2006) is more caudal (RC = -3.14mm) than the target investigated in this chapter (RC = -2.04mm). Of greater importance is the difference in frequencies studied. Sun *et al.* (2006) investigated only low frequency stimulation (1 & 10Hz). The experiments reported in this chapter characterise the neural substrates of stimulation of the mediodorsal thalamic nucleus at frequencies shown to be therapeutically effective in Parkinson's disease (130Hz).

Unilateral HF subthalamic nucleus DBS (monophasic; F: 80/130Hz, PW: 60μs, A: 300μA) yields increases in the expression of the immediate early genes *c-fos, c-Jun, zif-268*) in the stimulated nucleus (Schulte *et al.*, 2006; Salin *et al.*, 2002) and

its efferent targets whereas low frequency stimulation (5Hz) had no effect on IEG immunoreactivity (Schulte *et al.*, 2006). Similarly unilateral HF stimulation of the centrolateral thalamic nucleus (F, 100Hz; PW, - ; A, 1.5mA) yields increased expression of *c-fos* in its efferent targets. Similar increases were reported for *zif-268* expression (Shirvalkar *et al.*, 2006). These studies demonstrate the utility of IEG expression as a means to identify and map the neural targets affected through electrical stimulation of discrete brain regions.

3.5.1 Experimental aims

The aim of this experiment was to determine the brain regions affected by high frequency stimulation of the mediodorsal thalamic nucleus as assessed by the expression of the immediate early genes encoding the mRNA of both *zif-268* and *c-fos*. The distribution of changes in these IEGs provides a putative map of the substrates involved in the neural response to DBS of the mediodorsal thalamic nucleus.

3.6 Pilot study

The electrodes, DBS devices and surgical technique were uniquely developed as an integral part of this project. As such the techniques were initially piloted in a small *in vivo* study.

3.6.1 Materials & methods

3.6.1.1 Stimulation electrodes

Stimulation electrodes were fabricated (see section 2.1.1.1, page 37), tested and sterilised as previously described (see section 2.1.1.2, page 38).

3.6.1.2 Deep brain stimulation devices

DBS devices WERE NOT constructed as previously described (see section 2.1.2, page 39). The device described in the General Methods is that which was developed as a result of this pilot and used in all subsequent experiments. As shall be made apparent the device described here has several short comings that were subsequently resolved.

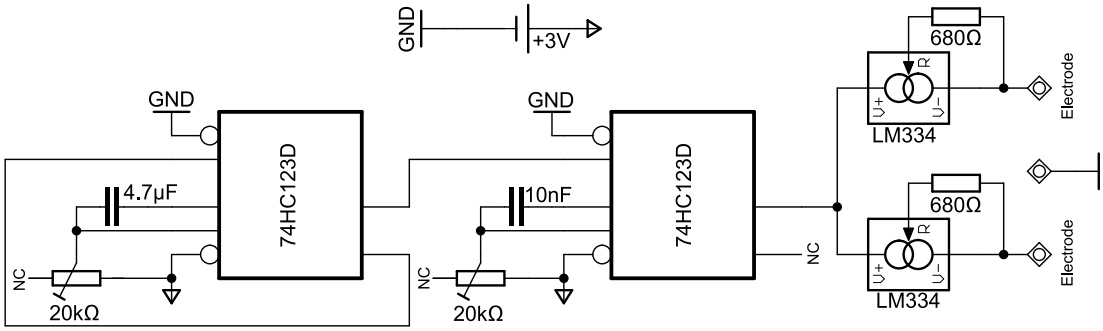

Figure 3.1: Pilot device schematic. As with the device described in section 2.1.2, page 39, monophasic square waves with short duration pulses, delivered at high frequency are generated by a dual retriggerable monostable multivibrator (74HC123D). Floating current sources (LM334) were used to provide the constant current output.

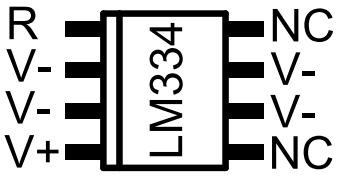

Figure 3.2: Floating current source, LM334. The LM334 is a fully programmable floating current source (*i.e:* requires no external power supply). The output current I_{set} is set by connecting a resistor between the pins labelled R and any pin labelled V- and flows from any pin labelled V-.

This prototype was considerably simpler than the final device relying on a mere 8 components. The 74HC123D dual monostable multivibrator, described earlier (see section 2.1.2, page 39), provides programmable pulse generation by means of two external resistor-capacitor networks. This prototype uses the output from the 74HC123D to drive two programmable floating current sources. The output current I_{set} is set by connecting a resistor between the pins labelled R and any pin labelled V- and flows from any pin labelled V- (see figure 3.2). The whole device runs from a single 3V battery and has no charge pump to increase the available voltage to the current sources.

3.6.1.3 Animals

Male Sprague-Dawley rats (bred in house) weighing 300g and 312g (n = 2), were housed together in a temperature regulated room maintained at 20°C with a 12 hour light/dark cycle. Lights on at 8:00am. Food and water was available *ad libitum*. Environmental enrichment was provided by the addition of a wooden house to the cage. All procedures were carried out in accordance with Home Office regulations.

3.6.1.4 Surgical protocol

Surgery was performed as previously described (see section 2.2.1, page 45). Briefly; animals were anaesthetised by the inhalation of isoflurane (Abbott Animal Health) and mounted in a stereotaxic frame using atraumatic earbars (David Kopf Instruments). Analgesia was omitted since the surgery was performed without recovery. Body temperature was maintained using a small heatpad (Fine Science Tools Inc.). A single rostral-caudal incision was made, the skull exposed and bregma identified. 1mm diameter burr holes were drilled bilaterally at the following coordinates (RC; -2.04mm, ML; ±2.43mm) (Paxinos & Watson, 2007).

The dura beneath the holes was excised with a small needle. Deep brain electrodes were implanted through the holes, bilaterally, at 20° to the perpendicular, in the coronal plane, into the mediodorsal thalamic nucleus (DV: ↓5.60mm). All electrodes were secured to screws anchored in the skull using dental cement (Kemdent) and the incision sutured around the implant. Post surgery animals were maintained under the lowest possible level of anaesthetic (isoflurane between 1 and 1.4%) whilst monitored for consciousness via the pedal reflex and tailpinch.

3.6.1.5 Stimulation protocol

Devices were configured to deliver a constant current of 100μA at a frequency of 130Hz delivered in pulses of 100μs duration. Stimulation was delivered unilaterally to the left hemisphere continuously for 2 hours.

3.6.1.6 Euthanasia & dissection

Animals were euthanased, decapitated, brains dissected, frozen and stored as previously described (see 2.3.1, page 48).

3.6.1.7 Cryotomy & fixation

Brains were sectioned, mounted and fixed as previously described (see 2.3.3.1, page 50). Briefly, 20μm frozen coronal sections were cut, thaw mounted onto poly-L-lysine coated slides, dried and fixed in depolymerised PFA and dehydrated through graded concentrations of ethanol.

3.6.1.8 Quantification of IEG expression

IEG expression was measured via the *in situ* hybridisation technique described previously (see 2.3.3.2, page 50). Briefly, radio-labelled probes for the detection of *zif-268* were hybridised to brain sections overnight. After excess probe was washed away the sections were exposed directly to x-ray film for several days. Resulting autoradiograms were then used to measure the relative optical density of a variety of brain regions.

3.6.1.9 Data analysis

The groups size (n = 2) is insufficient for statistical analysis. The appropriate paired Student's t test requires a minimum of 3 pairs for analysis. Data are thus presented as individual case studies. The ROD for the regions of interest are tabulated as absolute values for each region, for the hemispheres both ipsilateral (ipsi) and contralateral (contra) to stimulation.

3.6.2 Pilot results

Case 1		
Region	**Contra**	**Ipsi**
PrL	0.0993	0.1421
MO	0.0898	0.1354
VO	0.0921	0.1283
LO	0.0812	0.1169
DLO	0.0809	0.1349
M2	0.0965	0.1482
PrL	0.1021	0.1190
IL	0.0842	0.1128
VO	0.0966	0.1429
LO	0.0813	0.1227
Cg1	0.0995	0.1316
M2	0.1021	0.1526

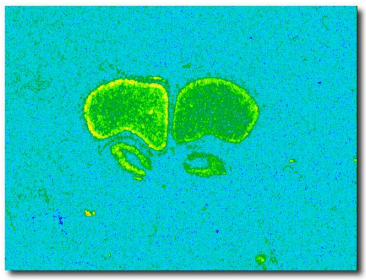

(a) Case 1: level of rostral prefrontal cortex

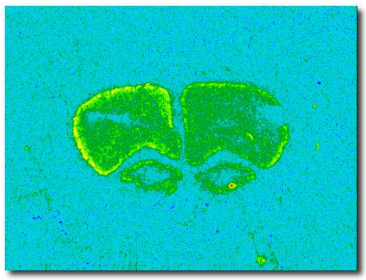

(b) Case 1: level of caudal prefrontal cortex

Case 2		
Region	**Contra**	**Ipsi**
PrL	0.0790	0.1054
MO	0.0761	0.0997
VO	0.0835	0.1018
LO	0.0667	0.1094
DLO	0.0764	0.1374
M2	0.0823	0.1375
PrL	0.0835	0.1030
IL	0.0733	0.0836
VO	0.0823	0.1158
LO	0.0620	0.0951
Cg1	0.0952	0.1399
M2	0.0981	0.1384

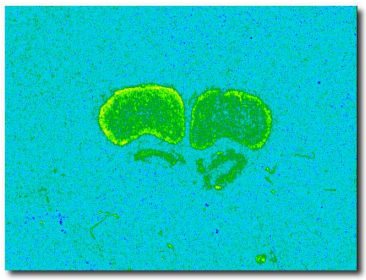

(c) Case 2: level of rostral prefrontal cortex

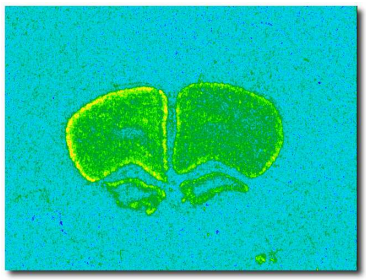

(d) Case 2: level of caudal prefrontal cortex

Figure 3.3: Effects of mediodorsal thalamic nucleus stimulation on *zif-268* expression in the prefrontal cortex - Pilot data, n = 2. Increases in the *zif-268* mRNA expression seem apparent in the hemisphere ipsilateral (ipsi) to stimulation when compared with the contralateral (contra) hemisphere. Values represent the relative optical density (ROD) in each brain region. **Abbreviations:** PrL, prelimbic cortex; IL, infralimbic cortex; MO, medial orbital cortex; VO, ventral orbital cortex; LO, lateral orbital cortex; DLO, dorsolateral orbital cortex; M2, secondary motor cortex; Cg1, cingulate cortex - area 1

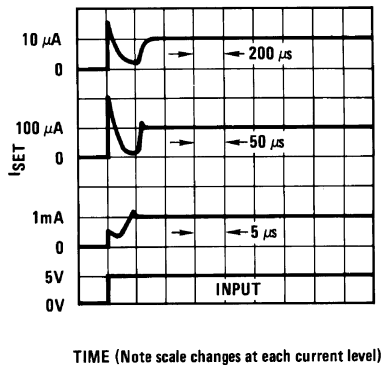

(a) Turn on time for the LM334 for various output currents (I_{set}) given a constant 5V input (adapted from datasheet).

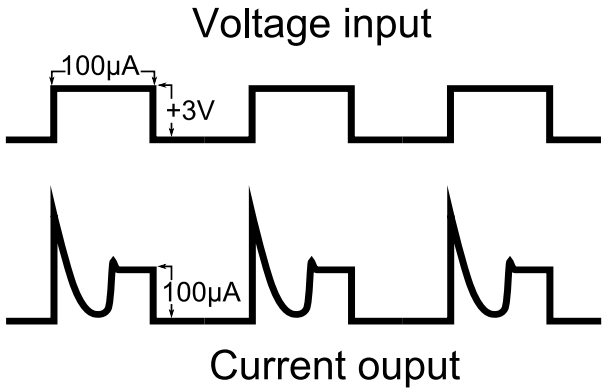

(b) Schematic representation of the output waveform for the device used in the pilot experiment.

Figure 3.4: Turn-on time for the LM334 and its consequence on the output waveform for the pilot device. The LM334 has a start-up time of approximately 50μs with I_{set} = 100μA. The consequence of this is a peculiar waveform on the output. The current sources, upon receiving a 100μs pulse on their input respond initially by producing a current at the output that is approximately twice that of the set current. This current decays rapidly to zero before the device powers up at approximately 50μs. The device then delivers the correct output current for the remainder of the input pulse.

3.6.3 Discussion

Whilst this pilot lacks the sample size to generate any statistical significance the results, at the very least, make some positive indications. The methodology, in the greater part, was successful. DBS was administered to 2 rats using custom designed and built electrodes and devices. Furthermore the IEG expression in the stimulated hemisphere appears considerably higher than in the contralateral control hemisphere at the level of the prefrontal cortex. These tentative results indicate a putative increase in cellular activity as a result of mediodorsal thalamic nucleus stimulation.

Of particular interest, and the primary reason for the inclusion of this pilot in this chapter, are the conditions in which these results were collected. The device used in this pilot was a very early prototype containing a couple of design flaws. The first of these was the minimal headroom in the voltage supply to the current sources. The device contains no charge pump so, assuming no voltage drop across the components preceding the current sources, the maximum voltage available to the current sources is that of the supply; 3V. With the output set to 100μA the maximum load resistance for the device is then limited to 30kΩ. The more serious concern is the current sources themselves. Whilst initially appealing given their

simplicity and small PCB footprint they have an inherent limitation making them inappropriate for this application. The LM334 has a start-up time of approximately 50μs with I_{set} = 100μA (see figure 3.4(a)). The consequence of this is a very peculiar waveform on the output of the device. The current sources, upon receiving a 100μs pulse on their input respond initially by producing a current at the output that is approximately twice that of the set current. This current decays rapidly to zero before the device powers up at approximately 50μs. The device then delivers the correct output current for the remainder of the input pulse (see figure 3.4(b)).

The limited headroom of the device is only a mild concern unless one is staunchly concerned with maintaining the current output over a broad range of tissue impedences. However it is worth recalling at this stage that clinical DBS is performed in a constant voltage mode *not* a constant current mode and that these voltages are commonly of the order of 3V. The more serious fault is with the unusual output waveform. Whilst pulse widths are a commonly varied parameter, pulse shapes are *always* square. Yet despite this flaw the pilot study succeeded in putatively demonstrating an increase in neuronal activation through DBS of the mediodorsal thalamic nucleus. The flaws in the device design have been amended and this optimised device has been described in some detail earlier (see 2.1.2, page 39). However, it is interesting to observe that the IEG response seems relatively robust to the "flaws" in the applied signal. Neuronal activation was putatively increased with voltages that may have been insufficient to drive the output current at the desired level and with a waveform that delivered approximately half the energy of that of the intended waveform. Given the absence of statistical weight in these putative results it is unwise to be overly speculative yet there is an indication that activation of the prefrontal cortex may be achievable through high frequency stimulation of the mediodorsal thalamic nucleus.

3.7 Experimental Study

3.7.1 Materials & methods

3.7.1.1 Stimulation electrodes

Stimulation electrodes were fabricated (see section 2.1.1.1, page 37), tested and sterilised as previously described (see section 2.1.1.2, page 38).

3.7.1.2 Deep brain stimulation devices

DBS devices were constructed and tested as previously described (see section 2.1.2, page 39).

3.7.1.3 Animals

Male hooded Lister rats (Harlan) weighing between 288 and 444g (n = 10), were housed in pairs in a temperature regulated room maintained at 20°C with a 12 hour light/dark cycle. Lights on at 8:00am. Food and water was available *ad libitum*. Environmental enrichment was provided by the addition of a wooden house to the cage. All procedures were carried out in accordance with Home Office regulations.

3.7.1.4 Surgical protocol

Surgery was performed as previously described (see section 2.2.1, page 45). Briefly; animals were anaesthetised by the inhalation of isoflurane (Abbott Animal Health) and mounted in a stereotaxic frame using atraumatic earbars (David Kopf Instruments). Analgesia was omitted since the surgery was performed without recovery. Body temperature was maintained using a small heatpad (Fine Science Tools Inc.). A single rostral-caudal incision was made, the skull exposed and bregma identified. 1mm diameter burr holes were drilled at the following coordinates (RC; -2.04mm, ML; ±2.43mm) (Paxinos & Watson, 2007).

The dura beneath the holes was excised with a small needle. Deep brain electrodes were implanted through the holes, bilaterally, at 20° to the perpendicular, in the coronal plane, into the mediodorsal thalamic nucleus (DV: ↓5.60mm). All electrodes were secured to screws anchored in the skull using dental cement (Kemdent) and the incision sutured around the implant. Post surgery animals were maintained under the lowest possible level of anaesthetic (isoflurane between 1 and 1.4%) whilst monitored for consciousness via the pedal reflex and tailpinch.

3.7.1.5 Stimulation protocol

Animals were prescribed stimulation to either the right or left hemisphere randomly. Devices were configured to deliver a constant current of 200μA at a frequency of 130Hz delivered in pulses of 100μs duration. Stimulation was delivered unilaterally continuously to the mediodorsal thalamic nucleus for 3 hours to either the left or right hemisphere whilst the contralateral side acted as a control. It is worth noting that the stimulation current employed in the experimental study is twice that used in the pilot study (see section 3.6.1.5, page 61). The reason for this is that it cannot be known whether the IEG response in the pilot study is driven by (a) the initial output of the device (*i.e:* its peculiar waveform, see figure 3.4, page 63) or (b) the total output of the device. Recall that the initial current output from the prototype, due to the turn-on time, may have been as high as 200μA whilst the total output was likely to be lower than that which would have been delivered by a rectangular 100μA pulse. To err on the side of caution stimulation was delivered at 200μA in the experimental study.

3.7.1.6 Euthanasia & dissection

Animals were euthanased, brains dissected, frozen and stored as previously described (see 2.3.1, page 48).

3.7.1.7 Cryotomy & fixation

Brains were sectioned, mounted and fixed as previously described (see 2.3.3.1, page 50). Briefly, 20μm frozen coronal sections were cut, thaw mounted onto poly-L-lysine coated slides, dried and fixed in depolymerised PFA and dehydrated through graded concentrations of ethanol. In the region of the mediodorsal thalamic nucleus electrode tracks were identified as previously described (see section 2.3.2, page 49).

3.7.1.8 Quantification of IEG expression

IEG expression was measured via the *in situ* hybridisation technique described previously (see 2.3.3.2, page 50). Briefly, radio-labelled probes for the detection of *c-fos* and *zif-268* were hybridised to brain sections overnight. After excess probe was washed away the sections were exposed directly to x-ray film for several days. Resulting autoradiograms were then used to measure the relative optical density of a variety of brain regions.

3.7.1.9 Statistical analysis

The ROD of specific anatomical regions in the hemispheres ipsilateral and contralateral to stimulation were compared via a two-tailed paired Student's t-test in `Prism5` (Graphpad Software Inc.) with significance defined at the 5% level. All data are presented as the mean ±SEM.

3.7.2.2 Electrode placements

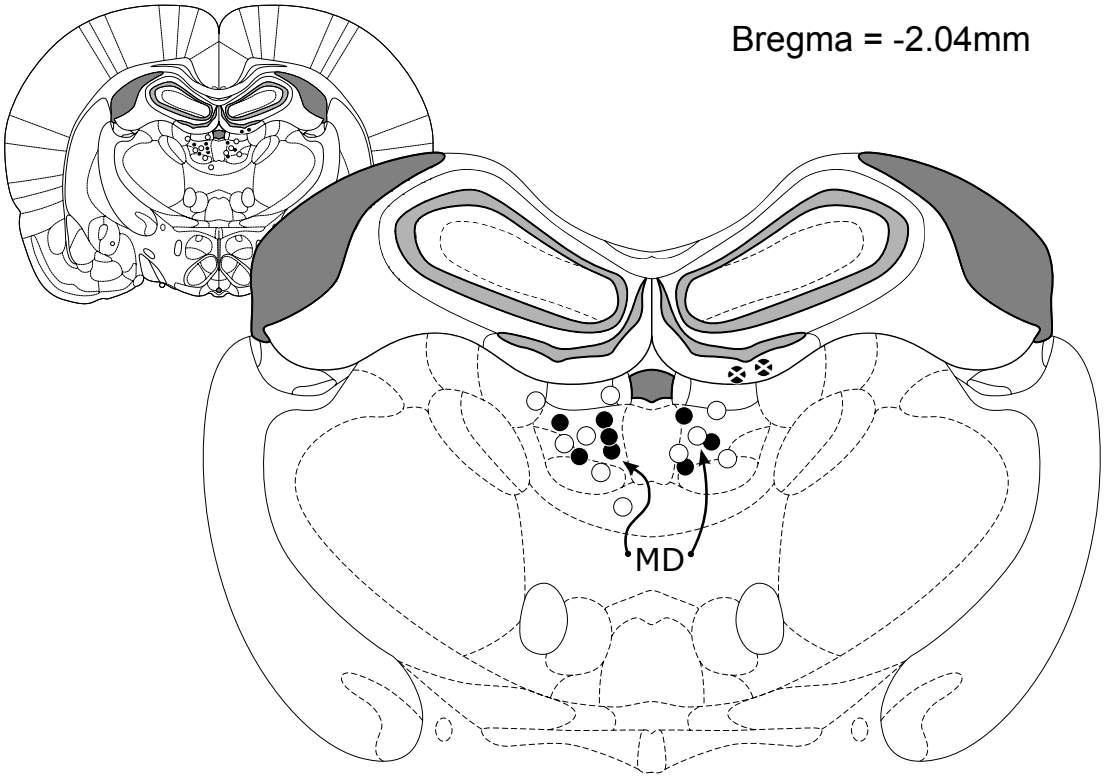

Figure 3.5: Electrode placements. Filled black circles indicate the positions of stimulating electrodes. Open white circles indicate the positions of sham electrodes. Animals were excluded from the analysis if their stimulating electrode was misplaced leading to the exclusion of two animals (n = 8). Misplaced electrode locations may be identified by a filled black circle overlaid with a white '×'.

3.7.2 Results

3.7.2.1 Electrode placements & exclusions

Animals were excluded from the analysis if their stimulating electrode was misplaced leading to the exclusion of two animals (n = 8) (see figure 3.5).

3.7.2.3 *c-fos* expression in mediodorsal thalamic nucleus stimulated rats

No effects of mediodorsal thalamic nucleus stimulation on *c-fos* mRNA expression were observed within any of the brain regions explored. Thus there were no changes in *c-fos* expression apparent at the level of the prefrontal cortex (see figure 3.6, page 71), the caudate-putamen (see figure 3.7, page 72) or the thalamus (see figure 3.8, page 73).

3.7.2.4 *zif-268* expression in mediodorsal thalamic nucleus stimulated rats

Expression of *zif-268* was significantly greater in many of the frontal cortical regions ipsilateral to stimulation when compared to the same regions contralateral to stimulation. Specifically, increases were seen, at the level of the rostral prefrontal cortex, in the prelimbic cortex (↑44%, $p = 0.0015$, $t = 5.056$); the orbital cortices, including the medial orbital cortex (↑56%, $p = 0.0031$, $t = 4.419$), ventral orbital cortex (↑73%, $p = 0.0001$, $t = 7.691$), dorsolateral orbital cortex (↑74%, $p < 0.0001$, $t = 15.000$), lateral orbital cortex (↑70%, $p < 0.0001$, $t = 10.24$) and the secondary motor cortex (↑66%, $p = 0.0012$, $t = 5.274$) (see figure 3.9(a)-(b), page 74). The magnitude of these increases is seen to diminish more caudally with the median increase in regions of the rostral prefrontal cortex = 68% and the median increase in regions of the caudal prefrontal cortex = 28%. Significant increases were also seen, at the level of the caudal prefrontal cortex, in the prelimbic cortex (↑23%, $p = 0.0079$, $t = 3.679$), cingulate cortex - area 1 (↑26%, $p = 0.0052$, $t = 4.003$), secondary motor cortex (↑31%, $p = 0.0057$, $t = 3.928$) and ventral orbital cortex (↑27%, $p = 0.0196$, $t = 3.013$) although no significant changes were detected in the caudal lateral orbital cortex or the infralimbic cortex (see figure 3.9(c)-(d), page 74)

Examination of autoradiograms from increasingly more caudal sections reveals no significant changes in any brain regions (see figures 3.10 - 3.11, page 75), including regions that more rostrally showed highly significant increases (secondary motor cortex, cingulate cortex - area 1, cingulate cortex - area 2 (see figures 3.9, page 74 and 3.10(b) - 3.10(d), page 75 for comparison). In addition no changes are observed in the accumbens core or accumbens shell (see figure 3.10(b), page 75) - a major recipient of prefrontal cortex efferents. No effects of stimulation were observed within the thalamus (reuniens thalamic nucleus, reticular thalamic nucleus, mediodorsal thalamic nucleus, centromedian thalamic nucleus and paratenial thalamic nucleus), hippocampus (CA1, CA2 and CA3 regions) or the amygdala (basolateral amygdaloid nucleus, lateral amygdaloid nucleus and centeromedial amygdaloid nucleus) (see figure 3.11, page 76).

These findings are summarised in figure 3.12 on page 77. Deep brain stimulation of the mediodorsal thalamic nucleus with parameters known to be of therapeutic benefit in diseases such as Parkinson's disease (F, 130Hz; PW, 100μs; A, 200μA) yields significant increases in the expression *zif-268* but not *c-fos* restricted to regions of the prefrontal cortex. These increases are seen to be largest in magnitude

in regions of the rostral prefrontal cortex with smaller significant increases found in regions of the caudal prefrontal cortex and no significant increases evident in other regions of the brain.

c-fos **expression at the level of the prefrontal cortex**

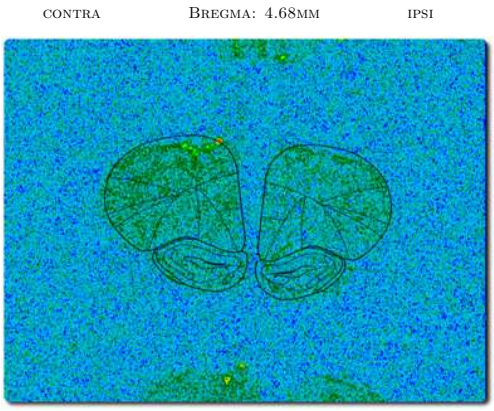

(a) Autoradiogram at the level of the rostral PFC

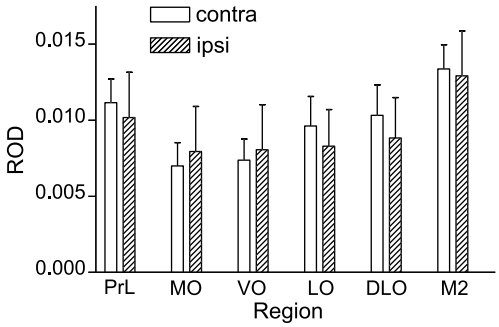

(b) ROD at the level of the rostral frontal cortex

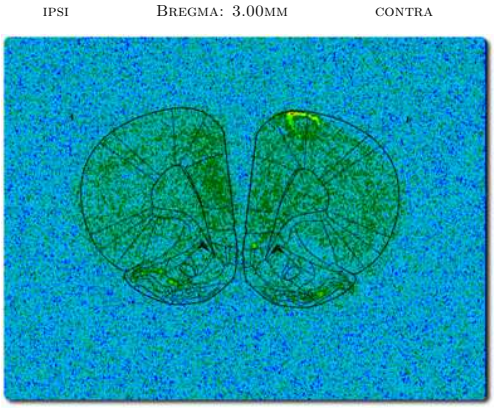

(c) Autoradiogram at the level of the caudal frontal cortex

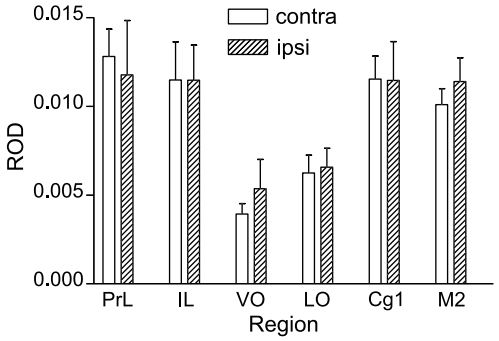

(d) ROD at the level of the caudal PFC

Figure 3.6: Effects of mediodorsal thalamic nucleus stimulation on the expression of *c-fos* in the regions of the prefrontal cortex in male hooded Lister rats. (a) and (b) depict an example autradiogram of a brain section at the level of the rostral prefrontal cortex and the measured relative optical density of the regions within it respectively. (c) and (d) depict an example autradiogram of a brain section at the level of the caudal prefrontal cortex and the measured relative optical density of the regions within it respectively. No changes are detected in any of the frontal cortices ipsilateral (ipsi) to stimulation when compared to the same regions contralateral (contra) to stimulation. Results are presented as the mean ±SEM (n = 8). **Abbreviations:** PrL, prelimbic cortex; MO, medial orbital cortex; VO, ventral orbital cortex; LO, lateral orbital cortex; DLO, dorsolateral orbital cortex; M2, secondary motor cortex; IL, infralimbic cortex; Cg1, cingulate cortex - area 1; ROD, relative optical density.

c-fos **expression at the level of the caudate putamen**

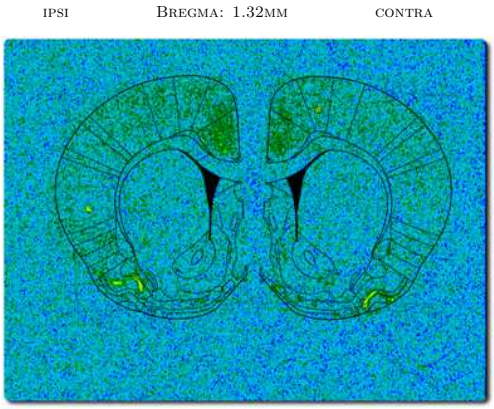

(a) Autoradiogram of a brain section at the level of the striatum

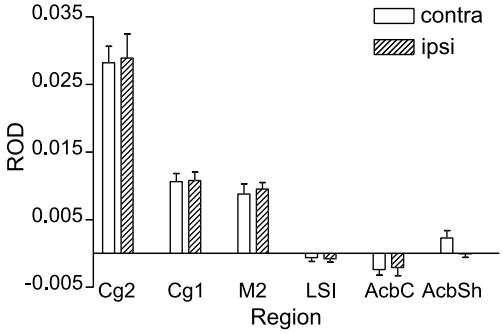

(b) ROD at the level of the striatum

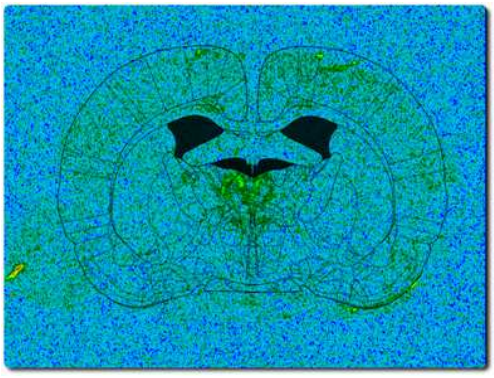

(c) Autoradiogram of a brain section at the level of the pallidum

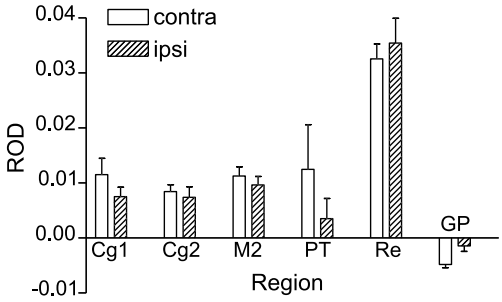

(d) ROD at the level of the pallidum

Figure 3.7: Effects of mediodorsal thalamic nucleus stimulation on the expression of *c-fos* at the level of the caudate putamen in male hooded Lister rats. (a) and (b) depict an example autradiogram of a brain section at the level of the striatum and the measured relative optical density of the regions within it respectively. (c) and (d) depict an example autradiogram of a brain section at the level of the pallidum and the measured relative optical density of the regions within it respectively. No changes are detected in any of the regions of interest ipsilateral (ipsi) to stimulation when compared to the same regions contralateral (contra) to stimulation. Results are presented as the mean ±SEM (n = 8). **Abbreviations:** Cg2, cingulate cortex - area 2; Cg1, cingulate cortex - area 1; M2, secondary motor cortex; LSI, lateral septal nucleus, intermediate part ; AcbC, accumbens core; AcbSh, accumbens shell; PT, paratenial thalamic nucleus; Re, reuniens thalamic nucleus; GP, globus pallidum; MD, mediodorsal thalamic nucleus; CM, centromedian thalamic nucleus; CeM, ; BLA, basolateral amygdala; ROD, relative optical density.

c-fos expression at the level of the thalamus

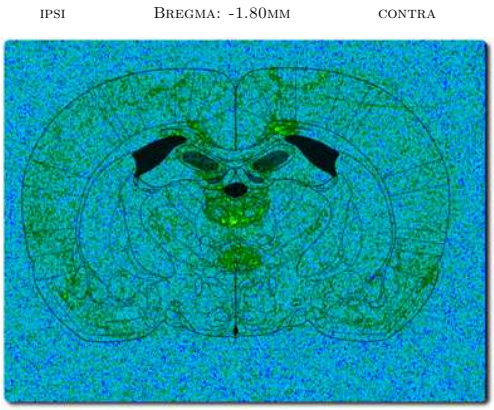

(a) Autoradiogram of a brain section at the level of the thalamus

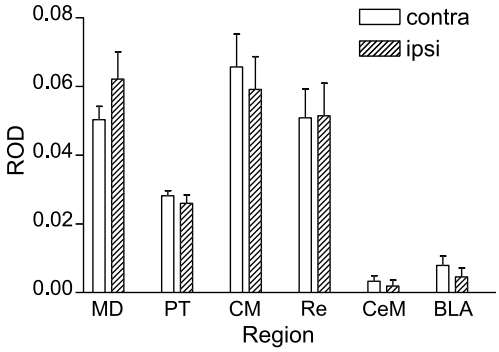

(b) ROD at the level of the thalamus

Figure 3.8: Effects of mediodorsal thalamic nucleus stimulation on the expression of *c-fos* in the regions of the thalamus and basolateral amygdaloid nucleus in male hooded Lister rats. (a) and (b) depict an example autradiogram of a brain section at the level of the mediodorsal thalamic nucleus and the measured relative optical density of the regions within it respectively. No changes are detected in any of the regions of interest ipsilateral (ipsi) to stimulation when compared to the same regions contralateral (contra) to stimulation. Results are presented as the mean ±SEM (n = 8). **Abbreviations:** PT, paratenial thalamic nucleus; Re, reuniens thalamic nucleus; MD, mediodorsal thalamic nucleus; CM, centromedian thalamic nucleus; CeM, central amygdaloid nucleus, medial part; BLA, basolateral amygdaloid nucleus; ROD, relative optical density.

zif-268 expression at the level of the prefrontal cortex

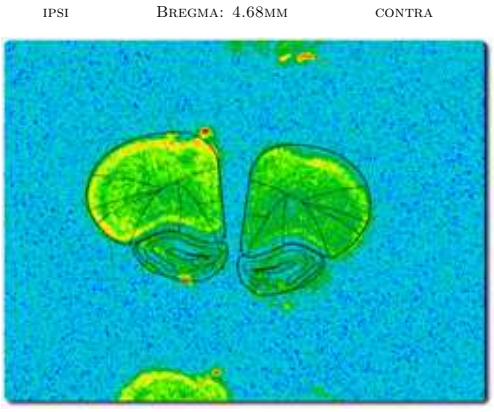

(a) Autoradiogram of a brain section at the level of the rostral frontal cortex

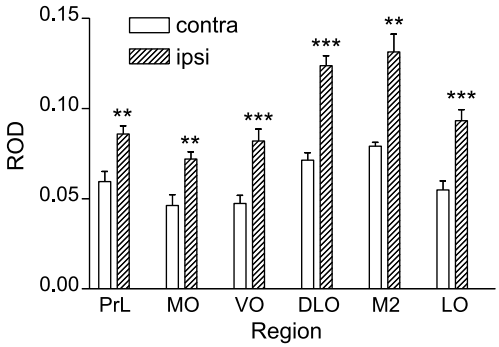

(b) ROD at the level of the rostral frontal cortex

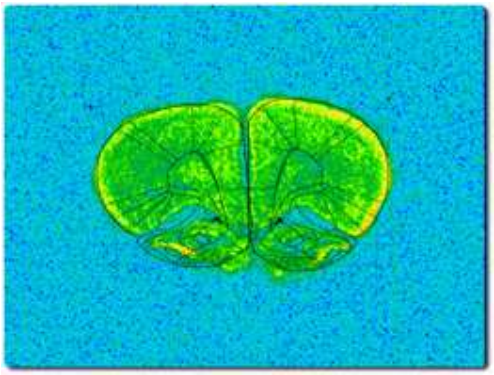

(c) Autoradiogram of a brain section at the level of the caudal frontal cortex

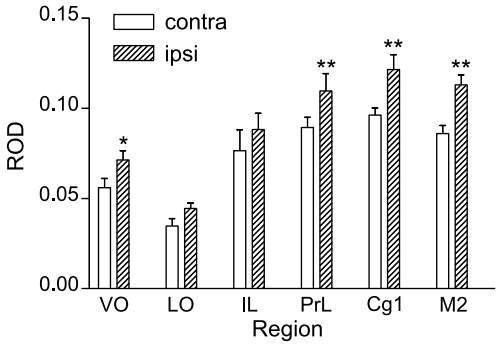

(d) ROD at the level of the caudal frontal cortex

Figure 3.9: Effects of mediodorsal thalamic nucleus stimulation on the expression of *zif-268* in the regions of the prefrontal cortex in male hooded Lister rats. (a) and (b) depict an example autradiogram of a brain section at the level of the rostral prefrontal cortex and the measured relative optical density of the regions within it respectively. (c) and (d) depict an example autradiogram of a brain section at the level of the caudal prefrontal cortex and the measured relative optical density of the regions within it respectively. Significant increases are seen in all of the frontal cortices ipsilateral (ipsi) to stimulation when compared to the same regions contralateral (contra) to stimulation. Results are presented as the mean ±SEM (n = 8). Specifically, increase are seen in the prelimbic cortex (PrL; $p < 0.01$); the orbital cortices, medial orbital cortex (MO; $p < 0.01$), ventral orbital cortex (VO; $p < 0.001$), dorsolateral orbital cortex (DLO; $p < 0.001$), lateral orbital cortex (LO; $p < 0.001$) and the secondary motor cortex (M2; $p < 0.001$) at bregma = 4.68mm. The magnitude of these increases is seen to diminish more caudally with significant increases seen in the prelimbic cortex (PrL; $p < 0.01$), cingulate cortex - area 1 (Cg1; $p < 0.01$), secondary motor cortex (M2; $p < 0.01$) and ventral orbital cortex (VO; $p < 0.05$) at bregma = 3.00mm. $\star = p < 0.05$, $\star\star = p < 0.01$, $\star\star\star = p < 0.001$. ROD, relative optical density.

zif-268 expression at the level of the caudate-putamen

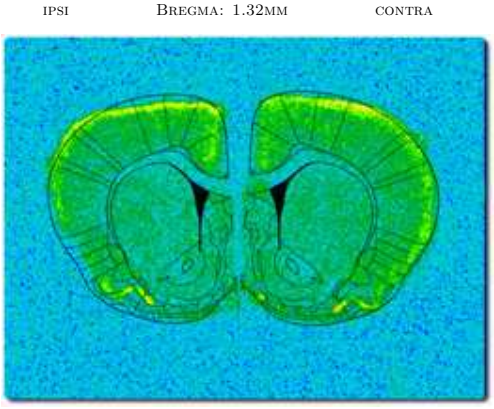

(a) Autoradiogram of a brain section at the level of the striatum

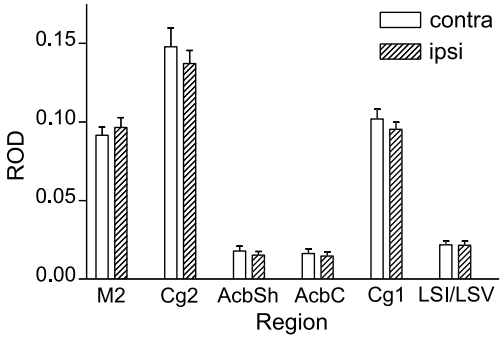

(b) ROD at the level of the striatum

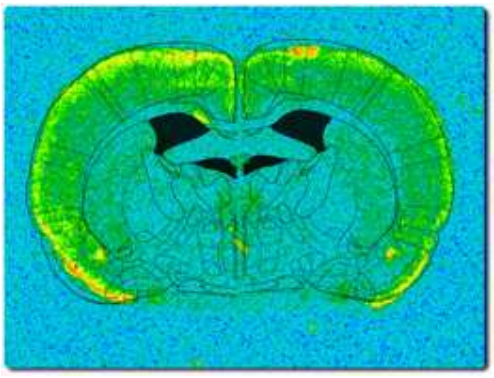

(c) Autoradiogram of a brain section at the level of the pallidum

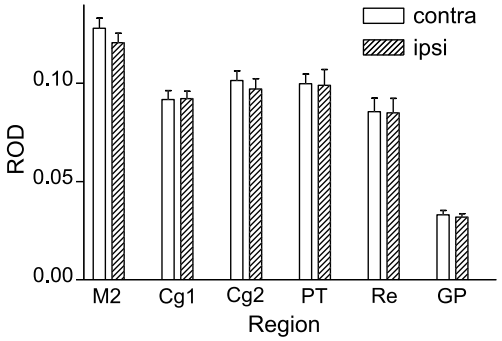

(d) ROD at the level of the pallidum

Figure 3.10: Effects of mediodorsal thalamic nucleus stimulation on the expression of *zif-268* in the regions of the prefrontal cortex in male hooded Lister rats. (a) and (b) depict an example autradiogram of a brain section at the level of the striatum and the measured relative optical density of the regions within it respectively. (c) and (d) depict an example autradiogram of a brain section at the level of the pallidum and the measured relative optical density of the regions within it respectively. No significant changes are seen between the hemisphere ipsilateral (ipsi) to stimulation when compared with the hemisphere contralateral (contra) to stimulation. Results are presented as the mean ±SEM (n = 8). **Abbreviations:** M2, secondary motor cortex; Cg2, cingulate cortex - area 2; Cg1, cingulate cortex - area 1; AcbSh, accumbens shell; AcbC, accumbens core; LSI, lateral septal nucleus, intermediate part; LSV, lateral septal nucleus, ventral part; PT, paratenial thalamic nucleus; Re, reuniens thalamic nucleus; GP, globus pallidum; ROD, relative optical density

zif-268 **expression at the level of the thalamus**

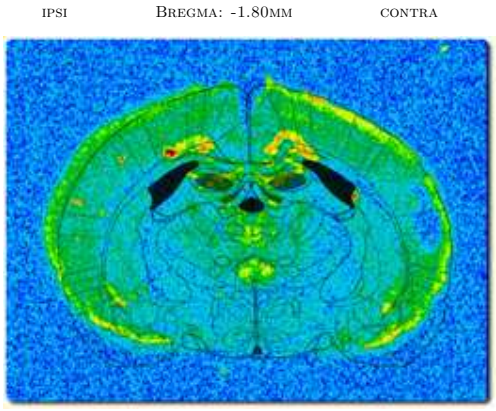

(a) Autoradiogram of a brain section at the level of the thalamus

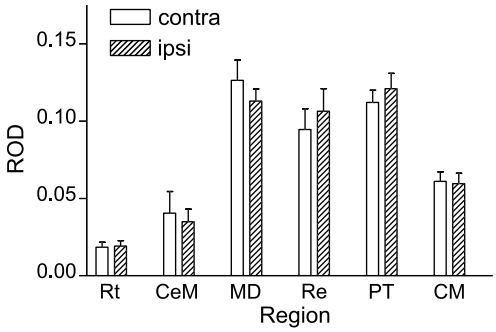

(b) ROD at the level of the thalamus

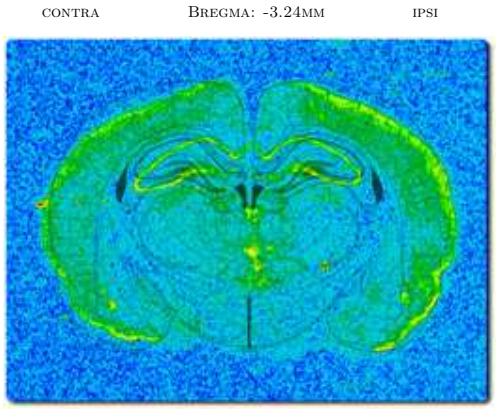

(c) Autoradiogram of a brain section at the level of the rostral hippocampus

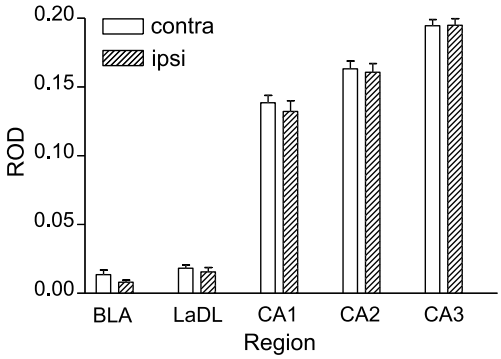

(d) ROD at the level of the rostral hippocampus

Figure 3.11: Effects of mediodorsal thalamic nucleus stimulation on the expression of *zif-268* in the regions of the prefrontal cortex in male hooded Lister rats. (a) and (b) depict an example autradiogram of a brain section at the level of the thalamus and the measured relative optical density of the regions within it respectively. (c) and (d) depict an example autradiogram of a brain section at the level of the hippocampus and the measured relative optical density of the regions within it respectively. No significant changes are seen between the stimulated and non stimulated hemisphere. Results are presented as the mean ±SEM (n = 8). **Abbreviations:** Rt, reticular thalamic nucleus; CeM, central amygdaloid nucleus, medial part; MD, mediodorsal thalamic nucleus; Re, reuniens thalamic nucleus; PT, paratenial thalamic nucleus; CM, centromedian thalamic nucleus; BLA, basolateral amygdaloid nucleus; LaDL, lateral amygdaloid nucleus, dorsolateral part; CA1, CA1 region of the hippocampus; CA2, CA2 region of the hippocampus; CA3, CA3 region of the hippocampus; ROD, relative optical density.

Summary of significant of findings

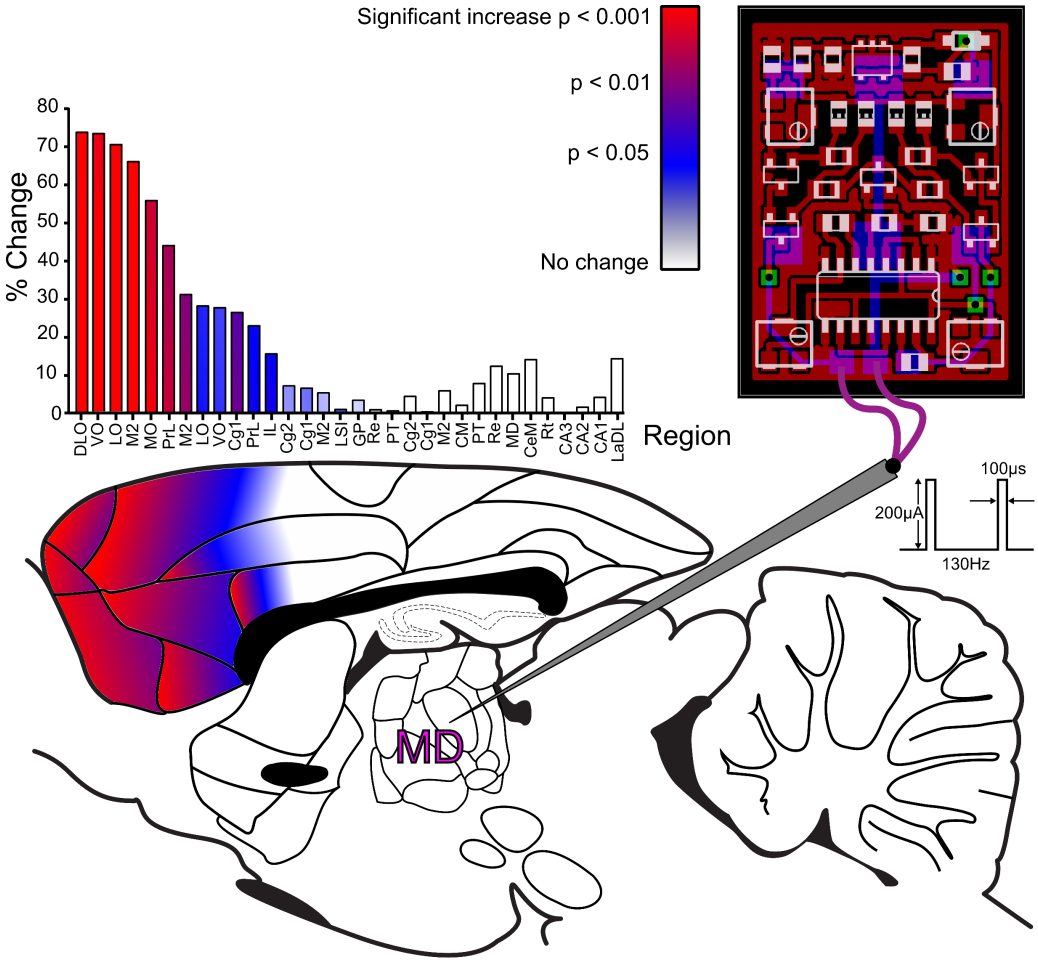

Figure 3.12: IEG summary. The percentage change in neuronal activity as assessed by the expression of *zif-268* is arranged rostral-caudally along the x-axis. The experimental set-up and results are displayed schematically - electrodes were implanted in the mediodorsal thalamic nucleus. Stimulation was delivered with an amplitude of 200µA, at a frequency of 130Hz with pulses 100µs in duration using custom designed and manufactured DBS devices. The graduated colours indicate the level of activity and give an approximate idea of the antomical distribution of these changes.

3.8 Discussion

High frequency stimulation (F, 130Hz; PW, 100μs; A, 200μA) of the mediodorsal thalamic nucleus results in the altered expression of mRNA encoding *zif-268* but not *c-fos*. These increases were apparent only in frontal cortical regions. Specifically, highly significant increases were detected in the medial, ventral, lateral and dorsolateral orbital cortices; the secondary motor cortex and the prelimbic cortex. The magnitude of these increases diminishes in sections taken more caudally. The more caudal sections also indicate significant increases in the cingulate cortex - area 1. No further increases in the expression of *zif-268* mRNA were found in brains regions other than those described including regions of the thalamus, hippocampus and amygdala. These increases suggest that HF DBS of the mediodorsal thalamic nucleus yields biochemical activation of neurons in the efferent targets of the mediodorsal thalamic nucleus. However, no changes were detected in the expression of *c-fos* mRNA - another marker of neuronal activation. These apparently contradictory statements, and there resolution, are considered in greater detail below (see section 3.8.2, page 82).

Induction of IEGs is unlikely to reflect a "microlesion" effect related to tissue damage associated with electrode implantation. Electrodes were implanted bilaterally into the mediodorsal thalamic nucleus although stimulation was delivered unilaterally to either the left or right hemisphere. The experimental design cannot explicitly rule out IEG induction due to electrode insertion since any such induction would presumably be manifest bilaterally. In addition this experiment cannot explicitly exclude IEG induction as a consequence of anaesthetic administration since again it is presumable that any such induction would be manifest bilaterally. Whilst either of these potential confounds may contribute to the IEG expression observed in this experiment their effects are controlled for by comparison of differently stimulated hemispheres from the same animal. Electrode implantation and anaesthesia may provoke bilateral IEG induction but it is only the unilateral induction due to stimulation that can account for the difference in induction between hemispheres. This said the observations reported here should probably be considered an interaction between the bilateral effects (anaesthesia, micro-lesion) and the unilateral effect (DBS). Anaesthesia is known to effect the induction of IEGs (Hamaya *et al.*, 2000) and the extent to which isoflurane anaesthesia effects the magnitude of the response cannot be determined in the present experiments. Furthermore it is impossible to account for any effects of stimulation that may manifest bilaterally despite the unilateral delivery of DBS.

Indeed where Sun *et al.* (2006) reported greater *c-fos* immunoreactivity in the hemisphere ipsilateral to 10Hz when compared with similar stimulation at 1Hz, it seems apparent that stimulation at higher frequencies (10Hz) elicits a greater *c-fos* immunoreactivity in the hemisphere contralateral to stimulation when compared with non-stimulated controls (see Sun *et al.* (2006)).

The effects in the non-stimulated hemisphere as a result of contralateral stimulation cannot be resolved in this experiment. As such all that can be reported with any certainty is the differences in IEG expression between the hemispheres ipsilateral and contralateral to stimulation.

3.8.1 Reproducibility of the results

The findings of the experimental study confirm the preliminary observations from the pilot study. Whilst the pilot study employed only two animals the detection of increased *zif-268* mRNA expression in the same brain regions in two separate experiments indicate that the effect of HF DBS of the mediodorsal thalamic nucleus is robust and reproducible. Furthermore the pilot and experimental studies harbour interesting methodological differences. As eluded to earlier the stimulation waveform deployed in the pilot study differed in terms of the current output and the shape of the waveform. Indeed the only similarity between the two stimulation waveforms was the frequency, indicating that the response, *in vivo*, is, to some degree, robust to alterations in current and pulse-width suggesting that frequency may be the most significant parameter. In addition the pilot and experimental studies were performed in different strains; sprague-dawley and hooded-lister respectively. The findings in the two strains, at least at the level of the frontal cortices, are strikingly similar indicating that the effects of HF DBS of the mediodorsal thalamic nucleus are reproducible across strains. These findings are the first to map the neural substrates of HF DBS of the mediodorsal thalamic nucleus. The general observation that DBS of subcortical nuclei yields increases in the induction of IEGs in the efferent targets of the stimulated nucleus is largely consistent with the observations reported in similar investigations, and these are discussed below.

Induction of IEGs by DBS is consistent with previous studies. Schulte *et al.* (2006) demonstrated that HFS of the subthalamic nucleus yielded expression of both c-Fos[‡] and Zif-268 (and c-Jun although this is not considered here) at the site of stimulation and in efferent targets of the stimulated nucleus. The observation

[‡]The convention of non-italicised, capitalised names indicates that the measure of IEG ac-

of increased Zif-268 expression in the efferent targets of the stimulated nucleus is consistent with the results reported here.

However the observation of increased c-Fos expression seems in apparent opposition of the findings of this study. It seems likely that this disparity can be ascribed to methodological differences. The ISH procedure used in this study was performed to detect IEG mRNA whereas Schulte *et al.* (2006) probed for the protein products of the expressed IEGs. In general IEG protein products are known to be up-regulated for upto 6 hours whereas the mRNA markers themselves **may** have returned to baseline levels after only 1 or 2 hours. Sun *et al.* (2006) and Shirvalkar *et al.* (2006) have also reported increased *c-fos* mRNA expression in the efferent targets of the stimulated nucleus. Of particular interest, Sun *et al.* (2006) investigated the effects of stimulation of medial thalamic nuclei including the medial, central, lateral and centrolateral subdivisions of the mediodorsal nucleus and reported increased *c-fos* activation in the prelimbic cortex, secondary motor cortex, cingulate cortex - area 1 and cingulate cortex - area 2. As shall be discussed below Sun *et al.* (2006) stimulated the the medial thalamus with low frequencies (1 & 10Hz) although it is unlikely that the apparent discrepancy in *c-fos* mRNA expression between the current study and the study by Sun *et al.* (2006) is due to the different stimulation frequencies. All investigators discussed here have demonstrated IEG induction, presumably as a consequence of increased synaptic output from the stimulated nucleus, regardless of frequency suggesting that IEGs may be a poor discriminator of DBS frequency. Again it seems more likely that time course in the study reported in this chapter (3hr as opposed to 1.5hr (Sun *et al.*, 2006)) was too long for the detection of transiently expressed *c-fos* mRNA. In addition to the *c-fos* induction, Shirvalkar *et al.* (2006) reported *zif-268* induction in the cortical targets of the centerolateral thalamic nucleus in response to HF stimulation (100Hz) of this region. The study by Shirvalkar *et al.* (2006) indicates *c-fos* induction as a consequence of HFS confirming that the differences between the results presented here and those of Sun *et al.* (2006) are more likely to be temporal rather than frequency related in nature.

In contrast with the results reported by Schulte *et al.* (2006), Sun *et al.* (2006) reported these IEG effects in response to low frequency stimulation. Schulte *et al.* (2006) reports no effect of stimulation at a frequency of 5Hz. A direct comparison of subthalamic nucleus and mediodorsal thalamic nucleus stimulation is arguably

tivity was determined through detection of the protein, rather than the mRNA, products of the IEG.

inappropriate and these studies serve as a timely reminder that it is unlikely that DBS has a *singular* mechanism of action. Whilst it *is* likely that there will be some commonality between different stimulation paradigms it is also to be expected that different nuclei respond differently to DBS. These studies both indicate that DBS affects changes in the efferent targets of the stimulated site. The implication being that DBS acts, at least in part, via synaptic mechanisms. The current study confirms this notion and adds particularly to the study by Sun *et al.* (2006) demonstrating that high, as well as low, frequency stimulation of the mediodorsal thalamic nucleus is effective in inducing changes in IEG expression in the efferent targets of the mediodorsal thalamic nucleus. Interestingly the changes in IEG mRNA induction reported by Sun *et al.* (2006) are in significantly more caudal regions of the cortex (Bregma = 2.2mm). The region of the medial thalamus stimulated was also significantly more caudal (Bregma = -3.14mm). The results reported here not only validate these findings but, from these two studies, one may reasonably infer that a relatively large portion of the frontal cortices (Bregma = <4.68mm $\rightarrow$ >2.2mm) may be activated by stimulation of a reasonably large portion of the medial thalamus (Bregma = -1.80mm $\rightarrow$ -3.14mm).

Schulte *et al.* (2006) also reported increased c-Fos expression at the site of stimulation, an observation corroborated by Salin *et al.* (2002). However this finding has not been reported by all. Henning *et al.* (2007) go further and suggest that the induction of *c-fos* at the site of stimulation reported by Salin *et al.* (2002) is an "artefact caused by electrochemical degradation of the surface of the stainless steel electrodes". Although Schulte *et al.* (2006) fails to report the composition of the electrodes used in his investigation, the bipolar electrodes (SNE-100, Rhodes Medical Instruments, Summerland, CA, USA) are reported to be constructed of stainless steel elsewhere (Degos *et al.*, 2005) indicating that the increases reported by Schulte *et al.* (2006) may also be an electrochemical artifact rather than a direct effect of stimulation. Whilst the electrodes used in this study were supported by stainless steel insect pins current delivery was via the attached nickel-chromium wires. The absence of any current delivery through the stainless steel components should minimise any electrochemical effects at the stainless steel tissue interface. Electrochemical processes at the electrode-tissue interface are unavoidable (Gimsa *et al.*, 2005). The absence of any lateral effects in the mediodorsal thalamic nucleus in the current study indicate that there has been no effect in the stimulated nucleus. This finding lends some support to the contention that IEG upregulation in the stimulated site may be a side effect of stainless steel

electrodes rather than a direct effect of stimulation.

Overall the conclusion that DBS of the mediodorsal thalamic nucleus results in the induction of expression of the mRNA encoding *zif-268* is consistent with similar observations made by Schulte *et al.* (2006) and Shirvalkar *et al.* (2006) and the more general observation that DBS yields induction of IEG expression in the efferent targets of the stimulated nuclei. Whilst the results presented here differ notably from previous studies with respect to *c-fos* mRNA induction it seems plausible that these differences can be ascribed to methodological differences including, time course of experiments and electrode design. This highlights the importance of considering the induction kinetics of various IEGs when designing experiments of this type.

3.8.2 Differential expression of *c-fos* and *zif-268*; a paradox?

3.8.2.1 Is *c-fos* expression too transient for detection after 3 hours?

The absence of expression of *c-fos* mRNA given the large increases in *zif-268* expression seems confounding. There are at least two plausible explanations; either *c-fos* mRNA expression was initially upregulated but returned to basal levels over the time course of the experiment, or there was never any change in *c-fos* mRNA expression. As discussed below what literature there is strongly indicates that DBS results in increased *c-fos* mRNA expression indicating that the former explanation is the more plausible.

Several authors have reported *c-fos* mRNA expression returning to basal levels in less than 2 hours (Tischmeyer *et al.*, 1990; Hamaya *et al.*, 2000; Zangenehpour & Chaudhuri, 2002). The induction of *c-fos* mRNA seems to habituate such that repeated stimulation results in only transient induction (see Kovács 1998). Perhaps the demonstration with the greatest relevance to the current discussion is that detailed by Zangenehpour & Chaudhuri (2002). This study demonstrates that both *c-fos* and *zif-268* mRNA expression induced by photic stimulation in the rat visual cortex peaks after only 30 minutes. After 120 minutes, expression of *c-fos* mRNA returns to baseline whereas expression of *zif-268 mRNA* remains near peak levels for the maximum duration studied (6 hours). Similar differential patterns of *c-fos* and *zif-268* mRNA expression in the visual cortex of rats are echoed elsewhere (Yamada *et al.*, 1999). Whilst the precise function of IEGs remains the subject of ongoing research these evidences indicate subtly different

roles for the IEGs *c-fos* and *zif-268* as markers of neuronal activity. *c-fos* seems to be only expressed transiently in response to continuous stimulation whereas *zif-268* seems to give a "running commentary" on ongoing synaptic activity. In other words *c-fos* may differentiate synaptic inputs providing a marker of *changes* in the inputs. *zif-268* however may provide a marker of simply whether or not inputs are active regardless of whether or not the inputs were previously active. In the context of the results reported here the differential IEG expression can be putatively explained by speculating that *c-fos* mRNA was induced in response to the initiation of DBS. Continuous HF DBS provided an increased but unchanging input to the frontal cortices and this increased synaptic input to the frontal cortices resulted in increased expression of *zif-268* - a putative marker of ongoing activity. However given the continuous nature of the stimulation no *change* in the synaptic inputs can be detected. As such *c-fos* expression - a putative marker of change in synaptic input - returns to basal levels.

However the time course of the experiment (3 hours) is insufficient to assert this with certainty so the possibility that *c-fos* expression was never upregulated must also be considered. An obvious extension to the current experiment would be to examine the protein products transcribed by *c-fos*. If *c-fos* has been upregulated in the past it is to be expected that its protein products (c-Fos) will persist for well in excess of 3 hours.

3.8.2.2 *zif-268* as a marker of LTP

Long-term potentiation (LTP) is the term used to described the activity dependent increase in synaptic efficacy. LTP can be further categorised depending on its duration; LTP1, approximately 2 hours; LTP2, approximately 4 days and LTP3, approximately 23 days although LTP lasting months has also been reported. The latter, LTP2 and LTP3, both require gene transcription and protein synthesis whereas LTP1 does not (see Knapska & Kaczmarek 2004). Various stimulation paradigms that generate the induction of LTP also result in the increased expression of *zif-268* mRNA but not in the expression of *c-fos* mRNA (see Hughes & Dragunow 1995; Davis *et al.* 2003). Whilst LTP data are most commonly derived from hippocampal studies similar results have been reported in thalamo-cortical circuits (see Davis *et al.* 2003). Invocation of LTP as the primary phenomenon reported here provides an alternative explanation for the discrepant *c-fos* and *zif-268* expression. However the literature supporting the role of *zif-268* in LTP, particularly in thalamo-cortical architectures, is relatively

sparse although Jones *et al.* (2001) report that *Zif-268* is required for the expression of late LTP and long-term memories. On the other hand, the weight of evidence in favour of the earlier argument - that of unapparent *c-fos* expression due to its temporal dynamics in response to unchanging stimuli - seems more compelling. That said the role of *zif-268* in synaptic plasticity should not be overlooked and it is a topic to which this discussion shall return in due course (see section 3.8.3).

3.8.3 Functional implications

The observation of increased expression of IEG mRNA in the frontal cortices is consistent with the anatomical connectivity discussed in section 1.4 (page 23). However, the pattern of expression is perhaps a little broader than had been initially hypothesised (see section 1.5.2, page 36) with increased IEG expression also seen in more dorsolateral and ventrolateral regions. One may be tempted to conclude that activation of these regions may be a consequence of "secondary" activation from increased outflow from the "activated" medial regions (see figure 1.3, page 27). However if this were the case then one would presumably expect to see increased activity in other efferent targets of the prefrontal cortex. A major target of the prefrontal cortex is the ventral striatum. The results reported in this chapter indicate no increased IEG expression in either the accumbens core or the accumbens shell. Indeed, the results reported here provide no evidence for increased cortical output as a result of the "activation" inferred from the increased induction of the *zif-268* mRNA, a point to which this discussion shall return shortly. Perhaps the more parsimonious explanation for increased induction of *zif-268* mRNA in the more dorsolateral and ventrolateral regions of the prefrontal cortex is simply "co-activation" of neighbouring thalamic nuclei. The midline thalamic nuclei of the rat are small and it is likely that stimulation of the mediodorsal thalamic nucleus was sufficiently large as to affect nuclei adjacent to the mediodorsal thalamic nucleus. The nuclei of the midline thalamus project to the prefrontal cortex in a topographic manner so co-activation of more lateral thalamic nuclei would likely result in a downstream response in the more lateral regions of the frontal cortex. Indeed, as discussed above, activation of the frontal cortex appears to be achievable via stimulation of a relatively large portion of the medial thalamus.

The activation of the efferent targets of the stimulated nucleus contributes to the growing body of evidence that indicates that DBS, rather than causing a

"functional lesion", actually modulates the activity of efferent nuclei by increasing the synaptic input in these nuclei. Increased neurotransmitter release in response to electrical stimulation of brain nuclei is well established (Windels *et al.*, 2000, 2003; Florin-Lechner *et al.*, 1996; Hiller *et al.*, 2006). Of particular interest Guillazo-Blanch *et al.* (2008) has reported increased glutamate release in the medial prefrontal cortex as a consequence of high frequency electrical stimulation (100Hz) of the parafasicular thalamic nucleus. The IEG results reported here and elsewhere support that DBS acts, at least in part, by synaptic mechanisms mediated by neurotransmitter release. As eluded to above the increased expression of IEGs, despite being indicative of an increase in neural "activity", does not necessarily indicate an increase in electrophysiological activity. The results from this study contain no indications of activation of the efferent targets of the frontal cortices. The absence of increased IEG expression in such nuclei, by the arguments presented throughout this chapter, implies that these targets have not received increased afferent input. From this one can logical infer that the output from the prefrontal cortex must have remained unaltered throughout this experiment.

The results indicate an increase in glutamatergic neurotransmission in the prefrontal cortex and one may superficially expect that an increase in excitatory input in the prefrontal cortex would naturally generate an increase in cortical output. These results are insufficient to make any hard conclusions but given that the thalamic afferents in the prefrontal cortex synapse onto both glutamatergic pyramidal cells and GABAergic interneurons in layers II and III of the cortex, then the increase in IEG expression may then plausibly represent an increase in activity in both glutamatergic and GABAergic cell types with a net excitatory/inhibitory influence that is insufficient to generate an output. It would be another logical extension to the molecular biological aspects of this continuing research to investigate the modulation of markers of GABAergic interneuron activity. Parvalbumin, although not an IEG, provides such a marker and is detectable using the *in situ* hybridisation techniques detailed earlier (see 2.3.3.2, page 50). It would also be of interest to examine the effects of this DBS paradigm in a situation in which there is diminished inhibitory influence through say the action of PCP. This thesis returns to this idea in later chapters (see 5, page 136).

An increase in neuronal activity without an increase in neuronal output may appear counter-intuitive but in reality simply serves as a reminder that IEGs *must*

reflect something other than electrophysiological activation. Neurons integrate, over a subsecond timescale, the action potentials from tens to thousands of discrete inputs and generate a single binary output. The timescale for the induction of IEGs is at best minutes, with the timescale for their protein products and for delayed early genes being significantly longer. The timescale alone is sufficient to argue that IEG induction contributes little to the generation of action potentials and cellular output, the implication being that IEG induction is a marker restricted to the detection of activity at synaptic inputs. Viewed in this context the somewhat classical interpretation, that expression of IEG mRNA can be used to map regions of neuronal activation seems vague. Despite this the literature supporting this approach is relatively mature and populated with an abundance of almost universally accepted publications confirming this methodology as a useful means by which to map the neural response to a particular intervention. IEG expression, as a precursor to changes in the genomic response, may then be more accurately described as a tool for the mapping of modifications in cellular morphology and plasticity. It is interesting to speculate, given this context, what the functional consequences of increases in *zif-268* may be in terms of the thalamo-cortical system investigated in this thesis. Alterations in LTP serve to modulate the influence of a particular neural pathway. If one considers that the increases reported here may reflect an increase in LTP then it is plausible to suggest that DBS of the mediodorsal thalamic nucleus, rather than simply increasing neural activity in the prefrontal cortex, may have increased the sensitivity of the prefrontal cortex to its input from the mediodorsal thalamic nucleus, through the potentiation of the thalamo-cortical inputs. Given the decrement in this particular pathway seen in schizophrenia such an increase in sensitivity may have therapeutic benefits.

3.8.4 Caveats & Extensions

Whilst discussed above it is important to stress the limitations of this experiment explicitly. The design of this experiment, despite being based upon the methods published by Schulte *et al.* (2006) are not beyond criticism. This experiment provides no control for effects in the hemisphere contralateral to stimulation. To account for this conclusively a significantly larger experiment should be performed containing 5 groups of 10 animals. These groups would be (a) a completely naive group, devoid of electrode implants and (obviously) stimulation, (b) a group which receives electrode implants but no stimulation, (c) a group which receive bilateral implants but unilateral stimulation to the left hemisphere, (d)

a group which receive bilateral implants but unilateral stimulation to the right hemisphere and (e) a group which receive bilateral implants and bilateral stimulation. Such an experiment could resolve any IEG expression caused purely by the implantation, any differences between each unilateral stimulation paradigm, whether there are any contralateral effects and the effects of bilateral stimulation. It is this authors assertion that this much larger experiment would yield very little additional information at the cost of a large number of animals and great experimental effort.

Considerably simpler and arguably of greater interest would be a reanalysis of the existing autoradiograms. The analysis described within this chapter examined the activity within each region as defined by the atlas of Paxinos & Watson (2007). However visual inspection of the autoradiograms indicates that the reported increases are likely to be specific to distinct cortical layers. In particular it appears that expression is mostly greatly increased in layer 1. Cortical layer 1 contains the dendritic arbors of the pyramidal output cells and is also richly populated with a pletora of interneurons. It is also the region in which the thalamic efferents terminate providing a ready explanation as to why increases in IEG expression, as a result of thalamic stimulation, may be most significant in this layer. However these experiments are unable to determine precisely where these increases occur; are they in the the synaptic terminals of the thalamic efferents, the dendrites of the output neurons or do they manifest in the interneurons? A significantly more refined technique would be required to answer such questions.

Whilst it is interesting to speculate it is important to remember that the aim of this experiment was to map the neural substrates of mediodorsal thalamic nucleus stimulation using techniques that are widely accepted as appropriate. To this end this experiment has identified the frontal cortices as the primary area of activation as a result of mediodorsal thalamic nucleus stimulation. This activation is explored further in the following chapter through spectral analysis of the electro-corticogram.

Part III

Electro-encephalography/corticography

Chapter 4

Investigation into the effects of sub-chronic administration of PCP in rats on the electrocorticogram and the influence of mediodorsal thalamic nucleus DBS

4.1 Introduction

The previous chapter served to demonstrate increases in cellular activity, as a result of high frequency stimulation of the mediodorsal thalamic nucleus, via the increased expression of the immediate early gene *zif-268* localised to the frontal cortices. However the nature, particularly any temporal dependencies, of this activation remains unclear given the nature of these markers. The electroencephalogram (EEG), first described in humans in 1929 (Bear *et al.*, 2001) provides a relatively simple, non-invasive, real-time means to investigate cortical activity and its analysis is likely to further elucidate the effects of the thalamic stimulation explored in this thesis. This chapter describes the methods developed to record the EEG in the anaesthetised rat and reports the results in terms of modulation in power in the delta and theta wave bands. The effects of high frequency mediodorsal thalamic nucleus stimulation in both normal animals and animals treated with sub-chronic PCP are detailed. Furthermore these experiments act to further validate the sub-chronic PCP model as a putative animal model for

the investigation of schizophrenia-like deficits in cortical activity.

4.1.1 Electrical activity in the brain

The activity of neuronal populations can be measured electrically in multiple modalities, including:

Single unit activity: The recording of spontaneous and evoked action potential firing can be recorded providing a measure of cellular *output*. Isolated action potentials contribute little, if not at all, to the recorded EEG (Fisch, 1999).

Local field potentials (LFP): LFPs record the summed postsynaptic potentials of localised neuronal populations and are thought to reflect the summed activity of the *input* to a region.

Electro-corticography (ECoG): The ECoG is essentially a LFP recorded from the surface of the cortex reflecting summed activity of the *input* to a cortical region.

Electro-encephalography (EEG): The EEG is essentially the ECoG but recorded from the surface of the scalp rather than the cortex thus suffering greater attenuation.

EEG recording in humans is non-invasive. Recordings in rodents is typically invasive with electrodes implanted in the skull (ECoG) or the brain (LFP) to improve the signal-to-noise ratio and spatial resolution. Whilst these modalities (LFP, ECoG, EEG) are methodologically distinct they are at least functionally similar, in that they all reflect summed postsynaptic potentials of the neuronal populations they record from. Thus the discussion of the experiments described in this chapter are not limited to discussion of the output variable alone (ECoG) but also include consideration of EEG and LFP data. There will however be little consideration of single unit activity.

4.1.2 The electroencephalogram

The EEG is a measure of the difference in voltage, associated with the central nervous system, between electrodes located on the scalp relative to a nearby reference point. Thus Fisch (1999) defines the EEG as *"the difference in voltage between two different recording locations plotted over time"*.

4.1.2.1 The origin of the EEG

The voltage recorded between EEG electrodes primarily represents the summation of inhibitory and excitatory postsynaptic potentials of pyramidal cells generated in the cortex (Fisch, 1999; Bear *et al.*, 2001). The electrical contribution of a single neuron is vanishingly small and is further attenuated as it propagates through the tissues separating the source and the recording electrodes. It follows that an observable EEG must reflect the summation of the *synchronous* activity of many cells. Postsynaptic potentials arise as a result of either the depolarization or hyperpolarization of the postsynaptic membrane due to the effects of neurotransmitter release (Martini, 2001). The potential difference between the postsynaptic membrane portion and other regions of the neuron cause an electric current to flow in the extracellular space.

The architecture of the cerebral cortex is ideally suited for the summation of the these postsynaptic potentials and thus the generation of an observable EEG. Cortical pyramidal cells are organised in columns oriented perpendicular to the cortical surface spanning the cortical layers between the white matter and the brain surface (Feldman *et al.*, 1997). Subpopulations of these neurons receive similar input and, therefore, generate similar extracellular currents. A single afferent axon may contact thousands of pyramidal cells yielding postsynaptic potentials with similar polarity and timing. These pyramidal cells are densely packed with their dendrites pervading the cortex thus guiding the current flow driven by postsynaptic potentials through its extent (Fisch, 1999). Thus many cells receiving similar input generate individual potentials that sum over space and propagate towards the cortical surface generating an observable EEG.

4.1.3 Recording the EEG

The EEG is recorded via the differential amplification of the signals between two electrodes placed on the scalp, *i.e:* the input to any one amplifier consists of the potentials recorded at two different electrode locations and the amplifier's output is the difference between these potentials. This differential amplification is employed (a) because it is impossible to place a reference electrode in an electrically "silent" position and (b) because the subtraction removes the equal contribution from electrical noise present on both inputs, leaving a relatively noise-free recording. As such it is impossible to resolve, from a single channel, whether the recorded potential arises due to the changes in potential at electrode 1, electrode 2 or through contributions from both. As such multichannel recordings from

many electrodes distributed over the scalp are used to better estimate the spatial distribution of cortical potentials. Different combinations of electrode locations are referred to as *montages*, two of which are considered in this chapter. For a full description see Fisch (1999).

4.1.3.1 Common reference montage

The common reference montage is recorded by using the same electrode as the negative input to each amplifier. It has an advantage of minimising the number of electrodes required to record the EEG since only one electrode is required for the negative inputs to all amplifiers. However due to the larger spatial separation between the electrodes connected to the positive and negative inputs the common reference montage records wide spread oscillations, obscuring more localised activity.

4.1.3.2 Bipolar montage

In any one amplifier channel, adjacent electrodes on the scalp form the positive and negative inputs to the amplifier. Given that the negative input is subtracted from the positive, the signals recorded using a bipolar montage filter out widespread activity and provide the best means for recording localised potentials.

4.1.3.3 Montage derivation

Given that the EEG signal from any one channel is the subtraction of the signal from one electrode from the signal from another electrode it is possible to calculate the potentials from electrode combinations that have not been recorded from. By way of example: if a recording was made from electrodes labeled 'A' and'Neg' (refer to figure 4.1, 100) then the recording reflects the difference in voltage between A and Neg, *i.e:* A - Neg. The same follows for the signal recorded between the electrodes labelled 'B' and 'Neg'. The subtraction of the two recorded signals (A - Neg) and (B - Neg) yields;

$$(\mathrm{A} - \mathrm{Neg}) - (\mathrm{B} - \mathrm{Neg}) = \mathrm{A} - \mathrm{Neg} - \mathrm{B} + \mathrm{Neg} = \mathrm{A} - \mathrm{B} \tag{4.1}$$

As such it is possible to compute the signal that would be recorded between electrodes A and B. This has important ramifications in the context of the study described in this chapter. The space available to implant electrodes in the rat skull is limited, so recording with a montage that minimises the number of electrodes required was chosen - the common reference montage. However this montage

has poor spatial resolution and it is the aim of this chapter to best estimate the cortical origin of any effects. The bipolar montage can then be derived, as above, from the common reference montage by subtracting the signals recorded from adjacent electrodes.

4.1.4 Quantitative EEG

The voltage wave form recorded between a pair of electrodes can be represented by a myriad of descriptors for which the reader is directed to Fisch (1999) for a complete description. Of those most frequently reported it is the discussion of rhythmical activity that predominates. The cortical EEG exhibits rhythmical oscillations which are commonly classified by their frequency.

Name	Symbol	Freq.	Associated with
Delta	δ	0 - 4Hz	deep sleep and anaesthesia
Theta	θ	4 - 8Hz	states of meditation, drowsiness and some stages of sleep
Alpha	α	8 - 12Hz	wakeful relaxation with eyes closed
Beta	β	12 - 30Hz	normal waking consciousness
Gamma	γ	30 - 80Hz	cognitive processing and neural synchronisation

The standard nomenclature arises as a result of the chronology in which different bandwidths were described rather than there frequency. Oscillations with frequencies as high as 600Hz have been described (see Herrmann & Demiralp 2005).

The most common technique employed for quantifying EEG data is *spectral analysis* whereby signals in the time domain (amplitude $\times$ time) can be represented in the frequency domain (amplitude $\times$ frequency). This transformation is most commonly computed using Fourier methods - specifically the *fast Fourier transform* (FFT), although other methods exist (wavelet analysis (Roach & Mathalon, 2008)). The *power spectrum* of a signal in the time domain can be computed by calculating the absolute magnitude of its Fourier transform. This representation of the data provides a means to examine the contribution, in terms of power, of different frequency components to the recorded signal. Having derived the power spectrum certain features may be computed to characterise the signal. These include: the absolute band power, the relative band power, the spectral edge frequency, the mean peak frequency and the absolute peak frequency. For details

see Fisch (1999). The data presented in this chapter are concerned with the computation of the relative band power calculated by integrating the power between the two frequencies that define the bandwidth, in this case the delta and theta bands. This power is then expressed as a proportion of the total power beneath a limiting value (in this case 100Hz).

4.1.5 The EEG in schizophrenia

Reports of increased delta activity in schizophrenia patients are consistent across a large number of studies, including studies in treatment naïve schizophrenics. The implication being that these effects are not a consequence of medication. Indeed such is the prevalence of this increase within the literature that Boutros *et al.* (2008) goes as far as to suggest that it may be a useful as a diagnostic marker for the disease. Furthermore the majority of studies agree that this anomaly is largely localised to frontal regions although a small number report spectral EEG anomalies localized to more posterior regions. These differences are more likely attributable to differences between subpopulations of schizophrenics (see Boutros *et al.* 2008). Indeed John (2009) reports higher delta power and reduced theta power in schizophrenics when compared with healthy controls. The observed increase in delta power is more attributable to patients exhibiting negative rather than positive symptoms. Whilst it is the low frequency powers that are of primary interest in this chapter[†] it is important to note that schizophrenics exhibit broad spectral anomalies in their EEG.

In addition to differences in delta power bands, subpopulations of schizophrenia sufferers can be further discriminated by anomalies in the alpha band. John (2009) further subdivides the alpha band into "low" and "high" alpha (8.5-10 and 10.5-12.5Hz respectively) with positive symptoms associated with increases in low alpha and negative symptoms associated with reductions in high alpha. It has been suggested that the alpha rhythm may be a marker for the hypofrontality associated with schizophrenia (Knyazeva *et al.*, 2008). Studies have shown deficits in task dependent gamma activity in schizophrenics as well as reductions in both beta and gamma coherence (see Başar & Güntekin 2008). It has been suggested that reductions in gamma amplitudes correlate with the negative symptoms of schizophrenia whilst the increases in gamma amplitude correlate with the positive symptoms (see Herrmann & Demiralp 2005). Whilst spectral anomalies are commonly reported in schizophrenics it is important to note that they are

[†]Primarily due to effects of anaesthesia in the experimental methods

also reported in a myriad of other neuropsychiatric disorders. Gamma anomalies are associated with epilepsy, ADHD and Alzeimer's disease (see Herrmann & Demiralp 2005).

4.1.6 Modeling deficits associated with schizophrenia

In general there are three principle approaches for modeling some of the deficits associated with schizophrenia in animals (Lodge & Grace, 2009). These include:

Pharmacological models: generated by the administration of pharmacological agents, typically NDMA antagonists including MK-801, PCP and ketamine and dopaminergic agents such as amphetamine.

Genetic models: including mutations in DISC-1 and over expression of the D_2 receptor in the striatum.

Developmental models: including neonatal hippocampal lesions, isolation rearing, maternal infection and MAM-GD17 (administration of a mitotoxin during gestation)

The model explored in this chapter is the pharmacological model first described by Cochran *et al.* (2003). Phencyclidine (PCP) is well known for its ability to replicate, in otherwise healthy humans, a psychosis that closely resembles that seen in schizophrenics (see Morris *et al.* 2005). Whilst acute administration yields a behavioural phenotype that mirrors some of abnormalities associated with schizophrenia (impaired social interaction and cognitive disruption) it is chronic exposure to PCP that is most likely to yield a schizophrenia-like phenotype in man (see Morris *et al.* 2005). As such the paradigm developed by Cochran *et al.* (2003) requires chonic exposure to PCP since it is believed to better model the condition.

The model requires rats to be administered PCP once daily, at 2.58mg.kg^{-1}, for 5 days followed by a 3 day period of no drug administration before testing. This treatment paradigm induces a pattern of metabolic anomalies analogous to those reported in human schizophrenics, primarily metabolic hypofunction in the prefrontal cortex. Furthermore this sub-chronic administration of PCP also yields a reduction in the expression of parvalbumin in the prefrontal cortex, indicating impairment of GABAergic interneurons in the frontal cortices. Coupled with these cellular deficits the model exhibits behavioural deficits akin to those observed in schizophrenia, including cognitive deficits in an attentional set shifting

task (the rodent analogue of the human Wisconsin card sorting task) (Egerton *et al.* (2008), for reviews see Morris *et al.* 2005; Pratt *et al.* 2008).

4.1.7 Experimental aims

The aims of the experiments described herein are:

1. To determine the electrophysiological correlates, in terms of the ECoG, of the phenotype generated by sub-chronic PCP treatment in rats.

2. To determine the effects, by analysis of the ECoG, of high frequency DBS of the mediodorsal thalamic nucleus in both normal (vehicle treated) and "schizophrenic" rats (PCP treated).

4.2 Materials & methods

4.2.1 Stimulation & recording electrodes

Stimulation electrodes were fabricated, tested and sterilised as previously described (see section 2.1.1.1, page 37). ECoG electrodes were fabricated by soldering the female end of a pin, taken from an 8 pin DIL socket (RS Components), to the flat head of a stainless steel screw (M1×2mm (Royem Scientific Limited)). Stainless steel is difficult to solder due to the oxide layer on the surface. To remove this the surface is painted with a drop of phosphoric acid (Sigma-Aldrich) and the solder applied directly to the liquid deposited on the surface. The recording electrodes are then cleaned and sterilised in 70% ethanol.

4.2.2 Deep brain stimulation device

DBS devices were constructed and tested as previously described (see section 2.1.2, page 39).

4.2.3 Animals

Male Hooded Lister rats (Harlan UK Limited) weighing between 360g and 415g (N = 20; PCP treated group, n = 10; Vehicle treated group, n = 10), were housed in pairs in a temperature regulated room maintained at 20°C with a 12 hour light/dark cycle prior to surgery. Lights on at 8:00am. Food and water was available *ad libitum*. Environmental enrichment was provided by the addition of a wooden house to the cage. All procedures were carried out in accordance with Home Office regulations.

4.2.4 Drug administration

Animals were randomly allocated a drug treatment and received either vehicle (0.9% sterile saline administered at $1ml.mg^{-1}$) or PCP.HCl (Sigma-Aldrich) according to the sub-chronic paradigm first described by Cochran *et al.* (2003) ($2.6mg.kg^{-1}$ administered at $1ml.mg^{-1}$ once daily for 5 consecutive days). Subsequent testing was done 72 hours after the final drug administration.

4.2.5 Surgery

Animals were anaesthetised, shaved, mounted in a stereotaxic frame, the scalp resected and bregma identified as previously described (see section 2.2.1, page

45). Local anaesthesia and analgesia were omitted since the surgical procedure was terminal. The small heatpad (Fine Science Tools Inc.) described in previous procedures was found to be the single greatest cause of electrical noise in the ECoG recordings and was not used in this experiment. To maintain the animal's body temperature the whole stereotaxic frame was mounted on top of a large metal cage heater. The metal exterior of the cage heater effectively shields the noise generated by its internal electronics and heating element.

8× 0.8mm diameter holes were then drilled through the skull but without breaching the dura to accommodate the ECoG electrodes; 7 distributed over the left hemisphere and 1 posterior of lambda directly above the cerebellum (see figure 4.1). The recording electrodes were implanted by gripping them with a pair of needle grips and turning them in by hand. The ECoG electrode montage described here makes it impossible to implant a DBS electrode in the ipsilateral hemisphere as previously described (see section 3.7.1.4). In this experiment the stimulating electrode was implanted into the mediodorsal thalamic nucleus ipsilateral to the ECoG electrode montage by driving it through the contralateral hemisphere. As such a ninth 1mm diameter hole was drilled over the contralateral hemisphere. Coordinates for all holes are detailed in table 4.1. All electrodes were secured with dental cement as previously described.

4.2.6 Data acquisition

ECoG data were fed to the amplifier with custom made connectors and cables. Signals were differentially amplified by a Cyberamp 380 computer-controllable 8 channel signal conditioner (Axon Instruments, Inc.) under software control. ECoG signals were AC coupled at 1Hz, amplified with a total gain of 10 000, notch filtered to remove 50Hz noise and low pass filtered at 100Hz. Analogue signals were digitised with a National Instruments laboratory interface card (NI-DAQ (PCI-MIO-16E-1) (National Instruments Corporation)) and recorded with `WinEDR v3.0.0` (Strathclyde Electrophysiology software)[†] sampling at 1kHz.

The ECoG electrodes were arranged in a common reference montage. The 7 electrodes implanted above the left hemisphere formed the positive inputs to 7 differential amplifiers. The 7 negative inputs were all connected to the electrode implanted at lambda. The ground for each amplifier was connected to the ear bars of the stereotaxic frame.

[†]http://spider.science.strath.ac.uk/sipbs/page.php?show=software_winEDR/

Table 4.1: Electrode coordinates for both the ECoG electrodes and DBS electrode. Corrdinates derived from Paxinos & Watson (2007)

	Coordinates (mm)			Cortical contact	
#	**RC**	**ML**	**DV**	**Abrev.**	**Region**
A	+5.16	+1.00	-	M2	secondary motor cortex
B	+3.41	+3.55	-	M1	primary motor cortex
C	+1.66	+1.00	-	Cg1	cingulate cortex - area 1
D	−0.09	+3.55	-	S1FL/ S1HL	primary somatosensory cortex, forelimb/hindlimb
E	−1.84	+1.00	-	M2	secondary motor cortex
F	−3.59	+3.55	-	LPtA	lateral parietal association cortex
G	−5.34	+1.00	-	RSD	retrosplenial dysgranular cortex
-ve	−10.0	0.00	-	5Cb	5^{th} cerebellar lobule
				Deep Brain Target	
DBS	−2.04	−1.20	−5.5	MD	mediodorsal thalamic nucleus

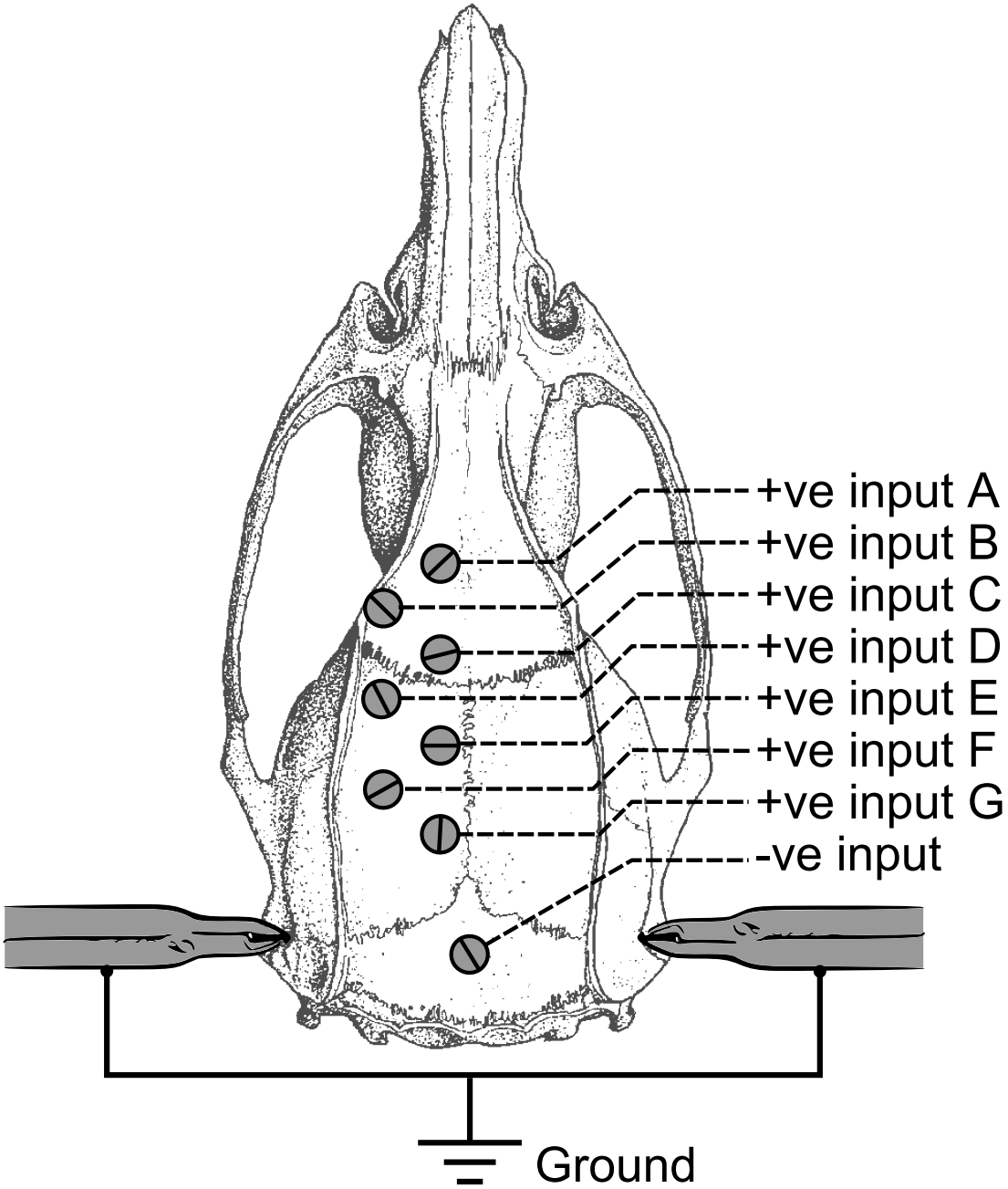

Figure 4.1: Common reference montage electrode placements. The positive inputs to 7 of the differential amplifiers were connected to stainless steel electrodes screwed into the skull overlying a large area of the cortex as shown above. The negative inputs of these 7 amplifiers were all connected to a single stainless steel electrode screwed into the skull above the cerebellum. All 7 of these amplifiers were grounded to connections on the ear bars. Skull diagram adapted from Paxinos & Watson (2007)

4.2.7 Deep brain stimulation & ECoG recording protocol

Devices were configured to deliver a constant current of 200μA at a frequency of 130Hz delivered in pulses of 100μs duration. Devices were tested immediately

before attachment to the animal by connecting them to an oscilloscope and observing the DBS device output waveform. Devices were tested again at the end of the experiment to confirm that they had functioned correctly throughout the experiment. Stimulation was delivered unilaterally to the left hemisphere in all cases.

Baseline ECoG recordings were made for 100 seconds every 5 minutes for 30 minutes. Stimulation (130Hz, 100μs, 200μA) was delivered for a further 90 minutes with 100 second recordings being made every 5 minutes.

Finally the animal was euthanased via anaesthetic overdose whilst continuing to record. Should the recorded signals be of a non-biological origin (*i.e:* noise) anaesthetic overdose will have no effect on the signal. Disappearance of the signals demonstrates that the signals are of a neural origin.

4.2.8 Analysis

Quantitative analysis of oscillating signals is commonly implemented using Fourier methods. However, Fourier methods make assumptions of the data that are violated in the present data set. Specifically the FFT assumes that signals are stationary (non-varying) in time. The signals recorded in this experiment are highly non-stationary, with significant variations in power and frequency over the recording epoch (100s). (see figure 4.2).

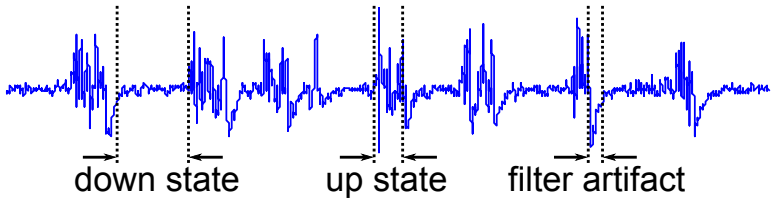

Figure 4.2: An example of an ECoG signal recorded from an isoflurane anaesthetised rat. The signal contains obvious low amplitude 'down' states and high amplitude 'up' states. The transition from an up state to a down state is marked by a large, slow negative going deflection. These deflections are filter artifacts caused as the analog recording electronics recover from the sudden change in the amplitude of the recorded signal.

These variations are of neural origin and reflect the well documented transitions between 'up' and 'down' states observed in the anaesthetised cortex. These large fluctuations induce filter artifacts in the recorded data - these fluctuations are of particular concern when considering the analysis of low frequency signals since

they contribute considerably to the power in these wavebands. Different physiological mechanisms underpin these different states so it is important to analyse these states independently. As such, an algorithm was devised to detect these different states and decompose the original signal into its up-states, down-states and the signal attributable to the filter artifacts.

4.2.8.1 State detection and signal reconstruction

The algorithm was devised and written in Matlab (Matlab) to automatically detect the various state transitions. This was achieved using wavelet methods. The raw signal was decomposed with a daubechies wavelet using a multilevel continuous 1D wavelet transform. The coefficients of a new 1D signal were reconstructed from the wavelet decomposition. The fifth level of detail was used to determine the location of the up states (see figure 4.3) by thresholding the reconstructed signal.

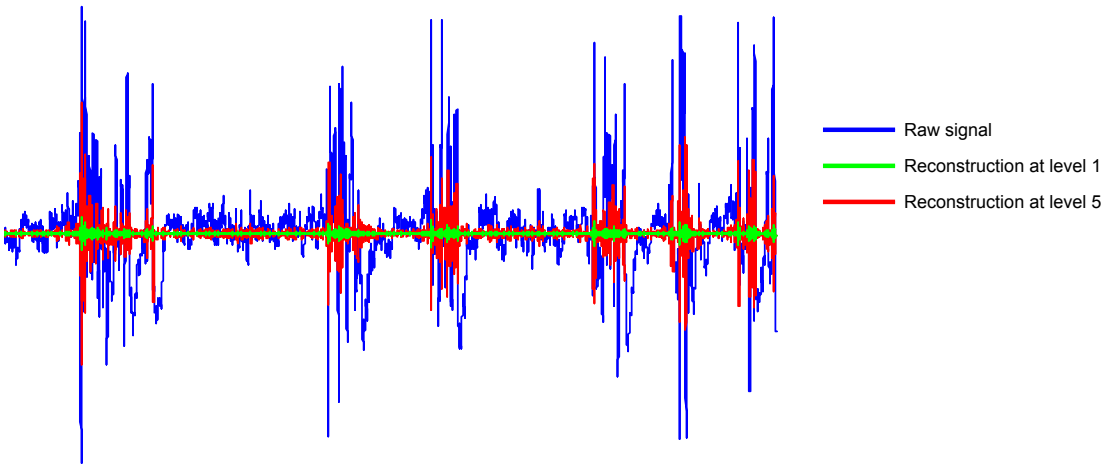

Figure 4.3: Reconstruction of the coefficients of the wavelet decomposition of the ECoG signal identifies different states at different levels of detail. The reconstruction of the first level of detail identifies very little of the features of the input signal (green). Reconstruction of the fifth level of detail highlights regions of higher frequency activity within the input signal (red).

The locations of the up states were used to create a windowing function that picked out the salient features of the signal - up states, down states and filter artifacts. This windowing function was then used to deconstruct the raw signal into 3 signals containing each of these features. The signal containing only the filter artifacts was discarded. This process is depicted in figure 4.4.

The remaining signals contain "gaps" since one of the states for each signal has been removed (see figure 4.4). These gaps were deleted yielding two "continuous"

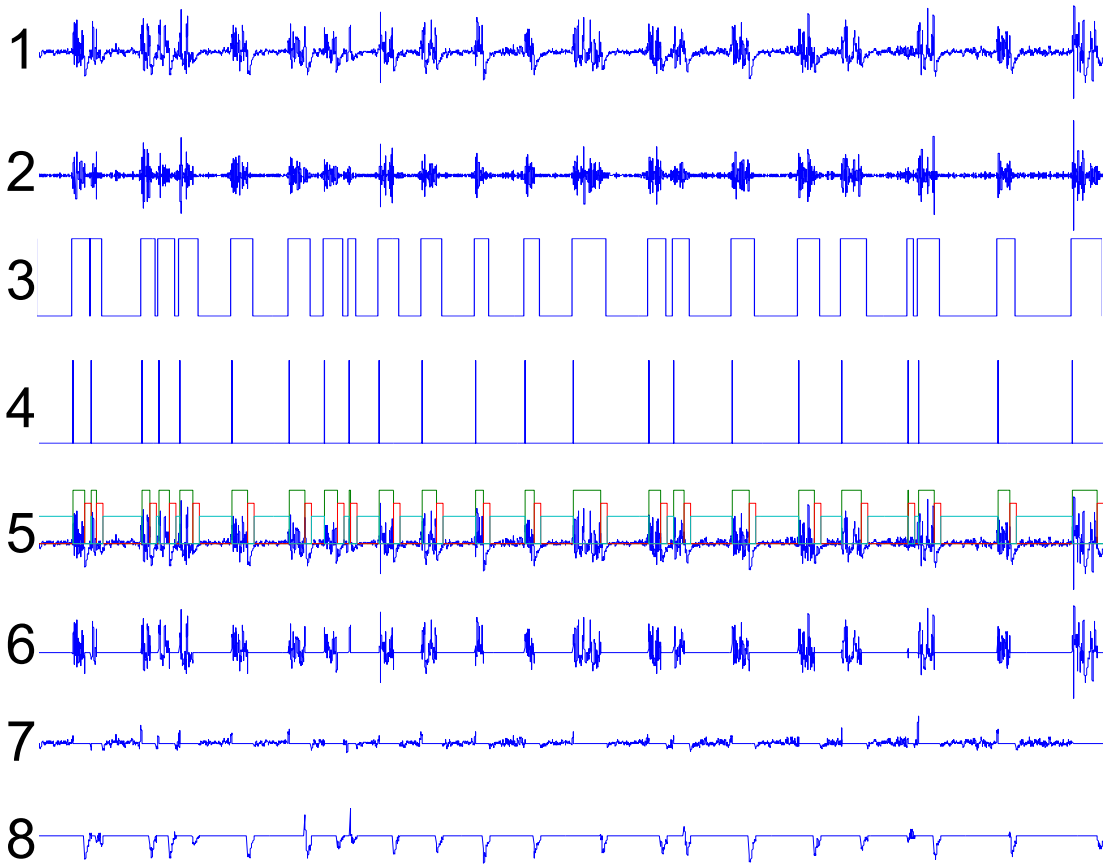

Figure 4.4: Processing steps in identifying up and down states in a typical signal. (1) The original signal is displayed. (2) The signal is decomposed via a wavelet transformation and the waveform corresponding to the 5th level of detail reconstructed. Values below a critical value are discarded and (3) a windowing function is constructed from the remaining non-zero values. (4) The leading edge of the windowing function is used to count the number of state transitions. (5) Three windowing functions are constructed from that constructed in (3) to identify the up-states (see (6)), down-states (see (7)) and filter artifacts (see (8)). Scale: The length of the signal in this example is 100s.

signals corresponding to the signal in the up state and the signal in the down state (see figure 4.5).

The resulting signals corresponding to up state and down state oscillations are at least approximately stationary and their analysis is amenable to conventional Fourier methods. These methods are described below. In addition the process of signal deconstruction and reconstruction allows the number of state transitions to be accurately computed and compared between groups.

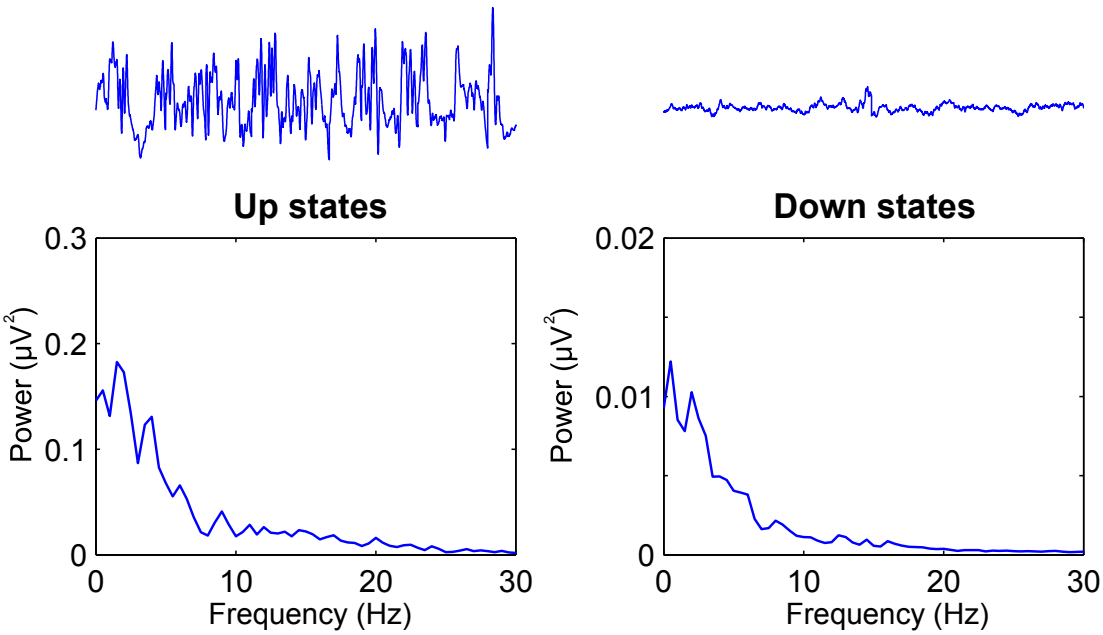

Figure 4.5: The empty spaces left in the signals from the initial processing were removed and the power spectra of the signals in the up and down states was computed using the modified periodogram method. Note the difference in scale - The up-states are approximately an order of magnitude more powerful, in all bandwidths, than the down-states. The traces above the power spectra show the reconstructions of up-state signals and down-state signals.

4.2.8.2 Relative band power

The power spectrum of a discrete signal $x_i(n)$ is defined as the magnitude squared of the signal's Fourier transform.

$$G_x(\omega) = \frac{1}{N}|X_i(\omega)|^2 \tag{4.2}$$

where $X_i(\omega)$ is;

$$X_i(\omega) = \sum_{n=0}^{N-1} x_i(n)e^{-i\omega n} \tag{4.3}$$

The magnitude squared of the Fourier transform provides, in isolation, a relatively poor estimation of the power spectrum of a discrete signal in the time domain. A greatly improved estimate is obtained via application of the modified periodogram method (see figure 4.6, page 105). Briefly, the signal is divided into overlapping segments. The magnitude squared of the Fourier transform is calculated for each segment and these averaged to yield the spectral estimate. Power spectra were estimated with a window size of 2 seconds, overlapping by 1 second using a rectangular window.

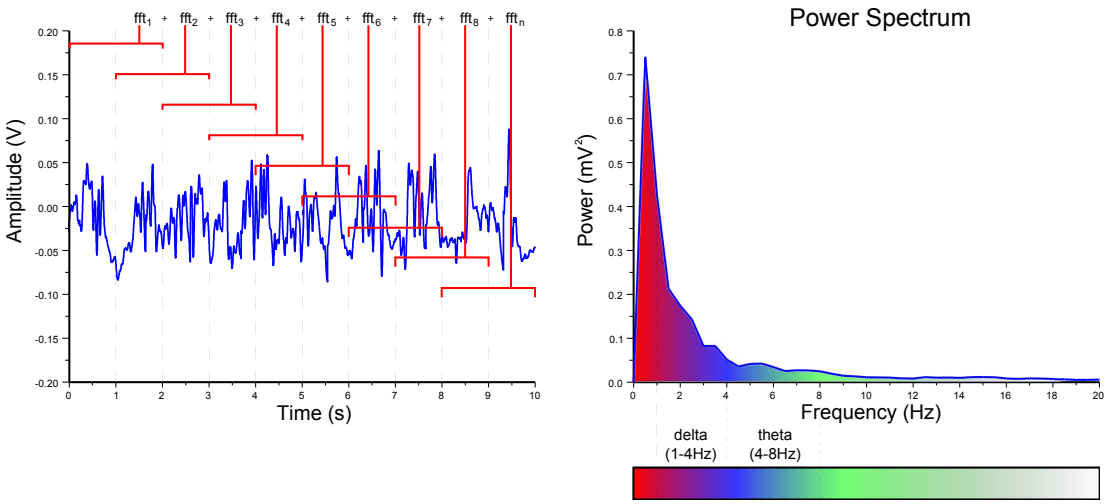

Figure 4.6: Computation of the power spectrum for a single channel. The signal is divided into 2s epochs which overlap each other by 1s. The Fourier transform for each epoch is calculated and all the epochs are averaged to estimate the power spectrum

The absolute band power in the delta and theta bands were then computed by integrating the power between the frequencies that define the respective bandwidths. The relative band power was then computed for each band by expressing it as a proportion of the total power under 100Hz.

4.2.8.3 Derived bipolar analysis

Each 100 second recording contains 7 signals (see figure 4.7, page 106). Signals were detrended by subtracting the mean value of the recorded ECoG signal from each sample value. The common reference montage records all potentials against the same reference. The detrended signals from each electrode in the common reference montage were then used to derive the bipolar montage by subtracting the signals in adjacent pairs of electrodes from each other (see table 4.2). The derived bipolar signals were then processed by the algorithm described above to construct the signals corresponding to the up and down states.

The power spectrum for both the up states and down states were computed for each derived signal with a frequency resolution 0.5Hz. It was calculated by subdividing the 100 seconds recording into 2 second epochs - each epoch overlapping the previous epoch by 1 second - and calculating the Fourier transform for each epoch. The Fourier transforms for each epoch were then averaged to estimate the power spectrum for each signal (see above).

The relative delta band power was then calculated by integrating the power spectrum between 1 and 4Hz and dividing it by the total power calculated by integrat-

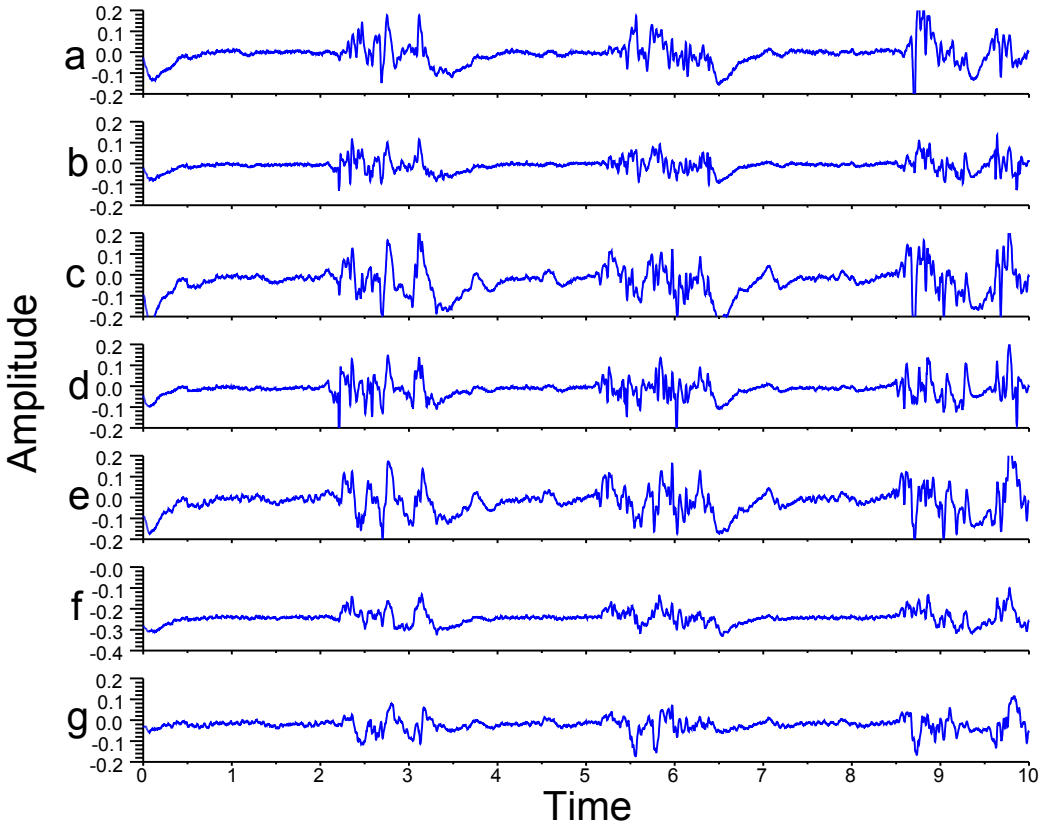

Figure 4.7: Representative data traces from one animal prior to stimulation showing the recorded signals for a 10 second epoch from the 7 ECoG electrodes (A-G) and the ECG electrodes.

ing the power spectrum betwen 1 and 100Hz. Similarly the relative theta band power then calculated by integrating the power spectrum between 4 and 8Hz and dividing it by the total power calculated by integrating the power spectrum betwen 1 and 100Hz.

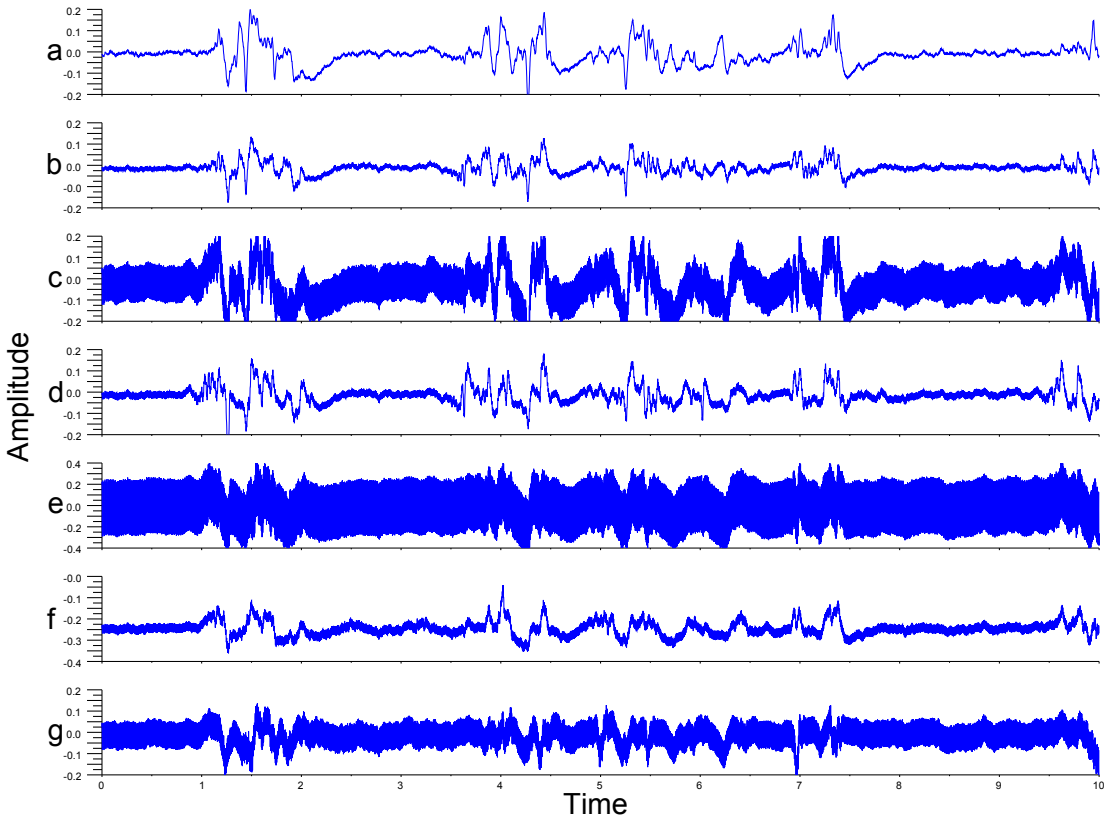

Figure 4.8: Representative data traces from one animal following the initiation of stimulation at 130Hz showing the recorded signals for a 10 second epoch from the 7 ECoG electrodes (A-G) and the ECG electrodes. Note the change of scale on the trace for electrode E - the artifacts were sufficiently large that this trace is plotted on a scale twice as large as the other traces. The stimulation artifacts pervade all of the electrodes being more prominent in electrodes located anterior/posterior to the site of stimulation (A, C, E & G) than those situated more laterally (B, D & F).

Table 4.2: Common reference and derived bipolar electrode combinations. Electrode G is located closest to the electrode connected to the negative inputs to all the amplifiers. As such it may be considered to belong to the common reference montage. Without further derivation it also represents a bipolar recording providing a recording of the ECoG between the retrosplenial dysgranular cortex and the cerebellum. As such it may also be considered to belong to the bipolar montage. In the description of the results in this chapter analysis of signals from electrode G have been reported as part of the bipolar montage.

Common reference	**Derived bipolar**	
A	A-B	D-E
B	A-C	D-F
C	B-C	E-F
D	B-D	E-G
E	C-D	F-G
F	C-E	G

4.2.8.4 Statistics

Data were plotted as delta/theta power as a function of time (temporal resolution = 5 minutes) using `gnuplot` (gnuplot). Data are presented as the mean ±SEM. Effects of drug treatment (VEH/PCP) are determined by repeated measures ANOVA over the five time points prior to the onset of stimulation. The combined effect of treatment and DBS is determined by repeated measures ANOVA over the five time points following the onset of stimulation. To determine if there was any effect of DBS itself data were scrutinised using a repeated measure ANOVA over the 3 time points including the time immediately prior to the onset of stimulation and the two time point immediately following the onset of stimulation. Statistics are tabulated as F(n,m) = x; p = y, where n and m denote the degrees of freedom in the numerator and denominator of the equation that computes the F value. p denotes the p-value.

4.3 Results

4.3.1 Electrode placements

Electrode locations were determined as described in section 2.3.2, page 49. Five electrodes were found to be misplaced (see figure 4.9). Animals with misplaced electrodes were excluded from the analysis of the stimulation effect since there contribution would represent the effect of non-specific stimulation. However the data from these animals was included in the analysis of the pre-stimulation group difference (effect of treatment) since it was estimated, that given the similar electrode trajectory (although different target), that the difference in target would contribute little to the treatment differences.

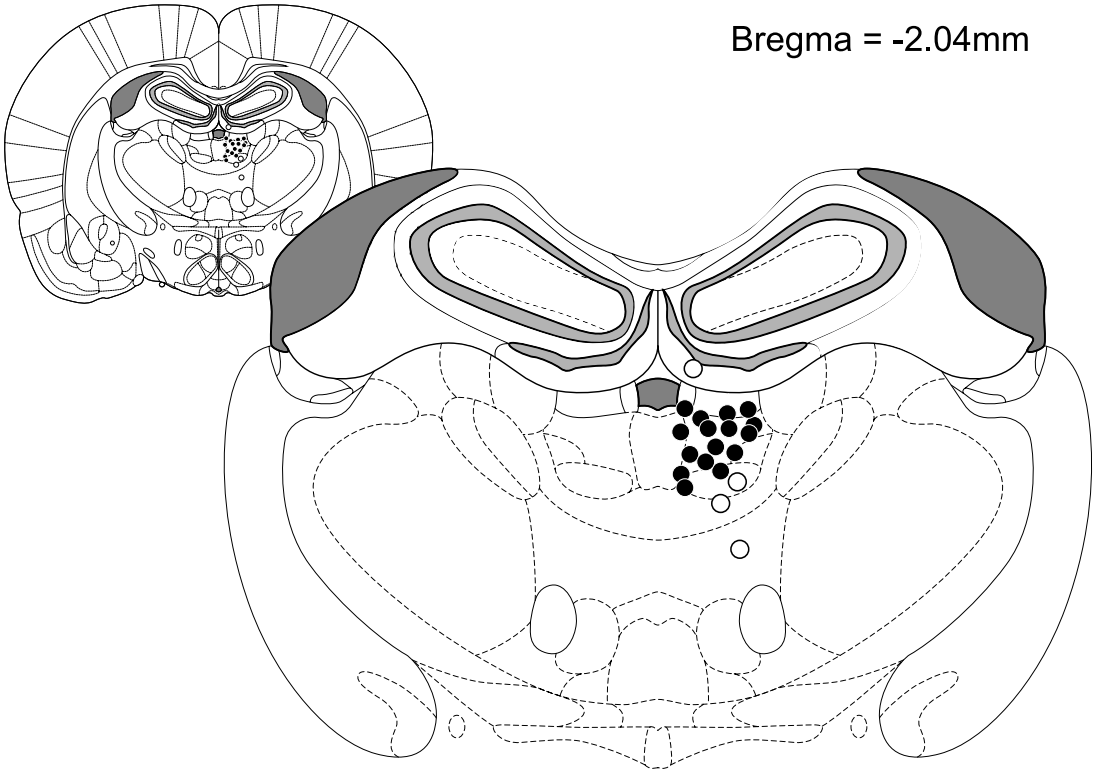

Figure 4.9: Electrode placements. Animals with misplaced electrodes were excluded from the analysis of DBS effects although were not excluded from the analysis of the treatment effects. Filled circles represent successful electrode placements. Open circles indicate the locations of electrodes in animals excluded from the analysis of the time (stimulation) effect.

4.3.2 Number of state transitions

Prior to surgery animals were administered either PCP or vehicle for 5 days followed by a 3 day washout (see section 4.2.4, page 97). The ECoG was recorded

differentially between 7 electrodes distributed over the cortex and 1 electrode over the cerebellum (see figure 4.1, page 100). Signals were processed to determine the number of state transitions in a 100s recording (see figure 4.4) for the recording immediately prior to beginning DBS and for the recording immediately after beginning DBS. No difference between PCP treated animals and vehicle treated controls was evident from examination of the number of state transitions. In addition DBS had no effect on the number of state transitions. These data were not computed for each channel since state transitions are apparent in every channel simultaneously.

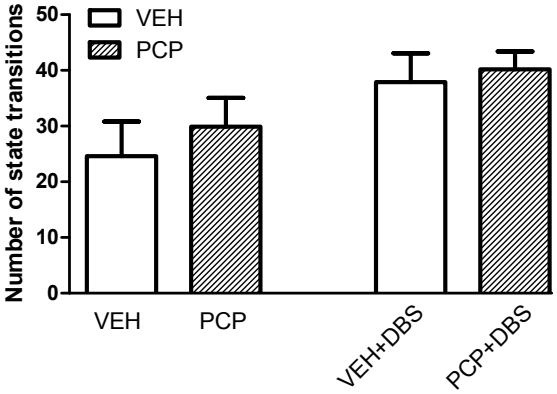

Figure 4.10: Number of state transitions. The number of state transitions were computed for each group in the time interval immediately prior to and immediately after beginning stimulation. No difference in the number of transitions was detected between groups in either condition. In addition the number of transitions was not seen to change as a consequence of stimulation.

4.3.3 Spectral analysis - derived bipolar montage

The signals from the 7 electrode combinations used to record the common reference ECoG were used to calculate a derived bipolar montage to better estimate the spatial distribution of the ECoG changes (see section 4.1.3.3, page 92). The derived signals were then processed to recover the signals that reflect the up-state and down-state activity. These signals were used to calculate the relative band power in the delta and theta bands using the modified periodogram method (see section 4.2.8.2, page 104) for signals recorded at 5 minute intervals. Differences between the differently treated groups for each oscillatory state were assessed via a repeated measures ANOVA over the 30 minutes of the baseline ECoG recordings. No effects of time were detected indicating a stable baseline. Differences between groups were detected at different electrode derivations and these are detailed below.

Effects of stimulation were assessed for each oscillatory state via a repeated measures ANOVA with time as the within subjects variable and treatment as the between subjects variable. The analysis was performed over three time points including the last time point of the baseline ECoG and the first two time points of the stimulation period.

Differences between groups were detected at different electrodes as a result of treatment and these are detailed below. Effects of time were evident from the analysis of the stimulation effect and group differences were modified by stimulation. These are also detailed below.

4.3.3.1 Effects of treatment on delta oscillations

Treatment effects were manifest in the delta power of the oscillations corresponding to both the the up-states and down-states of the signals. Significant increases in delta power in animals treated sub-chronically with PCP when compared with vehicle treated controls were detected at electrode locations B-C ($F(1,17) = 8.124$; $p = 0.011$), C-D ($F(1,17) = 7.754$; $p = 0.012$) and D-E ($F(1,17) = 4.857$; $p = 0.041$) indicating an increase in delta power during these states (see figure 4.11 and table 4.3). Similarly increases in delta power were observed at these locations during the down states, B-C ($F(1,17) = 7.624$; $p = 0.013$), C-D ($F(1,17) = 9.532$; $p = 0.006$) and D-E ($F(1,17) = 7.570$; $p = 0.013$). In addition further increases in delta power in animals treated sub-chronically with PCP were detected at C-E ($F(1,17) = 4.956$, $p = 0.039$), D-F ($F(1,17) = 5.935$; $p = 0.025$) and F-G ($F(1,17) = 6.016$; $p = 0.025$) during down-state oscillations (see figure 4.12 and table 4.4).

4.3.3.2 Effects of DBS of the mediodorsal thalamic nucleus on delta oscillations

Stimulation effects were markedly more noticeable in the down-states of the anaesthetised ECoG. Widespread effects of stimulation were detected at all but one (D-F) electrode combinations in the down state signals. Increases in delta power were seen at A-B ($F(2,26) = 6.385$, $p = 0.021$), A-C ($F(2,26) = 8.018$, $p = 0.011$), B-C ($F(2,26) = 6.533$, $p = 0.020$), B-D ($F(2,26) = 7.243$, $p = 0.015$), C-D ($F(2,26) = 4.644$, $p = 0.045$), C-E ($F(2,24) = 6.897$, $p = 0.017$), D-E ($F(2,24) = 6.708$, $p = 0.018$), E-F ($F(2,24) = 6.188$, $p = 0.023$), E-G ($F(2,24) = 6.660$, $p = 0.019$), F-G ($F(2,26) = 4.477$, $p = 0.049$) and G ($F(2,26) = 5.914$, $p = 0.026$) as a consequence of stimulation (see figure 4.12 and table 4.4). In addition this effect of stimulation modulates the differences between the two treatment groups in a state dependent

manner. Following DBS of the mediodorsal thalamic nucleus the differences between groups in up-state oscillations are no longer apparent (see figure 4.11 and table 4.3) whilst many of the pre-stimulation differences between PCP and vehicle treated animals are preserved in the down-states (see figure 4.12). Following stimulation differences in down-state delta power are apparent at C-E ($F(1,12) = 5.455$, $p = 0.031$), D-E ($F(1,12) = 6.505$ $p = 0.020$), D-F ($F(1,13) = 4.640$, $p = 0.045$) and E-F ($F(1,12) = 4.931$, $p = 0.040$) (see table 4.4). The apparent effect of stimulation on up-state delta oscillations (A-B $F(2,26) = 10.559$; $p = 0.004$) seems more likely attributable to the sudden reduction in delta power in the PCP group immediately prior to DBS. This dip probably reflects natural variation in power. The subsequent statistical effect is more likely due to this dip spontaneously recovering rather than a genuine stimulation effect.

4.3.3.3 Delta power - up states

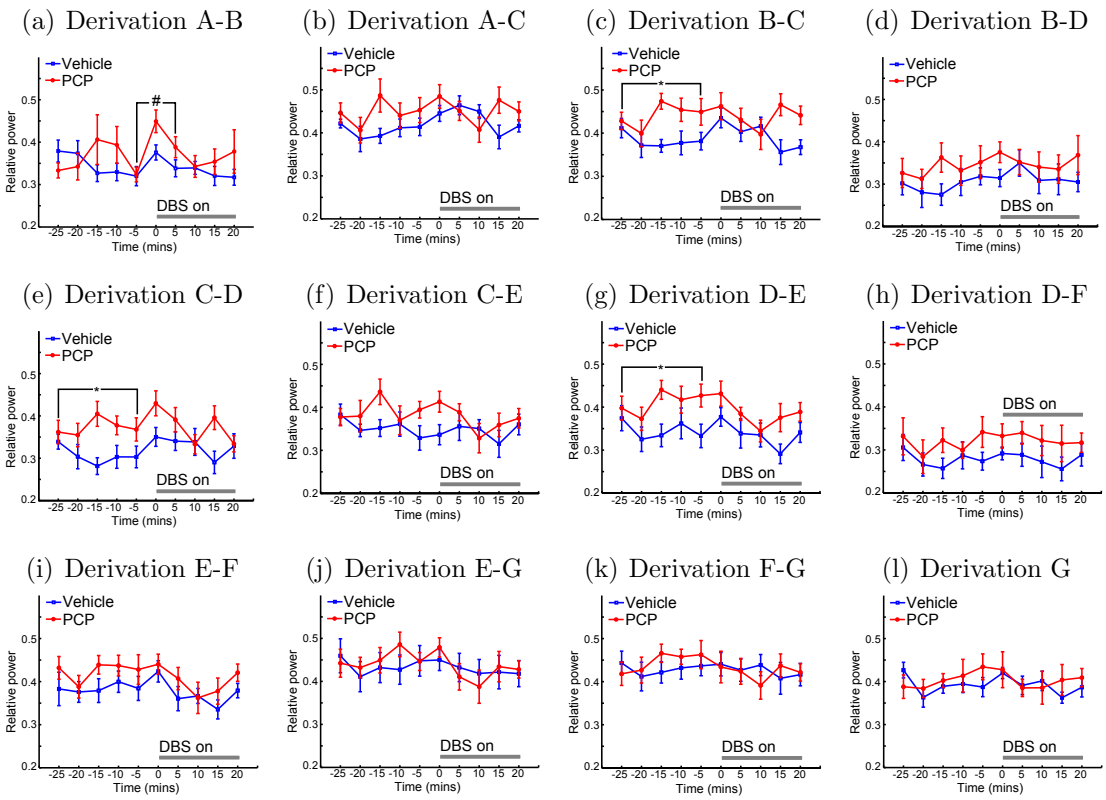

Figure 4.11: Effect of PCP treatment and mediodorsal thalamic nucleus stimulation on the delta power in the up states of signals from the bipolar montage derived from signals recorded from electrodes in the common reference montage. Stimulation on at t = 30 mins as indicated by the solid grey bar. Significant differences between groups are evident prior to stimulation at the bipolar derivation B-C ($F(1,17) = 8.124$; $p = 0.011$), C-D ($F(1,17) = 7.754$; $p = 0.012$) and D-E ($F(1,17) = 4.857$; $p = 0.041$) indicating an increase in delta power during the up states, at these locations, in the PCP treated group when compared with vehicle treated controls. Following the initiation of DBS the group difference at these bipolar electrode derivations are no longer apparent. A significant effect of time (stimulation) was detected at electrode derivation A-B $F(2,26) = 10.559$; $p = 0.004$. However, it seems unlikely that this effect reflects a real effect of DBS but rather is a consequence of the sudden reduced delta power in this channel immediately prior to stimulation. That is this result arises coincidentally due to the natural variation in delta power rather through any effect of DBS. Results are presented as the mean ±SEM, $\star$ indicates a significant pre-stimulation treatment effect, $p < 0.05$.

Table 4.3: Tabulated statistics for delta power in the up states for each electrode in the derived bipolar montage binned into 5 minute intervals over 60 minutes, stimulation on at 30 minutes. Within subjects statistics indicate the effects of time whilst the between subjects statistics indicate the effects of treatment either prior to stimulation (Time = 0 - 30 minutes) or the effects following the initiation of stimulation (Time = 30 - 50 minutes).

	Within Sub. (Time)				Between Sub. (Drug)		
	Electrode	**F**	**p**	**Sig.**	**F**	**p**	**Sig.**
Time = 0 - 30 min	A-B	F(4,72) = 0.973	0.337	-	F(1,17) = 0.211	0.652	-
	A-C	F(4,72) = 1.032	0.323	-	F(1,17) = 4.218	0.055	-
	B-C	F(4,72) = 0.917	0.351	-	F(1,17) = 8.124	0.011	$\star$
	B-D	F(4,72) = 0.851	0.368	-	F(1,17) = 1.356	0.259	-
	C-D	F(4,72) = 0.281	0.603	-	F(1,17) = 7.754	0.012	$\star$
	C-E	F(4,72) = 0.997	0.331	-	F(1,17) = 1.836	0.192	-
	D-E	F(4,72) = 1.234	0.281	-	F(1,17) = 4.857	0.041	$\star$
	D-F	F(4,72) = 1.596	0.223	-	F(1,17) = 1.085	0.311	-
	E-F	F(4,72) = 0.776	0.390	-	F(1,17) = 2.008	0.174	-
	E-G	F(4,72) = 0.833	0.373	-	F(1,17) = 0.182	0.674	-
	F-G	F(4,72) = 0.788	0.386	-	F(1,17) = 0.369	0.551	-
	G	F(4,72) = 1.414	0.250	-	F(1,17) = 0.235	0.634	-
Stimulation on at t = 30 minutes							
Time = 30 - 50 min	A-B	F(2,26) = 10.559	0.004	$\star\star$	F(1,13) = 2.696.	0.118	-
	A-C	F(2,26) = 1.071	0.314	-	F(1,13) = 2.663	0.298	-
	B-C	F(2,26) = 1.113	0.301	-	F(1,13) = 2.340	0.062	-
	B-D	F(2,26) = 0.239	0.631	-	F(1,13) = 0.556	0.281	-
	C-D	F(2,26) = 2.249	0.151	-	F(1,13) = 2.121	0.056	-
	C-E	F(2,24) = 0.383	0.544	-	F(1,12) = 1.450	0.273	-
	D-E	F(2,24) = 2.275	0.149	-	F(1,12) = 3.576	0.075	-
	D-F	F(2,26) = 0.097	0.759	-	F(1,13) = 2.652	0.121	-
	E-F	F(2,24) = 2.814	0.111	-	F(1,12) = 1.311	0.267	-
	E-G	F(2,24) = 2.364	0.142	-	F(1,12) = 0.004	0.952	-
	F-G	F(2,26) = 0.904	0.354	-	F(1,13) = 0.023	0.881	-
	G	F(2,26) = 1.655	0.215	-	F(1,13) = 0.308	0.586	-

4.3.3.4 Delta power - down states

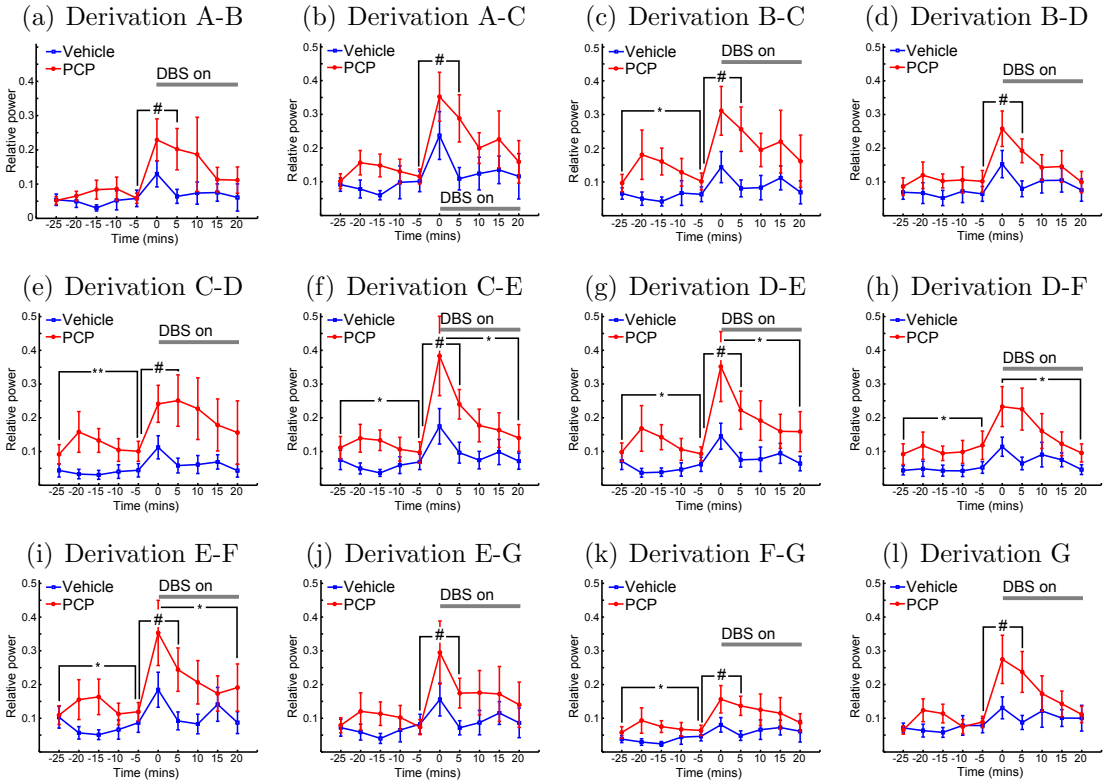

Figure 4.12: Effect of PCP treatment and mediodorsal thalamic nucleus stimulation on the delta power in the down-states of signals from the bipolar montage derived from signals recorded from electrodes in the common reference montage. Stimulation on at t = 30 mins as indicated by the solid grey bar. Significant differences between groups are evident prior to stimulation at the bipolar derivation B-C ($F(1,17) = 7.624$; $p = 0.013$), C-D ($F(1,17) = 9.532$; $p = 0.006$), C-E ($F(1,17) = 4.956$, $p = 0.039$), D-E ($F(1,17) = 7.570$; $p = 0.013$), D-F ($F(1,17) = 5.935$; $p = 0.025$) and F-G ($F(1,17) = 6.016$; $p = 0.025$) indicating an increase in delta power during the down-states, at these locations, in the PCP treated group when compared with vehicle treated controls. Following the initiation of DBS the group difference at these bipolar electrode derivations remain apparent at C-E ($F(1,12) = 5.455$, $p = 0.031$), D-E ($F(1,12) = 6.505$ $p = 0.020$), D-F ($F(1,13) = 4.640$, $p = 0.045$) and E-F ($F(1,12) = 4.931$, $p = 0.040$). A significant effect of time (stimulation) was detected at all but one electrode location: A-B ($F(2,26) = 6.385$, $p = 0.021$), A-C ($F(2,26) = 8.018$, $p = 0.011$), B-C ($F(2,26) = 6.533$, $p = 0.020$), B-D ($F(2,26) = 7.243$, $p = 0.015$), C-D ($F(2,26) = 4.644$, $p = 0.045$), C-E ($F(2,24) = 6.897$, $p = 0.017$), D-E ($F(2,24) = 6.708$, $p = 0.018$), E-F ($F(2,24) = 6.188$, $p = 0.023$), E-G ($F(2,24) = 6.660$, $p = 0.019$), F-G ($F(2,26) = 4.477$, $p = 0.049$) and G ($F(2,26) = 5.914$, $p = 0.026$). Results are presented as the mean ±SEM, $\star$ indicates a significant treatment effect, $p < 0.05$, $\star\star$ indicates p ¡ 0.01. # indicates a significant effect of stimulation, $p < 0.05$.

Table 4.4: Tabulated statistics for delta power in the up states for each electrode in the derived bipolar montage binned into 5 minute intervals over 60 minutes, stimulation on at 30 minutes. Within subjects statistics indicate the effects of time whilst the between subjects statistics indicate the effects of treatment either prior to stimulation (Time = 0 - 30 minutes) or the effects following the initiation of stimulation (Time = 30 - 50 minutes).

	Within Sub. (Time)				Between Sub. (Drug)		
	Electrode	**F**	**p**	**Sig.**	**F**	**p**	**Sig.**
Time = 0 - 30 min	A-B	F(4,72) = 0.216	0.648	-	F(1,17) = 1.145	0.299	-
	A-C	F(4,72) = 0.187	0.670	-	F(1,17) = 2.889	0.106	-
	B-C	F(4,72) = 0.371	0.550	-	F(1,17) = 7.624	0.013	⋆
	B-D	F(4,72) = 0.152	0.701	-	F(1,17) = 2.058	0.169	-
	C-D	F(4,72) = 0.326	0.575	-	F(1,17) = 9.532	0.006	⋆⋆
	C-E	F(4,72) = 0.106	0.748	-	F(1,17) = 4.956	0.039	⋆
	D-E	F(4,72) = 0.278	0.605	-	F(1,17) = 7.570	0.013	⋆
	D-F	F(4,72) = 0.237	0.632	-	F(1,17) = 5.935	0.025	⋆
	E-F	F(4,72) = 0.113	0.741	-	F(1,17) = 4.052	0.059	-
	E-G	F(4,72) = 0.081	0.779	-	F(1,17) = 1.773	0.200	-
	F-G	F(4,72) = 0.181	0.676	-	F(1,17) = 6.016	0.025	⋆
	G	F(4,72) = 0.440	0.516	-	F(1,17) = 1.761	0.201	-
Stimulation on at t = 30 minutes							
Time = 30 - 50 min	A-B	F(2,26) = 6.385	0.021	⋆	F(1,13) = 2.819	0.110	-
	A-C	F(2,26) = 8.018	0.011	⋆	F(1,13) = 2.359	0.142	-
	B-C	F(2,26) = 6.533	0.020	⋆	F(1,13) = 3.700	0.070	-
	B-D	F(2,26) = 7.243	0.015	⋆	F(1,13) = 3.166	0.092	-
	C-D	F(2,26) = 4.644	0.045	⋆	F(1,13) = 3.648	0.072	-
	C-E	F(2,24) = 6.897	0.017	⋆	F(1,12) = 5.456	0.031	⋆
	D-E	F(2,24) = 6.708	0.018	⋆	F(1,12) = 6.505	0.020	⋆
	D-F	F(2,26) = 3.564	0.075	-	F(1,13) = 4.640	0.045	⋆
	E-F	F(2,24) = 6.188	0.023	⋆	F(1,12) = 4.931	0.040	⋆
	E-G	F(2,24) = 6.660	0.019	⋆	F(1,12) = 2.603	0.124	-
	F-G	F(2,26) = 4.477	0.049	⋆	F(1,13) = 3.802	0.067	-
	G	F(2,26) = 5.914	0.026	⋆	F(1,13) = 3.257	0.088	-

4.3.3.5 Effects of treatment on theta oscillations

Treatment effects were negligible in the theta oscillations of animals treated with PCP or vehicle. No effects of treatment were evident in the up-state theta oscillations (see figure 4.13 and table 4.5). Similarly, with one exception (C-E ($F(1,17) = 4.617$; $p = 0.046$)) there were no differences between groups evident in the down-state theta oscillations.

4.3.3.6 Effects of DBS of the mediodorsal thalamic nucleus on theta oscillations

There were no effects of stimulation detected in the theta oscillations of the up-states (see figure 4.13 and table 4.5). However there were widespread effects of stimulation detected in the down-states with effects of stimulation detected at A-C ($F(2,26) = 5.825$, $p = 0.027$), B-D ($F(2,26) = 4.816$, $p = 0.042$), D-E ($F(2,24) = 5.772$, $p = 0.027$), D-F ($F(2,26) = 5.296$, $p = 0.034$) and E-F ($F(2,24) = 6.306$, $p = 0.022$). In addition group differences were observable at C-D ($F(1,13) = 5.135$, $p = 0.036$), C-E ($F(1,12) = 9.226$, $p = 0.007$), E-F ($F(1,12) = 4.764$, $p = 0.042$) and E-G ($F(1,12) = 4.545$, $p = 0.047$) following the onset of stimulation (see figure 4.14 and table 4.6).

4.3.3.7 Theta power - upstates

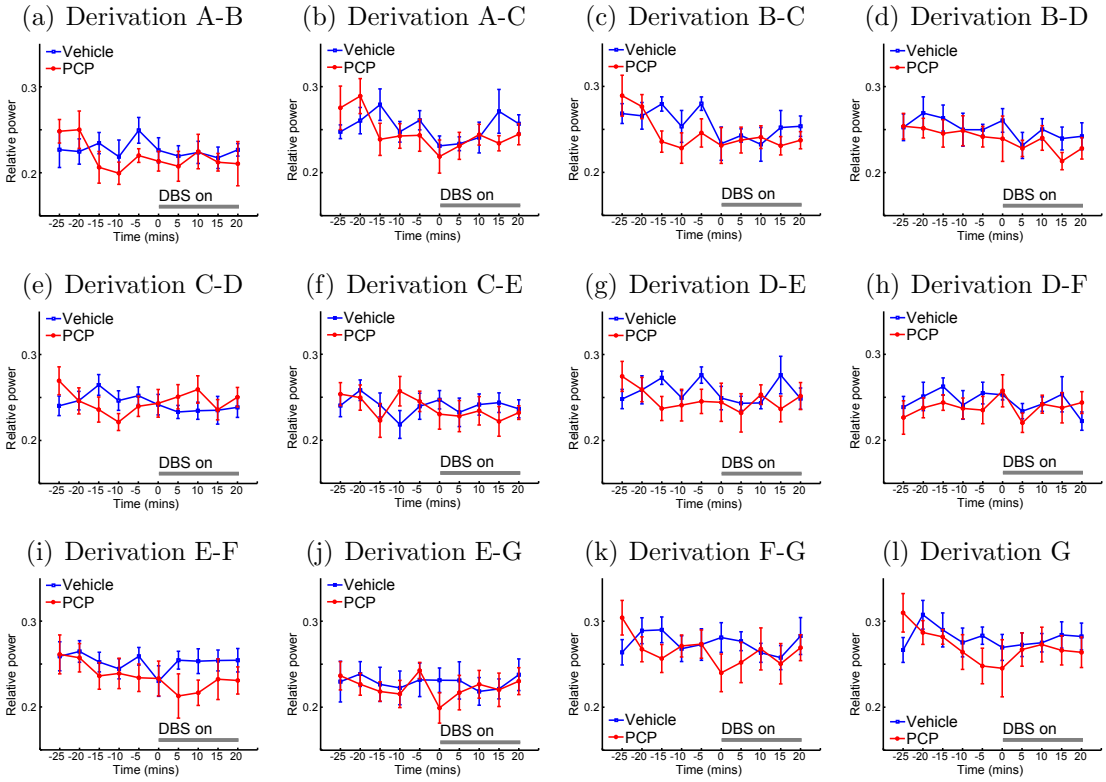

Figure 4.13: Effect of PCP treatment and mediodorsal thalamic nucleus stimulation on the theta power in the up states of signals from the bipolar montage derived from signals recorded from electrodes in the common reference montage. Stimulation on at t = 30 mins as indicated by the solid grey bar. No differences are seen between groups either before or after beginning DBS at any location indicating no effect of drug treatment on theta power of the up states of anaesthetised ECoG potentials. In addition no effect of time was detected at any location indicating no effect of stimulation on theta power in the up states.

Table 4.5: Tabulated statistics for theta power in the up states for each electrode in the derived bipolar montage binned into 5 minute intervals over 60 minutes, stimulation on at 30 minutes. Within subjects statistics indicate the effects of time whilst the between subjects statistics indicate the effects of treatment either prior to stimulation (Time = 0 - 30 minutes) or the effects following the initiation of stimulation (Time = 30 - 50 minutes).

	Within Sub. (Time)				Between Sub. (Drug)		
	Electrode	**F**	**p**	**Sig.**	**F**	**p**	**Sig.**
Time = 0 - 30 min	A-B	F(4,72) = 2.222	0.153	-	F(1,17) = 0.121	0.732	-
	A-C	F(4,72) = 0.979	0.336	-	F(1,17) = 0.010	0.923	-
	B-C	F(4,72) = 2.374	0.141	-	F(1,17) = 1.078	0.313	-
	B-D	F(4,72) = 0.398	0.536	-	F(1,17) = 0.357	0.557	-
	C-D	F(4,72) = 0.868	0.364	-	F(1,17) = 0.608	0.446	-
	C-E	F(4,72) = 0.818	0.378	-	F(1,17) = 0.231	0.637	-
	D-E	F(4,72) = 0.517	0.481	-	F(1,17) = 0.920	0.350	-
	D-F	F(4,72) = 0.800	0.383	-	F(1,17) = 1.177	0.292	-
	E-F	F(4,72) = 1.052	0.319	-	F(1,17) = 0.467	0.503	-
	E-G	F(4,72) = 0.796	0.384	-	F(1,17) = 0.012	0.914	-
	F-G	F(4,72) = 0.275	0.606	-	F(1,17) = 0.033	0.858	-
	G	F(4,72) = 1.610	0.221	-	F(1,17) = 0.182	0.657	-
Stimulation on at t = 30 minutes							
Time = 30 - 50 min	A-B	F(2,26) = 3.146	0.093	-	F(1,13) = 1.242	0.280	-
	A-C	F(2,26) = 2.053	0.171	-	F(1,13) = 0.691	0.417	-
	B-C	F(2,26) = 2.403	0.139	-	F(1,13) = 0.976	0.336	-
	B-D	F(2,26) = 1.091	0.310	-	F(1,13) = 0.640	0.434	-
	C-D	F(2,26) = 0.069	0.796	-	F(1,13) = 0.044	0.837	-
	C-E	F(2,24) = 0.467	0.503	-	F(1,12) = 0.109	0.745	-
	D-E	F(2,24) = 1.535	0.228	-	F(1,12) = 0.868	0.364	-
	D-F	F(2,26) = 2.911	0.105	-	F(1,13) = 0.613	0.444	-
	E-F	F(2,24) = 0.633	0.437	-	F(1,12) = 1.302	0.269	-
	E-G	F(2,24) = 1.759	0.201	-	F(1,12) = 0.326	0.575	-
	F-G	F(2,26) = 0.331	0.572	-	F(1,13) = 1.358	0.259	-
	G	F(2,26) = 0.221	0.638	-	F(1,13) = 1.370	0.257	-

4.3.3.8 Theta power - down states

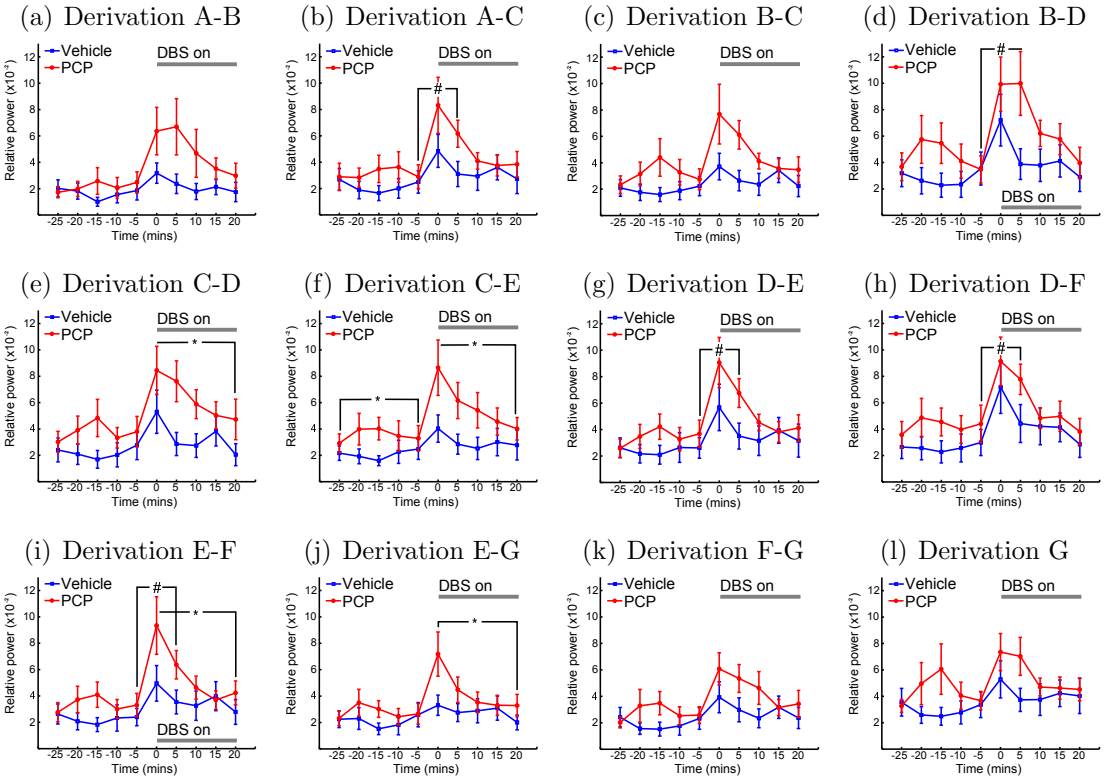

Figure 4.14: Effect of PCP treatment and mediodorsal thalamic nucleus stimulation on the theta power in the down states of signals from the bipolar montage derived from signals recorded from electrodes in the common reference montage. Stimulation on at t = 30 mins as indicated by the solid grey bar. Significant differences between groups are evident prior to stimulation at the bipolar derivation C-E ($F(1,17) = 4.617$; $p = 0.046$) indicating an increase in theta power during the down states, at these locations, in the PCP treated group when compared with vehicle treated controls. Following the initiation of DBS the group difference at the following bipolar electrode derivations become apparent at C-D ($F(1,13) = 5.135$, $p = 0.036$), C-E ($F(1,12) = 9.226$, $p = 0.007$), E-F ($F(1,12) = 4.764$, $p = 0.042$) and E-G ($F(1,12) = 4.545$, $p = 0.047$). A significant effect of time (stimulation) was detected at A-C ($F(2,26) = 5.825$, $p = 0.027$), B-D ($F(2,26) = 4.816$, $p = 0.042$), D-E ($F(2,24) = 5.772$, $p = 0.027$), D-F ($F(2,26) = 5.296$, $p = 0.034$) and E-F ($F(2,24) = 6.306$, $p = 0.022$). Results are presented as the mean ±SEM, $\star$ indicates a significant treatment effect, $p < 0.05$. # indicates a significant effect of stimulation, $p < 0.01$.

Table 4.6: Tabulated statistics for theta power in the down states for each electrode in the derived bipolar montage binned into 5 minute intervals over 60 minutes, stimulation on at 30 minutes. Within subjects statistics indicate the effects of time whilst the between subjects statistics indicate the effects of treatment either prior to stimulation (Time = 0 - 30 minutes) or the effects following the initiation of stimulation (Time = 30 - 50 minutes).

	Within Sub. (Time)				Between Sub. (Drug)		
	Electrode	**F**	**p**	**Sig.**	**F**	**p**	**Sig.**
Time = 0 - 30 min	A-B	F(4,72) = 0.143	0.709	-	F(1,17) = 0.650	0.431	-
	A-C	F(4,72) = 0.149	0.704	-	F(1,17) = 1.336	0.263	-
	B-C	F(4,72) = 0.323	0.577	-	F(1,17) = 2.820	0.110	-
	B-D	F(4,72) = 0.250	0.623	-	F(1,17) = 2.680	0.124	-
	C-D	F(4,72) = 0.222	0.643	-	F(1,17) = 3.441	0.080	-
	C-E	F(4,72) = 0.085	0.775	-	F(1,17) = 4.617	0.046	⋆
	D-E	F(4,72) = 0.186	0.671	-	F(1,17) = 1.856	0.190	-
	D-F	F(4,72) = 0.163	0.691	-	F(1,17) = 2.806	0.111	-
	E-F	F(4,72) = 0.064	0.803	-	F(1,17) = 2.615	0.123	-
	E-G	F(4,72) = 0.425	0.532	-	F(1,17) = 1.406	0.251	-
	F-G	F(4,72) = 0.101	0.754	-	F(1,17) = 2.234	0.152	-
	G	F(4,72) = 0.277	0.605	-	F(1,17) = 2.651	0.121	-
Stimulation on at t = 30 minutes							
Time = 30 - 50 min	A-B	F(2,26) = 3.381	0.083	-	F(1,13) = 3.943	0.078	-
	A-C	F(2,26) = 5.825	0.027	⋆	F(1,13) = 2.855	0.108	-
	B-C	F(2,26) = 4.400	0.050	-	F(1,13) = 3.989	0.061	-
	B-D	F(2,26) = 4.816	0.042	⋆	F(1,13) = 4.115	0.058	-
	C-D	F(2,26) = 3.926	0.063	-	F(1,13) = 5.135	0.036	⋆
	C-E	F(2,24) = 3.819	0.066	-	F(1,12) = 9.226	0.007	⋆⋆
	D-E	F(2,24) = 5.772	0.027	⋆	F(1,12) = 3.935	0.063	-
	D-F	F(2,26) = 5.296	0.034	⋆	F(1,13) = 1.717	0.201	-
	E-F	F(2,24) = 6.306	0.022	⋆	F(1,12) = 4.764	0.042	⋆
	E-G	F(2,24) = 4.123	0.057	-	F(1,12) = 4.545	0.047	⋆
	F-G	F(2,26) = 4.292	0.053	-	F(1,13) = 2.839	0.109	-
	G	F(2,26) = 2.973	0.102	-	F(1,13) = 2.802	0.111	-

4.3.4 Summary

In summary sub-chronic administration of PCP to rats for 5 days yields a spectral profile at 72 hours following the final drug administration of increased delta

power at frontal and medial-posterior electrode locations (B-C, C-D and D-E respectively) in the up-states. More widespread differences were seen in the down-states with increases seen in the PCP treated animals at frontal, medial and posterior locations (B-C, C-D, C-E, D-E, D-F and F-G respectively). Few differences were detected in the theta band between differently treated animals with no differences observed in the up-states and a single difference at electrode location C-E.

High frequency stimulation of the mediodorsal thalamic nucleus yields widespread but transiently increased cortical synchrony in delta and theta bands in the down-states only. No effect of stimulation was observed in the up-states. DBS effects were detected in the delta down-states at all electrode locations barring D-F. DBS effects on down-state theta oscillations were marginally more selective with increases only seen at frontal and medial-posterior electrode locations (A-C, B-D, D-E, D-F and E-F respectively).

4.3.4.1 Summary of treatment effects

Table 4.7: Summary of significant findings from the power spectra analysis from differentially treated (PCP vs. VEH).

	Power - Up states											
	A-B	A-C	B-C	B-D	C-D	C-E	D-E	D-F	E-F	E-G	F-G	G
δ			↑		↑		↑					
θ												
	Power - Down states											
δ			↑		↑↑	↑	↑	↑			↑	
θ						↑						

4.3.4.2 Summary of stimulation effects

Table 4.8: Summary of significant findings from the power spectra analysis from differentially treated (PCP vs. VEH) receiving stimulation of the mediodorsal thalamic nucleus.

	Power - Up states											
	A-B	A-C	B-C	B-D	C-D	C-E	D-E	D-F	E-F	E-G	F-G	G
δ												
θ												
	Power - Down states											
δ	↑	↑	↑	↑	↑	↑	↑	↑		↑	↑	↑
θ		↑		↑			↑	↑	↑			

4.4 Discussion

4.4.1 Effects of anaesthesia

EEG is used as an indicator of depth of anaesthesia in clinical procedures (Voss & Sleigh, 2007). As with all *in vivo* experiments conducted under anaesthesia the anaesthetic itself provides a significant confounding variable. This confound is arguable of greater significance in experiments investigating the ECoG given the sensitivity of these signals to anaesthesia. Whilst the interaction between the anaesthetic effects, drug effects and stimulation effects cannot be resolved, the experiment was performed to minimise and control for the effects of anaesthesia.

The isoflurane level was lowered to 1.5% (the surgical procedure is performed at an isoflurane level of 2%) 30 minutes before the start of the experiment. This length of time vastly exceeds that required for the ECoG to normalise after a change in anaesthesia. Experience from previous (unreported) pilot studies indicated that the ECoG suffers attenuation at an isoflurane level of 2%. Similar effects of isoflurane anaesthesia have been reported elsewhere (Li *et al.*, 2007). Whilst it is possible to lower the anaesthetic level beyond 1.5% without reinstatement of pedal withdrawal and responses to tail pinch, these lower anaesthetic doses occupy a "grey" area where some animals may come round at levels of 1.4% whereas others may remain acceptably anaesthetised at levels as low as 1%. An isoflurane level of 1.5%, therefore, represents a minimum level of anaesthesia for the recording of reliable ECoG signals whilst maintaining a consistent level of anaesthesia across animals.

It is likely that depth of anaesthesia by inhalation of isoflurane will be dependent on animal mass. Operationally, given a constant rate of isoflurane delivery, larger animals would receive a proportionally smaller anaesthetic dose and, from the author's experience, would exhibit more powerful ECoG recordings. A treatment strategy whereby all animals from "group x" were recorded from before all animals from "group y" may skew the results such that the latterly treated (presumably more massive) group may exhibit more powerful ECoGs. This potential confound was controlled for by randomising treatment such that animals treated with PCP and vehicle were randomly distributed with respect to their age, given their treatment, at the time of the surgical and recording protocol.

However the effect of this interaction is controlled for given that all recordings come from animals under similar anaesthetic conditions. Therefore the results re-

ported here are likely to represent differences due to treatment and/or stimulation rather than differences due to anaesthesia.

4.4.2 Effects of electrode insertion

It is likely that insertion of foreign objects, in this case an electrode into the mediodorsal thalamic nucleus and 8 screw electrodes into the skull overlying the cortex and cerebellum, will yield changes in the EEG/ECoG. As with the confounding effects of anaesthesia the effects due to electrode insertion and their interaction with treatment and/or stimulation cannot be resolved in these experiments. However any such effects are controlled for since animals in both groups underwent identical surgical procedures with identical electrode placements. Of particular note are the differences in delta and theta power reported around electrode E. This electrode contacts the cortex immediately above the mediodorsal thalamic nucleus and one may question whether these differences in anyway reflect an effect of electrode insertion. Given the identical electrode placements in both groups once can be confident that the effects are due to group differences and not electrode insertion. Furthermore, unlike previous surgical protocols, the DBS electrodes were introduced through the cortex contralateral to the hemisphere from which recordings were made, *i.e:* the recording hemisphere was **intact** (see section 4.2.5, page 97).

Skull defects, including fractures and burr holes, create low resistance pathways for ECoG currents. These can result in localised increase in beta activity referred to as a *breach rhythm* (Fisch, 1999). These breach rhythms are of little consequence in the context of the present findings since analysis is restricted to the low frequency delta and theta bands.

4.4.3 Effects of treatment

Analysis of the ECoG between differentialy treated groups of rats revealed that rats treated subchronically with PCP for 5 days have significantly elevated delta power, 72 hours after the final drug adminstration, primarily in frontal and medial-posterior regions. Theta power is also seen to be elevated but only in the most posterior electrode locations.

4.4.3.1 PCP induced changes in the EEG

Given their ability to induce psychosis in healthy volunteers and exacerbate psychosis in schizophrenics, acute administration of drugs which act as antagonists at *N*-methyl-D-aspartate (NMDA) receptors are believed to model some of the symptoms of schizophrenia (see Morris *et al.* 2005). Such drugs include dizocilipine (MK-801), phencyclidine (PCP) and ketamine. Acute administration of PCP in rats, induces hyperlocomotion (a model of psychosis (see section 5.1.3, page 140)), impairs social interaction and induces cognitive disruption including deficits in PPI (a model of sensory motor gating (see section 5.1.2, page 138), phenomena associated with schizophrenia (see Morris *et al.* 2005). Similarly acute administration of PCP appears to capture some of the electrophysiological deficits associated with schizophrenia.

PCP induces increases in delta power in the prefrontal and sensorimotor cortices in a dose dependent manner whilst decreasing power in higher frequency bandwidths (Marquis *et al.*, 1989; Sebban *et al.*, 2002). This effect has been reported to be resistant to administration of a plethora of antipsychotic medications, including haloperidol and clozapine (Sebban *et al.*, 2002). Whilst increased low frequency power is in general agreement with the results reported here the validity of this comparison is questionable. Acute and sub-chronic administration of PCP are well documented for their differing behavioral phenotypes (see Morris *et al.* 2005). It is then not unreasonable to assert that, rather than sub-chronic PCP administration yielding similar spectral anomalies as those seen in response to acute administration, it may plausibly yield different spectral anomalies. Indeed this may prove to be the case since the literature delivers conflicting reports as to the nature of the spectral changes in response to acute PCP adminstration. In addition to the purported increases, reductions in low frequency power have also been reported (Dimpfel & Spüler, 1990; Kargieman *et al.*, 2007) as have increases in cortical desynchronisation (Sagratella *et al.*, 1992), which presumably reflects a reduction in power.

Schizophrenia-like psychosis in humans is more likely to result from repeated administration of PCP than a single acute exposure (see Morris *et al.* 2005). Similarly sub-chronic PCP administration is likely to be a more plausible model of schizophrenia in rats. It is this model that has been explored in this chapter. Comparisons with acute models are then arguably invalid. To the author's knowledge this thesis provides the first demonstration that sub-chronic administration of PCP in rats yields disturbances in the spectral analysis of the EEG/ECoG

when compared with vehicle treated animals. This evidence is in general agreement with studies reporting similar effects in the acute paradigm. Of significantly greater importance is the parallels which may be drawn between the elevated power at low frequencies in this model and similar observations in the human condition. The sub-chronic PCP rat model of schizophrenia described here is not the only putative animal model of schizophrenia. Similar models exist with different dosing paradigms and time courses. To the author's knowledge these have not been validated through analysis of the EEG/ECoG. In addition there are genetic models and models requiring some sort of early insult leading to developmental disruption (Moore *et al.*, 2006; Lodge & Grace, 2009).

Of these at least one of which has been studied at the level of EEG/ECoG/LFP - the MAM-GD17 model. Administration of methylazoxymethanol acetate (MAM) to pregnant dams on gestational day 17 (GD17) yields a behavioural phenotype in adult rats that mirrors many of the core deficits seen in schizophenia, including: PPI deficits and heightened sensitivity to PCP induced hyperlocomotion (see sections 5.1.2 and 5.1.3 on pages 138 and 140 respectively), deficits in latent inhibition and working memory deficits (see Lodge & Grace 2009). As such the MAM-GD17 rat model of schizophrenia is claimed to be a robust developmental model of schizophrenia. In direct contrast to the results reported in this chapter local field potential recordings (LFP) made in MAM-GD17 animals show an absence of low frequency activity in the medial prefrontal cortex (Goto & Grace, 2006) although the same group have more recently reported no spectral differences between MAM-GD17 rats and control animals (Lodge *et al.*, 2009).

The prevalence of increased low frequency activity in the schizophrenia literature is so high that at least one author has suggested that it may be useful as a diagnostic tool (Boutros *et al.*, 2008). The bahavioural battery used to affirm the MAM-GD17 model as a putative model for schizophrenia is impressive. Similarly the sub-chronic PCP model demonstrates deficits in prefrontal cortical function including: reductions in prefrontal cortex glucose metabolism and parvalbumin expression (a marker of GABAergic interneuron activity) (see Pratt *et al.* 2008). Behaviourally these deficits manifest as deficits in an attenional set-shifting task - a rodent analogue of the human Wisconsin card sorting task - in which schizophrenia is associated with deficits in extradimensional shifts (Egerton *et al.*, 2008). In addition it is now suggested, given the findings reported in this chapter, that the sub-chronic PCP model, in addition to these cellular and behavioural deficits, exhibits anomalies in the EEG spectra similar to those reported in the human

condition. Whilst the MAM-GD17 model of schizophrenia fails to recapitulate the EEG anomalies reported in a majority of the schizophrenia literature it is important to restate that schizophrenia is a highly heterogenious disorder with at least some schizophrenics exhibiting a "normal" EEG. It is then likely that a battery of animal models will be required to fully examine this complex disease state with no one model being better or worse than any other. Amongst these models the sub-chronic PCP model can now claim to mirror many of the core cellular, behavioural **and** EEG spectral anomalies associated with this disease.

4.4.4 Effects of mediodorsal thalamic nucleus stimulation

Stimulation of the mediodorsal thalamic nucleus appears to produce acute (within 5 minutes) and transient (decays over approximately 30 minutes) elevation in delta and theta power at widespread cortical electrode locations. In addition the differences between groups in the simulation "on" condition compared with the stimulation "off" condition were modulated with differences between groups being detected at different electrode locations pre and post stim. Whilst the graphed data intimates that the effect of stimulation may be more greatly attributable to changes in the PCP treated group the statistics applied to individual groups lack the n numbers to draw valid conclusions.

4.4.4.1 DBS induced alterations is ECoG power

The increase in delta and theta power reported here as a consequence of DBS is in general agreement with similar studies although some conspicuous differences are apparent. McCracken & Grace (2007) originally reported increases in delta but not theta LFP power in the orbitofrontal cortex as a result of HF DBS of the nucleus accumbens, although this inference was drawn from a post-stimulation measurement. Furthermore this apparent increase took of the order of 30 minutes to manifest as opposed to the rapid onset of low frequency changes reported in this thesis. Consolidating this original assertion McCracken & Grace (2009) demonstrated significant increases in delta but not theta LFP power in the orbitofrontal cortex as a result of nucleus accumbens stimulation manifest only after 60 minutes of continuous stimulation. Furthermore the latter study demonstrated no changes in delta power in the medial prefrontal cortex, mediodorsal thalamic nucleus or in the nucleus accumbens itself. The implication being that modulation of orbitofrontal cortex delta power by nucleus accumbens DBS is mediated by an antidromic mechanism. The nature of the mechanism affecting the modulation

of delta power in the present study is difficult to resolve since thalamo-cortical connections are reciprocated (see section 1.4, page 23). As such stimulation of the mediodorsal thalamic nucleus could affect a response in the cortex by either antidromic or orthodromic mechanisms. Li *et al.* (2007) also report antidromic modulation of the cortical local field potentials and EEG via DBS of the subthalamic nucleus. In agreement with the findings reported in this chapter, and in contrast with the results reported by McCracken & Grace (2007, 2009), Li *et al.* (2007) indicate that modulation of the EEG happens rapidly with onset of stimulation and decays thereafter. However in contrast to both the present study and those of McCracken & Grace (2007, 2009), Li *et al.* (2007) indicate a reduction in both LFP and EEG oscillatory activity in the delta, theta and beta bands. To add grist to the mill Nishida *et al.* (2007) found no spectral differences in the frontal ECoG between animals receiving anterior thalamic stimulation and sham operated animals. Nishida *et al.* (2007) also reports modulation of cortical EEG delta and theta power through stimulation of nuclei of the posterior hypothalamus. In agreement with Li *et al.* (2007), Nishida *et al.* (2007) reports reductions in these power bands yet Nishida *et al.* (2007) associates the modulation of cortical rhythms with histamine release implicating an orthodromic mechanism. The differences between the studies discussed here are palpable (see table 4.9).

Increases *and* decreases in cortical synchronisation, as evidenced by modulation of power in low frequency band-widths, have been reported as a consequence of antidromic cortical activation (McCracken & Grace, 2009; Li *et al.*, 2007). In addition decreases in cortical synchonisation have been reported as a result of presumably orthodromic activation (Nishida *et al.*, 2007). Yet stimulation of the anterior thalamic nucleus failed to produce any modulation of cortical synchronisation (Nishida *et al.*, 2007). Furthermore the temporal profiles of these modulations varies from almost instantaneous to requiring of the order of an hour to manifest following the initiation of stimulation. Disparities abound. How then can these differences be reconciled? The most parsimonious explanation for these disparities is the different stimulated nuclei. Reports of instantaneous modulation of low frequency oscillatory activity are in agreement with those described in this chapter suggesting a degree of similarity in terms of mechanism of action. The temporal profile reported by McCracken & Grace (2009) is at odds with both the findings reported in this chapter and those reported elsewhere, indicating a largely different mechanism of action. The time-scale is reminiscent of the "genomic action potential" (Clayton, 2000) (see section 3.8.3, page 84) suggesting the possibility of modulation of rhythmic oscillations by changes in, for example,

cellular morphology or LTP/LTD.

Similarly the disparities between the increased power in low frequency oscillations reported here and the decreases reported by Li *et al.* (2007) and Nishida *et al.* (2007) are likely to be due to the anatomical loci of the DBS target. Nishida *et al.* (2007) demonstrates a concurrent increase in histamine release as a consequence of stimulation of the posterior hypothalamus (tuberomammillary nucleus and perifornical area) indicating an increase in synaptic transmission in the efferent targets of the stimulated nucleus. In general histamine has been shown to inhibit neuronal firing in the cortex (Feldman *et al.*, 1997). The EEG reflects the summation of inhibitory and excitatory post synaptic potentials (IPSPs and EPSPs respectively) in pyramidal cells in the cortex. Whilst individual action potentials contribute negligibly to the recorded EEG a reduction in neuronal firing, induced by increased histamine release, would be indicative of an increase in IPSPs. In contrast, the results reported in this chapter are likely to be mediated by increased glutamate transmission in the prefrontal cortex, presumably leading to an increase in EPSPs. The opposite actions of these neurotransmitters may provide sufficient explanation for the disparities between these studies. Whilst increased neurotransmission is indicative of an orthdromic mechanism it is impossible to discount a contribution due to an antidromic mechanism in the study by Nishida *et al.* (2007) via the projection from the prefrontal cortex to the posterior hypothalamus (Feldman *et al.*, 1997).

Li *et al.* (2007) also report a suppression of low frequency oscillations in the frontal EEG. In contrast to the results reported here and those reported by Nishida *et al.* (2007) and by corollary with those reported by McCracken & Grace (2009) DBS was targeted at a nucleus with no direct projection to the frontal cortices, in this case the subthalamic nucleus. In agreement with the results described in this chapter the temporal profile of changes due to subthalamic nucleus stimulation demonstrated a decay in the size of the initial effect despite the effect being essentially opposite.

In summary the results reported here provide support to the notion that the synchronous oscillatory activity of neural populations maybe modulated by DBS of various brain structures. Specifically this chapter demonstrates that DBS of the mediodorsal thalamic nucleus yields a transient increase in delta and theta power at frontal cortical regions. It remains unclear as to whether this effect is primarily a consequence of the functional disruption caused by the sub-chronic administration of PCP. The heterogeneity of the responses serves only to highlight

the heterogeneity of the stimulation targets and only furthers the idea that the mechanisms of action are neither singular nor simple. Whilst it is not uncommon to search for a "grand unified theory" for the mechanism by which DBS affects its therapeutic benefit it seems increasingly likely that no such unifying solution will be found. Initial theories of DBS action focused on the stimulated nucleus yielding the popularised "functional lesion" hypothesis. More recent investigations have focused on the efferent targets of the stimulated nucleus yielding the working hypothesis in this thesis; that of "functional deafferentation" (see section 1.3, page 17). One may well wonder where this expansion of exploration may stop. Modulation of neuronal output by DBS yields, by definition, modulation of neuronal input in connected brain regions. Modulation of input to these regions is likely to affect output from these regions. And so on and so forth, yielding potentially widespread effects in large interconnected networks. The complexity is further exacerbated by the addition of antidromic effects potentially yielding modulation in networks providing input to, rather than receiving input from, the stimulated network. The mechanisms of action of DBS are likely to remain the subject of continued research for some time. Despite this its effects can still be studied and the functional implications of these effects are considered herein.

Table 4.9: Summary of reported affects of DBS on modulation of low frequency oscillations in the frontal cortices. **Abbreviations:** Acb, nucleus accumbens; STN, subthalamic nucleus; ATN, anterior thalamic nucleus; TMN, tuberomammillary nucleus; PFN, perifornical area; PFC, prefrontal cortex; OFC, orbitofrontal cortex; HFS, high frequency stimulation; LFP, local field potential; EEG, electroencephalogram; Anti, antidromic; Ortho, orthodromic

Author	**Target**	**Parameters**	**Mode**	**Outcome**	**Mechanism**	**Comments**
McCracken & Grace (2007)	Acb	130/10Hz, 100μs, 100-400μA	LFP	HFS $\Rightarrow\uparrow \delta$ in OFC	Anti	Results reported from post stimulation period
McCracken & Grace (2009)	Acb	130/10Hz, 100μs, 200μA	LFP	HFS $\Rightarrow\uparrow \delta, \beta, \gamma$ in OFC, $\uparrow \gamma$ in mPFC, $\uparrow \beta, \gamma$ in MD	Anti	60 minutes required to attain effects
Li *et al.* (2007)	STN	40-160Hz, 100μs, 80-260μA	LFP/ EEG	$\downarrow \delta$, $\downarrow \theta$	Anti	Effects of "chronic" DBS studied for a maximum of 100s
Nishida *et al.* (2007)	TMN	100Hz, 300μs, 80/150μA	EEG	$\downarrow \delta, \uparrow$ histamine in PFC	Ortho	Effects of only 10 second stimulation burst studied.
	PFN	100Hz, 300μs, 80/150μA	EEG	$\downarrow \delta$ in PFC	Ortho	
	ATN	100Hz, 300μs, 80/150μA	EEG	No effect	-	

4.4.5 Functional implications

Functional interpretations of changes in ECoG oscillations and their relation to cognitive processes in anaesthetised rats is challenging. Furthermore evidence regarding the functional role of delta oscillations is thus far limited (Uhlhaas *et al.*, 2008). Despite this the results reported in this chapter demonstrate significant parallels between the the ECoG anomalies associated with an anaesthetised "schizophrenic" rat and similar anomalies reported in conscious humans. As already discussed the group differences due to treatment effects in the subchronic PCP model capture the increased delta activity reported in schizophrenic patients, particularly those exhibited by schizophrenics with a predominance of negative symptoms. This additional validation of this model suggests that the increased low frequency power in cortical regions may underpin the cognitive disruption reported in this model. In addition Babiloni *et al.* (2006) have indicated that increased delta power may be correlated with reductions in white matter volume in patients with mild cognitive impairment and Alzheimer's disease. The increased delta power seen in schizophrenics may be depend, at least in part, on the reported reduced white matter integrity reported in schizophrenia (see section 1.1.2.5, page 9). Increased delta power has been associated with significant reductions in regional cerebral blood flow (rCBF) in sleeping humans (Hofle *et al.*, 1997) suggesting a potential correlate between the increased delta power reported here and the reduced cerebral glucose metabolism reported by Cochran *et al.* (2003).

4.4.6 Caveats & extensions

The results reported in this chapter indicate that both subchronic PCP administration and DBS have the ability to modulate *something*. But what is the substance of this something? To describe the interpretation of results garnered from an anaesthetised preparation as "challenging" is an understatement. Whilst the effects described here attempt to control for the effects of the anaesthetic, there can be no doubt at all that the anaesthetic itself is having the greatest effect on the system. One only has to cast a cursory glance at an animal under anaesthesia to see the truth of this. In addition when trying to seek solace in the literature one only finds multiple confounds since the literature is scattered with multiple anaesthetics, all of which effect the observables in different ways. For example chloral hydrate is known to be a preferable anaesthetic when investigating monoamine systems. However the same anaesthetic would be detrimental to

cortical potentials where urethane may be preferred. Presumably cortical potentials have some dependence on their monoaminergic inputs so, whilst urethane may preserve cortical potentials to some extent, these potentials still reflect the physiology of a heavily biased system, in this case a system with a suppressed monoamine input.

In this study isoflurane was selected as the anaesthetic agent. Isoflurane is known to suppress cortical potentials in a dose dependent manner. Lloyd-Thomas *et al.* (1990) report that isoflurane inhaled at 2% completely suppresses the EEG. At lower concentrations the EEG alternates between states of complete suppression and states of high activity. These states correspond to the "up" and "down" states described in this chapter. This pattern of activity is entirely alien in an awake recording and reflects the physiology of a system that is heavily compromised. What then is one to make of the differences reported in this chapter? The treatment effects (PCP vs. VEH) reflect the action of PCP - an anaesthetic in itself - on an already anaesthetised system. The effect of DBS is similarly mired in this soup of anaesthesia. All one can say with anything approaching confidence is that *something* happened. Both of the interventions explored here demonstrated a potential to have an effect. The true nature of these effects though remains unclear - both the nature of the effect and the physiology underlying them.

These experiments need to be extended to provide more useful answers. The recording modality should be changed from recording ECoG to LFP. The ECoG signals recorded here lack the necessary specificity to really pin down the origin of the changes. Whilst the ECoG may allow one to easily map cortical potentials over the whole cortex it provides no means to explore deeper regions. Even when considering these cortical potentials the most frontal electrodes are most likely recording from the motor cortex when it is really the underlying prelimbic and infralimbic cortices that would be of most interest in an animal model of schizophrenia. The regions to be explored in an LFP study should be carefully considered and it is suggested here that at least the prelimbic and infralimbic cortices may be of interest. These loop back to themselves through striatal and thalamic subterritories which would make the nucleus accumbens and thalamus interesting targets also.

Having identified suitable targets it is vital that these recordings be made in the awake animal for reasons detailed above. Such methods require careful consideration. The oscillations will now be heavily dependent upon the behaviour of the animal and the problems of identifying "stationary" periods will need to be

addressed. In addition the signal is likely to be contaminated with movement artifacts which will heavily contaminate the power spectra if they are not identified and removed. An obvious solution would be to identify oscillations corresponding to periods where the animal is inactive - a wakeful, resting state. This is a common approach in the human literature. However one may find that the important differences manifest only when the animal performs a certain action and activates a certain neural pathway. Gruber *et al.* (2010) demonstrate no basal differences in oscillations between the ventral hippocampal lesion model (a model of schizophrenia like deficits in rats) and controls but a failure to activate certain oscillations during certain behaviours.

The study of neural oscillations is an exciting, dynamic and rapidly expanding field and it is reassuring that the interventions discussed in this chapter have the capacity to affect such oscillations. To better determine what these effects really are, where they originate and what they mean may be a life long study. Oscillations are open to multiple levels of analysis of which this chapter has only concerned itself with power spectral analysis. Of great interest would be the computation of additional variables including; coherence (a measure of functional connectivity), Granger causality (a statistical approach to causality between signals) and dynamic causal modeling (a measure of the strength of connections between regions). The complexity of such analyses arguably requires a higher quality data set (awake recordings) and such analyses are not considered further. The remainder of this thesis concerns itself with the possible behavioural consequences of the biomolecular and electrophysiological changes that have been reported in the previous chapters.

Part IV

Behaviour

Chapter 5

High frequency deep brain stimulation of the mediodorsal thalamic nucleus has no effect on motor function, modulates prepulse inhibition of the startle reflex and augments the hyperlocomotion induced by administration of PCP

5.1 Introduction

Having established that HFS DBS of the mediodorsal thalamic nucleus increases neural activity at the cellular level, as determined by increases in the expression of the IEG *zif-268*, and transiently through quantitative analysis of the ECoG, in anaesthetised animals it is pertinent to examine the behavioural consequences of such cellular activation. Before exploring behaviours in animal models which reflect some of the deficits seen in schizophrenia it is important to consider the possibility that such a DBS paradigm may generate undesirable behavioural side effects. Moreover the DBS paradigm explored in chapter 3 generated neuronal excitation in *all* regions of the prefrontal cortex, including the secondary motor

cortex. In the first instance general open-field behaviours were assessed to identify any possible motor side effects. Pre-pulse inhibition of the startle response was also explored given the well documented deficits seen in this task in human schizophrenics. Finally the effect of DBS on PCP induced hyperlocomotion, a putative rat model of psychosis, was assessed. The results of these experiments are described in this chapter.

5.1.1 Open-field locomotor activity

Assessment of locomotor activity in the open-field is one of the most commonly employed tests in the study of animal behaviour. Since its inception in 1934, in which defecation was used as an index of timidity, the number of observables measured and the means with which to measure them has vastly expanded. Variables typically measured using automated locomotion detection systems systems include total distance traveled, rearing and time spent in the centre of the arena when compared with the time spent in the perimeter (Crawley, 2000). The latter is known as thigmotaxis, a behaviour whereby fearful animals spend a disproportionate period of time close to the walls of the open-field and is thought to be an index of anxiety (Silverman, 1978). The popularity of the techniques are likely attributable to the ease with which such studies can be performed (see Walsh & Cummins 1976). As noted by Stanford (2007), "The procedure is apparently so straightforward that neither the rodents nor the humans require specialist training". Whilst this is in itself a criticism the point is none-the-less valid. The study of open-field behaviours *is* simple, providing a means to rapidly assess alteration in commonly recorded parameters due to some sort of intervention, in this case electrical stimulation of subcortical brain nuclei. But, whilst this is true, it is important to consider the limitations of studying open-field locomotor activity. The results of such studies are often difficult to interpret since the observable (locomotor activity) may depend on the intervention in a highly complicated manner. By way of example Hall (1934), the originator of the open-field test, observed that rats deprived of food traveled further and faster than those that were well fed (see Silverman 1978). Similarly, administration of certain drugs yields "hyperlocomotion" with an observed increase in distance traveled (see section 5.1.3, page 140). Furthermore comparison between studies performed in different laboratories is made difficult given the extensive variations in methodology (see Walsh & Cummins 1976; Stanford 2007; Kulkarni 1977). All things considered assessment of open-field behaviours provides an, albeit crude, indicator of the effect of an intervention on locomotor activity. Given the activation of the prefrontal

motor cortex (secondary motor cortex) demonstrated in chapter 3 it is pertinent to exclude any potential motor side effects of stimulation before exploring more complicated behaviours which may be confounded by such side effects.

5.1.2 Prepulse inhibition

The term "pre-pulse inhibition" (PPI) refers to a sensorimotor gating phenomenon whereby the prior presentation of a weak stimulus (pre-pulse) attenuates the response (startle reflex) normally induced by a sudden intense startling stimulus. PPI is thought to be manifest as a result of diminished attention to the startling stimulus due to the ongoing processing of the pre-pulse. As such PPI may reflect a mechanism by which organisms reduce the influence of potentially disruptive sensory information thereby reducing behavioural interference caused by the processing of discrete, simultaneous inputs. PPI represents a particularly useful behavioural measure since the phenomenon has been reported in a large number of species; humans and animals, including invertebrates (see Kumari *et al.* 2003; Li *et al.* 2009; Swerdlow *et al.* 2001).

5.1.2.1 PPI circuitry

Whilst PPI appears a relatively robust behavioural measure across species, Swerdlow *et al.* (2001) cautions against assuming homology between the circuits mediating the response in animal models and humans. Of particular importance in the current context; it cannot be assumed that the involvement of the medial prefrontal cortex in PPI reported in rats extrapolates to the regulation of PPI in humans. However much of what is known about the neural substrates of PPI has been identified in the rat.

The anatomical loci which contribute to the manifestation of PPI can be grouped as those which *mediate* PPI through brain stem nuclei; including the inferior and superior colliculus, pedunculopontine tegmental nucleus, laterodorsal tegmental nucleus, substantia nigra pars reticular and caudal pontine reticular nucleus (see Kumari *et al.* 2003; Swerdlow *et al.* 2001); and those which *regulate* PPI through forebrain nuclei; including the prefrontal cortex, thalamus, hippocampus, amygdala, ventral striatum, ventral pallidum and globus pallidum (see Swerdlow *et al.* 2001). The mediatory circuitry receives the input stimuli and affects the motor output. The regulatory circuitry impinges on the mediatory circuitry via the pedunculopontine tegmental nucleus providing a means to modulate the motor response (see figure 5.1).

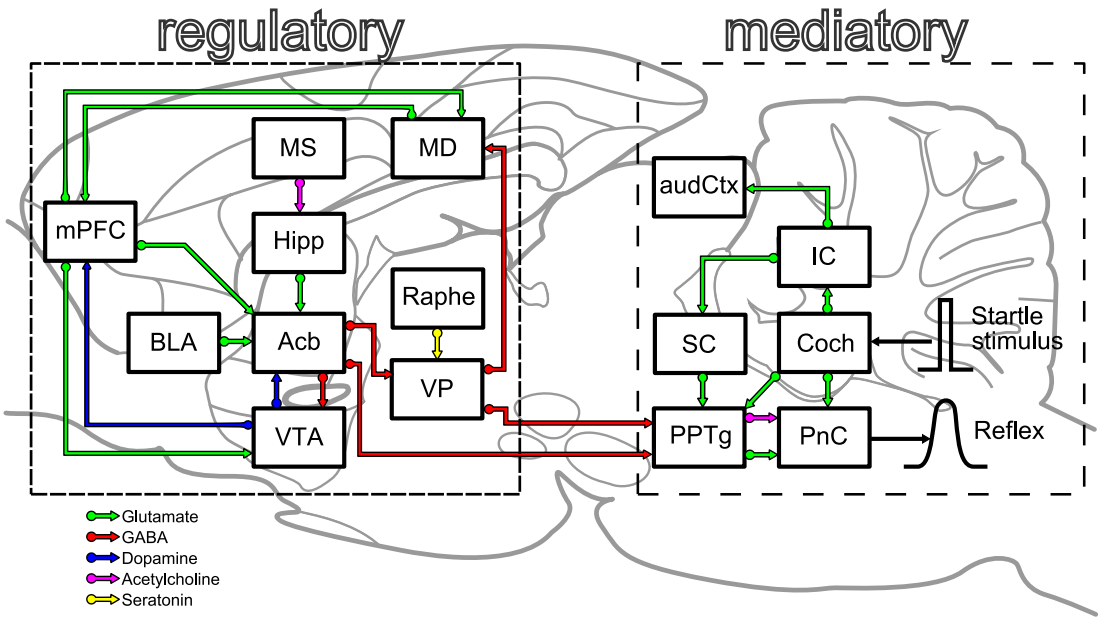

Figure 5.1: Neural circuitry involved in PPI (adapted from (Swerdlow *et al.*, 2001)). **Abbreviations:** mPFC, mprefrontal cortex; MS, medial septum; Hipp, hippocampus; BLA, basolateral amygdaloid nucleus; Acb, nucleus accumbens; VTA, ventral tegmental area; MD, mediodorsal thalamic nucleus; Raphe, raphe nucleus; VP, ventral pallidum; audCtx, auditory cortex; SC, superior colliculus; IC, inferior colliculus; Coch, cochleal neurons; PPTg, pedunculopontine tegmental nucleus, PnC; caudal pontine reticular nucleus.

5.1.2.2 PPI in schizophrenia

It is immediately apparent that the neural circuitry involved in regulating PPI is similar to the circuitry implicated in the pathophysiology of schizophrenia (see figures 1.4, page 32 and 5.1). However, many of the multiple nuclei of the regulatory circuitry are implicated in many disease states and, correspondingly, deficits in PPI have been reported in large number of disease states including schizophrenia as well as obsessive-compulsive disorder, Huntington's disease, nocturnal enuresis, attention deficit disorder and Tourette's syndrome (see Braff *et al.* 2001; Kumari *et al.* 2003).

A multitude of studies demonstrate deficits in PPI in schizophrenics across all commonly measured sensory modalities. Significant evidence indicates that these PPI anomalies correlate with the thought disorder associated with this disease (see Braff *et al.* 2001).

Whilst Swerdlow *et al.* (2001) advised caution when extrapolating between the circuitry regulating PPI in the rat and that regulating PPI in humans, more recent studies have indicated significant parallels between the two systems. The

study by Hazlett *et al.* (2001) indicates anterior and mediodorsal thalamic nuclei involvement in an "attention to pre-pulse" paradigm. Attention to pre-pulse paradigms require subjects to attend to a pre-pulse of a specific pitch but ignore pre-pulses delivered at other pitches. Furthermore Kumari *et al.* (2003) have demonstrated activation of the striatum, hippocampus and thalamus in healthy subjects with diminished activation in the same regions in schizophrenic subjects. The study by Kumari *et al.* (2003) required no "attention-to-prepulse" so is perhaps more analagous to PPI paradigms in animals. These reports have been further substantiated by Hazlett *et al.* (2008), demonstrating diminished activation in the dorsolateral prefrontal cortex, striatum and mediodorsal thalamic nucleus in schizophrenic patients when compared to healthy controls in an "attention to pre-pulse" paradigm.

5.1.3 PCP hyperlocomotion

Acute administration of PCP produces transient psychosis in healthy volunteers that closely mimics that seen in schizophrenic patients (see Mouri *et al.* 2007). Whilst NMDA antagonists such as PCP do not, in general, induce hyperlocomotion in primates (Takahata & Moghaddam, 2003), hyperlocomotor activity is considered, by some, to be a predictor of the propensity of a drug to induce or exacerbate psychosis (Adams & Moghaddam, 1998). This apparent disparity suggests that these behaviours are irrelevant with respect to the clinical effect of this class of drug. However, in rodents these behaviours are generally associated with limbic striatal function (Takahata & Moghaddam, 2003). So where in man aberrant limbic function might present as psychosis (see Takahata & Moghaddam 2003), in rodents it presents as locomotor disturbances, suggesting that this may be a useful model of the positive symptoms associated with schizophrenia (Mouri *et al.*, 2007).

PCP induces hyperlocomotion in rats (Jentsch *et al.*, 1998) through, it has been argued, increased dopamine release in the ventral striatum (see Takahata & Moghaddam 2003; Jentsch *et al.* 1998). Jentsch *et al.* (1998) showed that prefrontal cortex lesions abolished PCP-induced hyperlocomotion whilst attenuating the typically associated increase in dopamine usage in the nucleus accumbens. Despite this the role of the nucleus accumbens in PCP-induced hyperlocomotion is unclear. Moreover, it is likely that this hyperdopaminergic state is an effect like - rather than a cause of - PCP-induced hyperlocomotion. What *is* clear is that the behavioural phenotype involves the prefrontal cortex.

5.1.4 Experimental aims & rationale

The sections below describe the methods employed in the exploration of the behaviours described above. Electrodes, devices and surgery were performed as previously described (see sections 2.1.1.1, 2.1.2, 2.2.1, on pages 37, 39, 45) and behavioural tests are followed with little deviation from standard paradigms (see Egerton *et al.* 2008). However this chapter introduces the idea of a *stimulated* "control" rather than simply a *sham-operated* control. A sham-operated control would, as one would expect, have electrodes implanted in the same brain regions as the stimulated animals. This control group effectively controls for effects arising as a result of electrode implantation thereby providing confidence that any observed effects are due to stimulation and not a "micro-lesion" effect due to electrode insertion. However such a group provides no control for non-specific effects of stimulation. The ECoG recordings from the previous chapter indicate that stimulation artifacts propagate throughout the brain (see figure 4.8, page 107). One may reasonably wish to control for this to provide confidence that the effects arising from the stimulation are specific to the stimulated nucleus and not simply an effect of volume conduction of the applied current throughout the brain. To this end a group of animals had electrodes implanted bilaterally into the globus pallidum as well as the target of interest - the mediodorsal thalamic nucleus. As demonstrated in chapter 3 stimulation of the mediodorsal thalamic nucleus yields activation of the frontal cortices. The globus pallidum has no direct anatomical connections with the frontal cortices but is separated from it by a distance similar to that of the mediodorsal thalamic nucleus. Presumably the volume conduction of the DBS waveform from the mediodorsal thalamic nucleus and globus pallidum would be similar so stimulation of the globus pallidum should provide a control for any effects arising from this.

The aim of these experiments were:

1. To implement the methodology developed in section 2.1.2 (page 39) in conscious rodents and further refine the techniques necessary to investigate DBS in awake, freely moving animals.

2. To ascertain if HF DBS of the mediodorsal thalamic nucleus causes any motor side effects through activation of secondary motor cortex.

3. To determine the effects of HF DBS of the mediodorsal thalamic nucleus on pre-pulse inhibition of the startle response.

4. To determine the effects of HF DBS of the mediodorsal thalamic nucleus on PCP induced hyperlocomotion.

5.2 Methods

5.2.1 Stimulation electrodes

Stimulation electrodes were fabricated (see section 2.1.1.1, page 37), tested and sterilised as previously described (see section 2.1.1.1, page 37).

5.2.2 Deep brain stimulation device

DBS devices were constructed and tested as previously described (see section 2.1.2, page 39).

5.2.3 Animals & experimental groups

Male Hooded Lister rats (Harlan UK Limited) weighing between 360g and 415g (n = 20, 10 per group (*i.e:* 10 animals in the mediodorsal thalamic nucleus implanted group and 10 animals in the globus pallidum implanted group), were housed in pairs in a temperature regulated room maintained at 20°C with a 12 hour light/dark cycle prior to surgery. Lights on at 8:00am. Food and water were available *ad libitum*. All procedures were carried out in accordance with Home Office regulations. Pre-surgery, environmental enrichment was provided by the addition of a wooden house to the cage. Post surgery, the house was removed to prevent animals catching the externalised connectors on it and enrichment was provided by the addition of wooden chew sticks. Post surgery, animals were housed individually and access to the area under the food hopper was prevented by screening this area of the cage off with a metal partition again to afford additional protection to the externalised connectors. A detailed flow chart of the experimental procedures is included in section 5.2.7.1 (see figure 5.2, page 145).

5.2.4 Surgical protocol

Animals were randomly allocated a surgical procedure - either implantation of electrodes bilaterally into the mediodorsal thalamic nucleus or into the globus pallidum. Surgery was performed as previously described (see section 2.2.1, page 45). Briefly, animals were anaesthetised by the inhalation of isoflurane (Abbott Animal Health) and mounted in a stereotaxic frame using atraumatic earbars

(David Kopf Instruments). Analgesia and local anaesthesia was provided via a subcutaneous dose of Rimadyl™ and a bolus injection of a lidocaine/bupivacaine into the scalp. Body temperature was maintained using a small heatpad (Fine Science Tools Inc.). A single rostral-caudal incision was made, the skull exposed and bregma identified. 1mm diameter burr holes were drilled at the following coordinates: mediodorsal thalamic nucleus: RC; -2.04mm, ML; ±2.43mm, globus pallidum: RC; -1.32mm, ML; ±2.09mm (Paxinos & Watson, 2007).

The dura beneath the hole was excised with a small needle. Deep brain electrodes were implanted through the holes, bilaterally, at 20° to the perpendicular, in the coronal plane, into the mediodorsal thalamic nucleus (DV: ↓5.60mm) and into the globus pallidum, at 0° to the perpendicular, in the coronal plane (DV: ↓5.69mm). All electrodes were secured to screws anchored in the skull using dental cement (Kemdent) and the incision sutured around the implant. Animals were recovered for a minimum of 7 days before beginning to habituate them to the rodent jackets and stimulation devices. Animals were weighed daily following the start of the habituation to assess general health. All animals were found to have increased their mass from their surgical mass and continued to do so indicating that the animals were generally healthy post-operatively.

5.2.5 Habituation to jackets & sham-devices

Animals were habituated, over a period of 5 days, to the rodent jackets that would subsequently be used to hold the DBS device. Animals were weighed, to determine the appropriate size for the jacket, and handled for 2 minutes prior to placing them in a rodent jacket. Animals would then be handled for a further 2 minutes before being returned to their home cage. Over a period of several days animals would be left in the jackets for up to a maximum period of 2 hours. Having habituated to the rodent jacket animals were then habituated to the devices by placing them in the jackets, attaching dummy devices (see 2.1.2.7, page 44) and making the necessary connections between the device and the implant. Each animal was given at least 2 full 2 hour sessions wearing the full stimulation rig before behavioural testing. One animal failed to habituate to this procedure and was withdrawn from the study (mediodorsal thalamic nucleus group, n = 9).

5.2.6 Stimulation protocol

Devices were configured to deliver a constant current of 100μA at a frequency of 130Hz delivered in pulses of 100μs duration. The current used in the recovery

experiments was half that used in the anaesthetised studies. It has been shown that a current of approximately twice that required in a conscious animals is required to elicit the same response in an anaesthetised preparation (see Albert *et al.* 2009). Devices were quickly tested immediately before attachment to the animal by connecting them to an oscilloscope and observing the output from the DBS device. Devices were tested again at the end of the experiment to confirm that they had functioned correctly throughout the experiment. Stimulation was delivered unilaterally to the left hemisphere in the open field and PPI tests (either nucleus) and the right hemisphere in the PCP hyperlocomotion test for 60 minutes prior to beginning the behavioural tests and continuously throughout the tests. Unilateral stimulation was chosen for continuity since the previous chapters investigated unilateral stimulation. Stimulation of the right hemisphere was chosen in the PCP hyperlocomotion test since 2 animals broke the connections to the electrode implanted in the left hemisphere in the PPI task thereby making it impossible to deliver stimulation to the left hemisphere in all animals in the PCP hyperlocomotion test.

5.2.7 Behavioural tests

5.2.7.1 Experimental timeline

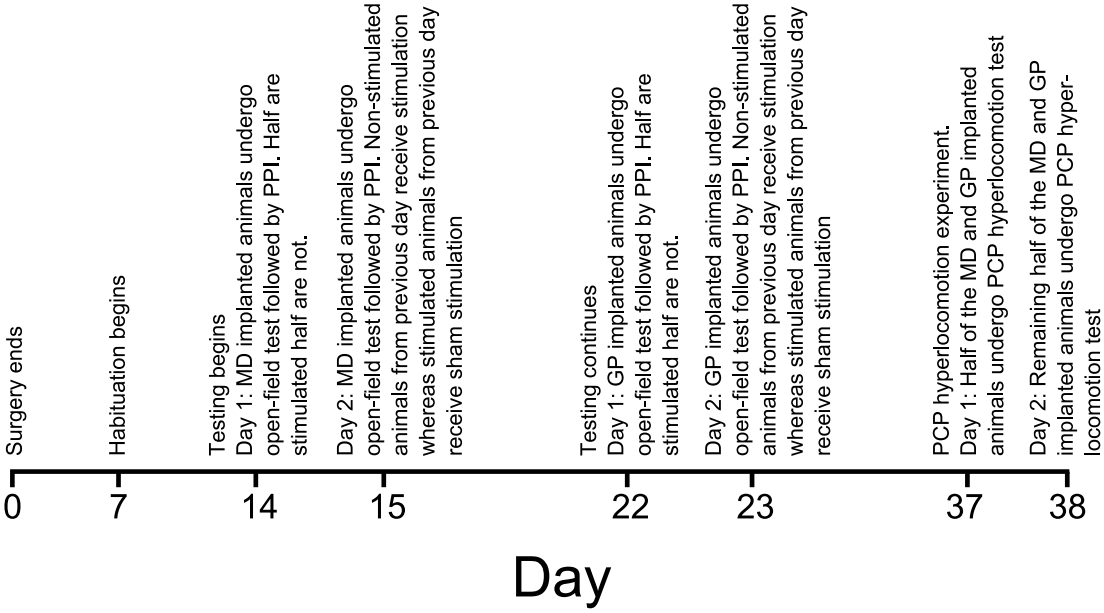

Figure 5.2: Experimental timeline. After completion of surgery in all 20 animals a minimum of 7 days was left before beginning the habituation procedure. This process lasted a week before the first stage of testing. All animals from the mediodorsal thalamic nucleus implanted group were tested in both the open-field and PPI tests on two consecutive days with their stimulation condition reversed on the second day. 1 week later the globus pallidum animals underwent the same protocol. 2 weeks later all animals from both groups underwent the PCP-induced hyperlocomotion experiment conducted over 2 consecutive days. Animals began receiving stimulation 60 minutes prior to the beginning of any of the behavioural tests. In the PCP hyperlocomotion test mediodorsal thalamic nucleus implanted animals received stimulation for 60 minutes prior to exposure to the open-field. After 30 minutes habituating to the open-field, animals were administered with PCP ($5mg.kg^{-1}$) and locomotor activity assessed for a further 60 minutes.

5.2.7.2 Open-field

On the day of testing animals were placed in jackets, connections made and stimulated as described above prior to being placed into a large open-field (60×60cm high walled, open topped, IR transparent enclosure) for 15 minutes. All animals were initially placed into the centre of the open-field arena. The open-fields were placed on an infra-red lightbox and the video captured digitally via an infra-red CCD camera (Sanyo), an MPEG encoder (USB 2.0 Pro audio video grabber (Cypress Technology Co. Ltd.)) using USB-205 software (Cypress Technology Co. Ltd.). Animals were randomly allocated by stimulation protocol (stimulation or

sham) and time of day. They performed the open-field tests twice on consecutive days based on the double test cross-over design described by Leyland *et al.* (1979) which is purported to have greater sensitivity. Animals would either be receiving stimulation or sham-stimulation (attachment of devices and connectors but no delivery of current) in each of the two trials in a counterbalanced design with half the animals receiving stimulation on the first day of testing and sham-stimulation on the following day with these conditions reversed in the remaining animals. Two open-fields could be tracked simultaneously and each animal only experienced each open-field once (*i.e:* individual animals were always placed into the open-field in which they had not been previously on the second trial) in an attempt to negate habituation to the open-field after the first trial. The video files were then tracked using EthoVISION (Tracksys Ltd.) and the track information processed to determine; total distance travelled, speed, turn angle, rearing frequency, time in centre/time in perimeter.

5.2.7.3 Prepulse inhibition

Following exposure to the open-field animals were returned briefly to their home-cages before being placed into the PPI apparatus. By this point animals had received between 90 and 120 minutes of stimulation. Animals were restrained in a perspex tube (diameter: 7.5cm, length: 12.5cm) and the tube secured onto a piezo electric platform inside an acoustically isolated chamber (Med Associates Inc). The animals then underwent a series of randomised trials to test their ability to inhibit their startle response to a 120dB sound pulse when exposed to a preceding pulse of 4, 8 and 16dB louder than a background volume of 65dB (white noise) according to a protocol devised by Egerton *et al.* (2008). Following completion of the test animals were disconnected, undressed and returned to their home-cages.

Once restrained and secured within the startle chamber, animals were given 5 minutes to acclimitise to a 65dB background of white noise. Three blocks of trials followed in which the inter-trial interval was varied between 8 and 23 seconds. The variable inter-trial interval prevents the animal from predicting the period in which it might be startled. The first and last consisted of 6 startle-stimulus (120dB white noise presented for 40ms) alone trials. These trials given an indication of any habituation of the startle response through repeated exposure to the startle-stimulus. The central block consisted of 52 trials presented in a pseudorandom order. Of the 52 trials 12 were startle-stimulus alone trials and 10 were trials in which no-stimulus was presented. In the remaining trials the

startle-stimulus was preceded by a pre-pulse of white noise, 20ms in duration, presented 100ms before the startle-stimulus. The pre-pulse amplitudes were 4, 8 and 16dB louder than the background volume, there being 10 trials at each volume. The "startle response" was acquired using MED Associates Startle software (SOF-825) which records the displacement of the piezo electric platform over the 100ms period following the onset of the startle-stimulus. PPI for each prepulse amplitude was calculated from trials in the central block only via the following formula (Egerton *et al.*, 2008). "Startle magnitude" is the magnitude of the startle response determined by integrating the voltage delfection measure by the piezo electric platform on trials where only the startle pulse is delivered. Similarly "Prepulse startle magnitude" is the magnitude of the startle response on prepulse trials.

$$\%\text{PPI} = 100 \times \left(\frac{\text{Startle magnitude} - \text{Prepulse startle magnitude}}{\text{Startle magnitude}} \right) \quad (5.1)$$

5.2.7.4 PCP induced hyperlocomotion

On the day of testing animals were placed in jackets, connections made and stimulated as described above prior to being tested. In this test animals with electrodes implanted in their mediodorsal thalamic nucleus were stimulated whilst animals with electrodes implanted in their globus pallidum served as the non-stimulated controls. After an hour of stimulation/sham-stimulation animals were placed into a small open-field (40 × 40cm high walled, open topped, IR transparent enclosure) for a total of 90 minutes. After a 30 minute habituation period to the open-field animals were briefly removed and injected with PCP (5mg.kg^{-1} administered in 1ml.kg^{-1} i.p.) before being returned to the open-field for a further 60 minutes. The open-fields were placed on an infra-red lightbox and the video captured as described above.

The subsequent 90 minutes of digital video was binned into 9× 10 minute (3 pre-drug and 6 post drug) trials. The trials were tracked using Tracksys Ltd. software and the distance moved for each time bin computed.

Inspection of the video during track acquisition indicated that, in addition to the PCP induced hyperlocomotion, the animals also exhibited a number of other drug induced characteristics. The most prominent of these characteristics was head-bobbing, a rhythmical, stereotypic movement of the head from side to side in the plane of the floor. A loss of balance seemed apparent resulting in the animal lying

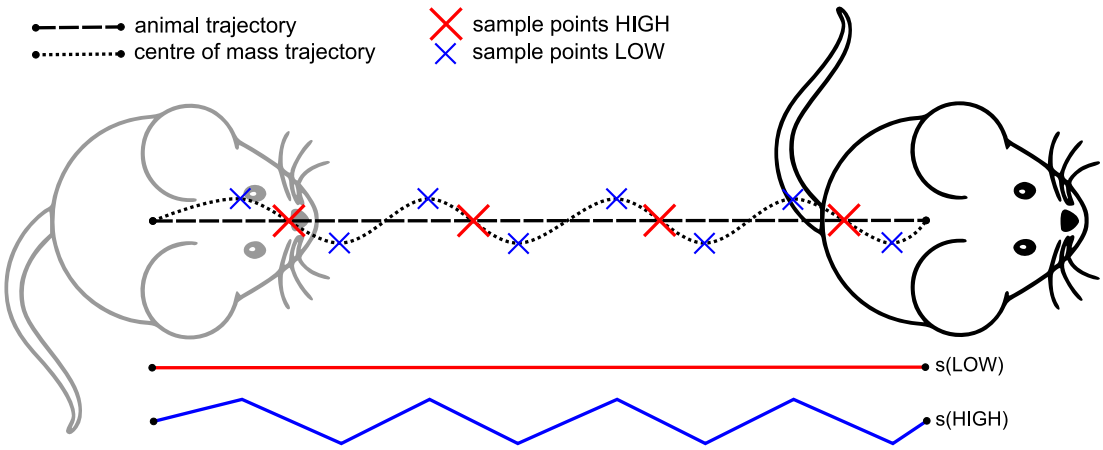

Figure 5.3: Measuring ataxia and stereotypy with EthoVISION. Measuring the distance travelled by an animal at a higher sample rate over estimates the distance travelled by the rat (s(HIGH)) by including the modulation in the position of the centre of mass. Measuring the distance at a lower sample rate gives a more accurate estimate of the "true" distance travelled (s(LOW)).

on its side whilst their limbs seemed to move without any net locomotion in any direction. Whilst rats naturally have a "shambling" gait whereby their centre of mass rocks gently from side to side as they ambulate this seemed accentuated in PCP treated animals. The net effect of these additional behaviours results in the oscillation of the animal's centre of mass without necessarily any net movement in any given direction which this author has described as ataxia (loss of coordinated body movements) and stereotypy (rhythmic stereotypical movements). In an attempt to characterise these behaviours using the EthoVISION software the following protocol was designed.

EthoVISION tracks the position of the animal's centre of mass by estimating its position from the 2 dimensional surface area (in the plane of the floor) of the animal. Even in an animal making no net movement in the horizontal plane this position is still modulated by movements of the head, limbs and body. This modulation in the position of the centre of mass, if captured at a high enough sample rate, contributes to the total distance traveled computed by the EthoVISION software. It follows that tracking the video at a lower sample rate will yield a better estimate of the *actual* horizontal distance traveled and that the differences in distance traveled between the two sample rates will provide an estimate of the distance traveled by the centre of mass outwith the distance it travels due to locomotion. As such it is suggested that the difference in distance traveled measured at a high and low sample rate provides an estimate of the modulation

in the position of the centre of mass, *i.e:* a measure of ataxic and stereotypical movements.

The video files were retracked at a high (5Hz) and a low (3.25Hz) sample rate and the distance traveled at each sample rate computed. The difference between these two distances was then calculated.

$$s(\text{ataxia}) = s(\text{LOW}) - s(\text{HIGH}) \tag{5.2}$$

5.2.7.5 Electrode marking & histology

The positions of electrode tips were marked with a small electrolytic lesion. Animals were briefly re-anaesthetised and a constant current of 100μA was passed through each electrode for 10 seconds. Animals were euthanased via cervical dislocation the brains removed, snap frozen and stored as previously described (see section 2.3.1, page 48). Brains were then sectioned and electrode tracks identified as previously described (see section 2.7, page 49).

5.2.7.6 Statistical analysis

Animals with misplaced electrodes were excluded from the analysis. Disconnection of the DBS device from the DBS electrodes was defined as a failure and animals that failed their behavioural test were also excluded from further analysis. No animals failed tests in the open field. However the restraints required for the PPI tests generally led to an approximate 50% failure rate in this test due to connections being broken due to repeated contact with the restraints. Data from the open field test were analyzed using paired Student's t-test in `Prism5` (Graphpad Software Inc.) with significance defined at the 5% level. Data from the PPI experiment were analysed with a repeated measures ANOVA with prepulse intensity as the within-subjects factor and stimulation status (on/off) as the between subjects factor using SPSS version 17.0. Startle responses were analysed by one-way ANOVA in SPSS version 17.0. The PCP hyperlocomotion experiment was analysed using a Student's t-test in `Prism5` (Graphpad Software Inc.) with significance defined at the 5% level to determine any difference between groups at the end of the habituation period. The data were then scrutinised with a repeated measures ANOVA with time as the repeated measure and stimulation status (on/off) as the between subjects factor using SPSS version 17.0.

5.3 Results & analysis

5.3.1 Electrode placements and exclusions

Animals were excluded from the analysis if electrodes were placed outwith the target. In the open-field and PCP hyperlocomotion experiments 3 animals were excluded from the mediodorsal thalamic nucleus implanted group. 3 animals were also excluded from the globus pallidum implanted group in these tests (see figure 5.4). In addition one further animal was excluded from the mediodorsal thalamic nucleus implanted group due to the animal's failure to habituate to the jackets and devices. The PPI experiment required further exclusions due to device failures (broken device connections during the task) during the experiment. This lead to 4 animals being used for the analysis of PPI effects in the mediodorsal thalamic nucleus group and 4 animals in the globus pallidum group.

5.3.2 Open-field

The effects of HF DBS of the mediodorsal thalamic nucleus on open-field behaviours are illustrated below (see figure 5.5). No significant differences between stimulated and sham-stimulated animals were found in any of the behaviours measured, including: total distance travelled (see figure 5.5(a)), the average velocity of movement (see figure 5.5(b)), the frequency of rearing (see figure 5.5(c)), the time spent in the centre/perimeter of the arena (see figure 5.5(d)) and the average angle turned by an animal (see figure 5.5(e)).

Similarly the effects of HF DBS of the globus pallidum on open-field behaviours are illustrated below (see figure 5.6). No significant differences between stimulated and sham-stimulated animals were found in any of the behaviours measured, including: total distance travelled (see figure 5.6(a)), the average velocity of movement (see figure 5.6(b)), the frequency of rearing (see figure 5.6(c)), the time spent in the centre/perimeter of the arena (see figure 5.6(d)) and the average angle turned by an animal (see figure 5.6(e)).

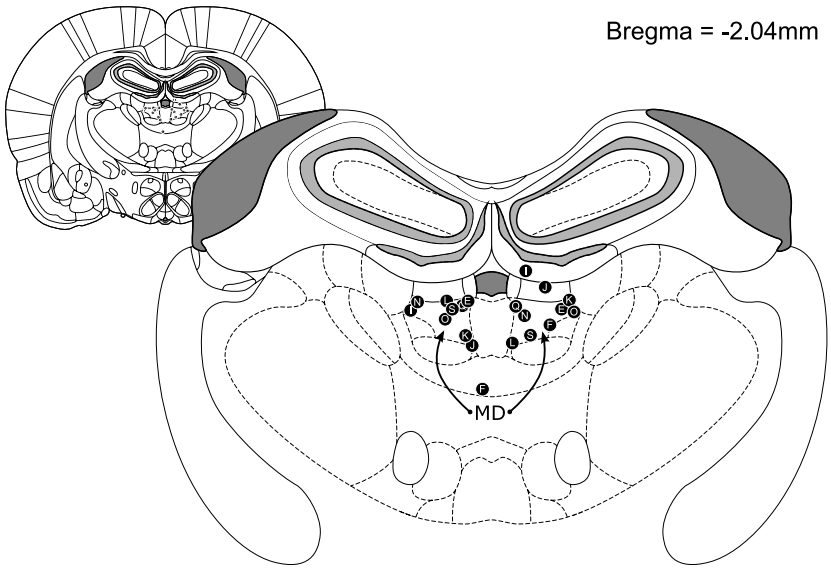

(a) In the mediodorsal thalamic nucleus

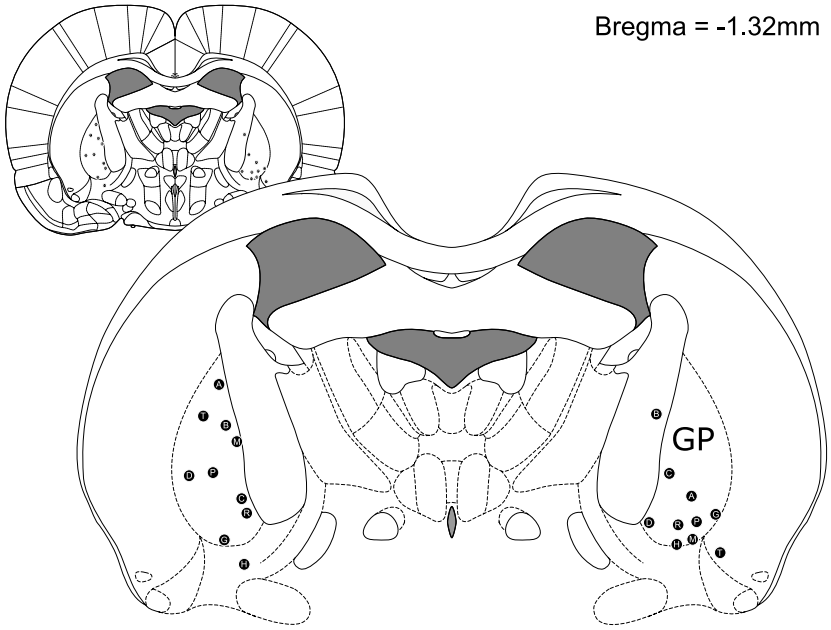

(b) In the globus pallidum

Figure 5.4: Location of the electrode placements in (a) the mediodorsal thalamic nucleusand (b) the globus pallidum. Animals were excluded from the analysis if electrodes were placed outwith the target. 3 animals were excluded from the mediodorsal thalamic nucleus group. 3 animals were also excluded from the globus pallidum group.

5.3.2.1 MD stimulation - open-field

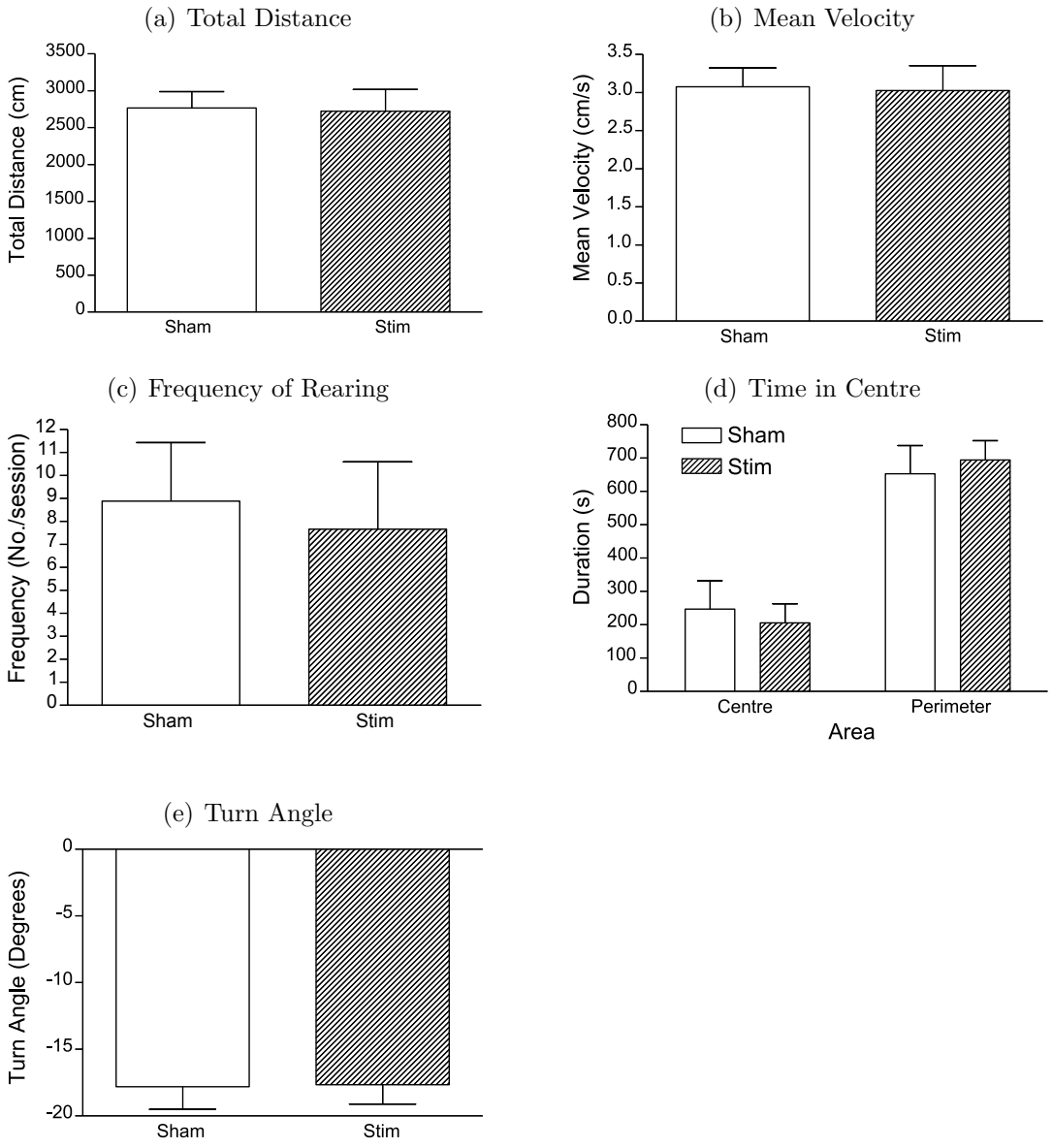

Figure 5.5: Effects of mediodorsal thalamic nucleus stimulation on measures of gross locomotor activity in the open-field. After 1 hour of continuous HFS DBS of the mediodorsal thalamic nucleus there is no difference in any of these behavioural measures between stimulated and non stimulated animals. Specifically no differences were found in (a) total distance travelled, (b) the average velocity of movement, (c) the frequency of rearing, (d) the time spent in the centre/perimeter of the arena and (e) the average angle turned by an animal. Results are expressed as the mean ±SEM with n = 6

5.3.2.2 GP stimulation - open-field

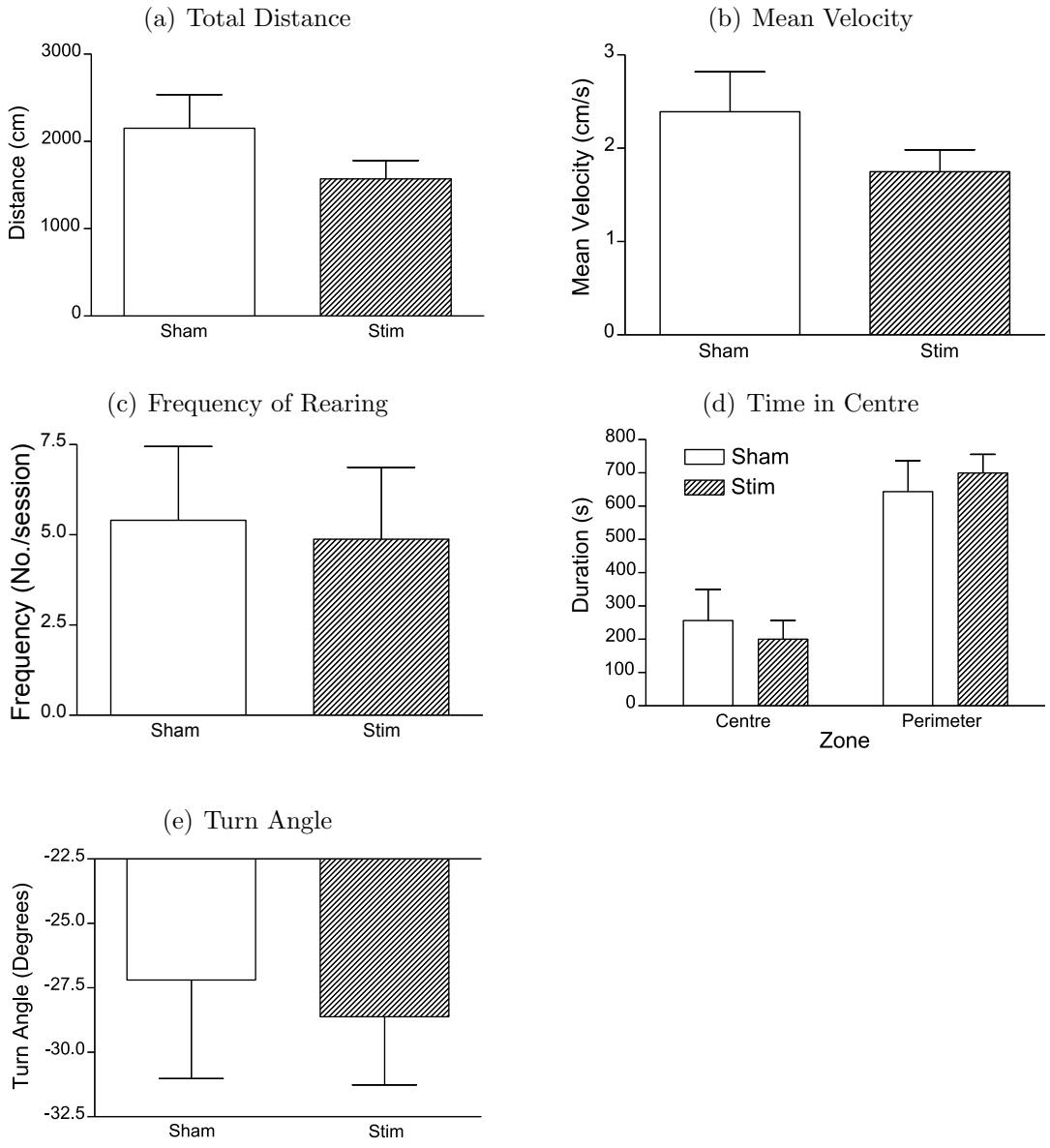

Figure 5.6: Effects of globus pallidum stimulation on measures of gross locomotor activity in the open-field. After 1 hour of continuous HFS DBS of the mediodorsal thalamic nucleus there is no difference in any of these behavioural measures between stimulated and non stimulated animals. Specifically no differences were found in (a) total distance travelled, (b) the average velocity of movement, (c) the frequency of rearing, (d) the time spent in the centre/perimeter of the arena and (e) the average angle turned by an animal. Results are expressed as the mean ±SEM with n = 7 per group

5.3.3 Pre-pulse inhibition of the startle response

Analysis of the startle response between globus pallidum implanted animals with and without stimulation indicates no effect of group ($F(1,7) = 0.000$; $p = 0.991$) (see figure 5.7(a), page 154). Analysis of the prepulse inhibition of the startle response between globus pallidum implanted animals with and without stimulation indicates a significant effect of prepulse intensity ($F(2,12) = 64.767$; $p = 0.000$) but no effect of group ($F(1,6) = 0.008$; $p = 0.931$) (see figure 5.7(b), page 154). Thus HF DBS of the globus pallidum did not affect the pre-pulse inhibition of the startle reflex in rats.

Analysis of the startle response between mediodorsal thalamic nucleus implanted animals with and without stimulation indicates no effect of group ($F(1,7) = 0.162$; $p = 0.701$) (see figure 5.8(a), page 155). Analysis of the prepulse inhibition of the startle response between mediodorsal thalamic nucleus implanted animals with and without stimulation indicates a significant effect of prepulse intensity ($F(2,12) = 25.367$; $p = 0.002$) with a significant effect of group ($F(1,6) = 16.166$; $p = 0.007$). Post hoc analysis of each prepulse intensity was performed via a one way ANOVA showing significant group differences at prepulse intensities of 4dB ($F(1,7) = 10.757$; $p = 0.017$) and 8dB ($F(1,7) = 64.913$; $p = 0.000$) although at a prepulse intensity of 16dB the differences only tended towards significance ($F(1,7) = 5.027$; $p = 0.066$) (see figure 5.8(b), page 155). Thus HF DBS of the mediodorsal thalamic nucleus appears to improve the prepulse inhibition of the startle reflex in rats.

5.3.3.1 GP stimulation - PPI

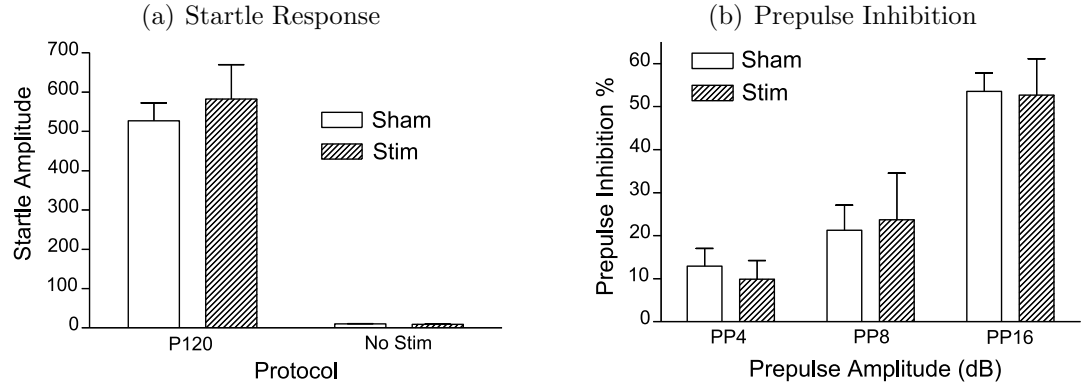

Figure 5.7: Effects of globus pallidum stimulation on measures of startle response and pre-pulse inhibition of the startle response. After approximately 90 minutes of continuous HFS DBS of the globus pallidum there is no difference in either basal levels of startle ($F(1,7) = 0.000$; $p = 0.991$) response nor any difference in PPI performance ($F(1,12) = 0.003$; $p = 0.954$). Results are expressed as the mean $\pm$SEM with $n = 4$.

5.3.3.2 MD stimulation - PPI

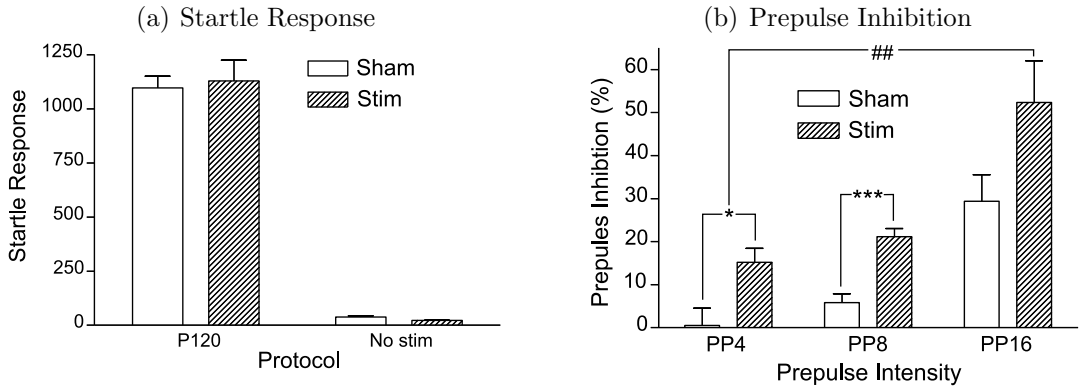

Figure 5.8: Effects of mediodorsal thalamic nucleus stimulation on measures of startle response and pre-pulse inhibition of the startle response. After approximately 90 minutes of continuous HFS DBS of the mediodorsal thalamic nucleus there is no difference in basal levels of startle response between stimulated and non-stimulated animals ($F(1,7) = 0.162$; $p = 0.701$). However significant differences in PPI performance were observed between stimulated and non-stimulated animals ($F(1,7) = 16.166$; $p = 0.007$). Post hoc analysis of each prepulse intensity was performed via a one way ANOVA showing significant group differences at prepulse intensities of 4dB ($F(1,7) = 10.757$; $p = 0.017$) and 8dB ($F(1,7) = 64.913$; $p = 0.000$) although at a prepulse intensity of 16dB the differences only tended towards significance ($F(1,7) = 5.027$; $p = 0.066$). Results are presented as the mean $\pm$SEM with $n = 4$. ## indicates an overall group effect ($p < 0.01$). Group effects at individual prepulse intensities are indicated by $\star$ $p<0.05$ and $\star\star\star$ $p<0.001$

5.3.4 Comparisons of locomotor activity and PPI between groups

Given the absence of differences between the mediodorsal thalamic nucleus sham-stimulated and mediodorsal thalamic nucleus stimulated animals in the open-field measures it was assumed that the data from these animals reflects "normal" locomotor activity. The data from these groups was pooled and used as a putative "control". The data from the globus pallidum sham-stimulated and stimulated animals was then compared with this control via an unpaired Student's t-test. No significant difference was demonstrated between the control group and the unstimulated globus pallidum implanted animals. However stimulation of the globus pallidum yielded significant reductions ($p = 0.007$) in ambulation when compared with mediodorsal thalamic nucleus implanted controls (see figure 5.9(a)).

Similarly, given the absence of differences between the globus pallidum sham-stimulated and globus pallidum stimulated animals in the PPI test it was assumed that the data from these animals reflects "normal" PPI performance. The data from these groups was pooled and used as a putative "control". No differences were demonstrated between this "control" and mediodorsal thalamic nucleus stimulated groups ($F(1,10) = 0.034$; $p = 0.857$). However animals with electrodes implanted in the mediodorsal thalamic nucleus, receiving no stimulation were found to have significantly diminished PPI when compared with both the mediodorsal thalamic nucleus stimulated group ($F(1,6) = 16.166$; $p = 0.007$) and the pooled globus pallidum group ($F(1,10) = 10.964$; $p = 0.008$) (see figure 5.9(b)).

5.3.5 PCP induced hyperlocomotion

Finally the animals were used to explore the effect of high frequency stimulation of the mediodorsal thalamic nucleus on PCP induced hyperlocomotion in rats. The globus pallidum implanted animals served as "controls" and received no DBS at any point in this experiment. Animals undergoing mediodorsal thalamic nucleus DBS were stimulated for 1 hour before being placed into the open-field. Control animals were placed in jackets and carried habituation devices for the course of the experiment. After 30 minutes habituating to the test environment all animals were administered PCP at $5mg.kg^{-1}$. Video capture was continued for a further hour. 2 animals from the globus pallidum implanted group removed their electrode implants prior to this experiment and were euthanased. Animals with misplaced electrodes from the globus pallidum implanted group were not

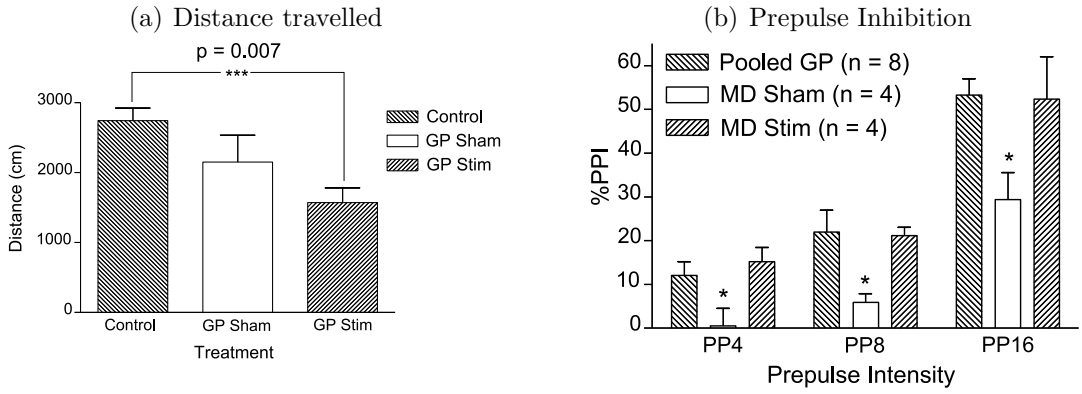

Figure 5.9: **(a)** After 60 minutes of continuous HF DBS of the globus pallidum stimulated animals show a marked reduction in ambulation in the open-field. **(b)** Animals with electrodes implanted in the mediodorsal thalamic nucleus appear to show marked reduction in the ability to inhibit their startle reflex, a deficit that appears to be restored by unilateral stimulation of the same region.

excluded from the analysis. The final group sizes were: globus pallidum group, n = 8; mediodorsal thalamic nucleus group, n = 6.

The time points -20, -10, 0 and 0, 10, 20 were analysed with a repeated measures ANOVA with time as the within subjects factor and group as the between subjects factor. The pre-drug analysis revealed a significant effect of time ($F(2,24) = 28.736$; $p = 0.000$) and a significant effect of group ($F(1,12) = 12.350$; $p = 0.003$). The post-drug analysis also revealed a significant effect of time ($F(2,24) = 17.919$; $p = 0.001$) and a significant effect of group ($F(1,12) = 15.770$; $p = 0.001$). The pre-drug time effect is indicative of habituation to the test arena. The pre-drug group effect indicates that the mediodorsal thalamic nucleus stimulated group move around the arena more than the globus pallidum implanted (no stimulation) group. However a comparison between groups immediately prior to drug administration indicates that the two groups habituated to the same level of activity ($t = 1.204$, $p = 0.2471$). The post drug time effect indicates a significant elevation in locomotion (hyperlocomotion) due to administration of PCP. The post drug between groups effect is likely to reflect an exacerbation of the PCP induced hyperlocomotion due to stimulation of the mediodorsal thalamic nucleus (see figure 5.10).

The differences between groups upon stereotypy and ataxia in the time points before and after drug administration were compared using a one way ANOVA. These time points included the 2 immediately prior to drug administration ($t = -10$ and 0) and the 2 immediately after drug administration ($t = 10$ and 20).

No significant difference in ataxia and stereotypy were detected at -10 minutes ($F(1,13) = 1.563$; $p = 0.235$) or 0 minutes ($F(1,13) = 0.104$; $p = 0.753$). Significant effects of drug administration were found between groups at 10 minutes ($F(1,13) = 9.522$; $p = 0.009$) and 20 minutes ($F(1,13) = 3.646$; $p = 0.080$). In contrast to the measure of ambulation above the measure of ataxia and stereotypy found no differences between groups prior to drug administration. Following drug administration the mediodorsal thalamic nucleus stimulated group were seen to have significantly greater ataxia and stereotypy than did the globus pallidum implanted group (see figure 5.11).

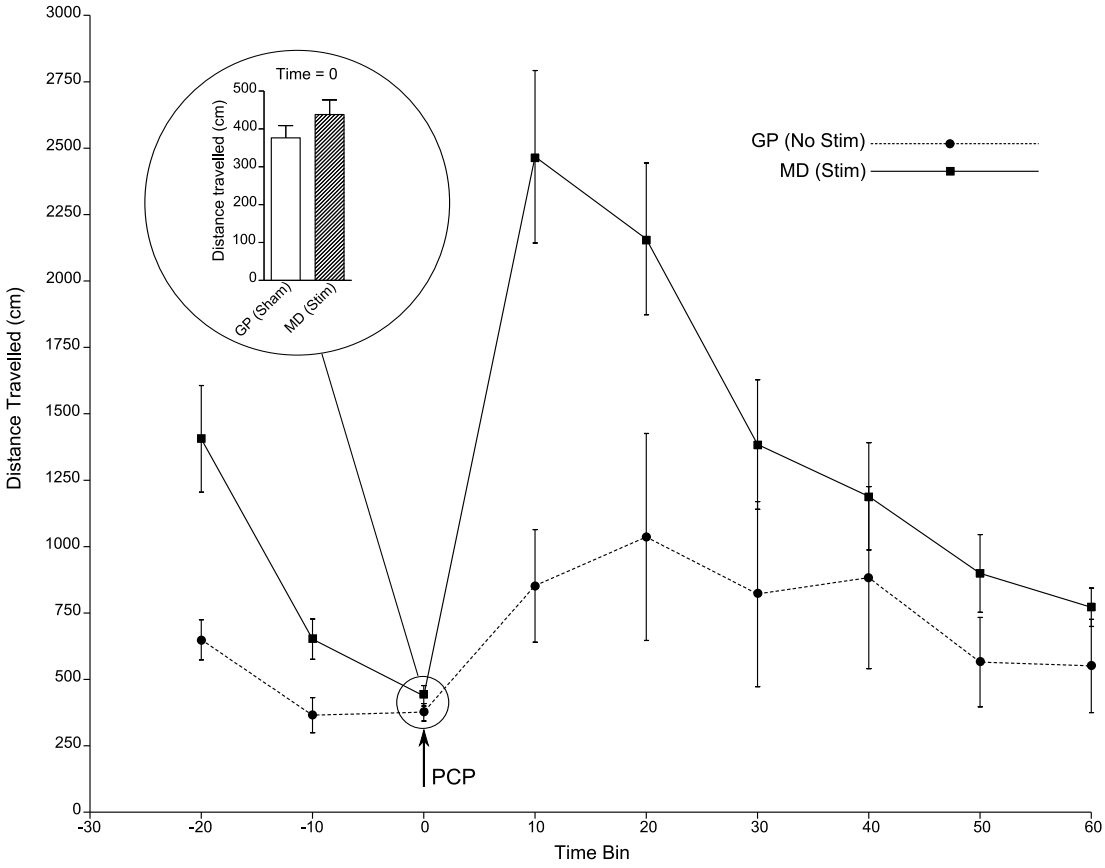

Figure 5.10: Putative effect of mediodorsal thalamic nucleus stimulation on PCP hyperlocomotion after 1 hour of continuous HFS DBS. **Inset:** After 30 minutes exposure to the open-field both stimulated (mediodorsal thalamic nucleus) and non stimulated (globus pallidum) animals habituate to similar levels of activity. After PCP administration both stimulated and non stimulated animals exhibit drug induced hyperlocomotion ($F(2,24) = 17.919$; $p = 0.001$). However this effect is observed to be significantly greater in stimulated animals than in non-stimulated controls ($F(1,12) = 15.770$; $p = 0.001$). Results are expressed as the mean $\pm$SEM, $n = 8$ (globus pallidum) and $n = 6$ (mediodorsal thalamic nucleus).

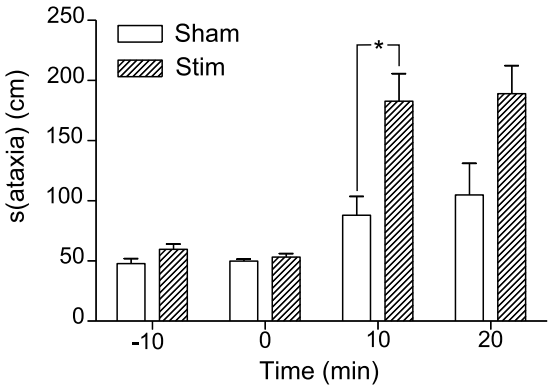

Figure 5.11: Effect of stimulation + acute administration of PCP on ataxia and stereotypy. Prior to drug administration (t = 0 min) the two groups do not differ with respect to the amount they exhibit ataxia and stereotypy. Post drug administration both groups exhibited greater ataxia and stereotypy although this increase is vastly more apparent in the stimulated animals ($F(1,13) = 9.522$; $p = 0.009$). Results are expressed as the mean ±SEM, n = 8 (globus pallidum) and n = 6 (mediodorsal thalamic nucleus). It should be noted that the "sham" animals in this comparison are drawn from the globus pallidum implanted animals whereas the "stim" animals are drawn from the mediodorsal thalamic nucleus implanted animals.

5.4 Discussion

5.4.1 Open-field

The results reported here demonstrate that neither stimulation of the globus pallidum nor the mediodorsal thalamic nucleus yields any deprecation of locomotor function when compared with sham-stimulated animals with identical electrode placements. Measures of distance traveled, velocity and rearing remained unchanged between stimulation on/off conditions as did measures of turn angle which it was thought may be more sensitive to differences specific to the unilateral nature of stimulation. No differences were observed in the time which animals occupied the centre of the arena. Thigmotaxis, a behaviour whereby fearful animals spend a disproportionate period of time close to the walls of the open-field, is though to be an index of anxiety. The region defined as the centre of the open-field occupied 1/3 of its total area. Animals typically spent approximately 1/3 of the test session in the central region indicating that animals spent, as a function of the area of the open-field, similar periods in the centre and periphery of the arena.

Despite the absence of differences between the stimulation on/off conditions within groups, the data may suggest a reduction in mobility in the globus pallidum implanted animals when compared to the mediodorsal thalamic nucleus implanted animals. There is a trend towards reduced ambulation in globus pallidum implanted animals (sham-stimulated) when compared with the pooled data from the mediodorsal thalamic nucleus group ($t = 1.597$, $p = 0.0612$). This trend appears to be exacerbated by stimulation with a significant reduction in the globus pallidum stimulated animals when compared with the pooled data from the mediodorsal thalamic nucleus group.

There are, however, confounds between the two experiments that make this a difficult assertion. Animals within each group were tested on two consecutive days. However the two groups were tested independently in blocks separated by 7 days although all other test conditions were consistent. Older rats tend to move less in the open-field than do younger rats (Bronstein, 1972), although Candland & Campbell (1962) and Bronstein (1972) agree that mature rats (40-200 days old) will travel similar distances upon their initial exposure to the open-field. These data suggest that the difference in distance traveled reported in this thesis are more likely to be an effect of electrode placement than an effect of animal age.

This assertion is supported by the pre-drug administration data collected in the

PCP induced hyperlocomotion experiment in which both mediodorsal thalamic nucleus and globus pallidum implanted animals performed the task simultaneously on two consecutive days. This experiment indicates that mediodorsal thalamic nucleus implanted animals, undergoing DBS, are more active upon exposure to a new open-field than are globus pallidum implanted rats receiving no stimulation. The initial within-subjects open-field task indicated no difference between stimulated and sham-stimulated animals with electrodes implanted in the mediodorsal thalamic nucleus. It seems safe to conclude then that this effect is not mediated by DBS of the mediodorsal thalamic nucleus but is simply an effect of the electrode placement, *i.e:* the micro-lesion generated by implantation of electrodes, bilaterally, into the globus pallidum is sufficient to affect a decrement in motor performance. This discussion shall return to the PCP hyperlocomotion experiment in due course.

5.4.1.1 Functional considerations

The absence of motor effects in mediodorsal thalamic nucleus stimulated animals provides some reassurance that DBS of the mediodorsal thalamic nucleus is "safe", at least at the level of motor function. In addition it provides a platform from which one could confidently explore more complex behaviours. Tasks used to explore cognition (5 choice serial reaction time for example) require some degree of motor accuracy from the animal so any motor dysfunction due to stimulation would presumably impair performance in such tasks and presumably confound results.

5.4.2 Prepulse inhibition

These results suggest that stimulation of the globus pallidum had no effect on the pre-pulse inhibition of the startle reflex in rats when compared to sham-stimulated animals with identical electrode placements. The initial interpretation of the PPI results reported here led this author to suggest that HF stimulation of the mediodorsal thalamic nucleus yielded improvements in the pre-pulse inhibition of the startle response in rats when compared to sham-stimulated animals with identical electrode placements. However a more recent interpretation of this data set indicates an arguably more intriguing possibility. The data from both globus pallidum and mediodorsal thalamic nucleus implanted groups, when viewed together, suggest that the increase in PPI reported in mediodorsal thalamic nucleus stimulated animals may be a restoration, rather than an increase, of

a deficit induced by a micro-lesion of the mediodorsal thalamic nucleus. However, there are several experimental shortcomings that muddy these waters.

As was the case in the open-field experiments the results from the mediodorsal thalamic nucleus and globus pallidum implanted animals were collected 7 days apart. However, to the authors knowledge, there is no indication in the literature to suggest that PPI in rats is age dependent. Of significantly greater concern is the difference in the calibration of the PPI apparatus between the two groups. As illustrated in the "Startle Response" results (see figures 5.7 and 5.8) the absolute startle response between the two groups seems significantly different. However, this apparent effect is not an effect at all - it merely reflects a difference in calibration between the two experiments. PPI, however, is not an absolute but a relative measure thereby negating differences in calibration between experiments. These results, viewed thus, therefore indicate no difference between the pooled globus pallidum implanted group and the mediodorsal thalamic nucleus stimulated group but a significant reduction in PPI in the sham-stimulated mediodorsal thalamic nucleus implanted group. The implication of this is that the micro-lesion generated by the implantation of electrodes, bilaterally, into the mediodorsal thalamic nucleus is sufficient to effect a reduction in PPI in rats when compared to animals with electrodes implanted in the globus pallidum. Unilateral stimulation of the mediodorsal thalamic nucleus (left hemisphere) is then sufficient to restore this deficit to levels seen in globus pallidum implanted animals. However due to the severity of the exclusions the sample sizes in these experiments is small and a larger repetition of these results is required before firm conclusions can be made.

5.4.2.1 Functional considerations

PPI is impaired in a plethora of disorders, perhaps most notably in schizophrenia. The results reported here, regardless of the two possible interpretations presented above, provide the first evidence that DBS of the mediodorsal thalamic nucleus may be an avenue of therapeutic interest in the restoration of impaired PPI. Should the data merely reflect improved PPI performance relative to controls then it is reasonable to hypothesise that the same paradigm may restore PPI deficits in, for example, a PCP model of schizophrenia (Egerton *et al.*, 2008).

It is at least plausible, if not more so than the previous explanation, that the effects reported here *are* a restoration of an induced PPI deficit. The evidence provides support for the notion that electrode insertion into the mediodorsal thalamic nucleus - the principal thalamic relay in the PPI regulatory circuit

(see figure 5.1, page 139) - is sufficient to impair PPI performance. This deficit then appears to be restored to "normal" levels by unilateral stimulation of the mediodorsal thalamic nucleus. Whilst a gross simplification it is interesting to note that some of the more robust findings reported in schizophrenia are that of PPI impairment and that of a modest reduction in mediodorsal thalamic nucleus volume. The results reported here suggest that a modest lesion (reduction in volume) of the mediodorsal thalamic nucleus is sufficient to impair PPI performance in rats, a deficit that can be restored by DBS.

5.4.3 PCP induced hyperlocomotion

The PCP induced hyperlocomotion indicates a significant difference between the sham-stimulated globus pallidum implanted group and the stimulated mediodorsal thalamic nucleus implanted group prior to the acute administration of PCP. As discussed above the absence of differences between the stimulation on/off condition within the mediodorsal thalamic nucleus group indicates that this is not a stimulation effect but a micro-lesion effect in the globus pallidum group. This result provides a difficult context in which to interpret the remainder of the results from this experiment. The two groups habituate to the same level of activity immediately prior to drug administration. Immediately after drug administration both groups show an increase in locomotor activity with a several fold greater increase in the mediodorsal thalamic nucleus stimulated group compared to the sham-stimulated globus pallidum implanted group. It is difficult to be certain whether this difference is attributable (a) to direct stimulation of the mediodorsal thalamic nucleus or (b) to a micro-lesion of the globus pallidum. At best it is safest to conclude that the significant difference between groups post drug administration is likely a combinatorial effect of both mediodorsal thalamic nucleus stimulation and globus pallidum micro-lesion. However several factors add weight to the assertion that this effect is primarily a consequence of mediodorsal thalamic nucleus stimulation. Animals in both groups habitutate to the same level of activity prior to drug administration, the implication being that the effect is not mediated by a decreased propensity for globus pallidum implanted animals to move around the arena. Furthermore the results of the measure tentatively introduced here - ataxia and stereotypy - indicate no difference between groups prior to drug administration with a significant exacerbation of the increased ataxia and stereotypy seen between groups post drug administration. These evidences compel this author to posit that the difference in hyperlocomotion between these inadequately matched groups is primarily a function of mediodorsal thalamic

nucleus stimulation and not of a globus pallidum micro-lesion.

5.4.3.1 Functional considerations

If one accepts the assertion above then it is interesting to consider its potential consequences. So far this chapter has argued that HF DBS of the mediodorsal thalamic nucleus may be of potential therapeutic benefit in schizophrenia. This stimulation paradigm appears to have no motor side effects whilst either improving or restoring PPI performance. Yet this final experiment seems to indicate that HF DBS of the mediodorsal thalamic nucleus exacerbates PCP induced hyperlocomotion - a putative animal model of psychosis. How can this be?

This data brings us back to some of the unanswered questions from the IEG and ECoG chapter (see chapters 3 and 4). It was unclear from the IEG experiment as to which cell types the increases in activity were manifest. The increases were arguably equally likely in either glutamatergic pyramidal prefrontal cortex neurons or GABAergic interneurons. Given the absence of secondary effects due to activation of the prefrontal cortex it was argued that there was no detectable increase in prefrontal cortex output, *i.e:* no increase in electrophysiological activity. Given the apparent increase in synaptic activity due to HF DBS of the mediodorsal thalamic nucleus demonstrated in chapter 3 it seems plausible that there *must* be an increase in glutamate release in the prefrontal cortex an assertion that has since been confirmed (Guillazo-Blanch *et al.*, 2008). In the absence of inhibition, sufficiently increased glutamate transmission in the prefrontal cortex would presumably yield increased action potential firing in the cortical output neurons. The paucity of evidence supporting increased output indicates sufficient cortical inhibition as to suppress output. This inhibition presumably arises from the GABAergic interneurons and it seems reasonable to posit that the increased glutamatergic transmission in the prefrontal cortex yields both excitation and inhibition of cortical neurons. The data from the hyperlocomotion experiment indicates significantly increased glutamatergic output from the prefrontal cortex under the conditions of mediodorsal thalamic nucleus stimulation and acute PCP administration. Stimulation of the mediodorsal thalamic nucleus is insufficient on its own to elicit hyperlocomotion, the implication being that there is no increased prefrontal cortex outflow. Co-administration of PCP, an NMDA receptor antagonist, acts to block glutamate-gated ion channels predominantly in the GABAergic interneurons. This would presumably reduce cortical inhibition and release the breaks on the prefrontal cortex yielding a dramatic increase in output due to the increased input from the mediodorsal thalamic nucleus.

In summary the findings reported in this chapter demonstrate that the methodology developed in this thesis is sufficient for the investigation of DBS in small rodents. The results demonstrate that stimulation of the mediodorsal thalamic nucleus yields no motor effects in the measures reported here despite the apparent activation of the secondary motor cortex. In addition there are indications that DBS of the mediodorsal thalamic nucleus may serve to improve PPI performance although it remains unclear as to the precise nature of this improvement. These indications, however, require further investigation before firm conclusions can be made. Finally the data from the PCP hyperlocomotion study suggest that DBS may exacerbate the increased glutamatergic output from the prefrontal cortex, a phenomenon that is believed to underpin PCP induced hyperlocomotion in rats.

5.4.4 Caveats & extensions

The PPI results while interesting require additional methodological improvement to reduce the attrition of devices under conditions where animals are restrained. In addition the experiments would need to be extended to include a suitable model of schizophrenia before more conclusive remarks could be made regarding the specificity of mediodorsal thalamic nucleus DBS to this disease state. As detailed above device failure was common during PPI with almost 50% of animals being excluded from the analysis. This failure occurred at the connectors between the cable that connects the device to the implant. This failure either occurred as a simple disconnection or by genuine damage to the connectors. Disconnection could be avoided by using a latching connector. However this does not solve the problem of cable breakage. Cables break as a result of flexion around a stiff point. Connectors is these experiments were reinforced with glue. This is too stiff. A better reinforcement of the connections could be made with silicon sealant which allows sufficient cable flexion to prevent damage. A better solution would be to implant the devices subcutaneously. This would require some means to (in the very least turn) the device on and off remotely. It is envisaged that the addition of some kind of magnetic latching switching circuitry would be of benefit, allowing the device to be switched on and off remotely using a magnet. However, once implanted it would no longer be possible to change the settings of the device. This could be addressed by replacing the multivibrator chip with some kind of micro-controller - the MSP4030 from Texas Instruments seems like a good candidate. This could be programmed either by complicated radio-frequency electronics or more simply by implanting a control input somewhere on the animal (the skull would be easiest). The device could then be

reprogrammed by briefly tethering the animal to the necessary control hardware with an appropriate commutator/cable set up. Plastics 1 (Plastisc 1) provide suitable commutators relatively cheaply.

These methodological improvements made one could confidently test the effects of DBS on PPI. Since no animal model of schizophrenia like deficits was employed in these experiments it is difficult to know if the effects reported here are specific to schizophrenia like deficits. Testing the effect in animals treated subchronically with PCP would be an excellent extension to the current work.

In addition the results from the PCP hyperlocomotion experiments are interesting but require further consolidation to provide conclusive proof. This experiment could be repeated with better matched controls. One would require at least the following groups: Vehicle, Vehicle+DBS, PCP and PCP+DBS. With these groups one could confirm or refute the observations made in this chapter.

Part V

Discussion, summary & Conclusions

Chapter 6

6.1 Summary & general discussion

The study of DBS in humans is restricted to the measure of non-invasive observables in small sample sizes. Research in rodents allows for the investigation of many variables, including invasive *in-vivo* and *ex-vivo* techniques that are far beyond the limits of clinical study. To this end the initial stages of this research were towards developing the methodology necessary for the application and study of DBS in rats. This methodological development has yielded the production of an easily manufactured and inexpensive device for the administration of high frequency, short pulse width, constant current stimulation. In addition a method for the production of disposable stimulating electrodes has been developed and described. For experiments in awake, freely-moving animals the methods necessary for recovery surgery, habituation to "sham" devices and for DBS in behavioural experiments have also been developed and described. This methodology was a key aim of this thesis which has been met and applied in the experiments described within it.

Whilst the exploration of DBS in rodents is not unique on the world stage the predominant contribution to the literature still originates in Parkinson's research with the focus largely on the subthalamic nucleus and the globus pallidum. More contemporary Parkinson's research is directed towards the pedunculopontine nucleus. The nucleus accumbens is a popular site for studies in rodent DBS given its implications in drug addiction, depression and obsessive-compulsive disorder. Epilepsy too receives considerable attention although the difficulty in identifying a suitable target makes research in this area particularly challenging. Schizophrenia, however, perhaps through the absence of success with any ablative surgical procedure, has received no attention from groups exploring DBS. This thesis describes, to the author's knowledge, the first attempts to explore DBS with specific reference to schizophrenia.

Through the arguments made in the introduction this thesis has focused on the investigation of high frequency (exclusively 130Hz) stimulation of the mediodorsal thalamic nucleus - a region consistently implicated in the primary pathology of schizophrenia. The experiments described here have demonstrated activation of the prefrontal cortex as evidenced by the increased expression of mRNA encoding the IEG *zif-268* but not *c-fos*. Whilst the functional implications of this remain elusive this experiment is sufficient to demonstrate increased synaptic input to the prefrontal cortex as a result of mediodorsal thalamic nucleus stimulation thereby satisfying the aims of this particular experiment. However the origin of this input remains unclear. It may arise as a consequence of increased efferent output from the stimulated region or as a consequence of antidromic activation of interneurons.

This activation of frontal cortical regions was further examined through analysis of the electrocorticogram (ECoG). This experiment describes the first attempt to explore DBS in a rodent model that produces schizophrenia like deficits - a sub-chronic PCP treatment regime. It was unknown what, if anything, the ECoG would reveal with respect to the differences between PCP treated "schizophrenic" rats and vehicle treated "normal" rats. It was, therefore, the aim of this experiment to (a) characterise this difference and (b) correct this difference (should it be found). This characterisation of the ECoG between PCP and vehicle treated rats revealed significantly increased low frequency (delta and theta) power in frontal and medial regions of PCP treated rats. These results largely reflect the evidence presented in the clinical literature that schizophrenics, particularly those with a predominance of negative symptoms, have elevated low frequency power in frontal regions. However, rather than normalising the increased low frequency power seen in the PCP treated rats, DBS of the mediodorsal thalamic nucleus further augmented this increase, albeit transiently. The idea that DBS of the mediodorsal thalamic nucleus may exacerbate some of the symptoms associated with schizophrenia is an idea that receives some, albeit small, support from the PCP hyperlocomotion experiment (discussed below).

Finally, the effects of DBS of the mediodorsal thalamic nucleus were scrutinised in awake freely moving animals. The widespread activation of the frontal cortices demonstrated in the IEG experiment included significantly increased activity in the secondary motor cortex. Investigation of general open-field locomotor activity demonstrated no motor side effects of mediodorsal thalamic nucleus stimulation. This thesis has accurately followed the nomenclature described by Paxinos &

Watson (2007) but in this case activation of a nominal motor cortex has yielded no observable outcome in measures of motor behaviour. This apparent oddity is plausibly due simply to interpretation of the atlas. Paxinos & Watson (2007) describes a frontal association cortex (FrA) in the most rostral regions of the frontal cortices (Bregma = 6.12mm $\rightarrow$ 5.64mm) which transforms abruptly into the secondary motor cortex at Bregma = 5.16mm. The rat cortex has no gyri to delineate functionally distinct regions so it seems plausible that the frontal association cortex may merge into the secondary motor cortex over a larger area. Indeed where Paxinos & Watson (2007) describes the secondary motor cortex at Bregma $\approx$ 5mm, Vertes (2004) describes a frontal polar cortex (FP) (more rostrally) and a medial agranular area (AGm) (more caudally). Furthermore Uylings *et al.* (2003) describes areas similar in location to the secondary motor cortex as the frontal cortical region 2 (Fr2). Whilst Paxinos & Watson (2007) provides the most commonly cited atlas there is far from a standardised nomenclature in the neural anatomy literature (Uylings *et al.*, 2003). It seems fair to assert then that where previously this thesis has reported increased expression of the mRNA encoding the IEG *zif-268* in the secondary motor cortex that it would be equally reasonable to describe this area as a frontal association cortex. Thus the absence of motor effects through activation of the "secondary motor cortex" requires no further explanation.

In addition to the open-field behaviours investigated in this thesis animals undergoing mediodorsal thalamic nucleus DBS were also tested to examine the effects of this stimulation paradigm on the pre-pulse inhibition of the startle response (PPI). PPI is a phenomenon which is well documented across many (if not all) species and is consistently found to be deficit in human schizophrenics. The PPI experiment represented arguably the greatest technical challenge in the experiments described in this thesis and as such requires significant effort in future research (see section 6.2). The connections between the device (mounted on the animals back) and the electrodes, whilst adequate for open-field investigations were easily broken once an animal was restrained in a perspex tube. This led to a significant reduction in the number of animals included in the analysis of this study. Whilst the PPI investigation has a small sample size the results indicate that DBS of the mediodorsal thalamic nucleus may be effective in restoring PPI in conditions where PPI is deficit. The reader may well question the absence of a repeat of this investigation in a situation where animals exhibit a reduced PPI, for example through the administration of PCP (Egerton *et al.*, 2008). Unfortunately this has not been achieved due to malfunction of the apparatus and

represents an obvious next step in the future of this research (see section 6.2).

As a consequence of the PPI malfunction the animals were then tested using the PCP-induced hyperlocomotion paradigm - a putative rodent model of psychosis. The pre-drug administration group differences (between mediodorsal thalamic nucleus stimulated and globus pallidum implanted (sham-stimulated)) make this data set difficult to interpret. Had these group differences been absent then it would have been straightforward to assert that mediodorsal thalamic nucleus stimulation exacerbates the hyperlocomotion induced by acute adminstration of PCP. The fact that the two groups habituate to the same level of activity prior to drug administration, and that the measure of ataxia and stereotypy introduced here normalised the pre-drug differences whilst still detecting the post drug differences lends support to this assertion. These data suggest that DBS of the mediodorsal thalamic nucleus may exacerbate the purported psychosis induced by acute administration of PCP. However, these data require further consolidation as part of this ongoing research (see section 6.2).

6.1.1 Functional implications

The results reported from the IEG experiment indicated no increased output from the prefrontal cortex despite its increased "activation" as a result of mediodorsal thalamic nucleus stimulation. On the other hand mediodorsal thalamic nucleus stimulation appears to augment the hyperlocomotion induced by acute administration of PCP - an effect that is reported to be mediated, in part, by prefrontal cortex glutamatergic efferents to the ventral tegmental area and/or ventral striatum since blockade of AMPA receptors in these regions inhibits PCP-induced locomotion and stereotypy (Takahata & Moghaddam, 2003). One may infer from these findings that increased prefrontal cortex glutamate neurotransmission, as a result of increased thalamic input, is dependent on the reduced cortical inhibition induced by administration of PCP. The subchronic PCP model exhibits reductions in parvalbumin expression (a marker of GABAergic inhibitory interneurons) indicating a reduction in cortical inhibition (Cochran *et al.*, 2003). All things considered the results reported here indicate that the consequences of mediodorsal thalamic nucleus stimulation depend intricately on a balance of cortical excitation and inhibition. In an "intact" animal it is suggested here that the increased activation of the prefrontal cortex arising from mediodorsal thalamic nucleus stimulation results in both increased excitation of both pyramidal cells and inhibitory interneurons, the cumulative effect of which is no detectable increase in corti-

cal output. The IEG experiment and the open-field tests support this assertion. PCP administration through antagonism of the inhibitory interneurons effectively "takes the brakes off" the frontal cortex allowing mediodorsal thalamic nucleus stimulation to drive cortical output as indicated by the PCP-induced hyperlocomotion data. This assertion is by no means proven and should be considered a new hypothesis for this continuing research.

6.2 Future research directions

The results reported in this thesis arguably generate more questions than they provide answers! Whilst the IEG chapter succeeded in mapping the neural substrates of mediodorsal thalamic nucleus stimulation the unexpected absence of increased *c-fos* expression raises interesting possibilities. Probing for the protein products of *c-fos* would conclusively demonstrate whether or not there had ever been any regulation of this IEG. This could similarly be achieved by reducing the time-scale of the experiment and probing for *c-fos* mRNA. Should it transpire that *c-fos* is not upregulated in the prefrontal cortex by stimulation of the mediodorsal thalamic nucleus it may indicate that LTP may play a part in the mechanism of action in this system. Potentiating thalamic input in the prefrontal cortex may have interesting functional consequences since deficits in this system are widely reported in schizophrenia.

The investigation of the ECoG has been limited in this thesis to analysis of the low frequency components commonly associated with sleep and anaesthesia. Abnormalities at higher frequencies are frequently reported in schizophrenia with a great deal of attention paid to oscillations at gamma frequencies. Gamma frequencies are low amplitude, high frequency oscillations that are difficult to observe from surface recordings in anaesthetised preparations. A logical and desirable extension to this work would examine the gamma frequency response of cortical regions to mediodorsal thalamic nucleus stimulation in both PCP and vehicle treated animals. The methodological challenges of such an investigation are significant since one would ideally perform such an experiment in conscious animals and record LFPs rather than ECoG.

The behavioural work reported here indicates that mediodorsal thalamic nucleus stimulation may be effective in restoring deficits in PPI, a deficit commonly reported in schizophrenia. This indication requires consolidation in the normal animal and it would be interesting to test the hypothesis that a micro-lesion of

this region is sufficient to generate an observable deficit in PPI. It would obviously be of great interest to see if this DBS paradigm is effective in restoring PCP induced deficits in PPI. This latter experiment however may be confounded by the exacerbation of the hyperlocomotion induced by PCP administration. This too requires further attention. The group differences between mediodorsal thalamic nucleus stimulated and globus pallidum implanted (non-stimulated) animals confound the interpretation of this data. The hypothesis one would seek to prove would be that DBS of the mediodorsal thalamic nucleus augments the hyperlocomotion induced by the acute administration of PCP. This should be tested using groups with identical electrode implants to account for the confound introduced by the globus pallidum implanted group. Furthermore to verify the role of the prefrontal cortex in this exacerbated hyperlocomotion it would be pertinent to examine the effects of mediodorsal thalamic nucleus stimulation on amphetamine-induced hyperlocomotion since this has no dependence on the prefrontal cortex (Jentsch *et al.*, 1998).

6.3 Concluding remarks

The methodology appears largely successful as evidenced by the data presented in this thesis. These data identify the prefrontal cortex as the primary affected region as evidenced by measures of IEG expression, spectral analysis of the ECoG and PCP-induced hyperlocomotion as a consequence of high frequency DBS of the mediodorsal thalamic nucleus. However there is also an indication that stimulation of the mediodorsal thalamic nucleus may exacerbate the psychosis associated with the positive symptoms of schizophrenia in situations where cortical inhibition is deprecated.

Finally, returning to the title of this thesis, what are the implications for the treatment of schizophrenia? At present DBS is not being realistically considered for a treatment strategy for schizophrenia. There is no support in the literature for its application and no "traditional" lesion target to invoke as a possible stimulation site. This thesis set out to investigate the possible consequences of stimulating the thalamo-cortical system given the well documented anatomical anomalies. Stimulation of the mediodorsal thalamic nucleus has yielded cellular activation of the prefrontal cortex as evidenced by the IEG data. However the nature of this activation is unclear. What is clear is that schizophrenia is associated with prefrontal cortex deficits. Identifying the mediodorsal thalamic nucleus as a DBS target capable of modulating prefrontal cortex activity is a step in the right direc-

tion. There are indications that this stimulation paradigm may also be of use in modulating the circuitry responsible for regulating PPI - a sensory motor gating phenomenon also seen top be deficit in schizophrenia. These evidences implicate the mediodorsal thalamic nucleus as a target worthy of future research in this disorder. The evidence from the PCP-hyperlocomotion experiment indicates that, rather than yielding an improvement, DBS of the mediodorsal thalamic nucleus may actually augment a dimension already seen to be aberrant in schizophrenia. It is worth noting that PCP-hyperlocomotion is most commonly associated with the positive symptoms of schizophrenia, the implication being that DBS of the mediodorsal thalamic nucleus may be a treatment strategy better suited to the treatment of the negative symptoms. However this research is still in its earliest stages and it would be a mistake to confuse statistical significance with clinical relevance. A great deal of research will be required before ANY target is considered for schizophrenia. The scientific challenges not withstanding this disease more than any other will face tough ethical challenges. Informed consent for these procedures will be difficult to obtain in human trials. Ask yourself this, if you believed someone was implanting thoughts in your mind, or if you believed that others were capable of reading your thoughts, would you let them implant foreign objects into your brain? Into your mind?

"The mind is its own place, and in itself
Can make a heav'n of hell, a hell of heav'n."

John Milton
Paradise Lost 1:254-255

References

Abelson, J L, Curtis, G C, Sagher, O, Albucher, R C, Harrigan, M, Taylor, S F, Martis, B, & Giordani, B. 2005. Deep brain stimulation for refractory obsessive-compulsive disorder. *Biol Psychiatry*, **57**, 510–516.

Ackermans, L, Temel, Y, Cath, D, van der Linden, C, Bruggeman, R, Kleijer, M, Nederveen, P, Schruers, K, Colle, H, Tijssen, M A J, & Visser-Vandewalle, V. 2006. Deep brain stimulation in tourettes syndrome: two targets? *Movement Disorders*, **21**(5), 709–713.

Ackermans, L, Temel, Y, & Visser-Vandewalle, V. 2008. Deep brain stimulation in tourettes syndrome. *Neurotherapeutics*, **5**(2), 339–344.

Adams, B, & Moghaddam, B. 1998. Corticolimbic dopamine neurotransmission is temporally dissociatedfrom the cognitive and locomotor effects of phencyclidine. *The Journal of Neuroscience*, **18**(14), 5545–5554.

Albert, G C, Cook, C M, Prato, & Thomas, A W. 2009. Deep brain stimulation, vagal nerve stimulation and transcranial stimulation: an overview of stimulation parameters and neurotransmitter release. *Neuroscience and Biobehavioral Reviews*, **33**, 1042–1060.

Anderson, D, & Ahmed, A. 2003. Treatment of patients with intractable obsessivecompulsive disorder with anterior capsular stimulation. *J Neurosurg*, **98**, 1104–1108.

Anderson, T, Hu, B, Pittman, Q, & Kiss, Z H T. 2004. Mechanisms of deep brain stimulation: an intracellular study in rat thalamus. *J Physiol*, **559**(1), 301–313.

Andreasen, N C, Arndt, S, Swayze, V, Cizadlo, T, Flaum, M, D O'Leary, J C Ehrhardt, & Yuh, W T C. 1994. Thalamic abnormalities in schizophrenia visualized through magnetic resonance image averaging. *Science*, **266**, 294–297.

Andreasen, NancyC. 1995. Symptoms, signs, and diagnosis of schizophrenia. *The Lancet*, **346**(8973), 477 – 481.

Andrews, J, Wang, L, Csernansky, J G, Gado, M H, & Barch, D M. 2006. Abnormalities of Thalamic Activation and Cognition in Schizophrenia. *Am J Psychiatry*, **163**, 463–469.

Antonova, E, Sharma, T, Morris, R, & Kumari, V. 2004. The relationship between brain structure and neurocognition in schizophrenia: a selective review. *Schizophr. Res.*, **70**, 117–145.

Aouizerate, B, Cuny, E, Martin-Guehl, C, Guehl, D, Amieva, H, Benazzouz, A, Fabrigoule, C, Allard, M, Rougier, A, Bioulac, B, Tignol, J, & Burbaud, P. 2004. Deep brain stimulation of the ventral caudate nucleus in the treatment of obsessivecompulsive disorder and major depression. *J Neurosurg*, **101**, 682–686.

Babiloni, C, Frisoni, G, Steriade, M, Bresciani, L, Binetti, G, Del Percio, C, Geroldi, C, Miniussi, C, Nobili, F, Rodriguez, G, Zappasodi, F, Carfagna, T, & Rossini, P M. 2006. Frontal white matter volume and delta EEG sources negatively correlate in awake subjects with mild cognitive impairment and Alzheimers disease. *Clinical Neurophysiology*, **117**, 1113–1129.

Başar, E, & Güntekin, B. 2008. A review of brain oscillations in cognitive disorders and the role of neurotransmitters. *Brain Research*, **1235**, 172–193.

Bajwa, R J, de Lotbiniére, A J, King, R A, Jabbari, B, Quatrano, S, Kunze, K, Scahill, L, & Leckman, J F. 2007. Deep brain stimulation in tourettes syndrome. *Movement Disorders*, **22**(9), 1346–1350.

Bar-Gad, I, Elias, Shlomo, Vaadia, E, & Bergman, H. 2004. Complex locking rather than complete cessation of neuronal activity in the globus pallidus of a 1-methyl-4-phenyl-1,2,3,6-tetrahydropyridine-treated primate in response to pallidal microstimulation. *The Journal of Neuroscience*, **24**(33), 7410–7419.

Barch, D M, Csernansky, J G, Conturo, T, & Snyder, A Z. 2002. Working and long-term memory deficits in schizophrenia: is there a common prefrontal mechanism? *Journal of Abnormal Psychology*, **111**(3), 478–494.

Barch, D M, Sheline, Y I, Csernansky, J G, & Snyder, A Z. 2003. Working memory and prefrontal cortex dysfunction: specificity to schizophrenia compared with major depression. *Biol Psychiatry*, **53**, 376–384.

Bear, M F, Connors, B W, & Paradiso, M A. 2001. *Neuroscience: exploring the brain 2nd edition.* Lippincott Williams & Wilkins.

Benazzouz, A, Piallat, B, Pollak, P, & Benabid, A. 1995. Responses of substantia nigra pars reticulata and globus pallidus complex to high frequency stimulation of the subthalamic nucleus in rats:electrophysiological data. *Neuroscience Letters*, **189**, 77–80.

Beurrier, C, Bioulac, B, Audin, J, & Hammond, C. 2001. High-frequency stimulation produces a transient blockade of voltage-gated currents in subthalamic neurons. *J Neurophysiol*, **85**, 1351–1356.

Birdno, M J, & Grill, W M. 2008. Mechanisms of Deep Brain Stimulation in Movement Disorders as Revealed by Changes in Stimulus Frequency. *Neurotherapeutics*, **5**, 14–25.

Black, Donald W, & Fisher, Ron. 1992. Mortality in DSM-IIIR schizophrenia. *Schizophrenia Research*, **7**(2), 109 – 116.

Boon, P, Vonck, K, De Herdt, V, Van Dycke, A, Goethals, M, Goossens, L, Van Zandijcke, M, De Smedt, T, Dewaele, I, Achten, R, Wadman, W, Dewaele, F, Caemaert, J, & Van Roost, D. 2007. Deep brain stimulation in patients with refractory temporal lobe epilepsy. *Epilepsis*, **48**(8), 1551–1560.

Boutros, N N, Arfken, C, Galderisi, S, Warrick, J, Pratt, G, & Iacono, W. 2008. The status of spectral EEG abnormality as a diagnostic test for schizophrenia. *schizophrenia Research*, **99**, 225–237.

Braff, D L, Geyer, M A, & Swerdlow, N R. 2001. Human studies of prepulse inhibition of startle: normal subjects, patient groups, and pharmacological studies. *Psychopharmacology*, **156**, 234–258.

Bronstein, P M. 1972. Open-field behavior of the rat as a function of age: cross-sectional and longitudinal investigations. *Journal of Comparative and Physiological Psychology*, **80**(2), 335–341.

Brown, A S, & Susser, E S. 2002. In utero infection and adult schizophrenia. *Ment. Retard. Dev. Disabil. Res. Rev.*, **8**, 51–57.

Brown, V J, & Bowman, E M. 2002. Rodent models of prefrontal cortical function. *TRENDS in Neurosciences*, **25**(7), 340–343.

Byne, W, Buchsbaum, M S, Mattiace, L A, Hazlett, E A, Kemether, E, Elhakem, S L, Purohit, D P, Haroutunian, V, & Jones, L. 2002. Postmortem Assessment of Thalamic Nuclear Volumes in Subjects With Schizophrenia. *Am J Psychiatry*, **159**, 59–65.

Byne, W, Fernandes, J, Haroutunian, V, Huacon, D, Kidkardnee, S, Kim, J, Tatusov, A, Thakur, U, & Yiannoulos, G. 2007. Reduction of right medial pulvinar volume and neuron number in schizophrenia. *Schizophrenia Research*, **90**, 71–75.

Callicott, Joseph H, Mattay, Venkata S, Verchinski, Beth A, Marenco, Stefano, Egan, Michael F, & Weinberger, Daniel R. 2003. Complexity of Prefrontal Cortical Dysfunction in Schizophrenia: More Than Up or Down. *Am J Psychiatry*, **160**(12), 2209–2215.

Candland, D K, & Campbell, B A. 1962. Development of fear in the rat as measured by behavior in the open field. *Journal of Comparative and Physiological Psychology*, **55**(4), 593–596.

Cannon, M, Jones, P B, & Murray, R M. 2002. Obstetric complications and schizophrenia: historical and meta-analytic review. *Am. J. Psychiatry*, **159**, 1080–1092.

Carpenter Jr, W T, & Gold, J M. 2002. Another view of therapy for cognition in schizophrenia. *Biol Psychiatry*, **52**, 969–971.

Chang, H, & Kitai, S. 1985. Projection neurons of the nucleus accumbens: an intracellular labeling study. *Brain Res*, **347**(1), 112–116.

Chkhenkeli, S A, Šramka, M, Lortkipanidze, G S, Rakviashvili, T N, Sh Bregvadze, E, Magalashvili, G E, Sh Gagoshidze, T, & Chkhenkeli, I S. 2004. Electrophysiological effects and clinical results of direct brain stimulation for intractable epilepsy. *Clinical Neurology and Neurosurgery*, **106**, 318–329.

Chua, S E, Cheung, C, Cheung, V, Tsang, J TK, Chen, E YH, Wong, J CH, Cheung, J P Y, Yip, L, Tai, K, Suckling, J, & McAlonan, Grinne M. 2007. Cerebral grey, white matter and csf in never-medicated, first-episode schizophrenia. *Schizophrenia Research*, **89**, 12–21.

Clayton, D F. 2000. The genomic action potential. *Neurobiology of Learning and Memory*, **74**, 185–216.

Cochran, S M, Steward, L J, Kennedy, M B, McKerchar, C E, Pratt, J A, & Morris, B J. 2003. Induction of metabolic hypofunction and neurochemical deficits after chronic intermittent exposure to phencyclidine: differential modulation by antipsychotic drugs. *Neuropsychopharmacology*, **28**, 265–275.

Coffey, R J. 2008. Deep brain stimulation devices:a brief technical history and review. *Artificial Organs*, **33**(3), 208–220.

Coscia, D M, Narr, K L, Robinson, D G, Hamilton, L S, Sevy, S, Burdick, K E, Gunduz-Bruce, H, McCormack, J, Bilder, R M, & Szeszko, P R. 2009. Volumetric and shape analysis of the thalamus in first-episode schizophrenia. *Human Brain Mapping*, **30**, 1236–1245.

Cota, V R, de Castro Medeiros, D, da Pscoa Vilela, M R S, Doretto, M C, & Moraes, M F D. 2009. Distinct patterns of electrical stimulation of the basolateral amygdala influence pentylenetetrazole seizure outcome. *Epilepsy & Behavior*, **14**, 26–31.

Crawley, J N. 2000. *What's wrong wih my mouse?* Wiley-Liss.

Csernansky, J G, Wang, L, Jones, D, Rastogi-Cruz, D, Posener, J A, Heydebrand, G, Miller, J P, & Miller, M I. 2002. Hippocampal deformities in schizophrenia characterized by high dimensional brain mapping. *Am J Psychiatry*, **159**, 2000–2006.

Danos, P, Baumann, B, Bernsteina, H, Staucha, R, Krella, D, Falkaib, P, & Bogertsa, B. 2002. The ventral lateral posterior nucleus of the thalamus in schizophrenia: a post-mortem study. *Psychiatry Research Neuroimaging*, **114**, 1–9.

Danos, P, Baumann, B, Kramer, A, Bernstein, H, Stauch, R, Krell, D, Falkai, P, & Bogerts, B. 2003. Volumes of association thalamic nuclei in schizophrenia: a postmortem study. *Schizophrenia Research*, **60**, 141–155.

Davis, S, Bozon, B, & Laroche, S. 2003. How necessary is the activation of the immediate early gene *zif 268* in synaptic plasticity and learning? *Behavioural Brain Research*, **142**, 17–30.

Degos, B, Deniau, J, Thierry, A, Glowinski, J, Pezard, L, & Maurice, N. 2005. Neuroleptic-induced catalepsy: electrophysiological mechanisms of functional recovery induced by high-frequency stimulation of the subthalamic nucleus. *Neurobiology of Disease*, **25**(33), 7687–7696.

Del-Fava, F, Hasue, R H, Ferreira, J G P, & Shammah-Lagnado, S J. 2007. Efferent connections of the rostral linear nucleus of the ventral tegmental area in the rat. *Neuroscience*, **145**, 1059–1076.

Diederich, N J, Kalteis, K, Stamenkovic, M, Pieri, V, & Alesch, F. 2005. Efficient internal pallidal stimulation in gilles de la tourette syndrome: a case report. *Movement Disorders*, **20**(11), 1496–1520.

Dimpfel, W, & Spüler, M. 1990. Dizocilpine (MK-801), ketamine and phencyclidine: low doses affect brain field potentials in the freely moving rat in the same way as activation of dopaminergic transmission. *Psychopharmacology*, **101**, 317–323.

Dinner, D S, Neme, S, Nair, D, Montgomery Jr, E B, Baker, K B, Rezai, A, & Lüders, H O. 2002. EEG and evoked potential recording from the subthalamic nucleus for deep brain stimulation of intractable epilepsy. *Clinical Neurophysiology*, **113**, 1391–1402.

Dostrovsky, J O, Levy, R, Wu, J P, Hutchison, W D, Tasker, R R, & Lozano, A M. 2000. Microstimulation-induced inhibition of neuronal firing in human globus pallidus. *J Neurophysiol*, **84**, 570–574.

Egerton, A, Reid, L, McGregor, S, Cochran, S M, Morris, B J, & Pratt, J A. 2008. Subchronic and chronic PCP treatment produces temporally distinct deficits in attentional set shifting and prepulse inhibition in rats. *Psychopharmacology*, **198**, 37–49.

Erro, M E, Lanciego, J L, & Giménez-Amaya, JM. 2002. Re-examination of the thalamostriatal projections in the rat with retrograde tracers. *Neuroscience Research*, **42**, 45–55.

Feldman, R S, Meyer, J S, & Quenzer, L F. 1997. *Principles of Neuropsychopharmacology*. Sinauer Associates, Inc.

Filali, M, Hutchison, W D, Palter, V N, Lozano, A M, & Dostrovsky, J O. 2004. Stimulation-induced inhibition of neuronal firing in human subthalamic nucleus. *Exp Brain Res*, **156**, 274–281.

Fisch, B J. 1999. *Fisch and Spehlmann's EEG Primer. Third revised and enlarged edition*. Elsevier.

Fitzsimmons, J, Kubicki, M, Smith, K, Bushell, G, Estepar, R San Jose, Westin, C-F, Nestor, PG, Niznikiewicz, MA, Kikinis, R, McCarley, RW, & Shenton, ME. 2009. Diffusion tractography of the fornix in schizophrenia. *Schizophrenia Research*, **107**, 39–46.

Flecknell, P. 1996. *Laboratory animal anaesthesia; second edition.* ACADEMIC PRESS LIMITED.

Florin-Lechner, S M, Druhan, J P, Aston-Jones, G, & Valentino, R J. 1996. Enhanced norepinephrine release in prefrontal cortex with burst stimulation of the locus coeruleus. *Brain Research*, **742**(1-2), 89–97.

Fontaine, D, Mattei, V, Borg, M, von Langsdorff, D, Magnie, M, Chanalet, S, Robert, P, & Paquis, P. 2004. Effect Of Subthalamic Nucleus stimulation on obsessivecompulsive disorder in a patient with parkinson disease. *J Neurosurg*, **100**, 1084–1086.

Friedman, D, Aggleton, J, & Saunders, R. 2002. Comparison of hippocampal, amygdala, and perirhinal projections to the nucleus accumbens: combined anterograde and retrograde tracing study in the Macaque brain. *J Comp Neurol*, **450**(4), 345–365.

Gabriëls, L, Cosyns, P, Nuttin, B, Demeulemeester, H, & Gybels, J. 2003. Deep brain stimulation for treatmentrefractory obsessive-compulsive disorder: psychopathological and neuropsychological outcome in three cases. *Acta Psychiatr Scand*, **107**, 275–282.

Gao, Feng, Guo, Yi, Zhang, Hong, Wang, Shuang, Wang, Jing, Wu, Ji-Min, Chen, Zhong, & Ding, Mei-Ping. 2009. Anterior thalamic nucleus stimulation modulates regional cerebral metabolism: an FDG-MicroPET study in rats. *Neurobiology of Disease.*

Garcia, L, D'Alessandro, G, Bioulac, B, & Hammond, C. 2005. High-frequency stimulation in Parkinsons disease: more or less? *TRENDS in Neurosciences*, **28**(4), 209–216.

Ghitza, U, Fabbricatore, A, Prokopenko, V, Pawlak, A, & West, M. 2003. Persistent cue-evoked activity of accumbens neurons after prolonged abstinence from self-administered cocaine. *J Neurosci*, **23**(19), 7239–7245.

Gilbert, A R, Rosenberg, D R, Harenski, K, Spencer, S, Sweeney, J A, & Keshavan, M S. 2001. Thalamic volumes in patients with first-episode schizophrenia. *Am J Psychiatry*, **158**(618), 624.

Gimsa, J, Habel, B, Schreiber, U, van Rienen, U, Strauss, U, & Gimsa, U. 2005. Choosing electrodes for deep brain stimulation experimentselectrochemical considerations. *Journal of Neuroscience Methods*, **142**, 251–265.

Goghari, V M, Sponheim, S R, & MacDonald III, A W. 2009. The functional neuroanatomy of symptom dimensions in schizophrenia: a qualitative and quantitative review of a persistent question. *Neuroscience and Biobehavioral Reviews*, **In press**.

Gold, J M. 2004. Cognitive deficits as treatment targets in schizophrenia. *Schizophr. Res*, **72**, 21–28.

Goto, Y, & Grace, A A. 2006. Alterations in medial prefrontal cortical activity and plasticity in rats with disruption of cortical development. *Biol Psychiatry*, **60**, 1259–1267.

Green, M F. 2006. Cognitive impairment and functional outcome in schizophrenia and bipolar disorder. *J Clin Psychiatry*, **67**(9), 3–8.

Greenberg, B D, Malone, D A, Friehs, G M, Rezai, A R, Kubu, C S, Malloy, P F, Salloway, S P, Okun, M S, Goodman, W K, & Rasmussen, S A. 2006. Three-year outcomes in deep brain stimulation for highly resistant obsessive-compulsive disorder. *Neuropsychopharmacology*, **31**, 2384–2393.

Groenewegen, H J, Galis-de Graaf, Y, & Smeets, W J A J. 1999. Integration and segregation of limbic cortico-striatal loops at the thalamic level: an experimental tracing study in rats. *Journal of Chemical Neuroanatomy*, **16**, 167–185.

Gruber, A J, Calhoon, G G, Shusterman, I, Schoenbaum, G, & O'Donnell, M R Roesch P. 2010. More is less: a disinhibited prefrontal cortex impairs cognitive felxibilty. *The Journal of Neuroscience*, **30**(50), 17102–17110.

Guillazo-Blanch, G, Miguéns, M, Villarejo-Rodríguez, I, Vale-Martínez, A, Ambrosio, E, & Martí-Nicolovius, M. 2008. Electrical stimulation of the thalamic parafascicular nucleas affects glutamate release in the medial prefrontal cortex: an in vivo microdialysis study in freely moving rats. Program No. 709.1. *2008 Neuroscience Meeting Planner*, Society for Neuroscience 2008, Online.

Gur, R E, Turetsky, B I, Cowell, P E, Finkelman, C, Maany, V, Grossman, R I, Arnold, S E, Bilker, W B, & Gur, R C. 2000. Temporolimbic volume reductions in schizophrenia. *Arch Gen Psychiatry*, **57**, 769–775.

Haber, S, & McFarland, N R. 2001. The place of the thalamus in frontal cortical-basal ganglia circuits. *The Neuroscientist*, **7**, 315–324.

Haber, S, Kunishio, K, Mizobuchi, M, , & Lynd-Balta, E. 1995. The orbital and medial prefrontal circuit through the primate basal ganglia. *J Neurosci*, **15**(7), 4851–4876.

Halpern, C H, Samadani, U, Litt, B, Jaggi, J L, & Baltuch, G H. 2008. Deep brain stimulation for epilepsy. *Neurotherapeutics*, **5**, 59–67.

Hamaya, Y, Takeda, T, Dohi, S, Nakashima, S, & Nozawa, Y. 2000. The effects of pentobarbital, isoflurane, and propofol on immediate-early gene expression in the vital organs of the rat. *Anesth Analg*, **90**, 1177–1183.

Handforth, A, DeSalles, A A F, & Krahl, S E. 2006. Deep brain stimulation of the subthalamic nucleus as adjunct treatment for refractory epilepsy. *Epilepsia*, **47**(7), 1239–1241.

Hardesty, D E, & Sackheim, H A. 2007. Deep brain stimulation in movement and psychiatric disorders. *Biol Psychiatry*, **61**, 831 – 835.

Harrison, P J, & Weinberger, D R. 2005. Schizophrenia genes, gene expression, and neuropathology: on the matter of their convergence. *Molecular Psychiatry*, **10**, 40–68.

Hazlett, E A, Buchsbaum, M S, Tang, C Y, Fleischman, M B, Wei, T C, Byne, W, & Haznedar, M M. 2001. Thalamic activation during an attention-to-prepulse startle modification paradigm: a functional MRI study. *Biol Psychiatry*, **50**, 281–291.

Hazlett, E A, Buchsbaum, M S, Kemether, E, Bloom, R, Platholi, J, Brickman, A M, Shihabuddin, L, Tang, C, & Byne, W. 2004. Abnormal glucose metabolism in the mediodorsal nucleus of the thalamus in schizophrenia. *Am J Psychiatry*, **161**, 305–314.

Hazlett, E A, Buchsbaum, M S, Zhang, J, Newmark, R E, Glanton, C F, Zelmanova, Y, Mehmet Haznedar, M, Chu, K, Nenadic, I, Kemether, E M, Tang, C Y, New, A S, & Siever, L J. 2008. Frontalstriatalthalamic mediodorsal nucleus dysfunction in schizophrenia-spectrum patients during sensorimotor gating. *NeuroImage*, **42**, 1164–1177.

Hazlett, Erin A, Buchsbaum, Monte S, Jeu, Lily Ann, Nenadic, Igor, Fleischman, Michael B, Shihabuddin, Lina, Haznedar, M Mehmet, & Harvey, Philip D. 2000. Hypofrontality in unmedicated schizophrenia patients studied with PET during performance of a serial verbal learning task. *Schizophrenia Research*, **43**(1), 33 – 46.

Heimer, L, Zahm, D, Churchill, L, Kalivas, P, & Wohltmann, C. 1991. Specivity in the projection patterns of accumbal core and shell in the rat. *Neuroscience*, **41**(1), 89–125.

Henning, J, Koczan, D, Glass, Ä, Karopka, T, Pahnke, J, Rolfs, A, Benecke, R, & Gimsa, U. 2007. deep brain stimulation in a rat model modulates TH, CaMKIIa and Homer1 gene expression. *European journal of Neuroscience*, **25**, 239–250.

Herdegen, T, & Leah, J D. 1998. Inducible and constitutive transcription factors in the mammalian nervous system: control of gene expression by Jun, Fos and Krox, and CREB/rATF proteins. *Brain Research Reviews*, **28**, 370–490.

Herrmann, C S, & Demiralp, T. 2005. Human EEG gamma oscillations in neuropsychiatric disorders. *Clinical Neurophysiology*, **116**, 2719–2733.

Hiller, A, Loeffler, S, Haupt, C, Litza, M, Hofmann, U, & Moser, A. 2006. Electrical high frequency stimulation of the caudate nucleus induces local GABA outflow in freely moving rats. *Journal of Neuroscience Methods*, **xxx**(xxx), xxx–xxx.

Hofle, N, Paus, T, Reutens, D, Fiset, P, Gotman, J, Evans, A C, & Jones, B E. 1997. Regional cerebral blood flow changes as a function of delta and spindle activity during slow wave sleep in humans. *The Journal of Neuroscience*, **17**(12), 4800–4808.

Hoover, W B, & Vertes, R P. 2007. Anatomical analysis of afferent projections to the medial prefrontal cortex in the rat. *Brain Struct Funct*, **212**, 149–179.

Houeto, J L, Karachi, C, Mallet, L, Pillon, B, Yelnik, J, Mesnage, V, Welter, M L, Navarro, S, Pelissolo, A, Damier, P, Pidoux, B, Dormont, D, Cornu, P, & Agid, Y. 2005. Tourettes syndrome and deep brain stimulation. *J Neurol Neurosurg Psychiatry*, **76**, 992–995.

Hughes, P, & Dragunow, M. 1995. Induction of immediate-early genes and the control of neurotransmitter-regulated gene expression within the nervous system. *Pharmacological Reviews*, **47**(1), 133–178.

Jentsch, J D, Tran, A, & Roth, J R Taylor R H. 1998. Prefrontal cortical involvement in phencyclidine-induced activation of the mesolimbic dopamine system: behavioural and neurochemical evidence. *Psychopharmacology*, **138**, 89–95.

John, J P. 2009. Fronto-temporal dysfunction in schizophenia: a selective review. *Indian J Psychiatry*, **51**(3), 180–190.

Jones, M W, Errington, M L, French, P J, Fine, A, Bliss, T V P, Garel, S, Charnay, P, Bozon, B, Laroche, S, & Davis, S. 2001. A requirement for the immediate early gene *Zif268* in the expression of late LTP and long-term memories. *Nature Neuroscience*, **4**(3), 289–296.

Kaczmarek, L, & Robertson, H J (eds). 2002. *Handbook of Chemical Neuroanatomy: Immediate early genes and inducible transcription factors in mapping of the central nervous system function and ddysfunction*. Vol. 19. Need Publisher.

Kargieman, Lucila, Santana, Noemi, Mengod, Guadalupe, Celada, Pau, & Artigas, Francesc. 2007. Antipsychotic drugs reverse the disruption in prefrontal cortex function produced by NMDA receptor blockade with phencyclidine. *PNAS*, **104**(37), 14843–14848.

Kelley, A E. 2004. Ventral striatal control of appetitive motivation: role in ingestive behaviour and reward-related learning. *Neuroscience and Biobehavioural Reviews*, **27**, 765–776.

Kemether, E M, Buchsbaum, M S, Byne, W, Hazlett, E A, Haznedar, M, Brickman, A M, Platholi, J, & Bloom, R. 2003. Magnetic resonance imaging of

mediodorsal, pulvinar, and centromedian nuclei of the thalamus in patients with schizophrenia. *Arch Gen Psychiatry*, **60**, 983–991.

Kerrigan, J F, Litt, B, Fisher, R S, Cranstoun, S, French, J A, Blum, D E, Dichter, M, Shetter, A, Baltuch, G, Jaggi, J, Krone, S, Brodie, M A, & Graves, M Rise N. 2004. Electrical stimulation of the anterior nucleus of the thalamus for the treatment of intractable epilepsy. *Epilepsia*, **45**(4), 346–354.

Keshavan, M S, Rosenberg, D, Sweeney, J A, & Pettegrew, J W. 1998. Decreased caudate volume in neuroleptic-naive psychotic patients. *Am J Psychiatry*, **155**, 744–778.

Kito, Shinsuke, Jung, Jiuk, Kobayashi, Tetsuo, & Koga, Yoshihiko. 2009. Fiber tracking of white matter integrity connecting the mediodorsal nucleus of the thalamus and the prefrontal cortex in schizophrenia: A diffusion tensor imaging study. *European Psychiatry*, **In Press, Corrected Proof**, –.

Klitenick, M A, Deutch, A Y, Churchill, L, & Kalivas, P W. 1992. Topography and functional role of dopaminergic projections from the ventral mesencephalic tegmentum to the ventral pallidum. *Neuroscience*, **50**(2), 371–386.

Knapska, E, & Kaczmarek, L. 2004. A gene for neuronal plasticity in the mammalian brain: Zif268/Egr-1/NGFI-A/Krox-24/TIS8/ZENK? *Progress in Neurobiology*, **74**, 183–211.

Knyazeva, M G, Jalili, M, Meuli, R, Hasler, M, De Feo, O, & Do, K Q. 2008. Alpha rhythm and hypofrontality in schizophrenia. *Schizophrenia Research*, **118**, 188–199.

Konick, L C, & Friedman, L. 2001. Meta-analysis of thalamic size in schizophrenia. *Biol Psychiatry*, **49**, 28–38.

Kovács, K J. 1998. *c-Fos* as a transcription factor: a stressful (re)view from a functional map. *Neurochem Int*, **33**, 287–297.

Krack, P, Pollak, P, Limousin, P, Hoffmann, D, Xie, J, Benazzouz, A, & Benabid, A L. 1998. Subthalamic nucleus or internal pallidal stimulation in young onset Parkinsons disease. *Brain*, **121**, 451–457.

Kuhn, J, Lenartz, D, Mai, J K, W, Lee, S, Koulousakis, A, Klosterkoetter, J, & Sturm, V. 2007. Deep brain stimulation of the nucleus accumbens and the internal capsule in therapeutically refractory Tourette-syndrome. *J Neurol*, **254**, 963–965.

Kulkarni, S K. 1977. Open field test: its status in psychopharmacology. *Ind J Pharmac*, **9**(4), 241–246.

Kumari, V, Gray, J A, Geyer, M A, Ffytche, D, Soni, W, Mitterschiffthaler, M T, Vythelingum, G N, Simmons, A, Williams, S C R, & Sharma, T. 2003. Neural correlates of tactile prepulse inhibition: a functional MRI study in normal and schizophrenic subjects. *Neuroimaging*, **122**, 99–113.

Lanahan, A, & Worley, P. 1998. Immediate-early genes and synaptic function. *Neurobiology of Learning and Memory*, **70**, 37–43.

Larson, P S. 2008. Deep brain stimulation for psychiatric disorders. *Neurotherapeutics*, **5**, 50–58.

Lavin, A, & Grace, A A. 1997. Response of the ventral pallidal/mediodorsalthalamic system to antipsychotic drugadministration: involvement of the prefrontal cortex. *Neuropsychopharmacology*, **18**(5), 352–363.

Lewis, D A, & Levitt, P. 2002. Schizophrenia as a disorder of neurodevelopment. *Annu. Rev. Neurosci.*, **25**, 409–32.

Leyland, C M, Gwyther, R J, & Ryiands, J M. 1979. An improved method for detecting drug effects in the open field. *Psychopharmacology*, **63**, 33–37.

Li, L, Du, Y, Li, N, Wu, X, & Wu, Y. 2009. Topdown modulation of prepulse inhibition of the startle reflex in humans and rats. *Neuroscience and Biobehavioral Reviews*, **33**, 1157–1167.

Li, S, Arbuthnott, G W, Jutras, M J, Goldberg, J A, & Jaeger, D. 2007. Resonant antidromic cortical circuit activation as a consequence of high-frequency subthalamic deep-brain stimulation. *J Neurophysiol*, **98**, 3525–3537.

Lieberman, J A, Stroup, T S, McEvoy, J P, Swartz, M S, Rosenheck, R A, Perkins, D O, Keefe, R S E, Davis, S M, Davis, C E, Lebowitz, B D, Severe, J, & Hsiao, J K. 2005. Effectiveness of Antipsychotic Drugs in Patients with Chronic Schizophrenia. *The New England Journal Of Medicine*, **353**(12), 1209–1223.

Limousin, P, Krack, P, Pollak, P, Benazzouz, A, Ardouin, C, Hoffmann, D, & Benabid, A L. 1998. Electrical stimulation of the subthalamic nucleus in advanced parkinsons disease. *N Engl J Med*, **339**, 1105–1111.

Lloyd-Thomas, A R, Cole, P V, & Prior, P F. 1990. Quantitative eeg and brainstem auditory evoked potentials: comparison of isoflurane with halothane using the cerebral function analysing monitor. *British Journal of Anaesthesia*, **65**, 306–312.

Lodge, D J, & Grace, A A. 2007. Aberrant hippocampal activity underlies the dopamine dysregulation in an animal model of schizophrenia. *Neurobiology of Disease*, **27**(42), 11424–11430.

Lodge, D J, & Grace, A A. 2009. Gestational methylazoxymethanol acetate administration: a developmental disruption model of schizophrenia. *Behavioural Brain Research*, **in press**.

Lodge, D J, Behrens, M M, & Grace, A A. 2009. A loss of parvalbumin-containing interneurons is associated with diminshed oscillatory activity in an animal model of schizophrenia. *The Journal of Neuroscience*, **29**(8), 2344–2354.

Loebrich, S, & Nedivi, E. 2009. The function of activity-regulated genes in the nervous system. *Physiol Rev*, **89**, 1079–1103.

Magariños-Ascone, C, Pazo, J H, Macadar, O, & Buño, W. 2002. High-frequency stimulation of the subthalamic nucleus silences subthalamic neurons: a possible cellular mechanism in parkinsons disease. *Neuroscience*, **115**(4), 1109–1117.

Mallet, L, Mesnage, V, Houeto, J, Pelissolo, A, Yelnik, J, Behar, C, Gargiulo, M, Welter, M, Bonnet, A, B Pillon, P Cornu, Dormont, D, Pidoux, B, Allilaire, J, & Agid, Y. 2002. Compulsions, parkinsons disease, and stimulation. *The Lancet*, **360**, 1302–1304.

Marquis, K L, Paquette, N C, Gusslo, R, & Moreton, J E. 1989. Comparative Electroencephalographic and Behavioral Effects of Phencyclidine, (+)-SKF-10,047 and MK-801 in Rats. *The Journal of Pharmacology And Experimental Therapeutics*, **252**(3), 1104–1112.

Martini, F H. 2001. *Fundamentals of Anatomy and Physiology; fifth edition.* Prentice and Hall.

Maurice, N, Deniau, J M, Menetrey, A, Glowinski, J, & Thierry, A M. 1997. Position of the ventral pallidum in the rat prefrontal cortexbasal ganglia circuit. *Neuroscience*, **80**(2), 523–534.

Mayberg, H S, Lozano, A M, Voon, V, McNeely, H E, Seminowicz, D, Hamani, C, Schwalb, J M, & Kennedy, S H. 2005. Deep brain stimulation for treatment-resistant depression. *Neuron*, **45**(5), 651–660.

Mazzone, P, Insola, A, Sposato, S, & Scarnati, E. 2009. The deep brain stimulation of the pedunculopontine tegmental nucleus. *Neuromodulation: Technology At The Neural Interface*, **12**(3), 191–204.

McCracken, C B, & Grace, A A. 2007. High frequency deep brain stimulation of the nucleus accumbens region suppresses neuronal activity and selectively modulates afferent drive in rat orbitofrontal cortex *in vivo*. *The Journal of Neuroscience*, **27**(46), 12601–12610.

McCracken, C B, & Grace, A A. 2009. Nucleus accumbens deep brain stimulation produces region-specific alterations in local field potential oscillations and evoked responses in vivo. *Neurobiology of Disease*, **29**(16), 5354–5363.

McCrone, P, Dhanasiri, S, Patel, A, Knapp, M, & Lawton-Smith, S. 2008. Paying the price, the cost of mental health care in England to 2026. *King's Fund*, **6**, 1–17.

McIntyre, C C, Sherman, W M Grill D L, & Thakor, N V. 2003. Cellular effects of deep brain stimulation: model-based analysis of activation and inhibition. *J Neurophysiol*, **91**, 1457–1469.

McIntyre, C C, Savasta, M, Goff, L Kerkerian-Le, & Vitek, J L. 2004. Uncovering the mechanism(s) of action of deep brain stimulation: activation, inhibition, or both. *Clinical Neurophysiology*, **115**, 1239–1248.

Meissner, W, Leblois, A, Hansel, D, Bioulac, B, Gross, C E, Benazzouz, A, & Boraud, T. 2005. Subthalamic high frequency stimulation resets subthalamic firing and reduces abnormal oscillations. *Brain*, **128**, 2372–2382.

Meredith, G, Pennartz, C, & Groenewegen, H. 1993. The cellular framework for chemical signalling in the nucleus accumbens. *Prog Brain Res*, **99**, 3–24.

Messias, E, Chen, C, & Eaton, W W. 2007. Epidemiology of schizophrenia: review of findings and myths. *Psychiatr Clin North Am.*, **30**(3), 323–338.

Mitelman, S A, Byne, W, Kemether, E M, Hazlett, E A, & Buchsbaum, M S. 2005. Metabolic disconnection between the mediodorsal nucleus of the thalamus and cortical Brodmanns areas of the left hemisphere in schizophrenia. *Am J Psychiatry*, **162**, 1733–1735.

Moore, H, Jentsch, J D, Ghajarnia, M, Geyer, M A, & Grace, A A. 2006. A neurobehavioural systems analysis of adult rats ecposed to methylazoxymethanol acetate on E17: implications for the neuropathology of schizophrenia. *Biol Psychiatry*, **60**, 253–264.

Morris, B J, Cochran, S M, & Pratt, J A. 2005. PCP: from pharmacology to modelling schizophrenia. *Current Opinion in Pharmacology*, **5**(1), 101 – 106.

Mouri, A, Noda, Y, Enomoto, T, & Nabeshima, T. 2007. Phencyclidine animal models of schizophrenia: Approaches from abnormality of glutamatergic neurotransmission and neurodevelopment. *Neurochemistry International*, **51**, 173–184.

Murthy, R Srinivasa, Bertolote, J M, Epping-Jordan, J, Funk, M, Prentice, T, Saraceno, B, & Saxena, S. 2001. *The World health report: 2001: Mental health: new understanding, new hope*. World Health Organization 2001.

Nakano, K. 2000. Neural circuits and topographic organization of the basal ganglia and related regions. *Brain Dev*, **22**(1), 5–16.

Nelson, M D, Saykin, A J, Flashman, L A, & Riordan, H J. 1998. Hippocampal volume reduction in schizophrenia as assessed by magnetic resonance imaging. *Arch Gen Psychiatry*, **55**, 433–440.

Nishida, N, Huang, Z, Mikuni, N, Miura, Y, Urade, Y, & Hashimoto, N. 2007. Deep brain stimulation of the posterior hypothalamus activates the histaminergic system to exert antiepileptic effect in rat pentylenetetrazol model. *Experimental Neurology*, **205**, 132–144.

Nowak, L G, & Bullier, J. 1998a. Axons, but not cell bodies, are activated by electrical stimulation in cortical gray matter. *Exp Brain Res*, **118**, 477–488.

Nowak, L G, & Bullier, J. 1998b. Axons, but not cell bodies, are activated by electrical stimulation in cortical gray matter. *Exp Brain Res*, **118**, 489–500.

Nuttin, B, Cosyns, P, Demeulemeester, H, Gybels, J, & Meyerson, B. 1999. Electrical stimulation in anterior limbs of internal capsules in patients with obsessive-compulsive disorder. *The Lancet*, **354**, 1526.

Otake, K, & Nakamura, Y. 2000. Possible pathways through which neurons of the shell of the nucleus accumbens influence the outflow of the core of the nucleus accumbens. *Brain Dev*, **Suppl**(1), 17–26.

Paxinos, G, & Watson, C. 2007. *The Rat Brain in Stereotaxic coordinates,* 6^{th} *edition*. Academic Press.

Perlstein, William M, Carter, Cameron S, Noll, Douglas C, & Cohen, Jonathan D. 2001. Relation of Prefrontal Cortex Dysfunction to Working Memory and Symptoms in Schizophrenia. *Am J Psychiatry*, **158**(7), 1105–1113.

Polikov, V S, Tresco, P A, & Reichert, W M. 2005. Response of brain tissue to chronically implanted neural electrodes. *Journal of Neuroscience Methods*, **148**, 1–18.

Popken, G J, Jr, W E Bunney, Potkin, S G, & Jones, E G. 2000. Subnucleus-specific loss of neurons in medial thalamus of schizophrenics. *PNAS*, **97**(16), 9276–9280.

Potkin, Steven G, Alva, Gustavo, Fleming, Kirsten, Anand, Ravi, Keator, David, Carreon, Danilo, Doo, Michael, Jin, Yi, Wu, Joseph C, & HFallon, James. 2002. A PET Study of the Pathophysiology of Negative Symptoms in Schizophrenia. *Am J Psychiatry*, **159**(2), 227–237.

Pratt, J A, Winchester, C, Egerton, A, Cochran, S M, & Morris, B J. 2008. Modelling prefrontal cortex deficits in schizophrenia: implications for treatment. *British Journal of Pharmacology*, **153**(S1), S465–S470.

Quinkert, A W, Schiff, N D, & Pfaff, D W. 2010. Temporal patterning of pulses during deep brain stimulation affects central nervous system arousal. *Behavioural Brain Research*, **214**, 377–385.

Ranck, J B. 1975. Which elements are excited in electrical stimulation of mammalian central nervous system: a review. *Brain Research*, **98**, 417–440.

Rapoport, J L, Addington, A M, Frangou, S, & Psych, M R. 2005. The neurodevelopmental model of schizophrenia: update 2005. *Mol. Psychiatry*, **10**, 434–449.

Rauch, S L, Dougherty, D D, Malone, D, Rezai, A, Friehs, G, Fischman, A J, Alpert, N M, Haber, S N, Stypulkowski, P H, Rise, M T, Rasmussen, S A, & Greenberg, B D. 2006. A functional neuroimaging investigation Of deep Brain stimulation in patients with obsessivecompulsive disorder. *J Neurosurg*, **104**, 558–565.

Razi, K, Greene, K P, Sakuma, M, Ge, S, Kushner, M, & DeLisi, L E. 1999. Reduction of the parahippocampal gyrus and the hippocampus in patients with chronic schizophrenia. *British Journal Of Psychiatry*, **174**, 512–519.

Roach, B J, & Mathalon, D H. 2008. Event-related eeg time-frequency analysis: an overview of measures and an analysis of early gamma band phase locking in schizophrenia. *Schizophrenia Bulletin*, **34**(5), 907–926.

Romanski, L M, Giguere, M, & andnd P S Goldman-Rakic, J F Bates. 1997. Topographic organization of medial pulvinar connections with the prefrontal cortex in the rhesus monkey. *The Journal Of Comparative Neurology*, **379**, 313–332.

Ross, C A, Margolis, R L, Reading, S A J, Pletnikov, M, & Coyle, J T. 2006. Neurobiology of Schizophrenia. *Neuron*, **52**, 139–153.

Sagar, S M, Sharp, F R, & Curran, T. 1988. Expression of *c-fos* protein in brain: metabolic mapping at the cellular level. *Science*, **240**, 1328–1331.

Sagratella, S, Pezzola, A, Popoli, P, & Scotti de Carolis, A. 1992. Different capability of *N*-methyl-D-aspartate antagonists to elicit EEG and behavioural phencyclidine-like effects in rats. *Psychopharmacology*, **109**, 277–282.

Salin, P, Manrique, C, Forni, C, & Kerkerian-Le Goff, L. 2002. High-frequency stimulation of the subthalamic nucleus selectively reverses dopamine denervation-induced cellular defects in the output structures of the basal ganglia in the rat. *The Journal of Neuroscience*, **22**(12), 5137–5148.

Satorius N, Jablensky, & Korten, A. 1986. Early manifestations and first-contact incidence of schizophrenia in different cultures. *Psychol Med*, **16**, 909–928.

Schiff, N D, Giacino, J T, Kalmar, K, Victor, J D, Baker, K, Gerber, M, Fritz, B, Eisenberg, B, OConnor, J, Kobylarz, E J, Machado, S FarrisVA, McCagg, C, Plum, F, Fins, J J, & Rezai, A R. 2007. Behavioural improvements with thalamic stimulation after severe traumatic brain injury. *Nature*, **448**, 600–603.

Schlaepfer, T E, Cohen, M X, Frick, C, Kosel, M, Brodesser, D, Axmacher, N, Joe, A Y, Kreft, M, Lenartz, D, & Sturm, V. 2008. Deep brain stimulation to reward circuitry alleviates anhedonia in refractory major depression. *Neuropsychopharmacology*, **33**, 368–377.

Schroder, Johannes, Buchsbaum, Monte S, Siegel, Benjamin V, Geider, Franz Josef, Lohr, James, Tang, Cheuk, Wu, Joseph, & Potkin, Stephen G. 1996. Cerebral metabolic activity correlates of subsyndromes in chronic schizophrenia. *Schizophrenia Research*, **19**(1), 41 – 53.

Schulte, T, Brecht, S, Herdegen, T, Illert, M, Mehdorn, HM, & Hamel, W. 2006. Induction of immediate early gene expression by high-frequency stimulation of the subthalamic nucleus in rats. *Neuroscience*, **138**(4), 1377 – 1385.

Sebban, C, Tesolin-Decros, B, Ciprian-Ollivier, J, Perret, L, & Spedding, M. 2002. Effects of phencyclidine (PCP) and MK 801 on the EEGq in the prefrontal cortex of conscious rats; antagonism by clozapine, and antagonists of AMPA-, a1- and 5-HT2A-receptors. *British Journal of Pharmacology*, **135**, 65–78.

Shimizu, M, Fujiwara, H, Hirao, K, Namik, C, Fukuyama, H, Hayashi, T, & Murai, T. 2008. Structural abnormalities of the adhesio interthalamica and mediodorsal nuclei of the thalamus in schizophrenia. *Schizophrenia Research*, **101**, 3311–338.

Shirvalkar, P, Seth, M, Schiff, N D, & Herrera, D G. 2006. Cognitive enhancement with central thalamic electrical stimulation. *PNAS*, **103**(45), 17007–17012.

Silverman, P. 1978. *Animal behaviour in the laboratory.* Pica Press New York.

Snitz, B E, III, A W Macdonald, & Carter, C S. 2006. Cognitive deficits in unaffected first-degree relatives of schizophrenia patients: a meta-analytic review of putative endophenotypes. *Schizophr. Bull.*, **32**, 179–194.

Stanford, S C. 2007. The open field test: reinventing the wheel. *Journal of Psychopharmacology*, **21**(2), 134–135.

Sun, J J, Kung, J C, Wang, C C, Chen, S L, & Shyu, B C. 2006. Short-term facilitation in the anterior cingulate cortex following stimulation of the medial thalamus in the rat. *Brain Research*, **1097**, 101 – 115.

Swerdlow, N R, Geyer, M A, & Braff, D L. 2001. Neural circuit regulation of prepulse inhibition of startle in the rat: current knowledge and future challenges. *Psychopharmacology*, **156**, 194–215.

Takahata, R, & Moghaddam, B. 2003. Activation of glutamate neurotransmission in the prefrontal cortex sustains the motoric and dopaminergic effects of phencyclidine. *Neuropsychopharmacology*, **28**, 1117–1124.

Temel, Y, & Visser-Vandewalle, V. 2004. Surgery in tourette syndrome. *Movement Disorders*, **91**(1), 3–14.

Temel, Y, Blokland, A, Steinbusch, H W M, & Visser-Vandewalle, V. 2005. The functional role of the subthalamic nucleus in cognitive and limbic circuits. *Progress in Neurobiology*, **76**, 393–413.

Theodore, W H, & Fisher, R S. 2004. Brain stimulation for epilepsy. *Lancet Neurol*, **3**, 111–118.

Tischmeyer, W, Kaczmarek, L, Strauss, M, & Jork, R. 1990. Accumulation of *c-fos* mRNA in rat hippocampus during acquisition of a brightness discrimination. *Behavioral & Neural Biology*, **54**(2), 165–171.

Uhlhaas, P J, Haenschel, C, Nikolić, D, & Singer, W. 2008. The role of oscillations and synchrony in cortical networks and their putative relevance for the pathophysiology of schizophrenia. *Schizophrenia Bulletin*, **34**(5), 927–943.

Usud, Iwao, Tanaka, Koichi, & Chiba, Tanemichi. 1998. Efferent projections of the nucleus accumbens in the rat with special reference to subdivision of the nucleus: biotinylated dextran amine study. *Brain research*, **797**, 73–93.

Uylings, H BM, Groenewegen, H J, & Kolb, B. 2003. Do rats have a prefrontal cortex? *Behavioural Brain Research*, **146**(3), 17.

Vertes, R P. 2004. Differential projections of the infralimbic and prelimbic cortex in the rat. *Synapse*, **51**, 32–58.

Vertes, R P. 2006. Interactions among the medial prefrontal cortex, hippocampus and midline thalamus in emotional and cognitive processing in the rat. *Neuroscience*, **142**, 1–20.

Vertes, R P, Hoover, W B, Szigeti-Buck, Kl, & Leranth, C. 2007. Nucleus reuniens of the midline thalamus: Link between the medial prefrontal cortex and the hippocampus. *Brain Research Bulletin*, **71**, 601–609.

Vesper, J, Steinhoff, B, Rona, S, Wille, C, Bilic, S, Nikkhah, G, & Ostertag, C. 2007. Chronic high-frequency deep brain stimulation of the STN/SNr for progressive myoclonic epilepsy. *Epilepsia*, **48**(10), 1984–1989.

Visser-Vandewalle, V, Teme, Y, Boon, P, Vreeling, F, Colle, H, Hoogland, G, Groenewegen, H J, & Linden, C Van Der. 2003. Chronic bilateral thalamic stimulation: a new therapeutic approach in intractable Tourette syndrome. *J Neurosurg*, **99**, 1094–1100.

Vitek, J L. 2002. Mechanisms of deep brain stimulation: excitation or inhibition. *Movement Disorders*, **17**(S3), S69–S72.

Voss, L, & Sleigh, J. 2007. Monitoring consciousness: the current status of EEG-based depth of anaesthesia monitors. *Best Practice & Research Clinical Anaesthesiology*, **21**(3), 313–325.

Walsh, R N, & Cummins, R A. 1976. The open-field test: a critical review. *Psychological Bulletin*, **83**(3), 482–504.

Wang, C C, & Shyu, B C. 2004. Differential projections from the mediodorsal and centrolateral thalamic nuclei to the frontal cortex in rats. *Brain Research*, **995**, 226–235.

Welter, M, Mallet, L, Houeto, J, Karachi, C, Czernecki, V, Cornu, P, Navarro, S, Pidoux, B, Dormont, D, Bardinet, E, Yelnik, J, Damier, P, & Agid, Y. 2008. Internal pallidal and thalamic stimulation in patients with tourette syndrome. *Arch Neurol*, **7**, 952–957.

Westby, G W M, & Wang, H. 1997. A floating microwire technique for multichannel chronic neural recording and stimulation in the awake freely moving rat. *Journal of Neuroscience Methods*, **76**, 123–133.

Wichmann, T, & DeLong, M R. 2006. Deep brain stimulation for neurologic and neuropsychiatric disorders. *Neuron*, **52**, 197–204.

Windels, F, Bruet, N, Poupard, A, Urbain, N, Chouvet, G, Feuerstain, C, & Savasta, M. 2000. Effects of high frequency stimulation of subthalamic nucleus on extracellular glutamate and GABA in substantia nigra and globus pallidus in the normal rat. *European Journal of Neuroscience*, **12**, 4141–4146.

Windels, F, Bruet, N, Poupard, A, Feuerstein, C, Bertrand, A, & Savasta, M. 2003. Influence of the frequency parameter on extracellular glutamate and γ-aminobutyric acid in substantia nigra and globus pallidus during electrical stimulation of subthalamic nucleus in rats. *Journal of Neuroscience Research*, **72**, 259–267.

Windels, F, Carcenac, C, Poupard, A, & Savasta, M. 2005. Pallidal origin of GABA release within the substantia nigra pars reticulata during high-frequency stimulation of the subthalamic nucleus. *The Journal of Neuroscience*, **25**(20), 5079–5086.

Wisden, W, & Morris, B J. 2002. *In situ hybridization protocols for the brain, 2^{nd} edition.* Academic Press.

Wright, I C, Rabe-Hesketh, S, Woodruff, P WR, David, A S, Murray, R M, & Bullmore, E T. 2000. Meta-analysis of regional brain volumes in schizophrenia. *Am J Psychiatry*, **157**, 16–25.

Wu, M, Hrycyshyn, A W, & Brudzynski, S M. 1996. Subpallidal outputs to the nucleus accumbens and the ventral tegmental area: anatomical and electrophysiological studies. *Brain research*, **740**, 151–161.

Wu, Y R, Levy, R, Ashby, P, Tasker, R R, & Dostrovsky, J O. 2001. Does stimulation of the GPi control dyskinesia by activating inhibitory axons? *Movement Disorders*, **16**(2), 208–216.

Yamada, Y, Hada, Y, Imamura, K, Mataga, N, Watanabe, Y, & Yamamot, M. 1999. Differential expression of immediate-early genes, *c-fos* and *zif268*, in the visual cortex of young rats: effects of a noradrenergic neurotoxin on their expression. *Neuroscience*, **92**(2), 473–484.

Young, K A, Manaye, K F, Liang, C, Hicks, P B, & German, D C. 2000. Reduced number of mediodorsal and anterior thalamic neurons in schizophrenia. *Biol Psychiatry*, **47**, 944–953.

Zaborszky, L, Alheid, G, Beinfeld, M, Eiden, L, Heimer, L, & Palkovits, M. 1985. Cholecystokinin innervation of the ventral striatum: a morphological and radioimmunological study. *Neuroscience*, **14**(2), 427–453.

Zahm, D. 2000. An integrative neuroanatomical perspective on some subcortical substrates of adaptive responding with emphasis on the nucleus accumbens. *Neurosci Biobehav Rev*, **24**(1), 85–105.

Zangenehpour, S, & Chaudhuri, A. 2002. Differential induction and decay curves of *c-fos* and *zif-268* revealed through dual activity maps. *Molecular Brain Research*, **109**, 221–225.

Zumsteg, D, Lozano, A M, Wieser, H G, & Wennberg, R A. 2006. Cortical activation with deep brain stimulation of the anterior thalamus for epilepsy. *Clinical Neurophysiology*, **117**, 192–207.

Part VI

Appendices

Suppliers

Abbott Animal Health Abbott Laboritories Ltd, Queensborough, Kent, ME11 5EL.

Allergen Pharmaceuticals (Ireland) Ltd. Castlebar Road, Westport, Co. Mayo., Ireland.

AstraZeneca UK Ltd 600 Capability Green, Luton, LU1 3LU.

Axon Instruments, Inc. 3280 Whipple Road, Union City, CA 94587, USA.

Coopers Needle Works Ltd. 261-263 Aston Lane, Birmingham, West Midlands, B20 3HS.

Cruachem Ltd. West of Scotland Business Park, Acre Road, Glasgow, G20 0UA.

Cypress Technology Co. Ltd. 6F-6, No. 130, Jian Kang Road, Chung Ho City, Taipei Hsien 23585, Taiwan, R.O.C.

David Kopf Instruments 7324 Elmo Street, Tujunga, California, 91042.

Dunlop's Vetinary Supplies College Mains Road, Dumfires, DG2 ONU.

EEE, The University of Glasgow Electronics & Electrical Engineering, The University of Glasgow, Rankine Building, Oakfield Avenue, Glasgow, G12 8LT.

Farnell Canal Road, Leeds, LS12 2TU.

Fine Science Tools Inc. Pentagon Business Park, Cambridge Road, Linton, CB21 4NN.

gnuplot www.gnuplot.info.

Graphpad Software Inc. 2236 Avenida de la Playa, La Jolla, CA 92037, USA.

Hameln Pharmaceuticals Ltd Gloucester, UK.

Harlan UK Limited Shaw's Farm, Blackthorn, Bicester, Oxon, OX25 1TP.

Harvard Apparatus Ltd. PO Box 126, Kent, TN8 6WF.

Imaging Research Inc. Interfocus Imaging Ltd. Cambridge Road, Linton, Cambridge, CB21 4NN.

Javis MFG. Co, Ltd. Lower Carr Mill, Hopes Carr, Stockport, SK11 1Y.

Kemdent Associated Dental Products Ltd, Purton, Swindon, Wiltshire, SN5 4HT.

Leica Microsystems (UK) Ltd Leica Microsystems (UK) Ltd, Davy Avenue, Knowlhill, Milton Keynes, MK5 8LB.

Maplin Electronics 30 St Enoch Square, Glasgow, G1 4DB.

Matlab Mathworks, 3 Apple Hill Drive, Natick, MA 01760-2098, USA.

Med Associates Inc PO Box 319, St Albans, VT 05478, USA.

National Instruments Corporation 11500 N Mopac Expwy, Austin, TX 78759-3504, USA.

PerkinElmer LAS (UK) Ltd Chalfont Road, Seer Green, Beaconsfield, Bucks, HP9 2FX.

Pfizer Animal Health Pfizer Ltd, Ramsgate Road, Sandwich, Kent, CT13 9NJ.

Plastisc 1 6591 Merriman Road, S.W.,Roanoke, VA, 24018-6664, USA.

QIAGEN Ltd QIAGEN House, Fleming Way, Crawley, West Sussex, RH10 9NQ.

Raymond A Lamb Ltd Units 4 5 Parkview Industrial Estate, Alder Close, Lottbridge Drove, Eastbourne, East Sussex, BN23 6QE.

Roche Applied Science Roche Diagnostics Ltd, Charles Avenue, Burgess Hill, West Sussex, RH15 9RY.

Royem Scientific Limited PO Box 961, Luton, Bedfordshire, LU2 0WB.

RS Components PO Box 99, Corby, Northants, NN17 9RS.

Sanyo Sales & Marketing Europe GmbH, 18 Colonial Way, Watford, Herts, WD24 4PT.

Seton Healthcare Group PLC. Tubiton House, Oldham, OL1 3HS.

Sigma-Aldrich Sigma-Aldrich Company Ltd, The Old Brickyard, New Road, Gillingham, Dorset, SP8 4XT.

SPSS version 17.0 SPSS UK Ltd., 1^{st} Floor, St. Andrew's House, West Street, Woking, Surrey, GU21 6EB.

Strathclyde Electrophysiology software The Strathclyde Institute of Pharmacy and Biomedical Sciences, University of Strathclyde, The John Arbuthnott Building, 27 Taylor Street, Glasgow, G4 ONR.

The Scientific Wire Company 18 Raven Road, South Woodford, London, E18 1HW.

Thermo Electron Corporation Anantomical Pathology International, 93/96 Chadwick Rd, Runcorn, Cheshire, WA7 1PR.

Tracksys Ltd. Unit 15, Faraday Building, Nottingham Science & Technology park, University Boulevard, Nottingham, NG7 2QP.

VWR International Ltd VWR International Ltd, Poole, BH15 1TD.

Watkins & Doncaster PO Box 5, Cranbrook, Kent, TN18 5EZ, UK.